Caspase 3 Cleavage of Pax7 Inhibits Self-Renewal of Satellite Cells

Sarah Dick

Thesis submitted to the
Faculty of Graduate and Postdoctoral Studies
in partial fulfillment of the requirements
for the Doctorate in Philosophy degree in
Cellular and Molecular Medicine

Department of Cellular and Molecular Medicine
Faculty of Medicine
University of Ottawa

Acknowledgments

Throughout my PhD I have had the opportunity to go on a journey of discovery that I am forever grateful for. Not only was I given the freedom to hone my skills in the lab but through many thoughtful discussions with colleagues at the OHRI or a conference I have learned to navigate the field of science with an air of excitement, wonder and criticism. I first and foremost have to thank my supervisor Dr. Lynn Megeney who opened his lab to me as an eager student straight out of my undergrad and encouraged me along the way. He provided helpful discussions when I needed some advice, in my science but also all aspects of graduate student life, and was my mentor in every aspect of the word. If not for his confidence in me I would not have been so daring to transfer to my PhD and embark on such a treacherous journey. Of course this path wasn't always easy, which is why those long coffee breaks with Alessandra, beers on a patio with Shannon or long talks on the phone with my family are as much a part of my success as my time in the lab doing experiments.

I also want to thank the members of my trainee advisory committee Drs. Jeffery Dilworth, Michael Rudnicki and Steffany Bennett for their guidance throughout my project. I also have to thank all members of the Megeney lab, past and present, for their help both on and off the bench. The friendship they provided made the lab a great place to work. A special thanks to Dr. Fabien Le Grand, an indispensable mentor during my early days in the lab, who taught me not only how to perform experiments but to critically evaluate my work and formulate hypotheses. And finally, I want to acknowledge my parents. At a young age they always told me I could achieve anything if I put my mind to it, a reminder I often needed after late nights at the lab with nothing but inconclusive data to show for it. They have stood by my side throughout this entire PhD and have done everything they could to make sure I achieved my dreams. Mom and Dad this thesis is dedicated to you.

Authorization

Figures 1-5

Permission for reproduction of material from Bentzinger, F.C., Wang, Y.X. and Rudnicki, M.A., Building Muscle: Molecular regulations of Myogenesis. Cold Spring Harb Perspect Biol. 2012; 4: a008342 for use in a thesis was obtained from © Cold Spring Harbor Laboratory Press.

Permission for reproduction of material from Fuentes-Prior, P. and Salvesen, GS., The protein structures that shape caspase activity, specificity, activation and inhibition. The Biochemical Journal 384(Pt2): 201-32 © 2004 for non-commercial use in a thesis is provided free of cost from Portland Press Ltd.

Permission for reproduction of material from D'Amelio, M., Cavallucci, V. and Cecconi, F. Neuronal caspase-3 signalling: not only cell death. Cell Death and Differentiation 17: 1104-14 © 2010 was obtained from Macmillan Publishers Ltd. License Number: 3461390324501

Permission for reproduction of material from Dick, S.A. and Megeney, L.A. (2013) Cell death proteins: An evolutionary role in cellular adaptation before the advent of apoptosis. BioEssays 35(11): 974-83 was obtained from John Wiley and Sons, Copyright © WILEY Periodicals, Inc. License Number: 3461390912878

Appendix Manuscripts

Permission to include the full article Alfaro, L. A., Dick, S.A., Siegel, A. L., Anonuevo, A. S., McNagny, K. M., Megeney, L.A., Cornelison, D. D., and Rossi, F. M. (2011) CD34 promotes satellite cell motility and entry into proliferation to facilitate efficient skeletal muscle regeneration. Stem Cells 29(12): 2030-41 as part of a dissertation/thesis was obtained from John Wiley and Sons, Copyright © 2011 AlphaMed Press. License Number: 3463751125023

Permission to include the full article Dick, S.A. and Megeney, L.A. (2013) Cell death proteins: An evolutionary role in cellular adaptation before the advent of apoptosis. BioEssays 35(11): 974-83 as part of a dissertation/thesis was obtained from John Wiley and Sons, Copyright © 2013 WILEY Periodicals, Inc. License Number: 3463750831621

Permission to include the paper Putinski, C., Abdul-Ghani, M., Stiles, R., Brunette, S., Dick, S.A., Fernando, P., and Megeney, L.A., Intrinsic-mediated caspase activation is essential for cardiomyocyte hypertrophy. Proceedings of the National Academy of Sciences USA 110(43): E4079-87 © 2013 as part of a dissertation/thesis is provided free of cost to authors from the National Academy of Sciences, USA.

Abstract

Compensatory growth and regeneration of skeletal muscle is dependent on the resident stem cell population, termed satellite cells. Self-renewal and maintenance of the satellite cell niche is coordinated by the transcription factor Pax7, yet continued expression of this protein inhibits the myoblast differentiation program. As such, the reduction or removal of Pax7 may denote a key prerequisite for satellite cells to abandon self-renewal and acquire differentiation competence. Here, we identify caspase 3 cleavage inactivation of Pax7 as a crucial step for terminating the self-renewal process. Inhibition of caspase 3 results in elevated Pax7 protein and satellite cell self-renewal, while caspase activation leads to Pax7 cleavage and initiation of the myogenic differentiation program. We have also noted that casein kinase 2 (CK2) directed phosphorylation of Pax7 attenuates caspase directed cleavage. Together, these results demonstrate that satellite cell fate is dependent on opposing post-translational modifications of the Pax7 protein.

Table of Contents

List of Figures

Chapter 1: Introduction

Chapter 3: Caspase 3 is required for commitment of satellite cells to differentiation

Chapter 4: Pax7 is a caspase 3 cleavage substrate

Chapter 5: The role of CK2 in modulating caspase 3 mediated cleavage of Pax7 Protein

Chapter 6: Discussion

List of Tables

Chapter 2: Materials and Methods

Chapter 4: Pax7 is a caspase 3 cleavage substrate

List of Abbreviations

Apaf-1	Apoptotic protease activating factor 1
ARMS	Alveolar Rhabdomyosarcoma
ARTS	Apoptosis-Related protein in the TGF-β Signalling pathway
ATP	Adenosine Triphosphate
(BAF)60	Brg/Brm-associated factor 60
Bak	Bcl-2-antagonist/Killer 1
Bax	Bcl-2-associated X protein
Bcl-2	B-cell CLL/Lymphoma 2
Bcl-xL	B-cell lymphoma-extra large
bFGF	basic Fibroblast Growth Factor
bHLH	basic helix-loop-helix
Bid	BH3 interacting domain death agonist
BIR	Baculoviral IAP repeat
BSA	Bovine Serum Albumin
CAD	Caspase Activated DNase
CARD	Caspase recruitment domain
Caspase	Cysteinyl-aspartate specific protease
Cdc48	Cell division cycle protein 48 (aka VCP)
CED	Cell death abnormal
CEE	Chick Embryo Extract
CIP	Calf Intestinal Phosphatase
CK2	Casein Kinase 2
DAPI	4',6-diamidino-2-phenylindole
Dcp-1	Death caspase 1
DED	Death effector domain
Diablo	IAP-binding Mitochondrial Protein
DISC	Death inducing signalling complex
DLK-1	Delta-like 1 homolog
DMEM	Dulbecco's Modified Eagle Medium
DMSO	Dimethyl Sulfoxide

DNA	Deoxyribonucleic Acid
Drice	Drosophila interleukin-1-converting enzyme
DSHB	Developmental Studies Hybridoma Bank
DTT	Dithiothreitol
ECM	Extracellular matrix
EDL	Extensor Digitorum Longus
EGL-1	Egg-laying defective
ERK	Extracellular signal-regulated kinase
ESC	Embryonic Stem Cell
EZH2	Enhancer of zeste 2
FACS	Fluorescence-activated cell sorting
FADD	Fas-associated death domain
Fas	Fas cell surface death receptor
FasL	Fas receptor ligand
FBS	Fetal Bovine Serum
FGF	Fibroblast growth factor
FOXO1	Forkhead box O1
Fzd7	Frizzled-7
GAPDH	glyceraldehyde-3-phosphate dehydrogenase
GFP	Green Fluorescent Protein
GST	Glutathione S-Transferase
HIPK2	Homeodomain Interacting Protein Kinase 2
HRP	Horseradish Peroxidase
HtrA2	High Temperature Requirement protein A2
IAP	Inhibitor of apoptosis
ICAD	Inhibitor of caspase-activated DNase
IRES	Internal ribosome entry site
LC-MS/MS	Liquid chromatography-mass spectrometry
LIF	Leukemia inhibitory factor
MAPK	Mitogen-activated protein kinase
MEF2	Myocyte Enhancer Factor 2
MEK	MAPK/ERK Kinase
MHC	Myosin heavy chain

miR/miRNA	Micro-RNA
MKK6	MAP Kinase Kinase 6
MOMP	Mitochondrial outer membrane permeabilization
MRFs	Muscle Regulatory Factors
MRF4	Muscle Regulatory Factor 4
MS	Mass Spectrometry
MST1	Mammalian Sterile Twenty-like kinase
mRNA	Messenger RNA
Myf5	Myogenic factor 5
MyoD	Myoblast determination protein
MyoG	Myogenin
Nek5	NIMA-related kinase 5
Oct4	Octamer-binding protein 4
Pac1	Procaspase 3 activating compound 1
PAGE	Polyacrylamide gel electrophoresis
Par3	Partitioning defective 3
PARP	Poly (ADP-ribose) polymerase
Pax3	Paired-box 3
Pax7	Paired-box 7
PBS	Phosphate-Buffered Saline
PCD	Programmed Cell Death
PCP	Planar cell polarity
PCR	Polymerase chain reaction
PCR2	Polycomb repressive complex
PE	Phycoerythrin
PFA	Paraformaldehyde
PI	Propidium iodide
PKC	Protein Kinase C
PVDF	Polyvinyl Difluoride
qPCR	Quantitative PCR
Raf	Rapidly accelerated fibrosarcoma
RBP-J	Recombination signal binding protein for immunoglobulin kappa J region

Rho	Rhodopsin
RNA	Ribonucleic Acid
ROCK1	Rho-associated, coiled-coil containing protein kinase 1
SEM	Standard error of the mean
Sept4	Septin 4
Sdc4	Syndecan 4
SDS	Sodium dodecyl sulfate
shRNA	Short hairpin RNA
SMAC	Second Mitochondria-derived Activator of Caspase
Sox2	SRY (sex determining region Y)-box 2
STS	Staurosporine
TBBt	Tetrabromobenzotriazole
tBid	Truncated Bid
TBS-T	Tris Buffered Saline with Tween 20
TNFα	Tumor necrosis factor α
UTR	Untranslated region
VCP	Valosin-Containing protien
Wnt	Wingless-iNTegration
XIAP	X-linked inhibitor of apoptosis
Yca1	Yeast Caspase 1
YFP	Yellow florescent protein
YY1	Yin Yang 1
z.DEVD.fmk	N-benzyloxycarbonyl-Asp-Glu-Val-Asp-fluomethylketone

CHAPTER 1

1.0 Introduction

"The scientist is not a person who gives the right answers; he's one who asks the right questions."

— Claude Lévi-Strauss, 1964

1.0 Introduction

In multi-cellular organisms the fate of a proliferating adult stem cell is, for the most part, restricted to divide, differentiate or die. Each of these outcomes holds great importance to the homeostasis of the organism's tissues and organs within which the stem cell resides. Division and replication is imperative for the self-renewal of the stem cell pool, thus ensuring the maintenance of a reserve population of cells, the loss of which is thought to contribute to the process of aging. The majority of these cells will carry out the most important job of differentiating and repairing/regenerating the tissue following injury or disease. This occurs through a complex succession of commitment, expansion (proliferation) and terminal differentiation. Finally, a small portion of these cells must die to prevent cellular overgrowth of abnormal/transformed cells as is seen in the many forms of cancer (Lockshin and Zakeri, 2007). The Megeney lab and others have shown caspases, specifically caspase 3, plays a central role not only in cell death but also in cellular differentiation (Abdul-Ghani and Megeney, 2008; Fernando et al., 2002). In addition, recent work out of the lab has implicated the yeast meta-caspase, Yca1, in regulating cell cycle dynamics (Lee et al., 2008) placing caspases as central regulators of basic cell fate decisions.

Following the work performed in the lab, highlighting a role for caspase 3 during the cellular differentiation of skeletal myoblasts into terminally differentiated muscle, we believe it is reasonable to predict caspase 3 is also playing a role in the differentiation/commitment of the adult stem cells residing in their specialized niche on the muscle fiber, termed satellite cells. Satellite cells are indispensable for the growth and extensive regeneration capacity of post-natal skeletal muscle (Chargé and Rudnicki, 2004). They express a number of distinct and well defined molecular markers including the most commonly used immunohistochemical marker Pax7 (Seale et al., 2000). A loss or defect in satellite cell

function has been attributed to several muscle wasting diseases and muscular dystrophies. This system offers several advantages in which to study adult stem cells due to the wide range of markers available to identify satellite cells throughout the differentiation/self-renewal process and the ability to study these cells within their specialized niche.

This body of work utilized an *ex vivo* model to study the effects of caspase 3 on the self-renewal, proliferation and differentiation of satellite cells associated with single isolated myofibers to investigate our hypothesis that caspase 3 regulates the cell fate decisions of muscle satellite cells.

1.1: Skeletal Muscle Development and Satellite Cell Specification

Skeletal muscle is a complex tissue responsible for all voluntary movement, remaining highly responsive to its systemic milieu. During embryogenesis, skeletal muscle is produced via differentiation and fusion of myoblasts which form a functional syncytium in a process referred to as myogenesis. The proliferation and differentiation of muscle precursor cells is a tightly regulated process during embryogenesis which requires strict temporal and spatial patterning in response to Wnt and FGF (fibroblast growth factor) signalling. All vertebrate skeletal muscle (with the exception of some head muscles) originates from segmented paraxial mesoderm-derived structures in the embryo called somites. Following the formation of embryonic (primary) fibers, and fetal (secondary) fibers, a basal lamina begins to form around each at E13.5 (in the mouse). Subsequently thereafter a subset of progenitor cells exits the cell cycle and the first satellite cells can be identified. These cells are anatomically located in a well-defined niche between the basal lamina and the sarcolemma of the muscle fiber (Mauro, 1961). Satellite cells are maintained in a quiescent state to elicit repair and homeostasis in the adult (Buckingham et al., 2003; Kang and Krauss;

Messina and Cossu, 2009). Embryonic myoblasts, fetal myoblasts and satellite cells have all been shown to have specific features characterizing them as distinct cell populations (Hutcheson et al., 2009). This raises the question of whether they represent a continuum of myogenic differentiation or derive from distinct progenitor populations in the embryo.

During development, myogenesis is regulated by, and dependent on, the expression patterns of two members of the paired-box family of transcription factors, Pax3 and Pax7; corroborated by the complete lack of myogenic progenitors in the dermomyotome region of the *Pax3*$^{-/-}$/*Pax7*$^{-/-}$ double knockout mouse (Relaix et al., 2004). Initially, Pax7 was believed to be the most important factor for satellite cell specification in the adult, as the *Pax7*$^{-/-}$ single mutant mouse lacked apparent satellite cells (Seale et al., 2000). Despite these mice having normal skeletal muscle at birth, they were unable to thrive due to the lack of post-natal muscle growth, particularly in the diaphragm, and quickly succumb to death around 2 weeks of age. Subsequent analysis revealed the Pax7 null mouse possess satellite cells immediately following birth, however, these cells were progressively lost during post-natal growth due to defects in cell cycle regulation and survival, highlighting an important role for Pax7 in satellite cell self-renewal and re-population of the satellite cell niche (Oustanina et al., 2004; Relaix et al., 2006).

Myogenic progenitors in the embryo express additional factors playing functional roles at defined stages of the myogenic program. Most notably is a family of basic helix-loop-helix (bHLH) transcription factors termed myogenic regulatory factors (MRFs), which include MyoD, Myf5, Myogenin and MRF4(Myf6). Ectopic expression of these MRFs in non-myogenic cells, such as fibroblast cell lines, results in their conversion to the muscle lineage (Braun et al., 1989; Davis et al., 1987). Gene targeting has provided great insight into the role of each of the MRFs to delineate their hierarchical framework of regulation. During

the proliferative phase of cell expansion, Pax7 positive progenitors co-express MyoD and Myf5. Mice lacking both MyoD and Myf5 are completely devoid of skeletal muscle and myoblasts, classifying them as myogenic determination factors (Rudnicki et al., 1993). Following exit from the cell cycle, Pax7 is down-regulated, along with Myf5, as expression of myogenin and MRF4(Myf6) is induced, indicative of their role during terminal differentiation (Figure 1). Consistent with this is the complete lack of myofibers in the myogenin knockout mouse, while the number of MyoD positive myogenic progenitors was unaltered (Hasty et al., 1993). Of note, expression of Pax7 and myogenin appear to be mutually exclusive, suggesting they may negatively regulate each other's expression (Olguin and Olwin, 2004). Late stage differentiation is often associated with expression of the structural proteins myosin heavy chain (MHC) and desmin, which provide the structure and contractibility of the resulting muscle fibers. *In vivo*, satellite cells of the adult perform muscle regeneration via sequential activation of the MRFs, allowing for a proliferative phase followed by terminal differentiation/fusion with existing myofibers, recapitulating myoblast function in the embryo.

With the striking phenotype observed in the MyoD/Myf5 double mutant mouse, further studies of the MyoD and the Myf5 single mutant mouse models revealed a redundant role for these two factors during development, yet an essential function for each during adult regeneration. The Myf5 null mouse is born with apparently normal skeletal muscle but die shortly after death due to rib abnormalities (Braun et al., 1992). Similarly, MyoD null mice also appear normal and thrive, likely due to the observed increase in Myf5 expression, yet they are unable to successfully repair muscle following damage (Megeney et al., 1996). With the observation of an increase in the number of satellite cells present in the *MyoD*$^{-/-}$ mice, it

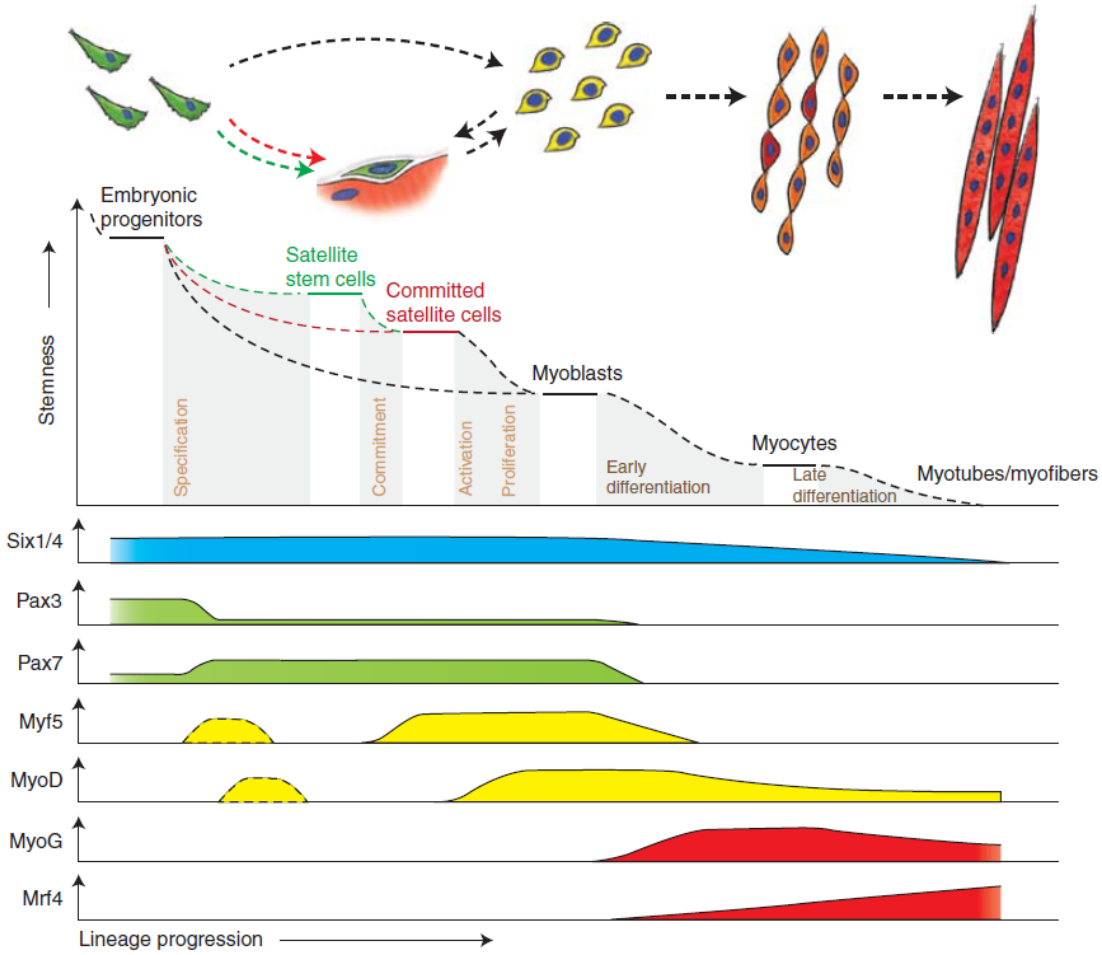

Figure 1: Hierarchy of transcription factors regulating progression through the myogenic lineage. Muscle progenitors that are involved in embryonic muscle differentiation skip the quiescent satellite cell stage and directly become myoblasts. Some progenitors remain as satellite cells in postnatal muscle and form a heterogeneous population of stem and committed cells. Activated committed satellite cells (Myoblasts) can eventually return to the quiescent state. Six1/4 and Pax3/7 are master regulators of early lineage specification, whereas Myf5 and MyoD commit cells to the myogenic program. Expression of the terminal differentiation genes, required for the fusion of myocytes and the formation of myotubes, are performed by both myogenin (MyoG) and MRF4. This figure was originally published in Cold Spring Harbor Perspectives in Biology. Bentzinger, F.C., Wang, Y.X. and Rudnicki, M.A., Building Muscle: Molecular regulations of Myogenesis. Cold Spring Harb Perspect Biol. 2012; 4: a008342 © Cold Spring Harbor Laboratory Press. (Bentzinger et al., 2012)

was hypothesized that these cells had a propensity for self-renewal over differentiation. This is consistent with the notion that a delicate balance between MyoD and Pax7 expression plays a major role in the cell fate decisions of these cells, wherein a lack of MyoD and/or over-expression of Pax7 favours self-renewal and a return to the quiescent state (Chargé and Rudnicki, 2004; Cossu and Biressi, 2005; Sabourin and Rudnicki, 2000).

The absolute requirement for Pax7 in satellite cell self-renewal (and thus an effective regeneration response) has given impetus to further examine its mode of regulation. In this regard, the use of satellite cells have proven indispensable, either as an *ex vivo* model attached to single isolated fibers or *in vitro* as a myogenic cell line. Notch signalling, extensively studied for its role in stem cell self-renewal, has been shown to promote Pax7 transcription (in a RBP-J-dependent manner) and repopulation of the satellite cell niche (Wen et al., 2012). Conversely, Pax7 must be removed from the cell in order for myogenesis and terminal differentiation to occur. Overexpression of Pax7 in satellite cells resulted in a down-regulation in MyoD, cell cycle exit and prevented myogenin expression (Olguin and Olwin, 2004). It is suggested that Pax7 regulates MyoD activity indirectly as a means to inhibit differentiation during the important phase of proliferation (Olguin and Olwin, 2004). When the cell is directed toward terminal differentiation, Pax7 is rapidly downgraded and removed while MyoD is de-repressed allowing it to bind to the promoters of a number of important skeletal muscle specific genes (Olguin and Olwin, 2004; Olguin et al., 2007). This may be, in part, due to MyoD–dependent micro-RNA expression (miR-206 and -486) which are expressed during differentiation and down-regulate Pax7 by directly targeting its 3' UTR (Dey et al., 2011).

Since the identification of Pax7 as a key satellite cell marker additional factors have been found which identify the quiescent satellite cell in resting muscle, such as Syndecan-3,

Syndecan-4 (Cornelison et al., 2001), CD34 (Beauchamp et al., 2000) and integrin α7β1 (Burkin and Kaufman, 1999). Each of which, have been characterized for specific functional roles during skeletal muscle regeneration. Specifically, CD34 has been shown to be essential for efficient entry into proliferation following activation as well as stem cell migration (Alfaro et al., 2011). Understanding the signalling pathways that regulate the balance between opposing myogenic factors is vital to evaluating the cell fate decision of myogenic progenitors and what makes a stem cell divide or differentiate.

1.2: Mechanisms Regulating Satellite Cell Mediated Skeletal Muscle Regeneration/ Repair

Skeletal muscle homeostasis and repair depends on the delicate balance between extrinsic and intrinsic factors and the constant communication of a satellite cell with its niche. Satellite cells, even in the quiescent state, are constantly engaging receptor-mediated signalling pathways to dictate its gene expression and metabolic activity. Upon activation of satellite cells, by either muscle injury or during homeostasis, they exit quiescence, enter the cell cycle and proliferate. Eventually, at around 3-4 days following activation in the mouse, a subset of these cells return to quiescence while the majority differentiate and fuse to form functional myofibers. The question as to whether the decision to return to quiescence (self-renewal) vs. differentiate is intrinsically mediated or extrinsically mediated is currently the topic of extensive research and likely involves cross-talk between the two pathways.

Seminal work using a Myf5-Cre/ROSA-YFP reporter mouse has shown satellite cells use asymmetric divisions for self-renewal, where a genetically upstream Myf5-ve cell can give rise to a Myf5-ve cell and a Myf5+ve cell (Kuang et al., 2007). These Myf5-ve satellite cells make up about 10% of the satellite cell population and are believed to represent a more

"stem-like" population. These cells demonstrate an extensive self-renewal capacity and can repopulate the satellite cell niche in transplantation experiments. In corroboration with this paradigm, the asymmetric co-segregation of DNA strands into different daughter cells has been shown for satellite cells (Rocheteau et al., 2012). The retention of template DNA strands in the "stem cell" is hypothesized to minimise acquisition of DNA mutations which could result in impaired function or tumorigenesis, often referred to as the "immortal DNA strand hypothesis" (Cairns, 2006). It was also noted that committed satellite cells (undergoing symmetric cell division) exhibited random DNA segregation further supporting the notion of a cell intrinsic mechanism of asymmetric cell division in satellite 'stem' cells specifically. Interestingly, the asymmetric division observed in the Myf5/YFP reporter mouse appeared to prefer an apical-basal orientation, relative to the host muscle fiber, with the YFP-ve cell located next to the basal lamina while the YFP+ve cells maintains contact with the plasma membrane of the muscle (Figure 2) (Kuang et al., 2007). This advocates extrinsic influences from its microenvironment and cell-to-cell contact with the muscle fiber may influence this asymmetry. Fittingly, the basal side of the satellite cell expresses the integrin α7β1 receptor which interacts with laminin in the basal lamina while the apical side expresses the adhesion molecule M-cadherin which interacts and binds with the host myofiber (Kuang et al., 2008). It remains to be determined if these signals form the basis for polarity during cell division.

Consistent with the asymmetry of cell surface markers, a variety of signalling molecules have been identified which are critical for muscle regeneration in the adult, a number of which recapitulate embryonic development. Recently, Wnt proteins have emerged as key regulators of satellite cell function mediating the decision between myogenic

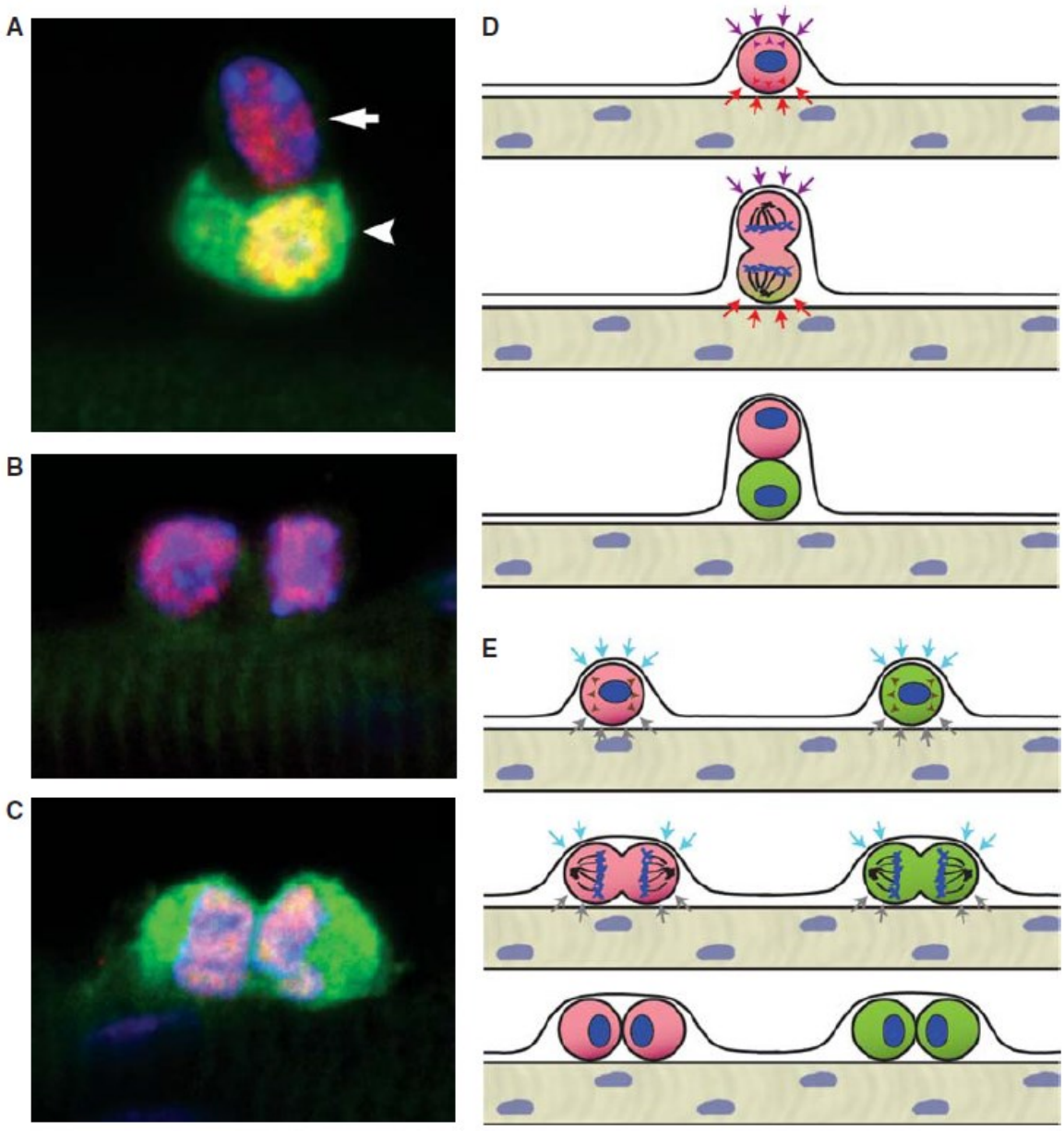
A
B
C
D
E

Figure 2: Asymmetric versus stochastic modes of satellite cell division. As determined by lineage tracing, 10% of adult satellite cells have never expressed Myf5 and are referred to as "satellite stem cells." (A) Satellite stem cells (arrow) undergo asymmetric division in an apical–basal orientation in which the daughter cell that is detached from the basal lamina up-regulates Myf5 and the fluorescent lineage tracer YFP (arrowhead). Pax7 (red); YFP (green); nuclei (blue). (B,C) In the stochastic mode of division, both types of satellite cells divide planar along the host fiber and give rise to two identical daughter cells. (D) Model of apical-basal divisions leading to an asymmetric outcome. Opposing signals from the basal lamina and the myofiber control the orientation of DNA spindles and the asymmetric cosegregation of proteins and DNA strands. Post-cytokinesis, daughter cells continue to be subjected to different signals leading to asymmetric cell fates. (E) Planar divisions lead to the symmetric expansion of cells. Signals such as the Wnt7a–PCP pathway drive the planar orientation of DNA spindles. Daughter cells in this outcome remain attached to the host fiber and the basal lamina, thus receiving similar signals, and maintain identical cell fates. This figure was originally published in Cold Spring Harbor Perspectives in Biology. Bentzinger, F.C., Wang, Y.X. and Rudnicki, M.A., Building Muscle: Molecular regulations of Myogenesis. Cold Spring Harb Perspect Biol. 2012; 4: a008342 © Cold Spring Harbor Laboratory Press.

commitment and self-renewal. One key family member, Wnt7a, is expressed by the regenerating myofiber and signals through the non-canonical planar cell polarity pathway to expand the satellite 'stem' cell population through symmetric cell divisions (Le Grand et al., 2009). On the other hand, Wnt3a has been shown to act through the canonical pathway to promote myoblast differentiation and efficient muscle regeneration (Brack et al., 2008). Interestingly, the manner in which a cell elicits a response to these signals is dependent on the state of the cell along the myogenic hierarchy. Satellite 'stem' cells, for example, have been shown to modulate their own extracellular matrix (ECM) via autologous expression of fibronectin, a ECM glycoprotein, following activation. This stimulates Wnt7a signalling through the syndecan-4 (Sdc4) and Frizzled-7 (Fzd7) co-receptor promoting stem cell expansion (Bentzinger et al., 2013). Although it is clear that Wnts play a major role in mediating extrinsic and intrinsic signalling events, the crosstalk between Wnts and other signalling pathways still needs to be elucidated.

One of the most well studied signalling pathways, which play a dynamic role in satellite cells during the regeneration process, involved the p38 MAPK family. Despite the crucial role of p38 signalling during myogenic differentiation its mechanism of action is still of some debate. Some inconsistencies in the literature may be because the wide range of protein targets is dependent on the cell state (ie. quiescent, proliferating or differentiating) and cell lines used. During satellite cell activation, p38α/β stimulates MyoD expression as cells enter a mitotically active state (Jones et al., 2005). During the first cell division about 12% of cells divide asymmetrically sequestering p38α/β to one daughter cell in a Par-3/PKCλ-dependent manner (Troy et al., 2012). This leaves the other daughter cell devoid of p38α/β activity, and therefore MyoD expression, and remains mitotically inactive after the first cell division (Troy et al., 2012). These cells re-enter a quiescent state to replenish the

satellite cell pool. This is consistent with observations that a defined population of low mitotically active cells are responsible for the majority of satellite cell self-renewal throughout life (Chakkalakal et al., 2014). Whether or not this corresponds to the same Myf5-ve satellite 'stem' cell population previously identified (Kuang et al., 2007) remains to be determined.

During myogenic differentiation TNFα activates p38α/β in an autocrine manner to promote myogenesis through multiple actions (Chen et al., 2007). In this context, p38α/β-mediated phosphorylation of chromatin remodelers EZH2 and (BAF)60 leads to repressive chromatin on the Pax7 promoter (Palacios et al., 2010) and activated chromatin at the myogenin promoter (Simone et al., 2004) respectively. Moreover, phosphorylation of the transcriptional co-activators MEF2 and E47 promotes their binding to MyoD to stimulate transcription of down-stream target genes (Lluis et al., 2005). Conversely, p38γ restricts differentiation to allow for expansion of the transiently amplifying pool of progenitors (Gillespie et al., 2009). Therefore, p38 signalling maintains the balance between quiescence, proliferation and differentiation in satellite cells and a block or misregulation of any of its isoforms results in a defect in muscle repair. Due to its broad spectrum of substrates working towards a similar outcome, p38 MAPKs provide a promising avenue for pharmacological intervention to modulate satellite cell populations.

1.3: Caspase Signalling and Regulation

Caspases are a family of cysteine proteases traditionally studied for their role as conserved cell death proteins. These proteases exist in cells as inactive pro-forms containing a pro-domain, a large subunit and a small subunit, which requires post-translational cleavage to form active enzymes (Nhan et al., 2006). Following cleavage, caspase enzymes form

heterodimers consisting of two large subunits and two small subunits forming a cleavage pocket, which contain the proteolytic cysteine and protein binding domains. Although each caspase is unique in their specificity for substrate binding and cleavage, they all require an aspartic acid in the P1 position (Fuentes-Prior and Salvesen, 2004; Lamkanfi et al., 2007; Nhan et al., 2006). In mammals there are variable numbers of caspases with humans having 13 and mice 12. There is also a degree of inconsistency regarding the nomenclature as human caspase 4 is homologous to murine caspase 11.

Caspases are categorized according to structural organization and cellular function. The first functional grouping is the cytokine activator caspases, comprised of caspase -1, -4, -5, -11 and -12, all of which contain a caspase recruitment domain (CARD) in their large pro-domain (Figure 3). These proteases are required to initiate the pro-inflammatory response through activation of interleukin-1β and interleukin-18 within the cell. The apoptotic initiator caspases form a distinct category and are responsible for activating death pathways through interactions with various signaling partners via oligomerization motifs in their pro-domain. These proteases are further divided into two sub-groups termed extrinsic and intrinsic initiator caspases. The extrinsic initiators (caspase -8 and -10) contain two death effector domains (DED) that allow for binding to cell surface receptors promoting oligomerization of a death inducing signaling complex (DISC), transducing death signals from outside the cell (Figure 4). The intrinsic initiator caspases, (caspase -9 and -2) contain a CARD domain that participates in the formation of a multiprotein complex termed the apoptosome. The formation of the apoptosome occurs in response to stress and genotoxic damage resulting in the depolarization of the outer mitochondrial membrane, leading to efflux of vital mitochondrial proteins such as cytochrome C, which spurs the formation of the tripartite protein complex (via binding to the adaptor protein Apaf-1 and the initiator caspase 9). These

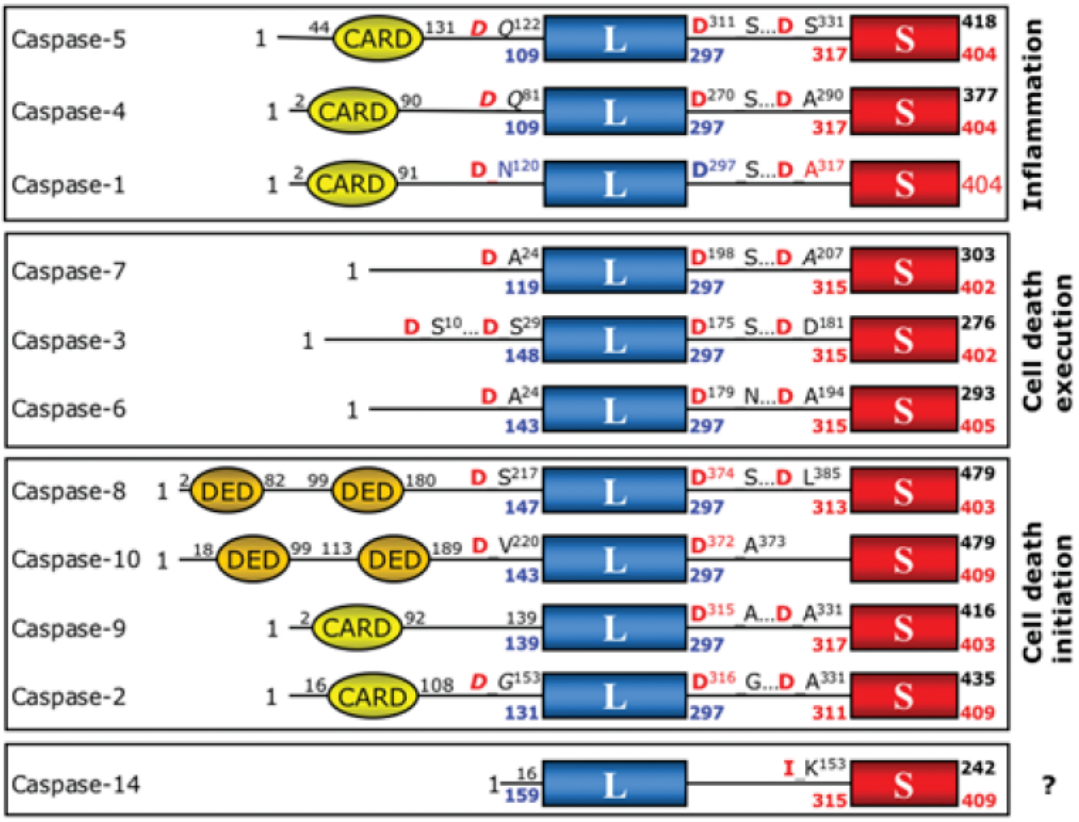

Figure 3: Domain organization of human caspases. Human caspases have been grouped according to their sequence similarities. Notice that sequence identity divides caspases-1 to -10 into three subfamilies, in accordance with the physiological distinction between inflammatory, initiator and effector caspases. In contrast with the widespread distribution of these family members, caspase-14 is found mainly in the epidermis, may be involved in keratinocyte differentiation, and is not activated *in vivo* at an Aspartic acid residue. The positions of maturation cleavage sites are given, with the P1 aspartate residue highlighted in red (in italics in cases where the usage of the site has not been confirmed experimentally). Numberings correspond either to the Swiss-Prot entries (with exception of caspase-10, for which the sequence of the more commonly expressed isoform 10/a is given) or to the caspase-1-based system used throughout this work (colour coded). This figure was originally published in The Biochemical Journal. Fuentes-Prior, P. and Salvesen, GS., The protein structures that shape caspase activity, specificity, activation and inhibition. The Biochemical Journal. 2004; 384(Pt2): 201-32 © the Biochemical Society.

protein complexes, the DISC and the apoptosome, promote the self-activation of the initiator caspases and provide a scaffold to recruit and activate the effector caspases.

The apoptotic effector caspases (caspase -3, -6 and -7) are the convergent point for the intrinsic and extrinsic death signaling cascades and are responsible for the majority of the proteolytic events that mediate the cellular and morphological changes associated with apoptosis. Recent proteomic studies have identified close to 300 protein targets of caspase 3 within a single cell type (Mahrus et al., 2008), confirming the centrality of this enzyme for the proteome wide alterations that occur during programmed cell death. Although caspase 3 activity is the convergent point for several death-signaling pathways, recent observations have implicated this protease in non-death roles such as stem cell self-renewal and differentiation (Abdul-Ghani and Megeney, 2008).

1.3.1: Mechanisms regulating caspase activity

As caspases and programmed cell death (PCD) play a critical role in development and defending against disease, the regulatory milieu provide a favourable avenue for intervention. The most well studied regulators are the Inhibitors of Apoptosis (IAPs). These are a family of E3 ubiquitin ligases which act as key signalling intermediates, participating in a wide array of cellular functions. Mammalian IAPs (IAP1, IAP2 and XIAP; X-linked inhibitor of apoptosis) were characterized for their ability to restrict the cell death machinery due to their BIR (baculoviral IAP repeat) domain which mediates protein-protein interactions, facilitating their ability to bind and inhibit caspases (Berthelet and Dubrez, 2013).

As an additional level of regulation, mammals also contain a number of IAP agonists; Smac/Diablo, Omi/HtrA2 and ARTS. During activation of the intrinsic cell death pathway,

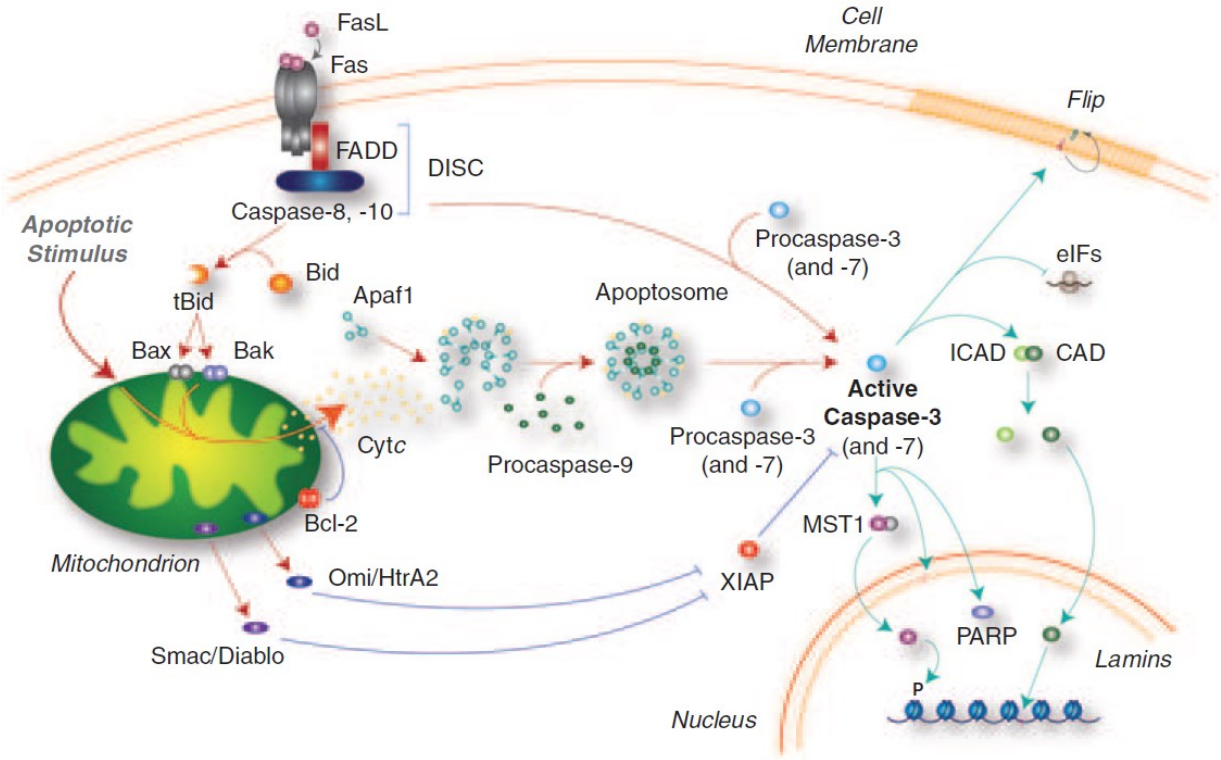
FasL
Fas
Cell Membrane
Flip
FADD
DISC
Caspase-8, -10
Apoptotic Stimulus
Procaspase-3 (and -7)
eIFs
Bid
tBid
Apaf1
Apoptosome
Bax
Bak
ICAD
CAD
Active Caspase-3 (and -7)
Cytc
Procaspase-9
Procaspase-3 (and -7)
MST1
Bcl-2
Mitochondrion
Omi/HtrA2
XIAP
PARP
Lamins
Smac/Diablo
P
Nucleus

Figure 4: Intrinsic and extrinsic pathways of caspase activation in mammals. Activation of executioner caspases-3 and -7 is the key event in mammalian apoptosis, and two major mechanisms exist to carry out this task. The intrinsic pathway involves the mitochondrion, which acts as an intracellular death receptor receiving a variety of proapoptotic signals that trigger oligomerization of proapoptotic proteins (Bcl-2-associated protein, Bax, and Bcl-2-antagonist killer, Bak, to produce mitochondrial outer membrane permeabilization, MOMP). This leads to the release of cytochrome C, which activates Apaf1, induction of apoptosome formation, procaspase-9 recruitment/ activation and direct processing and activation of procaspase-3 and -7. In the extrinsic pathway, Fas receptor ligand (FasL) triggers the membrane-bound Death-Inducing Signaling Complex (DISC), which recruits procasapase-8 and activates caspase-3 directly. In some cell types, caspase-8 can also cleave Bid to form tBid, which interacts with Bax/Bak to trigger MOMP, cytochrome C release and apoptosome formation. The activation of caspase-3 and -7 is antagonized by IAPs, which in turn can be inhibited by Smac/Diablo and Omi/HtrA2. Activation of caspase-3 and -7 orchestrates the demolition of the cell by cleavage of specific substrates, such as ICAD, Rho effector ROCK1, kinase MST1, PARP, transcription and translation initiation factors. Figure reprinted by permission from Macmillan Publishers Ltd: Cell Death and Differentiation D'Amelio, M., Cavallucci, V. and Cecconi, F. Neuronal caspase-3 signalling: not only cell death. Cell Death and Differentiation 17: 1104-14 © 2010.

mitochondrial outer membrane permeabilization (MOMP) results in Smac/Diablo and ARTS being released into the cytosol alongside cytochrome C. Smac/Diablo binds the BIR domain of IAP1/2 and XIAP interfering with their ability to bind caspases, as well as promoting the auto-ubiquitination/degradation in the case of IAP1 and IAP2 (Yang and Du, 2004). Due to their efficiency at engaging the cell death machinery, small molecules which mimic the inhibitory effects of Smac/Diablo (SMAC mimetics) are currently in clinical trials for their ability to kill death-resistant tumor cells (Bai et al., 2014; Beug et al., 2014).

In a similar fashion, ARTS binds and inhibits XIAP resulting in activation of caspase 9 and 3 (Mandel-Gutfreund et al., 2011). ARTS is produced from an internal splice site in the Sept4 gene (Larisch et al., 2000). Although it contains no canonical IAP binding domains it depends on a stretch of 27 amino acids residing in its unique C-terminal to bind XIAP (Gottfried et al., 2004). Despite little being known about this unusual IAP agonist, its importance is highlighted by evidence that shRNA mediated knockdown of ARTS blocks release of both Smac/Diablo and cytochrome C (Edison et al., 2012), suggesting ARTS itself is an upstream regulator of apoptotic induction in response to MOMP. The Sept4/ARTS-deficient mouse exhibits increased tumor incidence and an increase in the number of hematopoietic stem/progenitor cells (Garcia-Fernandez et al., 2010). This phenotype is exacerbated by combined inactivation of XIAP, suggesting ARTS may act as a tumor suppressor specifically through its role as an IAP agonist. The use of ARTS-based drugs to promote apoptosis in cancer, however, has yet to be tested. As we continue to uncover the diverse cellular outcomes that occur in response to caspase signalling it will be evermore important to identify and study the mechanisms by which they are regulated. With caspase activation, in the absence of cytochrome C release, being a key step in cellular differentiation (Murray et al., 2008) it will be interesting to see how the IAPs and IAP agonists play a role

in mediating an apoptotic response vs. a cell differentiation response. A requirement for Sept4/ARTS in regulating sperm terminal differentiation in mice (Kissel et al., 2005) confirms the requisite to study these agonists outside the context of apoptosis induction.

In addition to regulating the activity of caspases directly, a body of evidence is emerging implicating a number of proteins which bind to caspase substrates mediating the susceptibility of these targets to cleavage. This occurs by either binding the target, preventing caspases from subsequent binding (Ribeil et al., 2007), or via post-translational modification of the protein target modulating the ability of caspases to recognize/cleave the aspartic acid residue. With regard to the latter, caspase 3 and the CK2 kinase have been shown to share an overlapping recognition motif in targeted substrates (Duncan et al., 2011). CK2 phosphorylation of a wide range of proteins prevents cleavage by caspase 3, a biochemical event that extends even to pro-caspase 3 itself (Duncan et al., 2010). Specifically, CK2 phosphorylation has been implicated in mediating protein stability of the transcription factors, YY1 (Riman et al., 2012) and Pax3 (Iyengar et al., 2012), as well as the Pax3-FOXO translocation mutant, whose overexpression is responsible for the rare cancer, aveolar rhabdomyosarcoma (ARMS) (Dietz et al., 2011). Although this reciprocal relationship was only examined in conditions of apoptosis, one may envision this rheostat mechanism being directed to control caspase activity and drive non-death outcomes.

1.3.2: Evolutionary origin of caspase proteins. Non-death functions were an early adaptation of caspase/metacaspase like enzymes

It is suggested that caspase and PCD pathways co-evolved from a single cell ancestor, common to all multicellular eukaryotes. Indication of a conserved pathway for cell death was first gleaned from studies in the simple nematode *Caenorhabditis elegans.* Genetic

and biochemical evidence established a linear pathway of apoptotic induction in which there is only one caspase, CED-3 (Yuan et al., 1993). In response to a death signal EGL-1 is actively transcribed and acts as an antagonist against the anti-apoptotic protein CED-9. Under homeostatic conditions, CED-9 is bound to the adaptor protein CED-4. Once CED-4 is released from CED-9, CED-4 oligomerises and activates CED-3, which carries out the proteolysis typified of programmed cell death (Conradt and Horvitz, 1998) (Figure 5). In more complex organisms, the apoptotic program evolved additional modes of regulation, whereby multiple caspase enzymes interact in a coordinated signaling pathway (as previously discussed). This basic signal relationship emerged from the study of two key model systems, the fruit fly (*Drosophila melanogaster*) and the common mouse (*Mus musculus*). These diverse species share a remarkable number of functional orthologs with *C. elegans*, as well as each other, indicating these protein interactions evolved early as a requisite for normal development (Figure 5).

Ultimately, the discovery of caspase homologues in single-cell species, termed metacaspases (Uren et al., 2000), has provided support for the basic contention that PCD evolved from an ancient function in early eukaryotic organisms. Indeed, forced expression and activation of these caspase homologues has been shown to yield a PCD like phenotype in various model systems such as *Saccharomyces cerevisiae* (Madeo et al., 2002), suggesting that PCD is an ancient and conserved cell fate. Several prokaryotes, including various bacterial species, have now been shown to exhibit PCD in response to environmental stresses (Aizenman et al., 1996; Hazan et al., 2004) and during biofilm development (Asally et al., 2012; Bayles, 2007). Numerous hypotheses have been posited to rationalize PCD in single cell organisms, prominent among which is altruistic sacrifice of the individual cell for colony

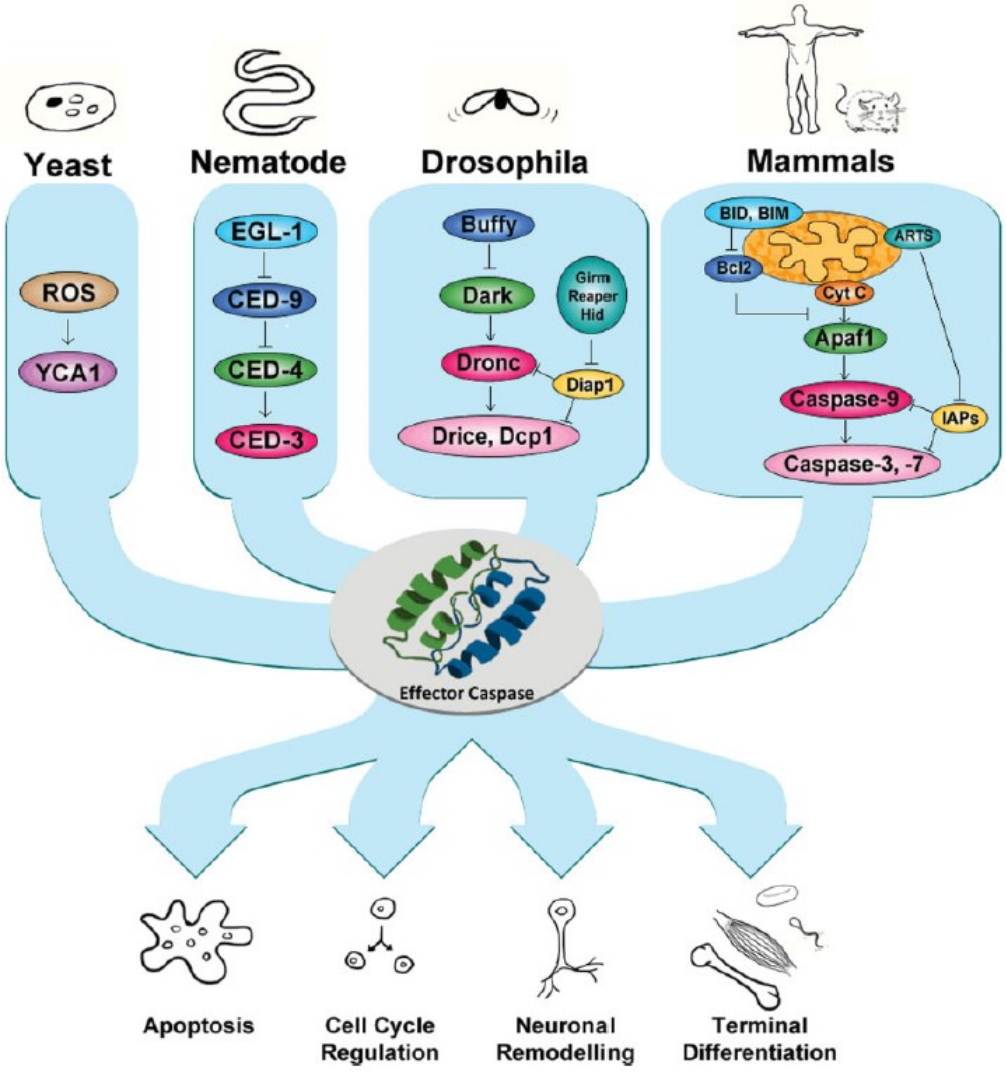
Yeast
Nematode
Drosophila
Mammals
ROS
YCA1
EGL-1
CED-9
CED-4
CED-3
Buffy
Dark
Grim
Reaper
Hid
Dronc
Diap1
Drice, Dcp1
BID, BIM
ARTS
Bcl2
Cyt C
Apaf1
Caspase-9
IAPs
Caspase-3, -7
Effector Caspase
Apoptosis
Cell Cycle
Regulation
Neuronal
Remodelling
Terminal
Differentiation

Figure 5: Conservation of the molecular pathway of caspase activation across the major species studied and its divergent physiological roles. Caspase 3 and caspase 7 in mammals, and Drice and Dcp1 in Drosophila, are classified as effector caspases. CED-3 in the nematode C. elegans functions as both the initiator and effector caspase. Effector caspases dictate diverse cell fates including apoptosis, cell cycle regulation, neuronal remodelling and terminal differentiation of a number of different cell types. The sole metacaspase in the yeast, *S. cerevisiae*, Yca1, functions similarly to an effector protease, and has been implicated in yeast apoptosis, cell cycle regulation and proteostasis. Functional homologs found within each species are indicated by the same colour. This figure was originally published in the journal Bioessays. Dick, S.A. and Megeney, L.A. Cell death proteins: An evolutionary role in cellular adaptation before the advent of apoptosis. *Bioessays* 35(11): 974-83

benefit (Duszenko et al., 2006; Frohlich and Madeo, 2000; Okasha, 2005; West et al., 2007): a reasonable notion given the clonal nature of such cellular communities. Within this context, two arguments are commonly put forth to support the evolution of PCD from a single cell organism. For example, PCD represents an efficient mechanism to remove otherwise damaged or aged cells from the population (Fabrizio and Longo, 2008; Gomes et al., 2008; Vachova and Palkova, 2005). In turn, self-sacrifice via PCD would act to provide nutrient supply for neighboring cells, maximizing population dynamism (Fabrizio et al., 2004; Mai-Prochnow et al., 2006; Segovia et al., 2003).

Despite the obvious theoretical appeal for an entrenched biochemical pathway devoted to inducing PCD, the utility of such a process in single cell organisms is not without controversy. Foremost in the argument against an exclusive evolved PCD pathway is the simple observation that there is no evolutionary advantage for PCD in a single cell entity. Cell death defies the basic precept of maintaining and replicating life; therefore the retention of an exclusive PCD pathway would be subject to strong negative selection pressures over the evolutionary timescale that would be required to entrench this cell fate. To rationalize this contradiction, we propose the hypothesis that apoptotic or death-centric proteins evolved from a primordial non-death role in the cell (Dick and Megeney, 2013). The corollary to this premise is that PCD is a process that evolved via co-option or co-evolution from a cohort of essential proteins with canonical functions unrelated to cell death (Dick and Megeney, 2013).

A non-death origin for apoptotic proteins and pathways is not a conventional perspective in the field. Indeed, while reviews over the preceding decade have highlighted the broad role of these biochemical cascades including non-death outcomes, the general consensus remains that any physiologic function is ancillary to the core death role (as reviewed in (Bozhkov et al., 2010; Galluzzi et al., 2012; Lamkanfi et al., 2007)). To support

the premise that the constituent proteins of PCD evolved from a non-death role in single cell organisms, it is essential to identify a corresponding physiologic activity (if any) for these proteins. A series of observations in the yeast model *S. cerevisiae,* provided the first robust evidence that apoptotic/PCD proteins in single cell life forms retain core non-death functions. Here, Lee *et al.* demonstrated that yeast strains with a genetic deletion of the single metacaspase Yca1, or expressing a catalytically inactive mutant strain of Yca1 (where the catalytic cysteine residue was mutated to an alanine) displayed significant reduction in cell growth/cell fitness (Lee et al., 2008). Both Yca1 mutant strains were characterized by a slower G1/S transition, and a failure to respond to reagents that induce G2/M checkpoint (Lee et al., 2008). In a subsequent study, Lee *et al.* characterized the precise molecular role for Yca1. Using a series of complimentary proteomic screens, these investigators noted that 1) Yca1 formed robust physical interactions with proteins that control basic proteostasis functions, including protein folding and aggregate control, and 2) that loss of Yca1 led to accumulation of vaculor structures and protein aggregates during cell cycle progression and heat stress (Lee et al., 2010). These results confirm that the core molecular function of Yca1 is to limit protein aggregation within the cell, rather than to promote cell death per se. In support of this notion, Yca1 overexpression resulted in decreased accumulation of unfolded proteins and an increase in the life span of *S. cerevisiae* (Hill et al., 2014). The observation that Yca1 has a positive rather than a negative effect on life span corroborates an evolutionary role for caspases as an integrated part of the protective response to help cells minimize the effects of toxic stress and cellular aging caused by the accumulation of misfolded protein.

These observations do not exclude a role for Yca1 in PCD, and suggest that such a role may have been derived from the general aggregate targeting capacity of the protease.

Indeed, one may envision conditions in the cell whereby unrestrained activation of Yca1 would lead to widespread protein aggregate disassembly, active inhibition of protein aggregate formation or limiting the formation of vital multi-protein structures, all changes that are not conducive for basic cell survival/function (Shrestha et al., 2013). The inescapable conclusion is that the PCD capacity of Yca1 may simply be the result of re-purposing a protein rather than *de novo* evolution of a death specific factor. Indeed, the very concept that Yca1 manages physiologic cell death is weakened by the observation that apoptosis in multicellular yeast structures occurs independent of Yca1 activity (Vachova and Palkova, 2005).

Lastly, a recent study in yeast supports the contention that the metacaspase/caspase targeting of insoluble aggregates may have a relevant bearing on a human disease (Shrestha et al., 2013). Here, Yca1 was observed to form a strong physical association with Cdc48, a protein that modifies protein aggregation. Loss of Yca1 led to a dramatic reduction in the recruitment of Cdc48 to the insoluble protein fraction, concurrent with increased aggregate formation (Shrestha et al., 2013). Cdc48 is the homologue of the human AAA^{+} ATPase VCP, and substitution mutations in VCP have been shown to give rise to a progressive form of damaging protein aggregation (Inclusion Body Myopathy with Pagets Disease of the Bone and Frontotemporal Dementia) (Kobayashi et al., 2007). How mutations in VCP give rise to progressive aggregate formation remains unknown; nonetheless, impaired recruitment of a caspase/disaggregase would be consistent with this disease etiology.

1.4: Caspases as Cell Fate Modulators

There is a predilection for regarding the non-death related function of caspases and PCD pathways as aberrant or recent adaptations of a core death activity (Fuchs and Steller,

2011). The wealth of data collected from single and multicellular organisms refute this core argument and suggest that PCD proteins evolved as general determinants of cell adaptation and cell fate. The new interpretation of PCD protein biology raises a number of critical questions. First, what is the range of physiologic functions (independent of cell death) that are attributed to caspase activity? Second, what are the constraints and factors that direct these proteins to engage death versus non-death outcomes?

1.4.1: Non-death roles of caspase proteases

As mentioned, elegant studies in yeast have provided support for the hypothesis that PCD proteins evolved from a non-death cellular function. However, the initial support for the hypothesis that PCD proteins retain conserved non-death functions were gleaned from observations involving complex cell types of vertebrate and invertebrate animals. Early studies using lens fiber epithelial cells (Ishizaki et al., 1998) and erythrocytes (Zermati et al., 2001) demonstrated that caspase 3 was essential for the differentiation of these cell types. The role of caspase 3 in these cell lineages was interpreted to simply be an attenuated form of apoptosis, as the differentiation program in each of these cell lineages is characterized by nuclei removal and dissolution akin to PCD. However, this death centric view of caspase function was challenged with the publication of three landmark papers. First, Fernando *et al.* reported that caspase 3 activation was essential for the differentiation and formation of murine skeletal muscle (Fernando et al., 2002). Loss of caspase 3 activity through peptide inhibition, or via the generation of caspase 3 null mice, led to a drastic reduction in the endogenous differentiation capacity of skeletal muscle progenitor cells. While skeletal muscle differentiation shares phenotypic characteristics of apoptosis, myofibers are long lived cell types that retain their nuclei in a functional syncytium. Next, Sordet *et al.*

demonstrated that the differentiation of monocytes into macrophages was dependent on the activity of a number of caspase proteases (Sordet et al., 2002), again macrophages being cell types that retain their nuclei and defy simple characterization as an attenuated apoptotic cell. Finally, a study examining *Drosophila* spermatid maturation, provided compelling evidence for a conserved non-death role of the intrinsic cell death pathway (Arama et al., 2003). Spermatid individualization, the final step in sperm development, is characterized by chromatin condensation along with bulk removal of the majority of cytoplasm and alterations in cytoarchitecture. Closer examination of this process revealed that Apaf-1 and cytochrome C, as well as the effector caspase Drice, were active during spermatid differentiation (Arama et al., 2003). Drice activity was initially restricted to the cytoplasmic bulge, known as the individualization complex, then traveled along the length of the elongated spermatid removing the bulk of the cytoplasm, a spatial and temporal regulation of caspase activity that was essential for maturation of the developing sperm.

Building on these initial observations, a plethora of studies have confirmed the requirement of PCD proteins for cell differentiation in general. To date, transient activation of caspase-mediated signaling has been found to be indispensable for the differentiation of the various hematopoietic cell lineages (Janzen et al., 2008), epithelial derivatives (Weber and Menko, 2005), skeletal muscle (Fernando et al., 2002; Larsen et al., 2010; Murray et al., 2008), neural progenitors (Fernando et al., 2005), cardiac myocytes (Abdul-Ghani et al., 2011), osteogenic derivatives (Miura et al., 2004) and embryonic stem cells (Fujita et al., 2008). This caspase dependent control of cell differentiation is also broadly conserved, having been demonstrated in vertebrate (zebrafish (Popgeorgiev et al., 2011), murine, human) and invertebrate (*Drosophila*) cells. This degree of conservation may also extend to the penultimate enzymatic step associated with PCD, caspase-directed genome wide DNA

damage. The differentiation of skeletal muscle myoblasts is characterized by genome wide DNA strand breaks (Larsen et al., 2010), a phenomenon that is essential for the differentiation program and has been demonstrated to be mediated by caspase 3 activation of caspase activated DNase (CAD). Most interesting is the degree to which the intrinsic PCD pathway is conserved in its entirety for the induction of these various differentiation programs. As noted above, this complete pathway conservation was initially demonstrated in *Drosophila* spermatid maturation (Arama et al., 2003), then corroborated in the study of differentiation in lens fiber epithelial cells (Weber and Menko, 2005), skeletal muscle myoblasts (Murray et al., 2008) and neural progenitor cells (Ohsawa et al., 2010). In an ironic twist, the intrinsic PCD pathway has also been implicated in the promotion of cell differentiation in *C. elegans* (Pinan-Lucarre et al., 2012): *C. elegans* was the pivotal model used to discover and construct the biochemical relationships that constitute caspase mediated PCD. CED-3, along with the cognate activator CED-4, acts in a calcium dependent manner to promote efficient regeneration initiation in part via the kinase DLK-1 and dependent on CED-3 protease activity (Pinan-Lucarre et al., 2012). Both the rate and extent of new outgrowth were dramatically reduced in CED-3 null nematodes, indicating defects in early filopodia extension. This phenotype was also observed in CED-4 null as well as the CED-3/CED-4 double mutants (Pinan-Lucarre et al., 2012), again highlighting the conservation of the intrinsic PCD pathway in a non-death cell fate.

In addition to cell death and differentiation, caspase proteases have also emerged as critical regulatory factors in neuronal adaptation. At the cellular level, the proteolytic activity of caspase 3 has been found to be indispensable for synaptic plasticity by regulating the formation and retraction of axonal projections and dendrites (reviewed in (D'Amelio et al., 2012). At the organ level, caspase 3 activity has been shown to be vital for memory,

learning, and consolidation, remarkable tasks for a protein that is often considered to be the primary mediator of PCD.

1.4.2: Constraints and factors that direct non-death outcomes

The available evidence suggests that altering the timing, duration or intensity of flux through PCD signalling pathways and proteins is a definitive step in directing divergent cell fates. The differentiation of lens fiber epithelial cells has provided an excellent model in this regard; demonstrating that cell differentiation was associated with intrinsic PCD pathway activation, accompanied by elevated expression of caspase inhibitory proteins (from the IAP family) (Weber and Menko, 2005). In contrast, cells displayed excessive levels of caspase activation during apoptosis, a level that was sufficient to overcome the threshold provided by the IAP content. PCD pathway selection of cell fate may also depend on reinforcing feedback loops between caspase proteases. Caspase 3 has been shown to cleavage-activate caspase 9, thus propagating the signal, during apoptosis (Fujita et al., 2001). Furthermore, cleavage of the caspase 7 ortholog, Dcp1, activates the caspase 3 ortholog, Drice, but not vice versa (Florentin and Arama, 2012). Despite having overlapping target sequences, Drice and Dcp1 have very different affinities for the same death-associated targets and Dcp1 is very inefficient at inducing cell death (Florentin and Arama, 2012). Post-translation modification of caspase enzymes may also provide a rapid and convenient mechanism for a cell to guide PCD pathways to divergent outcomes. Fbox proteins that mediate degradation of caspase inhibitory proteins and stimulate proteasome activation have been demonstrated to modify the Drice/caspase 3 activity during Drosophila spermatid differentiation (Bader et al., 2010; Bader et al., 2011). Despite an enormous amount of interest in recent years implicating

caspase 3 as a key player in cell fate decision making, the mechanism by which caspase activity can give rise to such diverse fates is just beginning to be examined.

1.4.3: Caspases and the cell death machinery during skeletal muscle differentiation

As previously noted, work from the Megeney lab has revealed caspase 3 activity is required for skeletal muscle differentiation (Fernando et al., 2002). Importantly, this study demonstrated that both inhibition and homologous deletion of caspase 3 resulted in the reduction of myoblast fusion and myotube formation. The mechanism of action, by which caspase 3 mediates differentiation in this context appears to share some protein substrates with the apoptotic pathway, as well as substrates that appear unique to differentiation. In the inaugural study, Fernando *et. al*. identified Mammalian Sterile Twenty-like kinase (MST1) as a crucial effector, being cleavage-activated by caspase 3. MST1 has been described to act upstream of kinases such as MKK6 and members of the p38 MAPK family (Graves et al., 2001). Transfection of primary myoblasts derived from caspase 3 null mice with active MST1 rescued the differentiation deficit, resulting in the formation of multi-nucleated myotubes (Fernando et al., 2002). Additional caspase substrates have been identified which promote myogenesis including inhibitor of caspase-activated DNase (ICAD) (Larsen et al., 2010), Nek5 (Shimizu and Sawasaki, 2013) and HIPK2 (de la Vega et al., 2013). The diversity of caspase substrates in this context highlights the role for this protease as an essential mediator of the differentiation program.

Interestingly, a number of upstream apoptotic inductive proteins have also been shown to play a role in skeletal muscle differentiation, confirming conservation of the prototypical PCD pathway in directing cell fate outcomes. Coordinating caspase 3 activation, caspase 9 and the intrinsic pathway protein Bcl-xL have been identified as key regulators of

myoblast differentiation (Murray et al., 2008). Caspase 9 itself is negatively regulated by the cytokine LIF (leukemia inhibitory factor) in proliferating myogenic progenitors, likely as a result of direct phosphorylation (an inhibition) via ERK (extracellular signal-regulated kinase) (Hunt et al., 2011). Furthermore, the myogenic marker Pax3, expressed in proliferating muscle progenitors, is a transcriptional regulator of the anti-apoptotic proteins Bcl-2 and Bcl-xL. MyoD dependent loss of Pax3 expression, via miR-1 and miR-206, results in a down-regulation of these factors and an increase in caspase activation (Hirai et al., 2010). The death receptor-mediated (extrinsic) pathway of caspase activation also participates in the regulation of satellite cell fate through FADD (Fas-associated death domain) phosphorylation (Cheng et al., 2014). C-terminal phosphorylation of FADD in a subset of satellite cells results in an increase in Pax7 and M-cadherin expression, suppression of myogenin and desmin and induced a phase of reversible cell cycle arrest indicating a propensity for self-renewal (Cheng et al., 2014). This ability of FADD to direct cell fate determination is mediated by its ability to modulate the Notch signaling pathway. Together, these observations suggest that the same strict regulations that impinge upon caspase activity in a death context are also maintained to regulate skeletal muscle differentiation. The factors that direct an activated satellite cell to self-renew versus initiate myogenesis are not fully defined, yet a reasonable hypothesis would envision that acquisition of these divergent cell fates requires a mutually exclusive molecular milieu.

1.4.4: Caspases as mediators of stem cell self-renewal

A probable mechanism that may influence satellite cell fate choice is the restricted deployment of directed proteolysis. The caspase 3 protease has been demonstrated to control cell fate determination independent of inducing cell death (Abdul-Ghani and Megeney,

2008). Transient activation of caspase 3 is essential for differentiation to occur across a broad range of lineage restricted progenitor cells (Dick and Megeney, 2013). The question remains as to whether this occurs directly, by engaging factors which promote the differentiation program, or indirectly, by limiting self-renewal, creating a permissive state for additional differentiation factors to act. Previous observations identifying a number of caspase substrates during differentiation provide a rationale for both occurring simultaneously. This is supported by the fact that caspases have the ability to target and cleave a wide number of protein substrates which could act in concert with each other to direct cell fate. However, complete mapping of caspase targets in a given cell type, in response to a given stimuli, would be required to gain a better understanding of this process.

With regards to stem cell self-renewal, caspase 3 has been observed to limit self-renewal of embryonic stem cells through direct proteolysis and inactivation of the key pluripotency factor Nanog (Fujita et al., 2008). Embryonic stem cells have a cell autonomous ability to self-renew due to their auto-regulatory circuit of pluripotency factors Oct4, Sox2 and Nanog (Boyer et al., 2005). However, they maintain the ability to rapidly differentiation down a specific lineage in response to developmental cues via post-transcriptional modification of core transcription factors. Caspase 3 mediated cleavage of Nanog allows embryonic stem cells to rapidly escape the constraints of their self-renewal machinery and further suppresses expression of other pluripotency factors, including Oct4 (Fujita et al., 2008). Additionally, caspase 3 has been implicated in negatively regulating cell cycle entry in primitive hematopoietic stem cells, leading to increased stem cell populations in the caspase 3 null mouse model (Janzen et al., 2008). Caspase 3 alters signal transduction in these cells by limiting activation of the Ras-Raf-MEK-ERK pathway, thus modulating the cytokine responsiveness required to maintain stem cell self-renewal and quiescence (Janzen

et al., 2008). It is still unclear whether the differentiation delay observed in caspase 3 null hematopoietic stem cells is due to the accumulation of self-renewal factors or an inability to activate differentiation factors. Further examination into the caspase 3 targets in this cell type will help elucidate these questions. In skeletal muscle myoblasts, caspase 3 directs a differentiation specific gene expression program by activating the caspase responsive DNase CAD. Once active, CAD reprograms the genome through targeted DNA damage/strand break events leading to P21 expression and cell cycle exit (Larsen et al., 2010). Together this data supports a novel role for proteases as central to the process regulating the stem cell compartment.

Here we examined whether limitation of satellite cell self-renewal was dependent on caspase 3 targeted cleavage of the transcription factor Pax7. Pax7 has been reported to regulate distinct panels of genes that promote proliferation and antagonize myogenic differentiation, a function that is consistent with maintaining the satellite cell niche (Soleimani et al., 2012). As such, the reduction or removal of Pax7 may denote a key prerequisite for satellite cells to abandon self-renewal and acquire differentiation competence. How the activated satellite cells retains or eliminates Pax7 protein activity remains unknown.

1.5: Hypothesis / Aims

Previous observations from our lab implicating caspase 3 in proper differentiation of skeletal muscle myoblasts, as well as work from other groups suggesting a role for caspases in stem cell maintenance, provide a critical rationale to further investigate whether caspase 3 activity alters muscle stem cell self-renewal. This work will greatly contribute to establishing a role for caspase 3 in skeletal muscle development and also to our overall understanding of satellite stem cell regulation. In order to approach this question we have outlined the following hypothesis and aims:

Hypothesis: Caspase 3 regulates the cell fate decisions of muscle satellite cells.

Aim 1: Examine the functional role of caspase 3 in activated fiber associated satellite cells

Aim 2: Determine how caspase 3 is affecting Pax7 protein levels

Aim 3: Determine the mechanisms regulating caspase 3 activity during myogenesis

We noted that inhibition of caspase 3 activity leads to the accumulation of Pax7 protein and expansion of the satellite cell self-renewing compartment. Conversely, small molecule stimulation of caspase 3 depletes Pax7 protein and results in a down-regulation of Pax7 target genes. Moreover, the ability of caspase 3 to target Pax7 is subject to an additional regulatory control via CK2. Here, quiescent and self-renewing satellite cells maintain elevated CK2 activity, which phosphorylates Pax7 and prevents caspase mediated degradation of Pax7. Together these results demonstrate that caspase cleavage of Pax7 is an early and essential step to limit satellite cell self-renewal, thereby establishing a cellular environment that is permissive for muscle differentiation.

CHAPTER 2

Materials and Methods

Single Fiber Isolation and Immunocytochemistry

Single muscle fibers were isolated from the EDL of 6-8 week old C57/B6 mice and cultured in floating conditions in Fiber Media (DMEM, 20% FBS, 2% CEE) as previously described (Kuang et al., 2007; Pasut et al., 2013). Fibers were fixed with 4% PFA at the indicated times and blocked using goat blocking buffer (5% goat serum; 2% BSA; 0.2% Triton; 1% NaAzide in 1xPBS) and incubated in primary antibody (Rabbit anti-Active-Caspase 3, Cell Signalling; Rabbit anti-Active-Caspase 7, SantaCruz; Rabbit anti-CK2α, Abcam; Mouse anti-Pax7, Developmental Studies Hybridoma Bank (DSHB); Rabbit anti-MyoD, SantaCruz; Rabbit anti-Syn4, Abcam) overnight at 4^{o}C followed by incubation with secondary antibody (Goat anti-Mouse 594 or Goat anti-Rabbit 488; AlexaFlour) and counterstained with DAPI. For analysis of satellite 'stem' cells the Myf5-Cre/ROSA-YFP mice were obtained from Dr. Michael Rudnicki and used for fiber isolation. Fibers were stained with Mouse anti-Pax7 (DSHB) and Goat anti-GFP(FITC) (Abcam).

For small molecule inhibitor treatments fiber cultures were plated in 6 well dishes and treated at T=0 with DMSO as a control and either z.DEVD.fmk (20 μM, BioVision) or TBBt (50 μM, Calbiochem). Fibers were plated on coverslips and the number of cells expressing each marker was counted. Data for 30-40 fibers/treatment were pooled and expressed as a percent of the total number of cells or as fold change relative to DMSO negative control. The average from 4 independent experiments were measured and expressed as +/- SEM (2400-3200 cells/treatment, N=4). Significance was considered $p \leq 0.05$ as determined by unpaired one-tailed student t-test.

Satellite Cell Primary Cultures

Primary myoblasts were isolated as previously described (Fernando et al., 2002) from 4 week old SV129 mice. Hind limb muscle was isolated and washed in PBS + 1% Pen/Strep followed by manual homogenization and incubation with Collagenase/Dispase solution (10% 100 mg/ml collagenase; 20% 12 mg/ml Dispase; 2.5% 100 mM $CaCl_2$ in DMEM) at 37^oC for 30 min. The muscle slurry was filtered with a netrix filter and cells were pelleted at 1,000 RPM (300xg). Cells were either pre-plated on plastic for 1 hour and immediately put into culture or processed for FACS purification as previously described (Pasut et al., 2012). FACS purification was used to isolate a highly pure population of satellite cells eliminating the need for pre-plating to remove fibroblasts and other contaminating cell types. Briefly, cell pellets were resuspended in 1 ml isolation media (10 mM Hepes, 2% FBS in DMEM) and incubated with mouse anti-α7-integrin for 15 min at room temperature followed by a wash step and incubation with IgG1-mouse 647, Hoechst and PE conjugated Sca-1, CD45, CD31 and CD11 for 15 min at 4^oC. Cells were washed, filtered and sorted using a BeckmanCoulter MoFlo XDP (StemCore Laboratories, Ottawa) gaiting for α7 positive and PE negative. Isolated satellite cells were then placed into culture and allowed to expand for down-stream studies.

Primary myoblasts and FACS sorted satellite cells were maintained in growth media (HAM F10 media, 20% FBS, 1% Pen/Strep, 1% heperin, 2.5 ng/µl bFGF) and induced to differentiate in low serum conditions (2% horse serum, 1% Pen/Strep in DMEM) in the presence of either DMSO or z.DEVD.fmk (20 µM; BioVision). Drug was refreshed after 24 hourss differentiation. Cell pellets were collected at indicated times for Immunoblotting or

RT-qPCR. Alternatively, cells were treated with TBBt (50 μM, Calbiochem) or staurosporine (STS) (1 μM, Sigma) in growth media for the indicated times.

Immunoblotting

Cell lysates were obtained by incubation of cell pellets with lysis buffer (0.05 M Hepes-NaOH, pH 7.5; 0.15 M NaCl; 10% (vol/vol) glycerol, 1% (vol/vol) Tx-100; 1 mM EGTA; 1.5 mM $MgCl_2$; 20 mM NaF; 10 mM sodium pyrophosphate) supplemented with protease inhibitors (4 mM Sodium Vanadate; 200 μM PMSF; 7.5 μg/mL Aprotonin; 7.5 μg/mL Pepstatin; 7.5 μg/mL Leupeptin) and incubated at 4^{o}C for 1 hour followed by centrifugation at 20,800xg for 10 min. Protein (50-100 μg) was separated by SDS/PAGE and transferred to PVDF membranes. Membranes were blocked with 5% (wt/vol) non-fat powdered milk in TBS-T (10 mM Tris, pH 7.4; 150 mM NaCl; 0.05% Tween-20), and incubated with primary antibody [mouse anti-Pax7 (Developmental Studies Hybridoma Bank); Rabbit anti-cleaved-caspase3 (Cell Signalling); mouse anti-β-tubulin (clone E7; Developmental Studies Hybridoma Bank); Mouse anti-MF20, Myosin Heavy Chain (MHC) (Developmental Studies Hybridoma Bank)] overnight at 4^{o}C followed by incubation with HRP-conjugated secondary antibody (goat anti-mouse or goat anti-rabbit, BioRad). The ECL detection kit (GE Healthcare) was used to detect protein expression. Relative densitometry was measured using ImageJ software, values were normalised to a tubulin loading control and expressed relative to growth (T=0).

Protein Expression and Purification

C-terminally 3xFLAG-tagged Pax7 was expressed using the baculovirus system as in (Kawabe et al., 2012). Pax7(WT), previously cloned into the pFastBac™1 vector (using EcoRI/XbaI), was used to produce single point mutations using site-directed mutagenesis. PCR was performed using primers containing the mutated nucleotide sequence corresponding to a single amino acid change (Table 1). The resultant vectors were then transformed into chemically competent E. coli (DH5α) for large scale production. Aliquots of the transformed E. coli were collected for miniprep isolation of the plasmid DNA and sequencing to confirm the mutation. Three to six individual clones were picked per mutation and sent for sequencing (Applied Biosystems 3730 DNA Analyzer, StemCore Laboratories). Sequencing data was analyzed using the Chromas software and one clone was selected for down-stream protein production. To produce double mutants, site-directed mutagenesis was performed on vectors containing the single mutation using the corresponding primer to induce the second mutation. Recombinant baculoviruses were generated using the Bac-to-Bac system (Invitrogen) and infected into Sf9 cells. Cells were lysed and pre-cleared by incubation with protein G sepharose (GE healthcare life science) at 4^{o}C for 30 min. Recombinant protein was purified using anti-FLAG M2-agarose beads (Sigma) at 4^{o}C for 3hrs and eluted by addition of 500 mM 3xFLAG peptide (Sigma). The purity of the eluted fractions was analyzed by SDS-PAGE followed by coommasie blue staining.

Table 1: Primers used for site-directed mutagenesis and cloning of Pax7 protein

Pax7 Primer		
D187A		5'-GCCAAACACAGCATCGCTG GCATCC-3'
D202A		5'-GAACCCGCCCTCCCCCTGAA-3'
D208A		5'-TGATTCCACAGCTGAGCCCTCATCC-3'
N-Term	FW	5'-ATAGGATCCACCATGGCGGCGCTGCCCGGC-3'
	RV	5'-TGTGCTCGAGATCTGAGCCCTCATCCAGACGGTT-3'
C-Term	FW	5'-ATAGGATCCACCATGGACCTCCCCCTGAAGCGCAA-3'
	RV	5'-TGTGCTCGAGGTAGGCTTGTCCCGTTTC-3'

***In Vitro* Cleavage Assay**

Recombinant Pax7 protein (100-300 ng) and recombinant active-caspase 3 or recombinant active-Caspase 7 (0.5 µg, Chemicon) were incubated for 0.5-8 hours in cleavage assay buffer (50mM Hepes, pH 7.5; 0.1 M NaCl; 10% glycerol; 0.1% Chaps; 10 mM DTT) containing either DMSO or z.DEVD.fmk (20 µM, BioVision) as indicated. Reactions were incubated at 37^{o}C and stopped by addition of running buffer and subjected to SDS-PAGE. Western blot analysis was performed using αPax7 as described.

To assess the cleavage of dephosphorylated Pax7, recombinant Pax7 (600 ng) was treated with 5 units Alkaline Phosphatase, Calf Intestinal (CIP) for 1 hour at 37^{o}C (or buffer lacking the phosphatase enzyme, in which case Pax7 remained partially phosphorylated). Aliquots were subsequently incubated with recombinant active-Caspase 3 (0.5 µg) as described. Reactions were subjected to SDS-PAGE and western blot analysis.

Bioinformatics Analysis of Pax7 Protein

To evaluate the Pax7 protein for caspase 3 cleavage sites we acquired the mouse a.a. sequence from the NCBI database and compared this to other closely related species using BLAST2 software. For help with cloning, site-directed mutagenesis and primer design we utilized the ApE software (A plasmid Editor © Wayne Davis).

Cloning of Pax7 Fragments and Retrovirus Production

To determine functionality of the Pax7 fragments Pax7(FL), N-Term [a.a. 1-208] and C-Term [a.a. 202-503] cDNA was cloned into the BamH1 and Xho1 sites of pHIT4-IRES-eGFP vector (for primers see Table 1). The resultant vectors were then transformed into chemically competent E. coli (DH5α) for large scale production. Aliquots of the transformed E. coli were collected for miniprep isolation of the plasmid DNA and sequencing to conform the mutation. Three to six individual clones were picked per mutation and sent for sequencing (Applied Biosystems 3730 DNA Analyzer, StemCore Laboratories, Ottawa). Sequencing data was analyzed using the Chromas software and one clone was selected for down-stream analysis.

Retrovirus was produced using the Phoenix helper-free retrovirus producer line PHX ECO (Stanford University). These cells were created by placing into 293T cells constructs capable of producing gag-pol and envelope (viral packaging) proteins for ecotropic viruses. PHX ECO cells were transfected at ~80% confluency using calcium phosphate mediated transfection for 16 hours, followed by washing in PBS and maintained in growth media (DMEM, 20% FBS and 1% Pen/Strep). 48 hours later, the virus containing media was removed from the cells, filtered using a 0.45 μm filter and supplemented with an additional

20% FBS. Virus was added to primary myoblasts cells maintained in growth conditions at ~60% confluency at a concentration of 50% overnight (50% virus media; 50% myoblast growth media; 1:1,000 5 mg/ml polybrene). The following day media was replaced with fresh myoblast growth media and cells split when they reach 80% confluent. At 4 days post-infection, primary myoblasts were trypsinized and prepared for FACS analysis to sort for GFP+ve cells containing the pHIT4 vector (gaiting for PE and GFP using a BeckmanCoulter MoFlo XDP, StemCore Laboratories, Ottawa). Cells which exhibited a side scatter positive for GFP were collected. This step was necessary to enhance the effect seen by over-expressing the Pax7 fragments as the transfection efficiency alone was very low (~4%). These cells were allowed to recover in culture and expand until enough GFP+ve cells were available for RNA isolation and qPCR analysis (as previously described).

Luciferase Assay

To measure the activity of the Pax7 fragments the previously mentioned N-terminal and C-terminal Pax7 pHIT4 expression vectors were used for luciferase assay. COS cells were seeded onto 48-well plates (0.7×10^5 cells per well), the following day cells were transfected using Lipofectamine 2000 (Invitrogen), SF Opti-MEMα (Gibco), 25 ng of internal *Renilla* luciferase internal control, 300ng of Firefly luciferase reporter DNA (*Myf5-57.5kb* enhancer in pGL4 vector, (Kawabe et al., 2012)) and 200ng of activator DNA containing either Pax7(FL), N-Term or C-Term for 8hrs at 37^{o}C with 5% CO_2. The reporter plasmids and the VP16-Pax7 were a gift from Dr. Michael Rudnicki (For a list of plasmids see Table 2). Luciferase activity was measured by using the Dual Luciferase Assay System per manufacturer's instructions (Promega). Luciferase values were normalized to *Renilla* luciferase internal control and empty pHIT4 vector.

Table 2: Description of plasmids used in luciferase assay

Activator Plasmids	
PHIT	pHIT4 Empty Vector, Negative Control
VP16--Pax7	Positive Control
Pax7	Full Length Protein in pHIT4
N-Term	a.a. 1-208 of Pax7 in pHIT4
C-Term	a.a. 208-503 of Pax7 in pHIT4

Reporter Plasmids	
PGL4	Empty Vector Negative Control
Myf5-57.5	in PGL4

Primary Myoblasts Viability

To evaluate primary myoblast viability following treatment with procaspase 3 activating compound 1 (Pac1; BioVision) (24 hours; 0 μM, 12.5 μM, 25 μM, 50 μM, 75 μM, 100 μM; dissolved in DMSO) propidium iodide (PI) in combination with flow cytometry was used. Following treatment, growth media was collected for identification of detached cells in culture and the attached cells were harvested with 1x trypsin and diluted in 1x PBS solution. Suspended and adherent cells were combined and pelleted by centrifugation at 250xg for 5 min. Cell pellet was washed and resuspended in 1mL 1x PBS solution. Incubation with PI (1 mg/mL) for 5 min at 4^{o}C was followed by analysis of PI-positive cells

by flow cytometry using 488-nm excitation and 617-nm emission (MoFlo instrument; Beckman Coulter). Analysis was conducted using Summit version 4.3 software.

Caspase 3-specific Small Molecule Activation

To examine the differentiation inducing capabilities of caspase 3 activation, primary myoblasts were incubated with Pac1 (25 μM or 50 μM dissolved in DMSO) for 24 hours in growth media. DMSO alone was used as a vehicle negative control and differentiation media (2% horse serum, 1% PS in DMEM; 24 hours) was used as a positive control. Cells were harvested by incubation with 1x trypsin and pelleted by centrifugation at 250xg for 5 min. Cell pellets were then processed for mRNA or protein lysate isolation.

To examine the cell fate inducing capabilities of caspase 3 activation, single isolated fibers were placed in activation media (15% FBS, 2% CEE in DMEM) for 48 hours. PAC1 (25 μM, 50 μM) or DMSO alone was added to media and left for an additional 24 hours. Fibers were collected 72 hours post-isolation for immunocytochemistry analysis as previously described. Fibers were plated on coverslips and the number of cells expressing each marker was counted. Data for 30-40 fibers/treatment were pooled and expressed as a percent of the total number of cells. The average from 4 independent experiments were measured and expressed as +/- SEM (2400-3200 cells/treatment, N=4). Significance was considered $p \leq 0.05$ as determined by unpaired one-tailed student t-test.

RNA isolation and qPCR

RNA was isolated from cell pellets using the RNeasy Mini Kit (Qiagen) with on-column DNase digestion followed by reverse transcription using the iScript cDNA synthesis

Kit (BioRad) using 1 µg of RNA. cDNA was then subjected to qPCR analysis using SYBR® Green Supermix (BioRad) in a Eco™ Real-Time PCR system (Illumina). QPCR primers (Table 3) were either previously published or designed using Primer-BLAST (NCBI). Gene expression was analysed using $\Delta\Delta C_T$ method and Eco™ Software v4.1.2, values were normalized to GAPDH.

Table 3: Primer pairs used for qPCR

Gene		qPCR Primer
Myf5	FW	5'-CACCTCCAACTGCTCTGACG-3'
	RV	5'-CTCGGATGGCTCTGTAGACG-3'
MyoD	FW	5'-GCGCAACGCCATCCGCTAC-3'
	RV	5'-TCGACACAGCCGCACTCTTCC-3'
Myogenin	FW	5'-AGCAGGGAGGGTTTAAATGG-3'
	RV	5'-GTCCCCAGTCCCTTTTCTTC-3'
Mef2C	FW	5'-GGCAGCAAGAACACGATGCCA-3'
	RV	5'-AAGCTCCCAACTGACTGAGGGCAG-3'
P21	FW	5'-TGTCCAATCCTGGTGATGTCC-3'
	RV	5'-TCAGACACCAGAGTGCAAGAC-3'
Pax7	FW	5'-GACGACGAGGAAGGAGAGAA-3'
	RV	5'-ACATCTGAGCCCTCATCCAG-3'
MHC	FW	5'-ACCTTGCCAAGAAGAAGGACTCCA-3'
	RV	5'-TGGATGCGGATGAACTTGCCAAAC-3'
GAPDH	FW	5'-TGACTCCACTCACGGCAAATTCAA-3'
	RV	5'-TGCCTGCTTCACCACCTTCTTGAT-3'

Kinase Assay

Recombinant Pax7 (100 ng) was incubated with purified GST-CK2 (0.1 µg/µl; obtained as a gift from Dr. Litchfield) and either DMSO or TBBt (50 µM, Calbiochem) in kinase buffer (50 mM Tris, pH 7.5; 150 mM NaCl; 11.25 mM $MgCl_2$, 0.075 mM ATP) containing γ^{32}P-ATP (0.04 µCi/µl) for 1 hour at 30^{o}C. Aliquots were subjected to SDS-PAGE and autoradiography. For pre-treatment prior to caspase 3 cleavage GST-CK2 (0.1 µg/µl) was incubated with Pax7 (100 ng) in kinase buffer containing cold ATP (0.075 mM) for 1 hour at 30^{o}C. Aliquots were subsequently subjected to caspase 3 cleavage and immunoblot analysis as previously described.

Mass Spectrometry

To confirm caspase 3 cleavage of Pax7 protein an *in vitro* cleavage reaction, performed as previously described, was subjected to SDS-PAGE followed by silver stain using Silver Nitrate. The protein bands corresponding to the cleavage fragments were excised and processed for LC-MS/MS via trypsin digest (OHRI Proteomics Core Facility, Ottawa). The results were analyzed by MASCOT and the identified peptides were mapped to either the N-Terminus or the C-Terminus of the Pax7 protein sequence.

To identify the site at which caspase 3 cleaves the Pax7 protein the cleavage reaction mixes were directly reduced using dithiothreitol, akylated using iodoacetamide and divided into 3 aliquots which were digested with trypsin, chymotrypsin and GluC respectively. A portion of the peptide digests were mixed and then processed for LC-MS/MS. MASCOT 2.3.01 software (Matrix Science, UK) was used to match the acquired mass spectral data against a custom database comprised of mouse sequences in SwissProt (2011_07 version of

uniprot_sprot.fasta.gz from ftp.uniprot.org) concatenated with a database of common contaminants (Contaminant db downloaded from maxquant.org, downloaded june 9th 2011). Data set was queried for Pax7 peptides produced via a cleavage following an aspartic acid (D) residue.

To identify the serine residue phosphorylated via CK2, recombinant Pax7 (600 ng) was treated with 5 units Alkaline Phosphatase, Calf Intestinal (CIP) for 1hr at 37^{o}C. Aliquots were subsequently incubated with GST-CK2 (0.1 µg/µl) (or buffer only) in a cold kinase assay, as previously described. Recombinant protein was subjected to SDS-PAGE and silver stained, +CK2 and –CK2 bands were isolated and processed for LC-MS/MS. MASCOT software version 2.4 (Matrix Science) was used to infer peptide and protein identities from the mass spectra. Phosphorylation of serine or threonine, oxidation of methionine, carbamidomethylation of cysteine, protein N-terminal acetylation, deamidation, and conversion of glutamate or glutamine to pyro-glutamate were allowed as variable modifications.

Statistical Analysis

All data are expressed as mean +/- SEM. The student *t* test was used for comparisons between treatments, with $p \leq 0.05$ considered significant.

CHAPTER 3

Caspase 3 is Required for Commitment of Satellite Cells to Differentiation

3.1: Caspase 3 is active during myogenic differentiation

During the early stages of myoblast differentiation (12-24 hours post low-serum induction) low-levels of transient caspase 3 activity is observed using a flourometric assay of cell lysate (Fernando et al., 2002). Initial examination of the expression of active-caspase 3 in cultured myogenic cells revealed an increase in active(cleaved)-caspase 3 during early stages of differentiation, as previously reported. This activation appeared to be tightly regulated with punctate foci observable at 24hrs following differentiation (2% HS; Figure 6A). In contrast, caspase 3 activity present following 24hrs treatment with low levels of Staurosporine (STS) appeared brighter and cytoplasmic.

To address the role of caspase 3 activity in satellite cell function we isolated single muscle fibers from juvenile mice and performed immunofluorescence for active caspase 3. Isolated and cultured myofibers provide an amenable model that accurately reconstructs the transition of satellite cells from quiescence to activation/early cell divisions, with well-defined temporal kinetics (T=0 post culture, quiescence; T=48hrs post culture, early activation; and T=72hrs full activation) recapitulate *in vivo* regeneration of a damaged muscle fiber (Zammit et al., 2004). In this system, the first division of satellite cells occurs between 24 and 48 hours post-isolation (Siegel et al., 2011). Subsequently, satellite cells rapidly divide with an average cycling time of 10 hours (Siegel et al., 2011) producing large clusters of cells residing adjacent to the myofiber. By about 72 hours post-isolation a majority of these cells will have begun the differentiation process by down-regulating expression of Pax7 while a small number are fated for self-renewal, indicative of their high-levels of Pax7 expression and loss of MyoD expression.

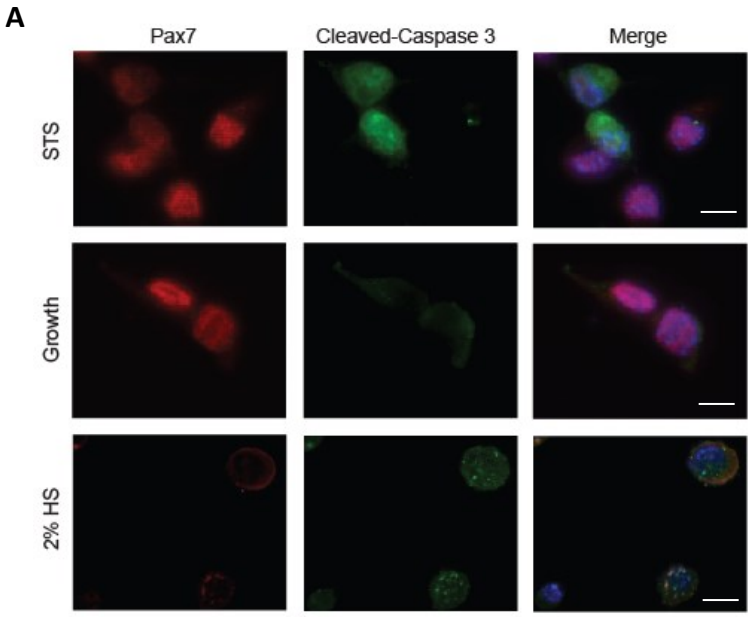
A
Pax7
Cleaved-Caspase 3
Merge
STS
Growth
2% HS

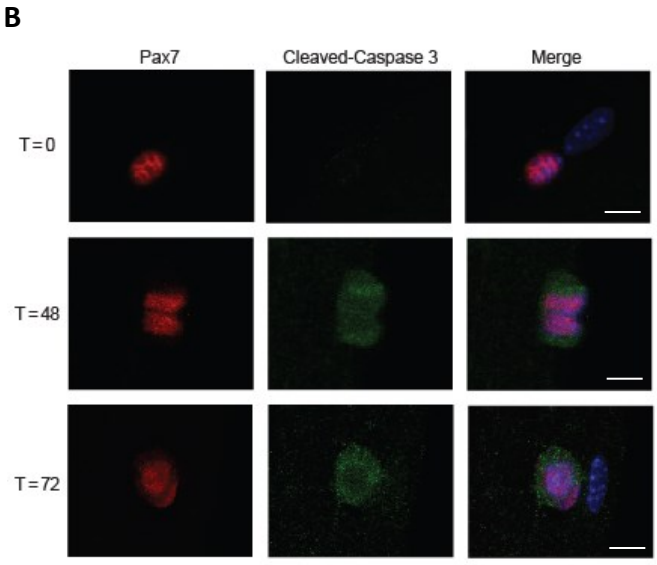
B
Pax7
Cleaved-Caspase 3
Merge
T=0
T=48
T=72

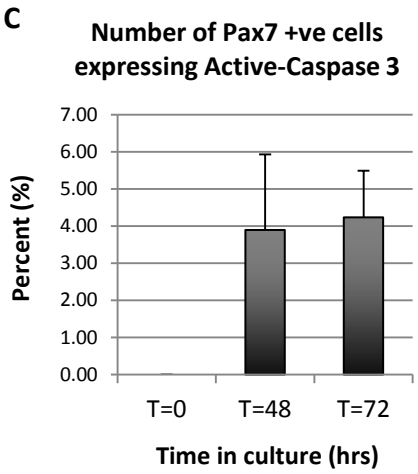
C
Number of Pax7 +ve cells expressing Active-Caspase 3
Percent (%)
7.00
6.00
5.00
4.00
3.00
2.00
1.00
0.00
T=0
T=48
T=72
Time in culture (hrs)

Figure 6 – Active caspase 3 is present in activated satellite cells. (A) FACS purified satellite cells were cultured in growth media and either induced to undergo apoptosis (STS) or differentiate (2% HS) for 24hrs. Immunoflorescence analysis showed active (cleaved)-caspase 3 (green) was present in both STS and 2% HS treated cells which were low or absent for Pax7 expression (red). (B) Single fibers were isolated from the EDL of juvenile mice cultured for the indicated times in growth media. Active (cleaved)-caspase 3 (green) was observed in Pax7 positive (red) fiber associated satellite cells at 48 and 72 hours following isolation at a low frequency, quantified in (C). No active caspase 3 signal was observed at time 0 in quiescent satellite cells. Scale bars are 10μm.

Satellite cells showed low-level expression of cleaved-caspase 3 in a subset of activated fiber associated satellite cells (Figure 6B). Examination at different time points following single fiber isolation showed a low frequency of active-caspase 3 expression at 48 (3.9%) and 72 (4.2%) hours post-isolation in Pax7 positive satellite cells (Figure 6C). Based on the transient nature of caspase 3 activity during a non-death phenomenon, compared to prolonged and constant activity during cell death, we predict low prevalence of active-caspase 3 in Pax7 satellite cells when fixed at a given moment in time. No caspase 3 activity was observed immediately following fiber isolation at the 0 hour time point when cells are viewed in their quiescent state, confirming a role for caspase 3 in activated satellite cells.

3.2: The role of Caspase 3 during Satellite cell activation

To address the function of caspase 3 in satellite cell activation and self-renewal, isolated myofibers were incubated with a cell permeable caspase 3 specific peptide inhibitor (20μM, z.DEVD.fmk) and assessed for markers of self-renewal (Pax7) vs. commitment to differentiation (MyoD). Sustained Pax7 expression in the absence of myogenic markers is indicative of the self-renewing population (Olguin and Olwin, 2004). Alternatively, satellite cells with down-regulation of Pax7 and up-regulation of the transcription factors MyoD and myogenin are considered to be a cell population committed to differentiation. Satellite cells expressing both Pax7 and MyoD are understood to be committed cells that remain in a proliferative state. Inactivation of caspase 3 resulted in a significant increase in the number of Pax7+/MyoD- satellite cells on fibers (34.85±3.13% in treated versus 15.74±4.61% in control conditions) (Figure 7A, B). The total number of satellite cells per fiber did not

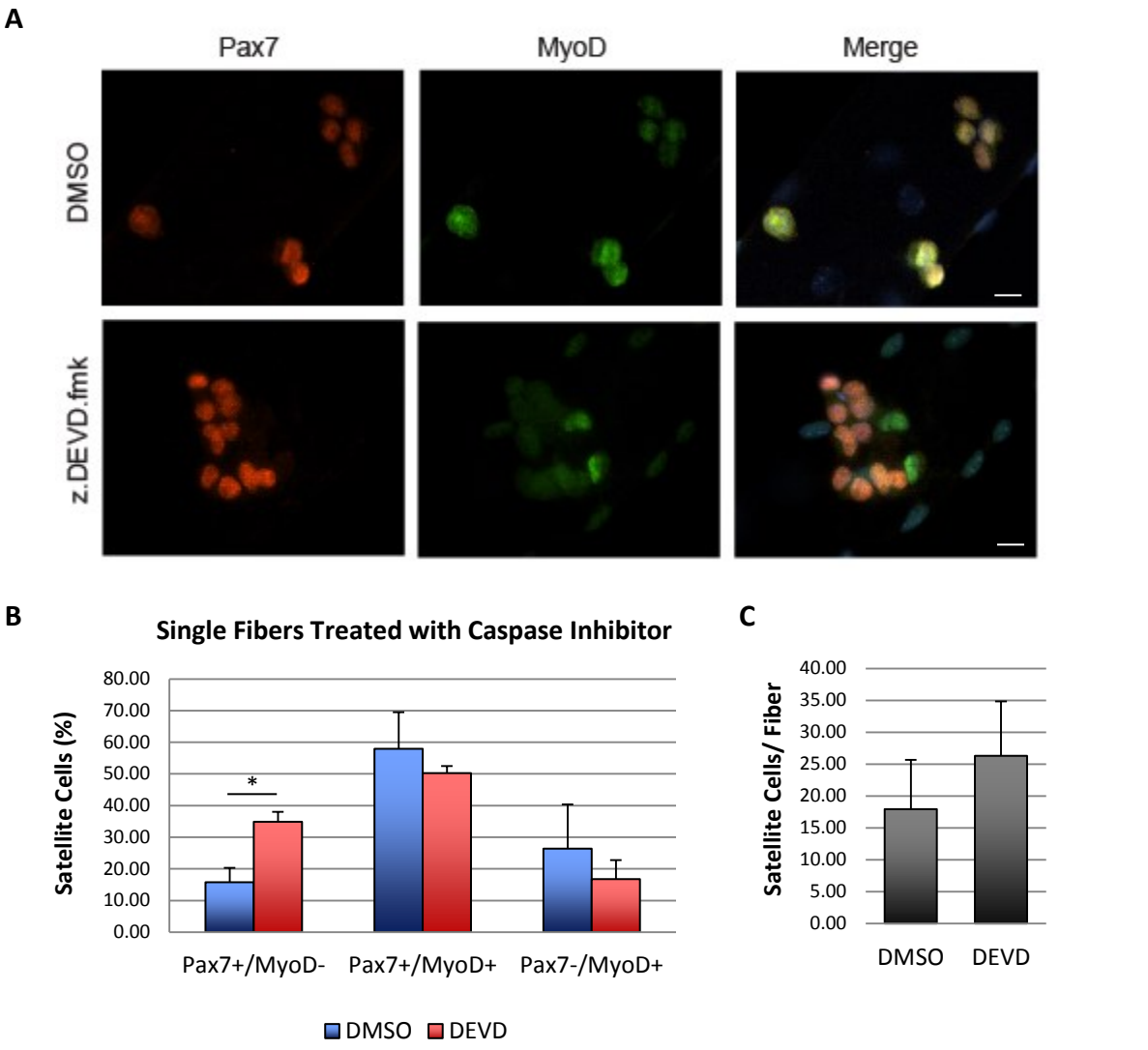

Figure 7 - Caspase 3 activity is required during early satellite cell fate decisions. (A) Single fibers were isolated from juvenile mice and cultured in 20μM z.DEVD.fmk (bottom) or DMSO (top; control) for 72 hours, fixed and stained with Pax7 (red) and MyoD (green). (B) Quantification of the number of satellite cells expressing each marker expressed as a percentage of the total number of satellite cells (+/- SEM). (C) Quantification of total number of satellite cells per fiber (+/- SEM). *$p<0.05$ unpaired student t-test. Scale bars are 10 μM.

change with caspase 3 inhibition (Figure 7C), confirming that caspase activation in the activated satellite cell population impacts the self-renewal process rather than influencing cell death/cell survival per se.

Published work out of Dr. Rudnicki's lab demonstrates the use of a Myf5-cre reporter mouse to identify a new population of satellite cells that express Pax7 and reside in the satellite cell niche, however at no time in their development had ever expressed the myogenic marker Myf5. These are now generally recognized as the hierarchical subpopulation of stem cells that has not yet been committed to muscle differentiation and are hypothesized to be more pluripotent then their Myf5+ daughters (Kuang and Rudnicki, 2008). During satellite cell activation Myf5- cells divide either symmetrically to give rise to two daughter cells or asymmetrically to produce one Myf5- stem cell and one Myf5+ committed muscle progenitor (Kuang et al., 2007). To test if caspase 3 inhibition has an effect on the regulation of Myf5+ commitment within these cells, we analyzed this population at 72 hours post fiber isolation as previously described. We found no significant differences in the number of uncommitted Myf5- satellite cells indicating caspase 3 is acting downstream of this cell fate decision (Figure 8A, B). A significant decrease in the differentiating Myf5+/Pax7- population was observed confirming a role for caspase 3 in satellite cell differentiation. We did not observe any changes in the total number of satellite cells per fiber (Figure 8C). These results, along with the experiments looking at Pax7/MyoD expression, indicate caspase 3 affects the decision of a satellite cell to either differentiate or return to quiescence for future rounds of regeneration but not the decision to commit to the myogenic lineage from a Pax7+/Myf5- stem cell population.

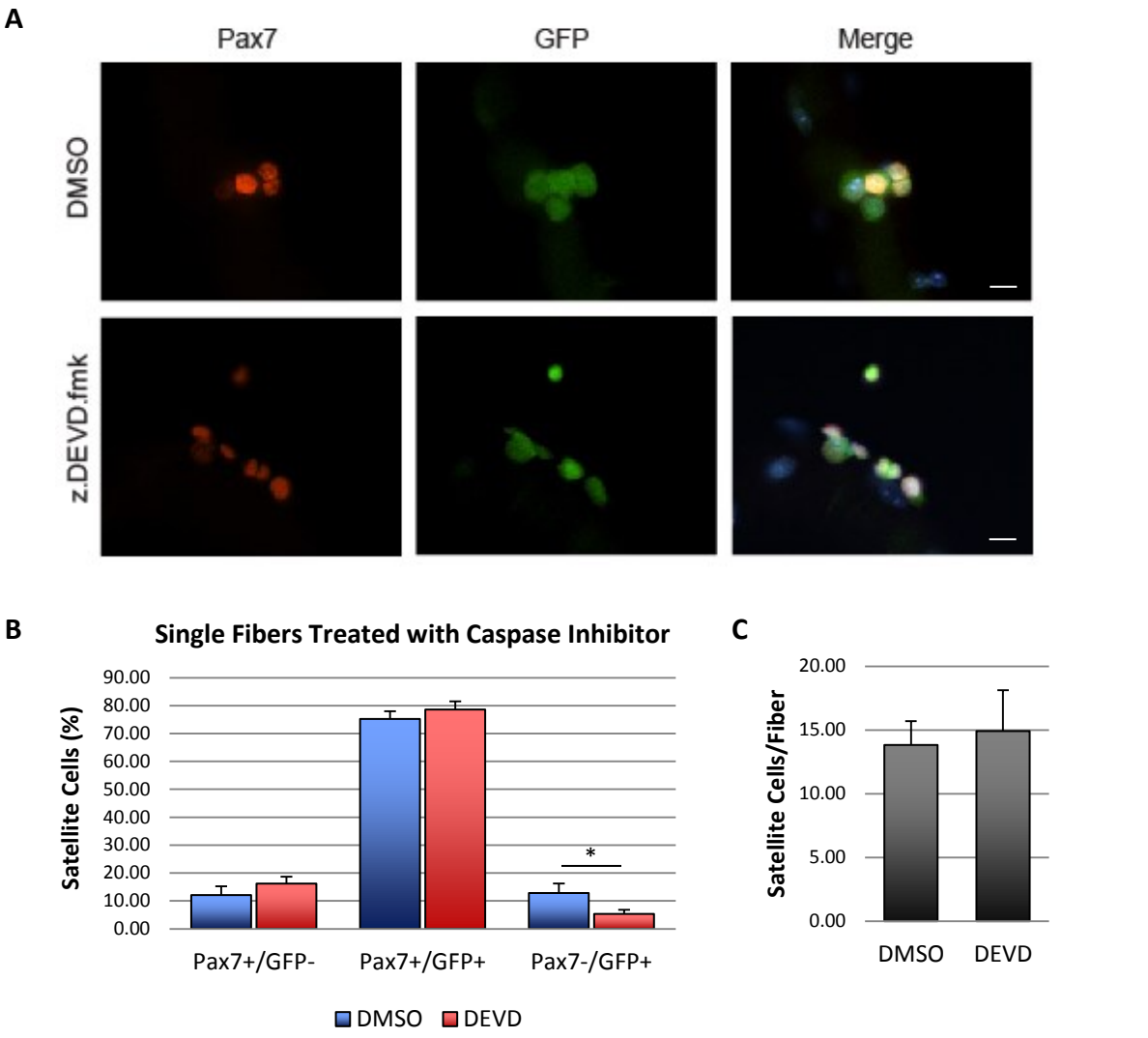

Figure 8 – Caspase 3 activity has no effect on the satellite 'stem' cell population. (A) Single fibers were isolated from juvenile Myf5/Cre-Rosa/YFP mice and cultured in 20μM z.DEVD.fmk (bottom) or DMSO (top; control) for 72 hours, fixed and stained with Pax7 (red) and GFP (green). (B) Quantification of the number of satellite cells expressing each marker expressed as a percentage of the total number of satellite cells (+/- SEM). (C) Quantification of total number of satellite cells per fiber (+/- SEM). *$p<0.05$ unpaired student t-test. Scale bars are 10μM.

3.3: The effect of exogenous caspase activation on myogenic differentiation

To determine whether caspase 3 activation is a dominant (sufficient) signal in determining satellite cell fate, we used a specific small molecule activator of caspase 3, termed Procaspase 3 Activating Compound 1 (Pac1), to engage protease activity. Pac1 is a potent and specific procaspase 3 targeted molecule, that chelates the inhibitory zinc ions from the catalytic site of the enzyme, leading to auto activation (Putt et al., 2006). A previous report has successfully utilized Pac1 to produce non-lethal levels of caspase 3 activation, confirming a role for this protease in the induction of cardiac hypertrophy (Putinski et al., 2013). Isolated myofibers treated with low levels of Pac1 (50μM) displayed a significant reduction in the number of Pax7 positive satellite cells compared to control treated myofibers (Pax7+/Syndecan4+ cells, Figure 9A, B). This suggests caspase 3 activity is sufficient to push these cells from a Pax7+ve (self-renewing) state to one permissive for differentiation, indicated by an increase in the Pax7-ve population (Pax7-/syndecan4+, Figure 9B). Although a slight decrease in the number of satellite cells per fiber was seen, indicating in some cultures Pac1 (and thus caspase 3 activity) induce a small amount of cell death, this was not found significant (Figure 9C).

To independently confirm these observations, we also tested the capacity of Pac1 to alter Pax7 levels and the commitment of FACS isolated satellite cells. We treated cultured satellite cells with various concentrations of Pac1 for 24hrs in growth media, using DMSO as a vehicle control. Cells cultured in low-serum differentiation media for 24 hours were used as a positive control. Following treatment cells were processed for viability assay, protein isolation or RNA isolation (Figure 10A). The viability was determined using PI/FACS analysis of floating and attached cells following treatment. We ascertained all concentrations

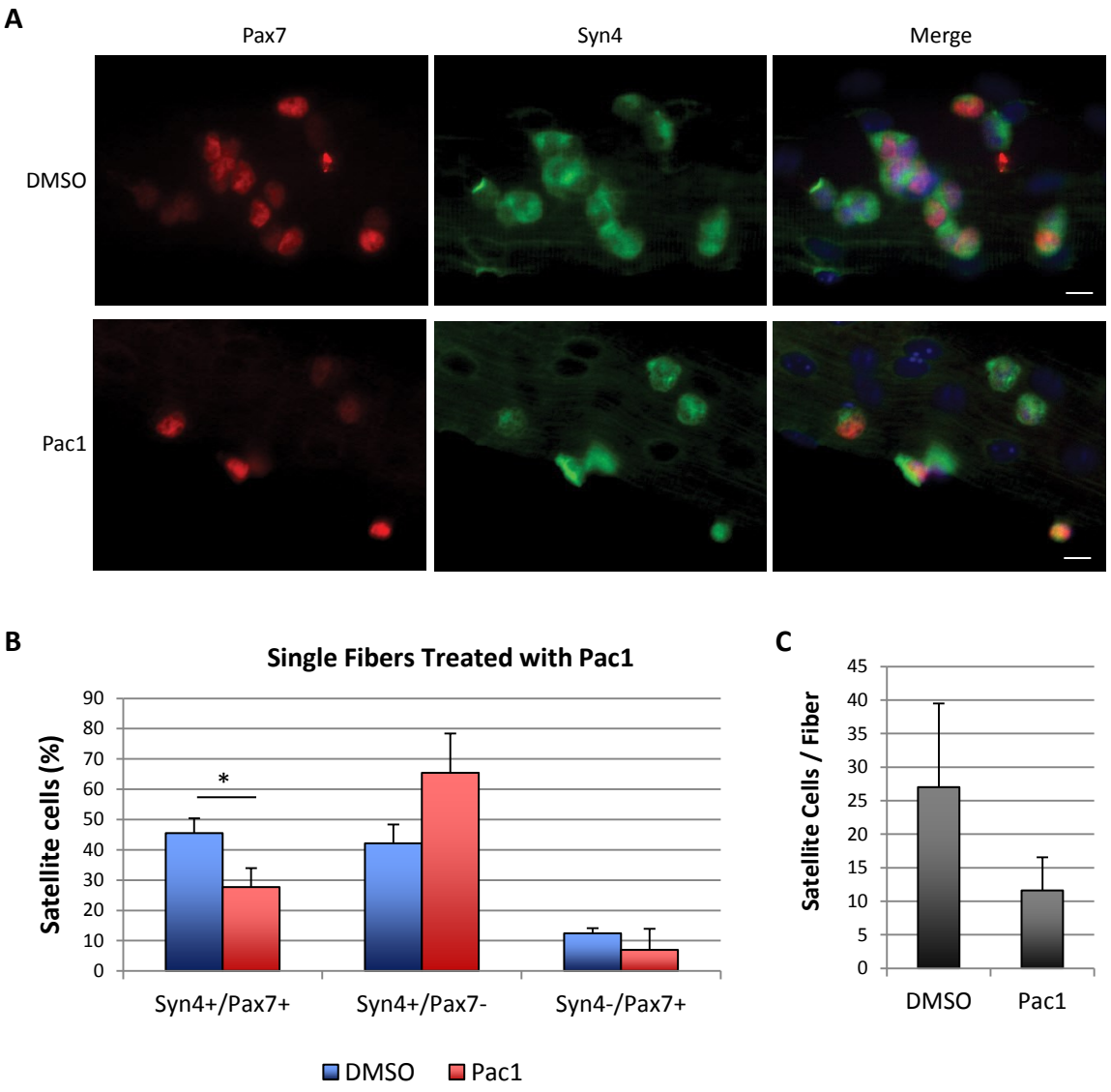

Figure 9 - Small molecule (PAC-1) activation of caspase 3 induces loss of Pax7 positive satellite cells. (A) Single fibers were treated with either 50µM Pac1(bottom) or DMSO (top) 48hrs following isolation and left for an additional 24 hours. At 72 hours post-isolation fibers were fixed and stained with syndecan 4 (green) and Pax7 (red). (B) The number of satellite cells expressing each marker was counted and expressed as a percentage of total number of satellite cells (+/- SEM). (C) Quantification of total number of satellite cells per fiber (+/- SEM). *$p<0.05$ unpaired student t-test. Scale bars are 10µM.

over 50μM Pac1 induced a significant level of cell death (Figure 10B). Therefore, we decided to use two viable concentrations of Pac1 (25μM and 50μM) to induce caspase 3 to functional levels without inducing cell death, a known outcome of sustained high-levels of caspase 3 activity.

Western blot analysis revealed that satellite cells treated with 25 or 50μM Pac1 displayed a dramatic reduction in Pax7 protein in growth media conditions, a loss that was comparable to cells exposed to low serum induction of differentiation (Figure 10C, D). Consistent with these results, we also observed activation of caspase 3 in these cells to levels similar to that seen in differentiation (Figure 10C, middle panel), confirming the need for a tight regulation of caspase 3 activity during differentiation to keep it at low-levels thus preventing cell death. Moreover, the Pac1 induced loss of Pax7 was concurrent to a reduction in the expression of the Pax7 target genes *Myf5* and *MyoD* (Figure 10E). Collectively, these results support the hypothesis that caspase 3 is necessary and sufficient to limit satellite cell self-renewal and establish the molecular conditions that are conducive for differentiation. Surprisingly, we did not see an increase in the expression levels of the differentiation markers *myogenin*, *Mef2C* and *P21*, suggesting additional cues may be required to sustain precocious differentiation in these conditions. We predict this is due to the high-levels of growth factors present in the media restricting the progression through differentiation. Unfortunately, administration of Pac1 at levels viable in growth media result in extensive cell death when used in combination with differentiation media. Likely due to the delicate balance in caspase 3 activity already produced during myoblast differentiation.

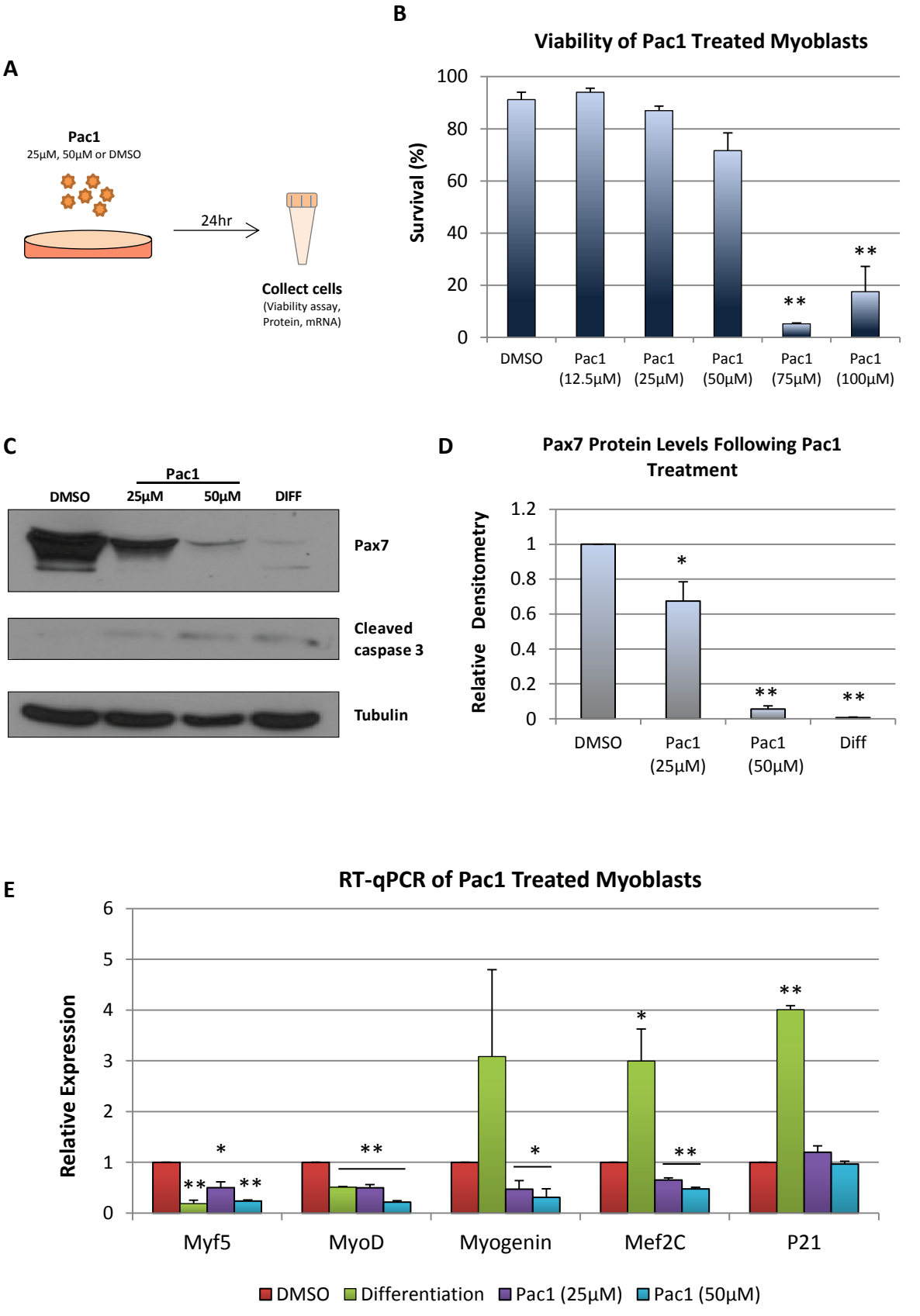
A
Pac1
25µM, 50µM or DMSO
24hr
Collect cells
(Viability assay,
Protein, mRNA)
B
Viability of Pac1 Treated Myoblasts
Survival (%)
100
80
60
40
20
0
**
**
DMSO
Pac1 (12.5µM)
Pac1 (25µM)
Pac1 (50µM)
Pac1 (75µM)
Pac1 (100µM)
C
Pac1
DMSO
25µM
50µM
DIFF
Pax7
Cleaved caspase 3
Tubulin
D
Pax7 Protein Levels Following Pac1 Treatment
Relative Densitometry
1.2
1
0.8
0.6
0.4
0.2
0
*
**
**
DMSO
Pac1 (25µM)
Pac1 (50µM)
Diff
E
RT-qPCR of Pac1 Treated Myoblasts
Relative Expression
6
5
4
3
2
1
0
Myf5
MyoD
Myogenin
Mef2C
P21
DMSO
Differentiation
Pac1 (25µM)
Pac1 (50µM)

Figure 10 - Small molecule (PAC-1) activation of caspase 3 induces cleavage of Pax7 and down-regulation of Pax7 target genes. (A) Cultured FACS purified satellite cells were treated with PAC-1 for 24 hours prior to collection for down-stream analysis. (B) Viability was evaluated by PI staining and FACS analysis. Percent of PI negative cells were plotted for each treatment group (+/-SEM). (C) Western blot analysis of PAC-1 treated cells at the indicated concentrations. Lysates were probed with αPax7, Cleaved-Caspase3 and αTubulin. (D) Densitometry analysis of Pax7 protein levels determined using imagej software and normalized to tubulin (loading control) shows a decrease similar to that seen in differentiation conditions. (E) Primary myoblasts treated with 25μM or 50μM Pac1, DMSO (control) or differentiation (2% HS) for 24 hours. RT-qPCR analysis was performed using primers indicated in Table 3. Error bars represent SEM. *$p<0.05$; **$p<0.005$, unpaired student t-test.

CHAPTER 4

Pax7 is a Caspase 3 Cleavage Substrate

4.1: Caspase 3 activity alters Pax7 protein levels

The increased numbers of self-renewing satellite cells following caspase 3 inhibition is consistent with the premise that this protease may act to cleave and inactivate the factor(s) that governs the self-renewal process. To test the influence of caspase 3 inhibition on Pax7 levels under differentiation conditions, primary myoblasts were placed in culture under growth conditions until confluent, at which time the media was replaced with low-serum media to induce myogenic differentiation. We observed inhibition of caspase 3 resulted in the persistent expression of Pax7 protein levels at 12 hours after the initiation of differentiation compared to loss of Pax7 protein at this time in control conditions (Figure 11A). Pax7 is a logical target in this regard, as 1) the protein content has been shown to decline faster than message content in differentiating myoblasts (Figure 11B, C) and (Dey et al., 2011), and 2) simple inspection of the Pax7 protein reveals conserved caspase 3 cleavage sites (Figure 14A).

4.2: Caspase 3 cleaves Pax7 *in vitro*

To determine whether caspase 3 directly targets the Pax7 protein, we conducted an *in vitro* cleavage assay using recombinant active-caspase 3 and recombinant Pax7 proteins. Addition of active-caspase 3 was sufficient to induce an immune-reactive Pax7 cleavage product of approximately 40KDa (Figure 12A). This cleavage event was blocked by addition of the caspase 3 peptide inhibitor, confirming the specificity of Pax7 as a caspase 3 substrate.

In an attempt to determine the kinetics of this cleavage event, we incubated recombinant Pax7 (100ng) with caspase 3 enzyme (3 units) for various times at 37^{o}C (Figure 12B). We observed cleavage of Pax7 at all time-points examined with a slight increase in cleavage product as time increased. In addition, we performed titration experiments in which

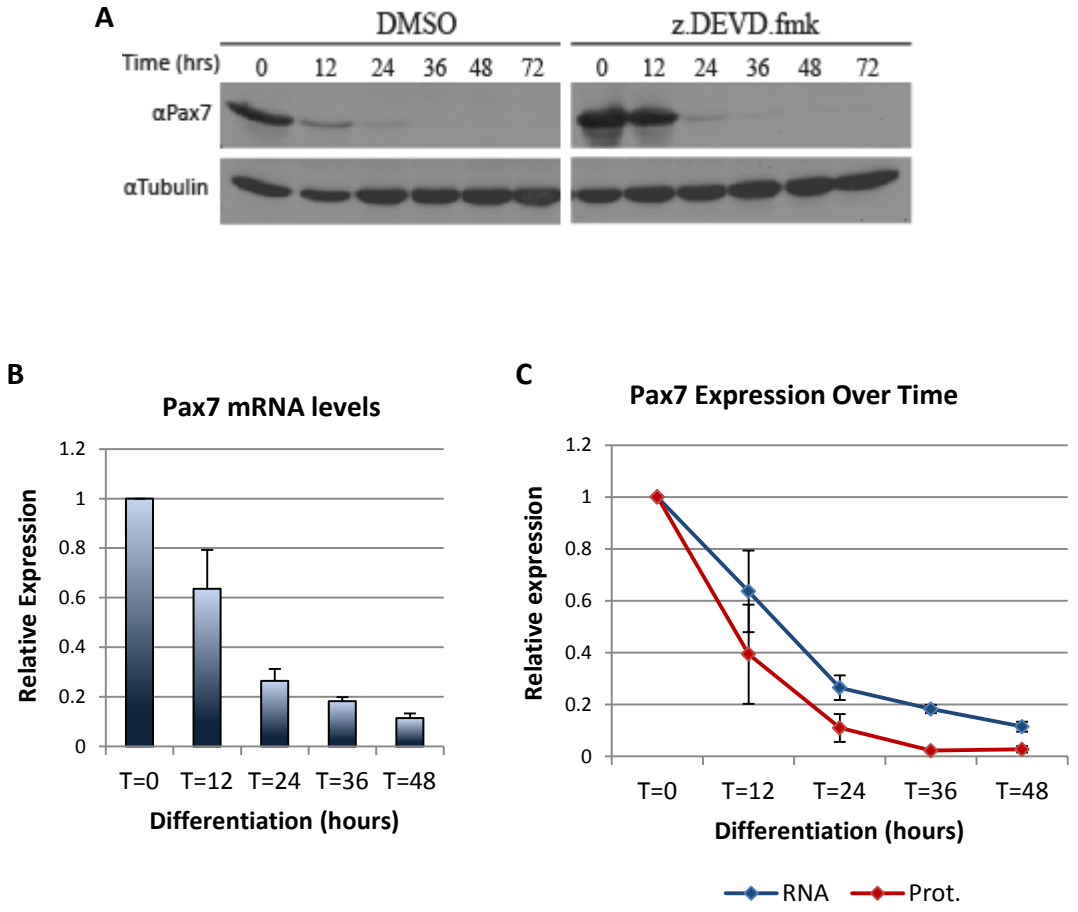

Figure 11 – Pax7 protein stability is affected by caspase 3 activity. (A) Differentiation time course of primary myoblasts treated with the caspase 3 peptide inhibitor z.DEVD.fmk (20μM) or DMSO control. Lysates were probed for αPax7 (top blot) and α-tubulin (bottom blot; loading control). (B) Primary myoblasts were induced to differentiate and collected at the indicated times for RT-qPCR analysis of Pax7 mRNA expression. (C) Relative mRNA expression from the RT-qPCR and relative densitometry analysis of Pax7 Protein (using ImageJ for western blot) was plotted together to show kinetics of Pax7 protein decrease is accelerated in comparison to the mRNA. Error bars represent SEM.

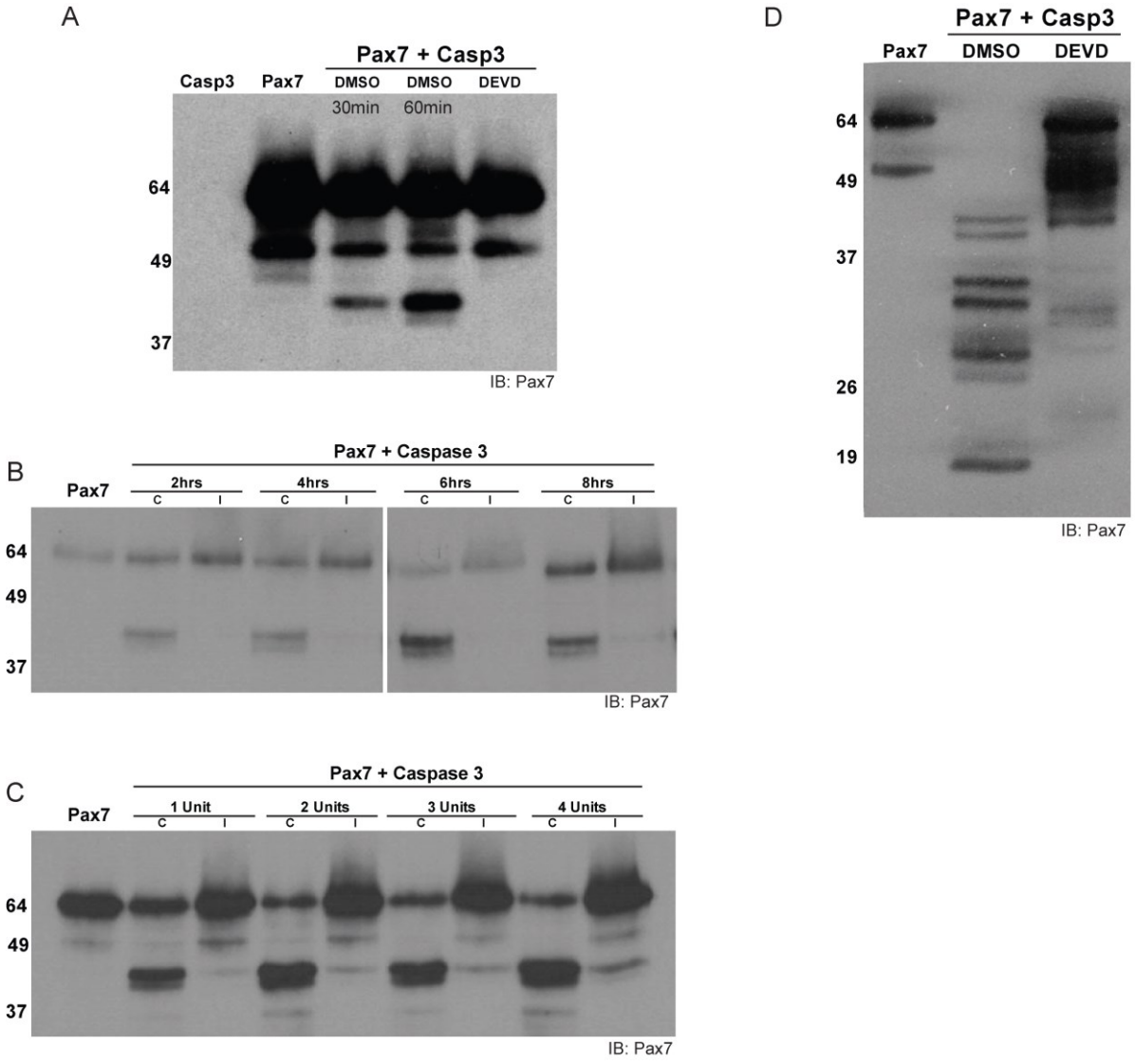
A
Pax7 + Casp3
Casp3
Pax7
DMSO
DMSO
DEVD
30min
60min
64
49
37
IB: Pax7
B
Pax7 + Caspase 3
Pax7
2hrs
4hrs
6hrs
8hrs
C
I
64
49
37
IB: Pax7
C
Pax7 + Caspase 3
Pax7
1 Unit
2 Units
3 Units
4 Units
C
I
64
49
37
IB: Pax7
D
Pax7 + Casp3
Pax7
DMSO
DEVD
64
49
37
26
19
IB: Pax7

Figure 12 - Pax7 protein is cleaved by caspase 3 at a cryptic cleavage site. (A) Recombinant Pax7 protein and recombinant active caspase 3 were incubated in standard cleavage assay conditions containing either DMSO or z.DEVD.fmk (20μM) for the indicated times. (B) Cleavage reactions were performed using static amounts of Pax7 (100ng) and caspase 3 (3 units) which the duration of the reaction was altered between 2 and 8 hours. (C) Cleavage reactions were performed using static amounts of Pax7 (100ng) and time (4 hours) while the amount of caspase 3 was altered between 1 and 4 units. Lanes marked with c (Cleaved; Caspase 3) or I (Inhibited; Caspase 3 and z.DEVD.fmk). (D) Cleavage reaction in which 100ng of Pax7 and 3 units of caspase 3 were incubated in cleavage conditions at 37^{o}C overnight (~16 hours). All reactions were subjected to SDS-PAGE and western blot analysis using αPax7 indicating a caspase 3 specific cleavage event at around 40kDa.

the amount of Pax7 remained constant (100ng) while the amount of recombinant caspase 3 was gradually increased from 1 to 4 units (Figure 12C). Reactions were incubated at 37^{o}C for 4hrs. As predicted the amount of cleavage product produced increased when incubated with 2 units compared to 1 unit of caspase 3, however, we did not observe an appreciable increase at higher concentrations. Although we observed a plateau in the amount of cleavage product produced (at concentrations higher than 2 units for 4hrs) we never observed complete loss of the full length protein. This suggests there may be more than one species of Pax7 protein present, a cleavable and an uncleavable form. This is most likely due to post-translational modifications present on the protein during production via the baculovirus system in Sf9 cells. This, however, was overcome by incubation of 100ng Pax7 with 3 units of Caspase 3 overnight (~16hrs) (Figure 12D). In addition to the 40kDa fragment, we observed a number of smaller immune-reactive fragments and complete loss of the full length species. Complete loss of this cleavage by addition of the caspase 3 specific inhibitor z.DEVD.fmk confirms the presence of multiple caspase cleavage sites in the Pax7 protein. That these are only cleaved during long exposure to the caspase 3 enzyme suggests low affinity of caspase 3 for these sites compared to the one which produces the 40kDa fragment, observable with as little as a 30min incubation (Figure 12A). Whether one or all anticipated cleavage sites are physiologically relevant remains to be determined. Due to the high affinity of caspase 3 for the site producing the 40kDa fragment we focused on this as the most relevant, with the assumption that cleavage at any other site would be secondary to this cleavage event.

4.3: Identification of the caspase 3 cleavage site within Pax7

Next, we sought to identify the caspase 3 cleavage site(s) within Pax7 and whether the cleavage event is consistent with producing a loss of function for Pax7. Importantly, we

observed both a 40kDa band on a silver stained gel which corresponded to the immune-reactive fragment identified via western blot analysis, as well as a 20kDa fragment, as predicted, upon addition of active-caspase 3 (Figure 13A, red and green box). These two bands were excised and processed for LC-MS/MS, identifying peptides which clustered to either the N-terminus (and within the paired domain) in the case of the 20kDa fragment or the C-terminus (including the homeodomain) for the 40kDa fragment (Figure 13B). This analysis suggested a physiologic cleavage event that parsed these two regions. To identify the precise caspase 3 cleavage site (an exposed N-terminal aspartic acid), we subjected aliquots of the whole cleavage reaction to enzymatic digestion using 3 different endoproteases (Chymotrypsin, Trypsin, GluC). Analysis of the Pax7 cleavage reaction products revealed a number of peptides with a common N-terminal aspartic acid at D187 that could not be attributed to cleavage via the selected diagnostic endoproteases (Table 4). Importantly, D187 mapped to a region that was not detected in either the 40kDa or the 20kDa fragments, and was localized between the paired and the homeodomain in which the respective peptides clustered (Figure 13B and Figure 14A).

To confirm this cleavage site, we produced recombinant Pax7 protein which harbored an aspartic acid to alanine mutation at site D187. For this we utilized the baculovirus system. A point mutation was introduced into the cDNA of Pax7 (previously cloned into the FastBac1 vector, containing a C-terminal 3xFLAG tag) via site-directed mutagenesis (For primers see Table 1). Following sequencing and confirmation of the point mutation, the FastBac1 plasmid containing D187A Pax7 was transfected into Sf9 cells and recombinant Pax7 was isolated using M2Flag beads. To confirm recombinant protein purification aliquots of the elute was run on a SDS-PAGE gel stained with coommassie blue (Figure 14B). This work was in collaboration with Yoichi Kawabie and Natasha Chang of the Rudnicki lab.

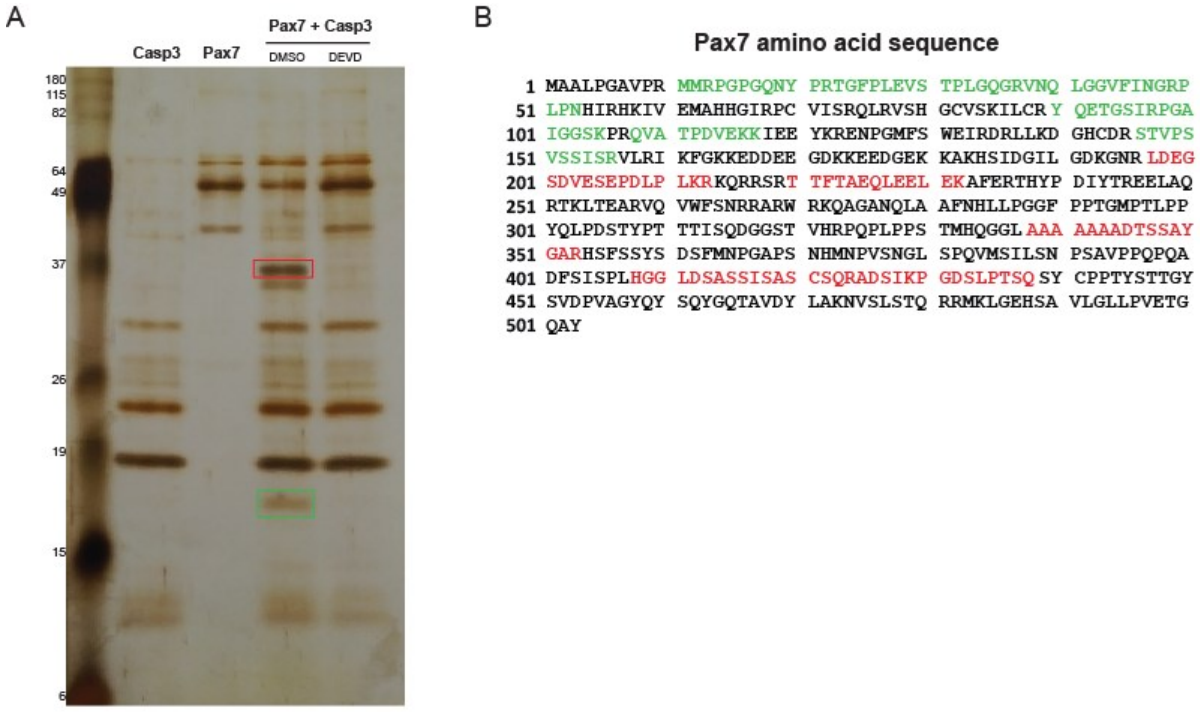

Figure 13 - Fragments produced via caspase 3 cleavage map to the N- or C- Terminus of the Pax7 protein. (A) Recombinant Pax7 (1µg) was subjected to an *in vitro* caspase 3 cleavage reaction followed by SDS-PAGE and silver stain. The protein fragments produced (red and green boxes) were isolated and processed for LC-MS/MS. (B) Pax7 amino acid sequence with the identified peptides indicated. Peptides indicated by green were identified in the ~20kDa fragment and the peptides indicated by red were identified in the ~40kDa fragment.

Table 4 – Mass spectrometry results identifying D187 as a caspase 3 cleavage site. Recombinant Pax7 was subjected to an in vitro caspase 3 cleavage assay and directly processed for LC-MS/MS using 3 different endoproteases (Chymotrypsin, Trypsin, GluC). MASCOT software was used to analyse the identified peptides mapping to the Pax7 protein. The peptides identified were queried for cleavage events following an aspartic acid residues which could not be attributed to cleavage via one of the endopeptide used for LC-MS/MS processing (red).

Start	-	End	Observed	Mr (expt)	Mr (calc)	Sequence	Interpretation
2	-	10	893.5179	892.5107	892.513	M.AALPGAVPR.M	tryptic peptide from N-terminus of protein following loss of N-term Met plus acetylation
2	-	10	447.2626	892.5107	892.513	M.AALPGAVPR.M	tryptic peptide from N-terminus of protein following loss of N-term Met plus acetylation
23	-	37	779.9136	1557.813	1557.815	R.TGFPLEVSTPLGQGR.V	trypsin cleavage (also seen in control)
29	-	42	713.3931	1424.772	1424.774	E.VSTPLGQGRVNQLG.G	non-specific (also seen in control)
34	-	45	616.3296	1230.645	1230.647	L.GQGRVNQLGGVF.I	chymotrypsin cleavage
38	-	56	526.0481	2100.163	2100.171	R.VNQLGGVFINGRPLPNHIR.H	trypsin cleavage
38	-	56	701.0637	2100.169	2100.171	R.VNQLGGVFINGRPLPNHIR.H	trypsin cleavage
38	-	56	701.3901	2101.148	2101.155	R.VNQLGGVFINGRPLPNHIR.H	trypsin cleavage
38	-	56	526.2949	2101.15	2101.155	R.VNQLGGVFINGRPLPNHIR.H	trypsin cleavage
62	-	74	511.9333	1532.778	1532.782	E.MAHHGIRPCVISR.Q	???
78	-	92	612.6333	1834.878	1834.882	R.VSHGCVSKILCRYQE.T	???
93	-	107	485.278	1452.812	1452.816	E.TGSIRPGAIGGSKPR.Q	???
93	-	120	730.8995	2919.569	2919.578	E.TGSIRPGAIGGSKPRQVATPDVEKKIEE.Y	GluC cleavage
121	-	132	772.3531	1542.692	1542.693	E.YKRENPGMFSWE.I	GluC cleavage
137	-	156	554.2861	2213.115	2213.122	R.LLKDGHCDRSTVPSVSSISR.V	trypsin cleavage
137	-	156	738.7123	2213.115	2213.122	R.LLKDGHCDRSTVPSVSSISR.V	trypsin cleavage

184	-	213	816.1625	3260.621	3260.627	K.HSIDGILGDKGNRLDEGSDVESEPDLPLKR.K	seen in control sample only
184	-	214	678.7504	3388.716	3388.722	K.HSIDGILGDKGNRLDEGSDVESEPDLPLKRK.Q	seen in control sample only
188	-	208	1101.508	2201.002	2201.008	D.GILGDKGNRLDEGSDVESEPD.L	caspase plus GluC or caspase x2
188	-	208	734.6756	2201.005	2201.008	D.GILGDKGNRLDEGSDVESEPD.L	caspase plus GluC or caspase x2
188	-	211	842.4155	2524.225	2524.229	D.GILGDKGNRLDEGSDVESEPDLPL.K	caspase plus chymotrypsin
188	-	213	703.1121	2808.419	2808.425	D.GILGDKGNRLDEGSDVESEPDLPLKR.K	caspase plus trypsin
188	-	213	937.1475	2808.421	2808.425	D.GILGDKGNRLDEGSDVESEPDLPLKR.K	caspase plus trypsin
188	-	214	735.1355	2936.513	2936.52	D.GILGDKGNRLDEGSDVESEPDLPLKRK.Q	caspase plus trypsin
188	-	214	588.3104	2936.516	2936.52	D.GILGDKGNRLDEGSDVESEPDLPLKRK.Q	caspase plus trypsin
188	-	215	767.1497	3064.57	3064.579	D.GILGDKGNRLDEGSDVESEPDLPLKRKQ.R	caspase plus GluC
188	-	215	613.9221	3064.574	3064.579	D.GILGDKGNRLDEGSDVESEPDLPLKRKQ.R	caspase plus GluC
188	-	216	645.1409	3220.668	3220.68	D.GILGDKGNRLDEGSDVESEPDLPLKRKQR.R	caspase plus trypsin
230	-	247	766.3755	2296.105	2296.112	E.LEKAFERTHYPDIYTREE.L	GluC cleavage (also seen in control)
232	-	247	514.5022	2053.98	2053.986	E.KAFERTHYPDIYTREE.L	GluC cleavage
232	-	247	685.6674	2053.98	2053.986	E.KAFERTHYPDIYTREE.L	GluC cleavage
236	-	247	527.2528	1578.737	1578.743	E.RTHYPDIYTREE.L	GluC cleavage (also seen in control)
236	-	247	527.2534	1578.738	1578.743	E.RTHYPDIYTREE.L	GluC cleavage (also seen in control)
236	-	247	527.2535	1578.739	1578.743	E.RTHYPDIYTREE.L	GluC cleavage (also seen in control)
236	-	247	527.2537	1578.739	1578.743	E.RTHYPDIYTREE.L	GluC cleavage (also seen in control)
237	-	247	712.327	1422.639	1422.642	R.THYPDIYTREE.L	???
257	-	263	453.2513	904.488	904.4919	E.ARVQVWF.S	???
259	-	267	596.3213	1190.628	1190.631	R.VQVWFSNRR.A	trypsin cleavage
333	-	350	816.8837	1631.753	1631.754	M.HQGGLAAAAAAADTSSAY.G	chymotrypsin cleavage? seen in control sample only

317	-	350	819.6508	3274.574	3274.579	D.GGSTVHRPQPLPPSTMHQGGLAAAAAADTSSAY.G	caspase plus chymotrypsin
317	-	350	1092.535	3274.584	3274.579	D.GGSTVHRPQPLPPSTMHQGGLAAAAAADTSSAY.G	caspase plus chymotrypsin
317	-	353	890.6918	3558.738	3558.739	D.GGSTVHRPQPLPPSTMHQGGLAAAAAADTSSAYGAR.H	caspase plus trypsin
351	-	385	1236.882	3707.624	3707.619	Y.GARHSFSSYSDSFMNPGAPSNHMNPVSNGLSPQVM.S	chymotrypsin cleavage
355	-	406	1088.5	5437.462	5437.438	H.SFSSYSDSFMNPGAPSNHMNPVSNGLSPQVMSILSNPSAVPPQPQADFSISP.L	also seen in control
402	-	412	571.7947	1141.575	1141.577	D.FSISPLHGGLD.S	caspase or GluC?
464	-	477	739.8946	1477.775	1477.778	Y.GQTAVDYLAKNVSL.S	chymotrypsin cleavage
464	-	483	746.7256	2237.155	2237.159	Y.GQTAVDYLAKNVSLSTQRRM.K	chymotrypsin cleavage (also seen in control)
465	-	482	678.3622	2032.065	2032.07	G.QTAVDYLAKNVSLSTQRR.M	also seen in control
470	-	477	454.2649	906.5152	906.5174	D.YLAKNVSL.S	caspase plus chymotrypsin
470	-	480	612.334	1222.654	1222.656	D.YLAKNVSLSTQ.R	caspase plus GluC
470	-	483	556.304	1665.89	1665.898	D.YLAKNVSLSTQRRM.K	caspase plus chymotrypsin
470	-	487	1047.577	2093.14	2093.142	D.YLAKNVSLSTQRRMKLGE.H	caspase plus GluC
483	-	492	542.7934	1083.572	1083.575	R.MKLGEHSAVL.G	???
488	-	498	567.8281	1133.642	1133.645	E.HSAVLGLLPVE.T	GluC cleavage (also seen in control)
488	-	498	1134.65	1133.643	1133.645	E.HSAVLGLLPVE.T	GluC cleavage (also seen in control)

A

		PAIRED BOX	OCTAPEPTIDE	HOMEO DOMAIN	
Mus musculus	156	RVLR I K F	GKKEDDEEG D KKEEDGEKKAK	HSIDGILGD KGNRLDEGS DVESEP DLPLKRKQ	RRSRTTFTAEQLEELEKAFE 235
Rattus norvegicus	156	RVLR I K F	GKKEDDEEG D KKEEDGEKKAK	HSIDGILGD KGNRLDEGS DVESEP DLPLKRKQ	RRSRTTFTAEQLEELEKAFE 235
Gallus gallus	156	RVLR I K F	GKKEEEEE D CD KKEEDGEKKAK	HSIDGILGD KGNRLDEGS DVESEP DLPLKRKQ	RRSRTTFTAEQLEELEKAFE 235
Homo sapiens	158	RVLR I K F	GKKEEED E AD KKEDDGEKKAK	HSIDGILGD KGNRLDEGS DVESEP DLPLKRKQ	RRSRTTFTAEQLEELEKAFE 237
Danio rerio	161	RVLRAR F	GKKDDDDECDKKDEDGEKKTK	HSIDGILGD KGNRTDEGS DVESEP DLPLKRKQ	RRSRTTFTAEQLEELEKAFE 240

B

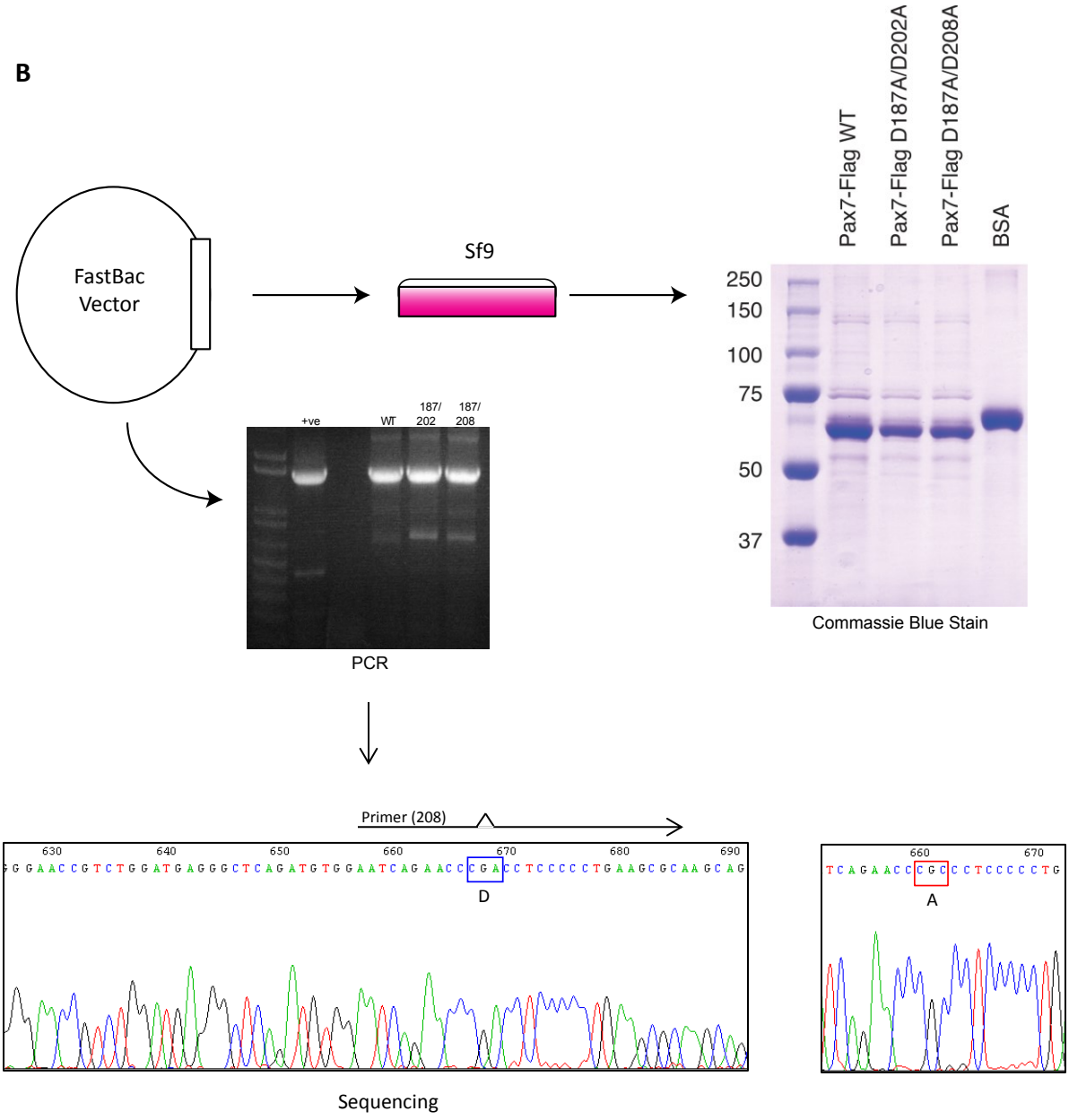

Figure 14 – Identification of the caspase 3 cleavage sites and site-directed mutagenesis. (A) The aspartic acid residues targeted by caspase 3 (highlighted in blue), as well as the serine residue targeted by CK2 (highlighted in red), is conserved across a broad range of phyla. Amino acid sequences obtained from NCBI (http://www.ncbi.nlm.nih.gov). (B) Pax7 protein containing a point mutation resulting in the loss of the aspartic acid responsible for caspase 3-mediated cleavage was produced via site-directed mutagenesis on Pax7(WT) containing FastBac1 vector and baculovirus production. PCR was performed using primers harbouring the mutations (indicated in Table 1) and resultant vectors were sequence verified. These vectors were transfected into Sf9 cells for baculovirus production and the protein was purified using their 3xFLAG-tag. Eluent was run on a SDS-PAGE gel and commassie stained to verify purity.

Interestingly, the recombinant D187A Pax7 protein displayed partial cleavage via caspase 3, suggesting that Pax7 contained additional cleavage site(s) attributing to production of the 40kDa fragment (Figure 15A). Examination of the Pax7 amino acid sequence indicated two additional aspartic acid residues (D202 and D208) that retain prototypical caspase 3 recognition sites (Thornberry et al., 1997). To test the caspase targeting of these residues we generated the single aspartic acid to alanine Pax7 mutations (D202A and D208A), as well as the relevant Pax7 double mutants (D187A/D202A and D187A/D208A) for use in the caspase cleavage assay. Recombinant Pax7 containing the D187A/D202A double mutant, or any of the single mutants did not provide effective blockade of caspase-directed cleavage (Figure 15A, B). However, Pax7 protein containing the dual D187A/D208A aspartic acid to alanine mutations was completely protected from caspase 3 cleavage (Figure 15B), establishing these aspartic acids as de facto caspase target sites.

4.4: Examining a role for the caspase 3 mediated cleavage fragments of Pax7

Following caspase 3-mediated cleavage at the indicated site(s) within Pax7, two fragments are produced which may contain residual activity. The N-terminal fragment of Pax7 is of particular interest as it retains the DNA binding capacity of Pax7 (Paired domain) unbound from the transactivation domain (Figure 16A). A dominant-negative effect has been documented following truncation of transcription factors, following loss of the transactivation domain (Choul-Li et al., 2010) providing a rationale to test the functional activity of the fragments produced via caspase 3 cleavage of Pax7.

We produced retroviral expression plasmids in the pHIT4 backbone containing the N-terminal (a.a. 1-208), the C-terminal (a.a. 208-503) or full length (a.a. 1-503) Pax7

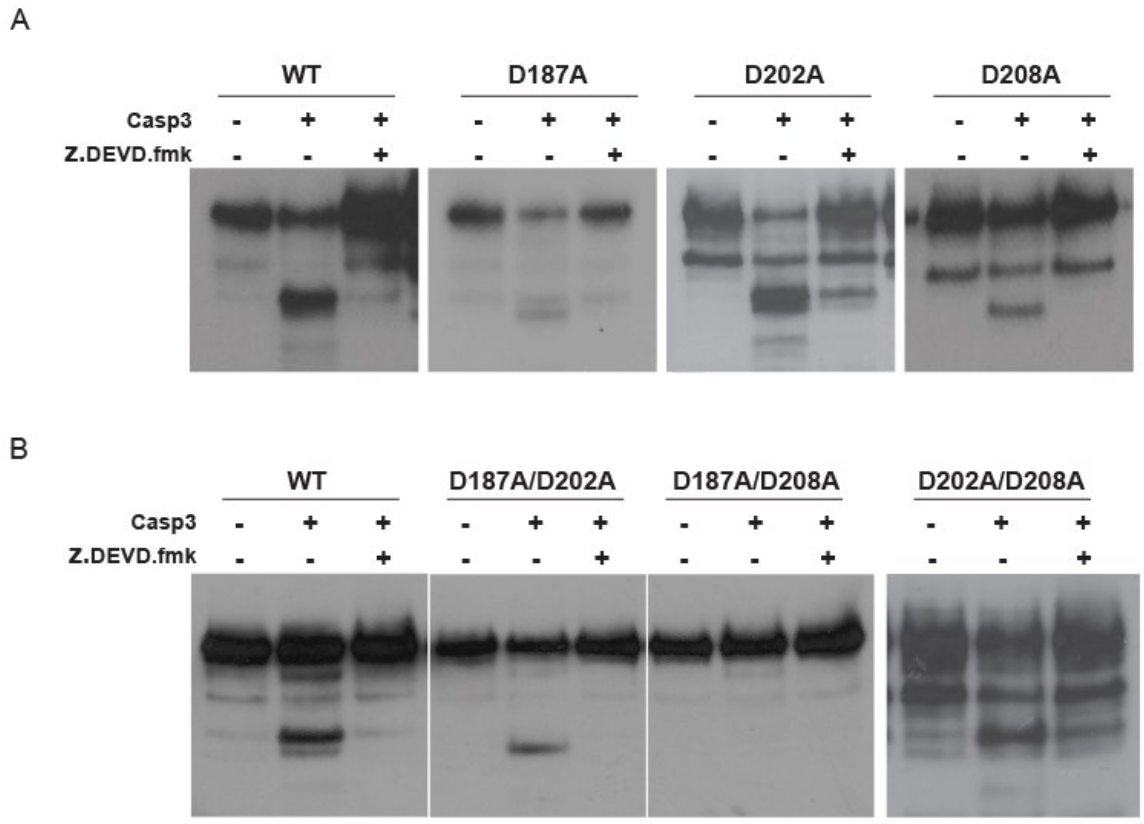

Figure 15 – Caspase 3 cleavage was abolished in the D187A/D208A double mutant only. (A) Recombinant Pax7 protein containing single aspartic acid to alanine point mutations at site D187A and D202A or D208A were subjected to caspase 3 cleavage followed by western blot analysis. (B) Recombinant Pax7 containing double point mutations at sites D187A/D202A, D187A/D208A and D202A/D208A were subjected to caspase 3 cleavage followed by western blot analysis. Only D187A/D208A completely blocked caspase 3 cleavage compared to wild-type.

containing a down-stream IRES-GFP (Figure 16A). Initially, we examined whether caspase cleavage of Pax7 resulted in loss of function for the resulting Pax7 fragments. COS cells were co-transfected with either full length or truncated Pax7 constructs and a Pax7 responsive promoter linked to a luciferase reporter (*Myf5*-57.5) (Table 2). COS cells transfected with full length Pax7 induced expression of the *Myf5* linked reporter, whereas COS cells expressing either caspase generated Pax7 fragment (N-Term or C-Term) did not activate the reporter (Figure 16B). These results suggest that caspase cleavage of Pax7 results in the generation of non-functional Pax7 fragments.

Based on previous observations of truncated/fragmented transcription factors having a dominant-negative affect on function we then tested the ability of the cleavage fragments of Pax7 to inhibit Pax7 function, thus further promoting differentiation. We hypothesize the N-terminal fragment of Pax7 (containing amino acids 1-208) would act as a dominant-negative by binding to Pax7 target elements and blocking the ability of full length Pax7 to successfully initiate transcription of its down-stream target. In accordance with our hypothesis, Zammit et. al. revealed, regardless of persistent Pax7 expression, via retroviral infection with a Pax7 expression construct, myoblast differentiation occurred. This supports the notion that a dominant-negative effect is acting to inhibit Pax7 function (specifically at the *Myf5* promoter) regardless of its mRNA levels (Zammit et al., 2006).

We observed no significant change in reporter activity when the N-Term or the C-Term of Pax7 was co-expressed with the full length Pax7 (Figure 16C). Due to the low baseline expression induced by the full length Pax7 protein we sought to observe the effect of the over-expression of either the N-Term or C-Term fragment on the function of a Pax7 transgene containing VP16 (a potent transcriptional activator). Similarly, we did not observe a significant change in reporter activity when either of the fragments were co-expressed with

VP16-Pax7 compared to co-expression with full length Pax7 (Figure 16D). Together these results indicate the N-Term and C-Term Pax7 fragments likely do not contain a residual function following caspase 3 mediated cleavage.

To confirm our results from the luciferase assay we produced retrovirus via transfection of the pHIT4 expression plasmids in PHX ECO cells, which was used for subsequent infection of primary myoblasts. Following expression and expansion of GFP positive cells (Day 6, Figure 17A), the myoblasts were FACS sorted to produce a pure population of Pax7 expressing cells (Figure 17B). These cells were allowed to recover for an additional 4 days in culture prior to collection and processing for RT-qPCR. Using primers for the Pax7 target genes *Myf5* and *MyoD* we observed no change in transcriptional activity at the *Myf5* promoter in cells expressing either the N-terminal or C-terminal of Pax7 (Figure 17C). We did however observe a decrease in transcription of *MyoD*, consistent with what has been reported for a dominant-negative form of Pax7 (Relaix et al., 2006). Further investigation into the role of the Pax7 fragments produced via caspase 3 cleavage is warranted with specific attention to the cell environment. Our results suggest these fragments may have a specific role in regulating Pax7 transcriptional activity as opposed to a global one.

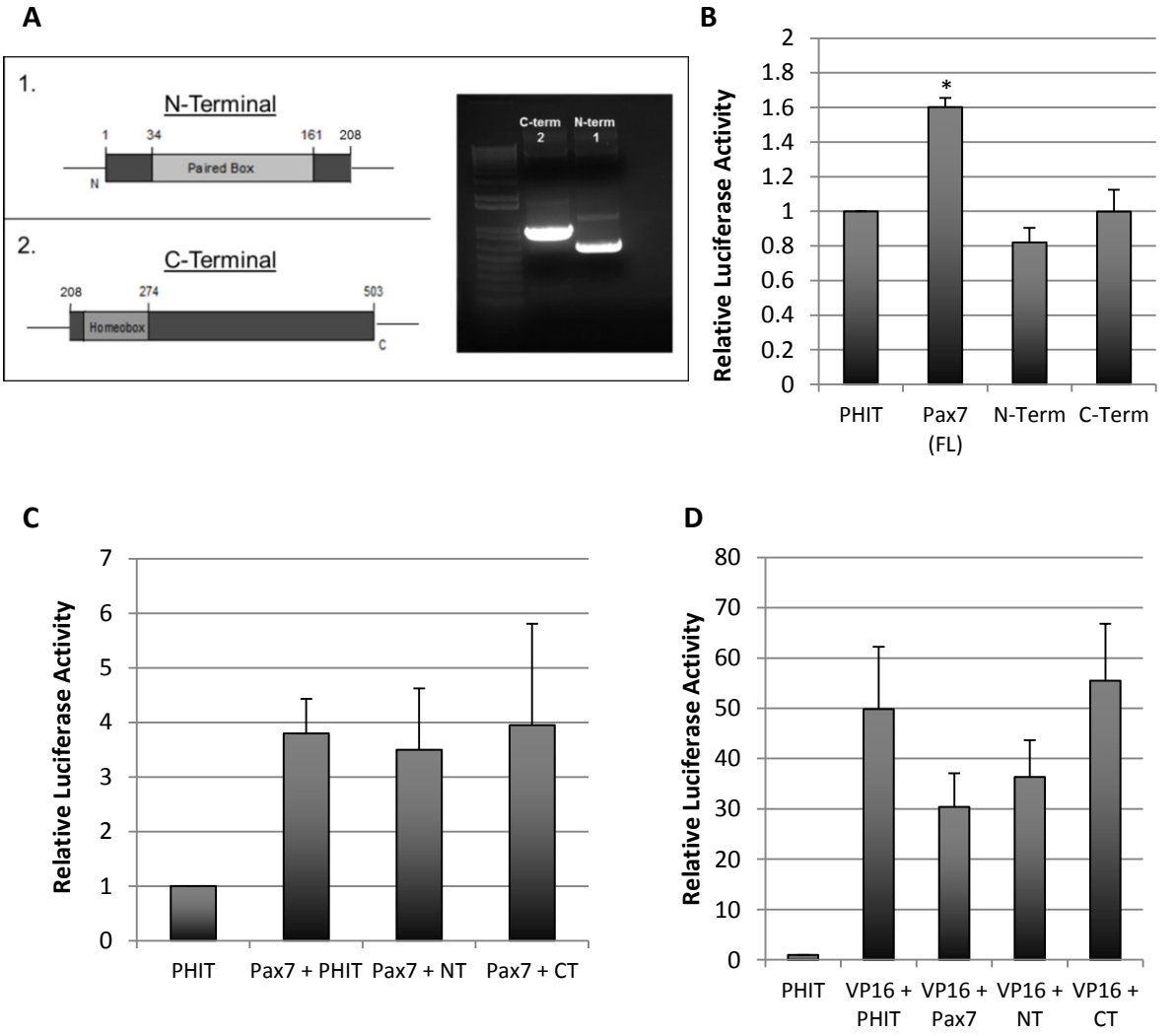
A
1.
N-Terminal
1
34
161
208
N
Paired Box
2.
C-Terminal
208
274
503
Homeobox
C
C-term 2
N-term 1
B
Relative Luciferase Activity
2
1.8
1.6
1.4
1.2
1
0.8
0.6
0.4
0.2
0
*
PHIT
Pax7 (FL)
N-Term
C-Term
C
Relative Luciferase Activity
7
6
5
4
3
2
1
0
PHIT
Pax7 + PHIT
Pax7 + NT
Pax7 + CT
D
Relative Luciferase Activity
80
70
60
50
40
30
20
10
0
PHIT
VP16 + PHIT
VP16 + Pax7
VP16 + NT
VP16 + CT

Figure 16 – Pax7 fragments produced via caspase 3 cleavage retain no transcriptional activity. (A) The N-Terminal (a.a. 1-208) and the C-Terminal (a.a. 208-503) of Pax7 was PCR cloned into the pHIT4 vector. (B) Luciferase assay was performed in COS cells co-transfected with a Pax7 containing plasmid and a luciferase reporter plasmid containing the *Myf5* promoter (see Table 2 for plasmid descriptions). Only Pax7 full-length induced expression of the Myf5 luciferase reporter indicating the fragments contained no transcriptional activity (C) Luciferase assay was performed using Pax7 full-length in conjunction with either the N-Terminus (NT) or the C-Terminus (CT) of Pax7 to determine if the fragments acted as a dominant negative to inhibit the transcriptional activity of full-length Pax7. (D) Luciferase assay was performed as in (C) using Pax7 (full-length) fused to VP16 (a strong transcription activation domain) to enhance any observable affect. In both cases there was no significant change in the reporter activity from Pax7 + PHIT (empty vector control) to Pax7 + NT or Pax7 + CT. Luciferase activity were normalized to *Renilla* for transfection efficiency and expressed as luciferase activity relative to empty vector (PHIT). Error bars represent SEM. *$p<0.05$; unpaired student t-test.

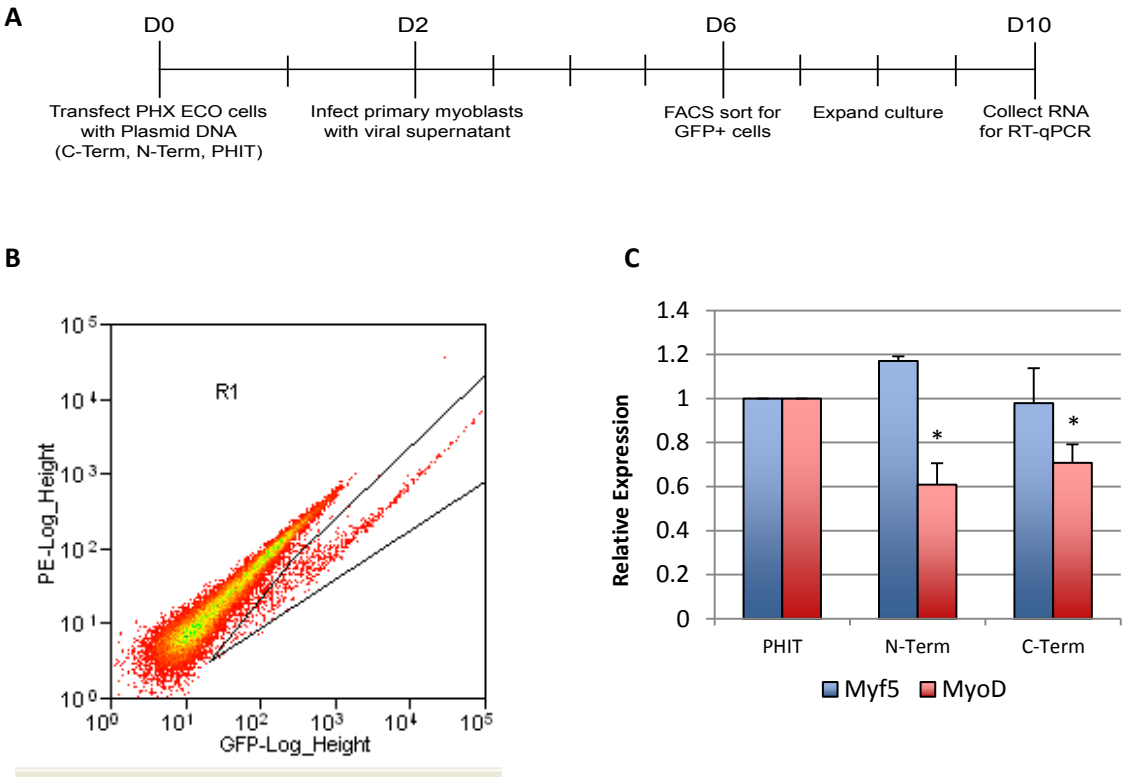

Figure 17 – Pax7 fragments retain some endogenous function. (A) pHIT4 vectors containing the Pax7 fragments (produced as in Figure 16A) were transfected into PHX ECO cells for retrovirus production. Retrovirus was then used to infect primary myoblasts in culture. (B) Following 4 days in culture, infected myoblasts were FACS purified gaiting for PE and GFP. Cells which exhibited a side scatter positive for GFP were collected (~4% of total cells). (C) RT-qPCR analysis showed no change in Myf5 mRNA expression and a significant decrease in MyoD mRNA expression. Error bars represent SEM. *p<0.05; unpaired student t-test.

CHAPTER 5

The Role of CK2 in Modulating Caspase 3 Mediated Cleavage of Pax7 Protein

5.1: CK2 is present and active in satellite cells

The stand alone capacity of caspase 3 to alter self-renewal implies that the satellite cell may have evolved or co-opted a mechanism(s) to restrain the protease targeting of Pax7. Interestingly, the constitutively active casein kinase 2 (CK2) has been shown to produce a steric inhibition on caspase 3 cleavage events via phosphorylation of serine residues that reside in close proximity to the caspase 3 cleavage site (Duncan et al., 2011). Indeed, comprehensive proteomic analysis has established that caspase 3 cleavage sites and CK2 phosphorylation sites strongly overlap (Duncan et al., 2011; Turowec et al., 2014). Here we show that CK2 is present in all activated satellite cells and the majority (73.0±3.5%) of quiescent satellite cells (Figure 18). There are a small percentage of cells (25.48±9.0%) that express CK2 but lack Pax7 (Figure 18C) which is cytoplasmically located, as determined via immunofluorescence microcopy (Figure 18A). Whether this represents CK2 in differentiating satellite cells or other fiber associated mononuclear cells (such as fibroblasts) was not determined. As CK2 plays an important role in general cell survival we favor the notion that CK2 activity is restricted during differentiation commitment allowing for cleavage of Pax7 protein, as opposed to transcriptional shut down of CK2 gene transcription. Further examination of CK2 activity at different times of satellite cell commitment would be required to further elucidate its function.

5.2: CK2 inhibition results in a differentiation defect

To address the physiological relevance of CK2 activity and whether this kinase modulates satellite cell self-renewal we tested the effect of the CK2 specific inhibitor TBBt on single fiber cultures. We observed an increase in the differentiation potential of satellite cells when treated with TBBt (50μM) compared to vehicle control (DMSO), as indicated by

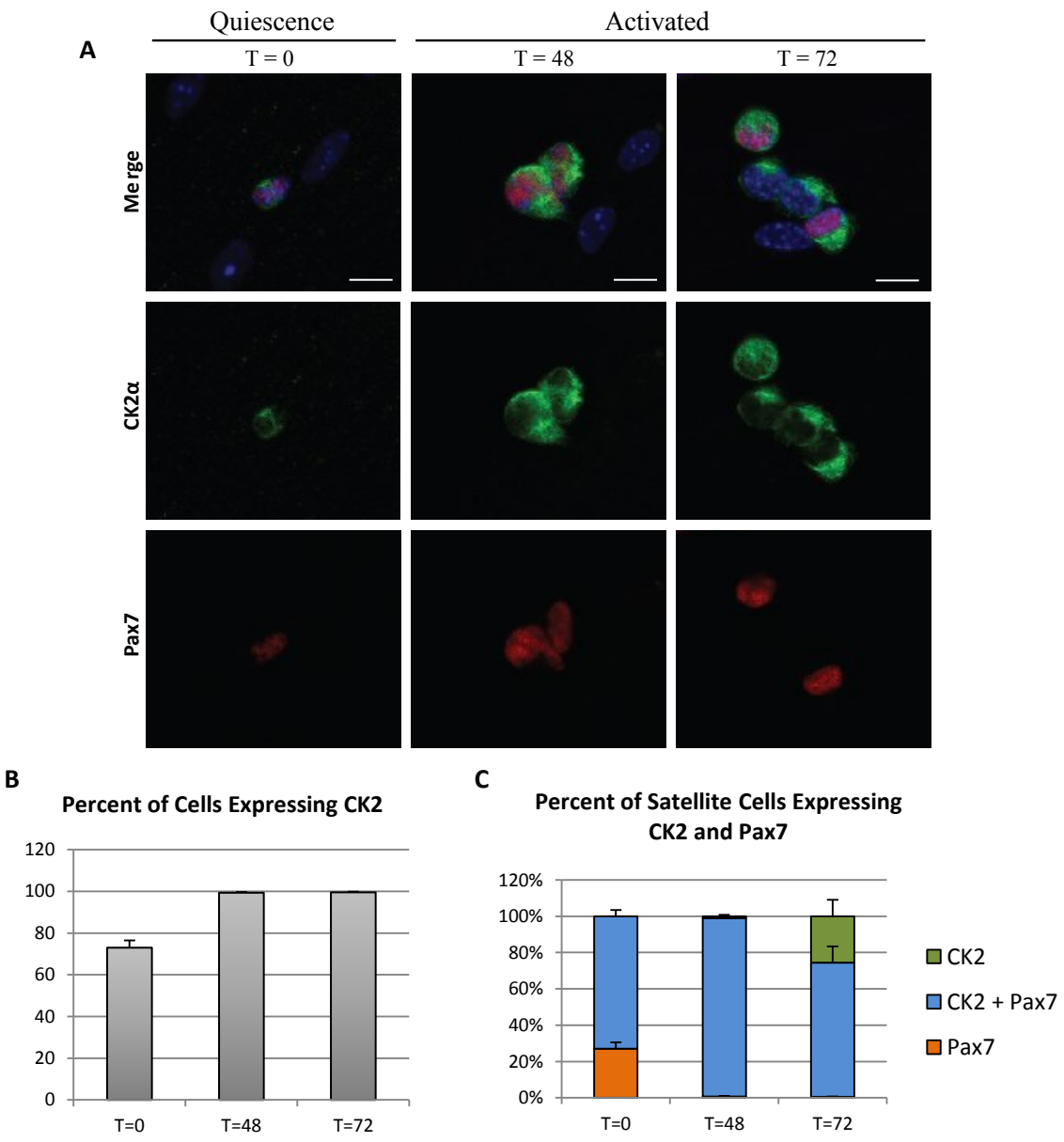

Figure 18 – Casein Kinase 2 (CK2) is present in fiber associated satellite cells. (A) CK2α (green) was observed in Pax7 positive (red) fiber associated satellite cells at all time points tested. (B) The number of mononuclear cells expressing CK2 was quantified at T=0, T=48 and T=72 hours post fiber isolation. (C) The number of cells expressing each marker was also quantified and expressed as a percentage of the total number of cells counted. Error bars represent SEM. Scale bars are 10μM.

the increase in Pax7-/MyoD+ satellite cells at day 3 following isolation (1.41±0.10 fold increase) (Figure 19A, B). There was no significant difference in the number of satellite cells per fiber indicating that inhibition of CK2 activity does not impair cell survival (Figure 19C). As we increased the amount of inhibitor from 10μM to 50μM we observed a step wise increase in the number of Pax7-/MyoD+ satellite cells indicating a dose dependent effect (Figure 19D). Together, these results suggest a role for CK2 in maintaining Pax7 protein stability during the proliferation/expansion of activated satellite cells.

To confirm these results, we treated FACS-isolated satellite cells in culture with the CK2 inhibitor TBBt (50μM) for 24 hours in growth media. RT-qPCR analysis revealed an increase in the differentiation marker *Mef2C* suggesting a propensity for these cells to differentiate (Figure 19E). Interestingly, the transcription of the Pax7 target gene *Myf5* remained unchanged (Figure 19E). This suggests CK2 may act to inhibit Mef2C and myogenic differentiation independent of its role in modulating caspase 3 targeted cleavage events, further elucidation of which is outside the scope of this thesis and was not further examined.

5.3: CK2 phosphorylates Pax7 at serine 201

To examine the direct role of CK2 in modulating caspase 3 cleavage of Pax7 we looked for potential CK2 phosphorylation sites in the Pax7 protein. The Pax7 amino acid sequence contains two evolutionarily conserved serine residues (S201 and S205) which are consistent with a CK2 consensus sequence, and in close proximity to the caspase targeted aspartic acid residue at position D208 (Figure 14A). To confirm Pax7 is a direct target of

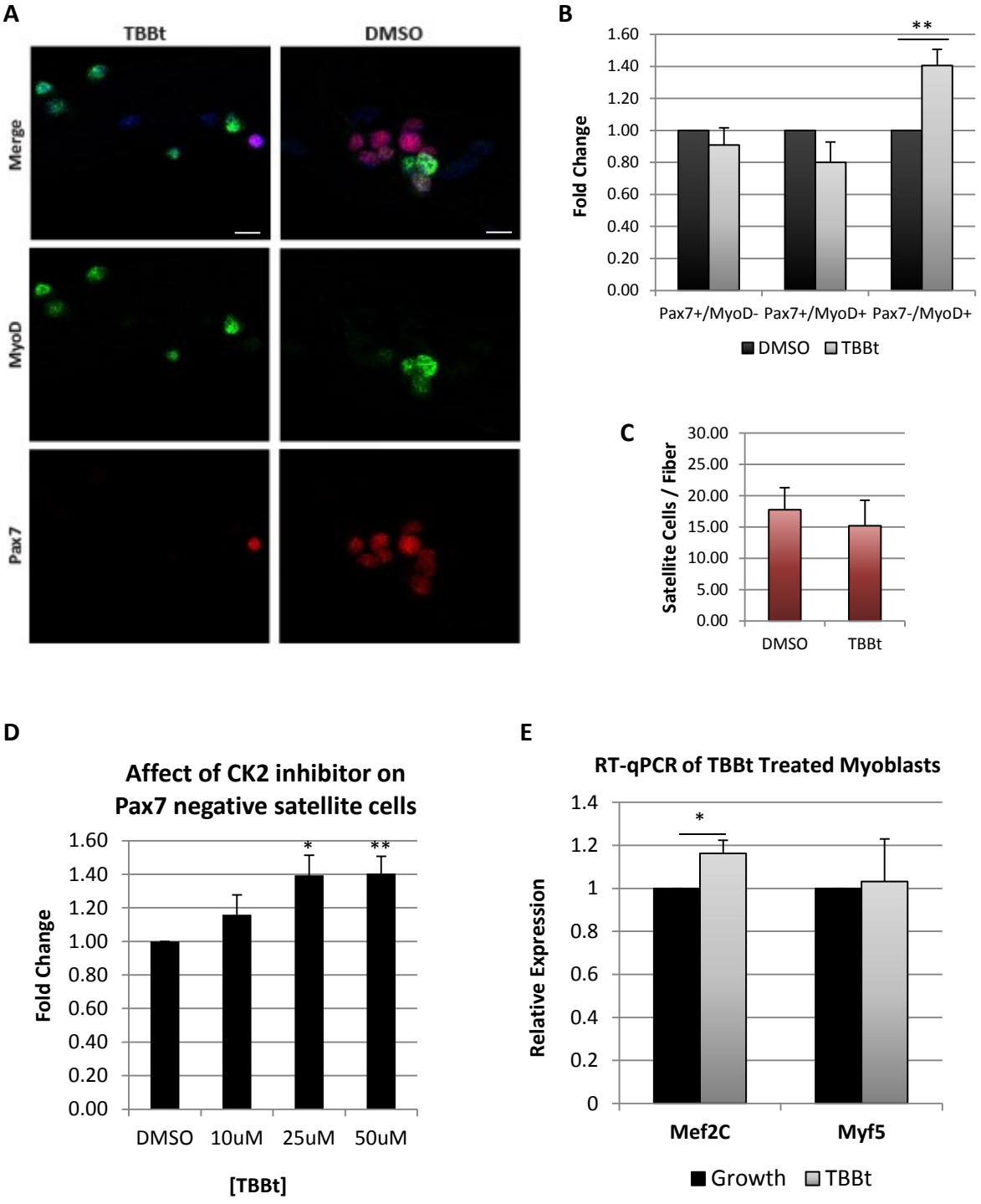
A
TBBt
DMSO
Merge
MyoD
Pax7
B
**
Fold Change
1.60
1.40
1.20
1.00
0.80
0.60
0.40
0.20
0.00
Pax7+/MyoD-
Pax7+/MyoD+
Pax7-/MyoD+
DMSO
TBBt
C
Satellite Cells / Fiber
30.00
25.00
20.00
15.00
10.00
5.00
0.00
DMSO
TBBt
D
Affect of CK2 inhibitor on
Pax7 negative satellite cells
Fold Change
1.60
1.40
1.20
1.00
0.80
0.60
0.40
0.20
0.00
*
**
DMSO
10uM
25uM
50uM
[TBBt]
E
RT-qPCR of TBBt Treated Myoblasts
Relative Expression
1.4
1.2
1
0.8
0.6
0.4
0.2
0
*
Mef2C
Myf5
Growth
TBBt

Figure 19 - Casein Kinase 2 (CK2) inhibition promotes satellite cell differentiation. (A) Individual fibers were incubated in the presence of the CK2 inhibitor TBBt (50μM) or DMSO and stained with αPax7 (red) and αMyoD (green). (B) Quantification of the number of satellite cells expressing each marker expressed as fold change relative to DMSO control. TBBt treated fibers had a significant increase in the number of differentiating (Pax7-/MyoD+) satellite cells. (C) There was no change in the number of satellite cells per fiber in treated and control conditions. (D) Fibers were incubated with various concentrations of the CK2 inhibitor TBBt for 72 hours. The number of Pax7-/MyoD+ (differentiating) satellite cells was quantified, indicating a dose-dependent effect of the inhibitor on increasing the number of cells in this population. (E) FACS isolated satellite cells were treated with TBBt (50μM) for 24 hours and collected for RT-PCR analysis, indicating an increase in Mef2C but not Myf5 expression. Error bars represent SEM. *$p<0.05$; **$p<0.005$, unpaired student t-test. Scale bars are 10μM.

CK2 we performed an *in vitro* kinase assay, observing phosphorylation of Pax7 protein which was completely blocked by addition of the CK2 inhibitor TBBt (Figure 20A). It is of note there was low levels of phosphorylation detected in the aliquot that contained only the recombinant Pax7 protein (without the addition of holo-CK2) that was purified via baculovirus. To determine if there was a kinase present in the purified protein we submitted an aliquot for Mass Spectrometry analysis. We identified traces of insect CK2 (both α and β subunits) in our sample that we believe is responsible for this low level of background detection. Importantly, both the CK2 specific phosphorylation, as well as all traces of background phosphorylation, was completely inhibited by addition of the CK2 inhibitor TBBt confirming the specific phosphorylation of Pax7 by CK2. Point mutations of Pax7 at S201 or S205 revealed that only S201 in recombinant Pax7 protein was directly phosphorylated by CK2 (Figure 20B) (This experiment was provided by Dr. Yoichi Kawabe in the Rudnicki lab). The specificity of this phosphorylation event was confirmed via Mass Spectrometry peptide mapping of Pax7 protein following incubation with CK2 (Figure 20C).

5.4: Phosphorylation of Pax7 via CK2 results in an inhibition of caspase 3 cleavage

Next, we tested whether prior CK2 phosphorylation of recombinant Pax7 was sufficient to inhibit cleavage via active-caspase 3. Interestingly, CK2 phosphorylation of Pax7 resulted in the generation of a partial cleavage of wild-type Pax7, compared to the cleavage products generated from unphosphorylated Pax7 protein (Figure 21A). This result suggested that CK2-mediated phosphorylation of Pax7 at S201 may shield only one of the caspase cleavage sites. To identify the CK2-protected caspase cleavage site we tested the D187A and D208A single Pax7 mutants in the same serial kinase/cleavage assay utilized above. CK2 phosphorylation followed by caspase 3 incubation of the D187A mutant

displayed a similar cleavage pattern to unphosphorylated Pax7, whereas the caspase cleavage products generated from the D208A mutant were unaffected by a prior CK2 mediated phosphorylation event (Figure 21A). This experiment revealed that CK2 phosphorylation at S201 was sufficient to block caspase 3 cleavage at a single cleavage site, D208 (Figure 21B).

Together these results demonstrate a physiologic interaction between CK2 and caspase 3 in the control of Pax7 protein stability. A remaining question to be answered is if one or both caspase 3 specific cleavage events occurs *in vivo* and the physiological role of having two caspase 3 cleavage sites in such close proximity to each other and under different regulatory mechanisms. We predict additional kinase(s) are required to phosphorylate Pax7 to either directly prevent caspase cleavage or prime the protein for additional phosphorylation events as seen in previous work published by Hollenbach and colleagues (Dietz et al., 2011).

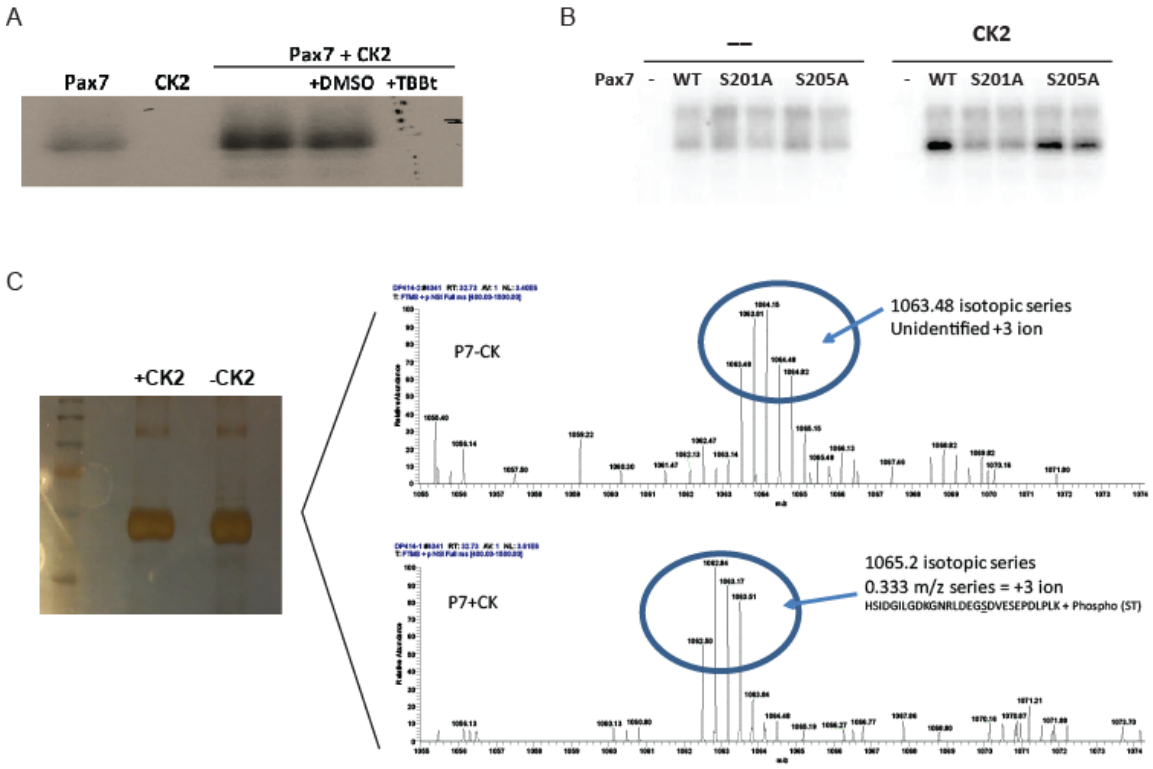

Figure 20 - Casein Kinase 2 (CK2) phosphorylates Pax7 at S201. (A) Autoradiography of recombinant Pax7 protein shows Pax7 is phosphorylated by CK2, which is completely lost by addition of the CK2 inhibitor TBBt (50µM). (B) An *in vitro* kinase assay of wild-type Pax7 or Pax7 with site mutations at S201A or S205A indicating loss of phosphorylation in the S201A mutant only (panel provided by Yoichi Kawabe). (C) Recombinant Pax7 was subjected to global dephosphorylation via Calf Intestinal Phosphatase (CIP) and subsequent phosphorylation with CK2 (+CK2) or buffer only (-CK2). Reactions were processed for LC-MS/MS and MASCOT analysis which revealed a phosphorylated event on S201 in the +CK2 sample which was absent from the –CK2 sample.

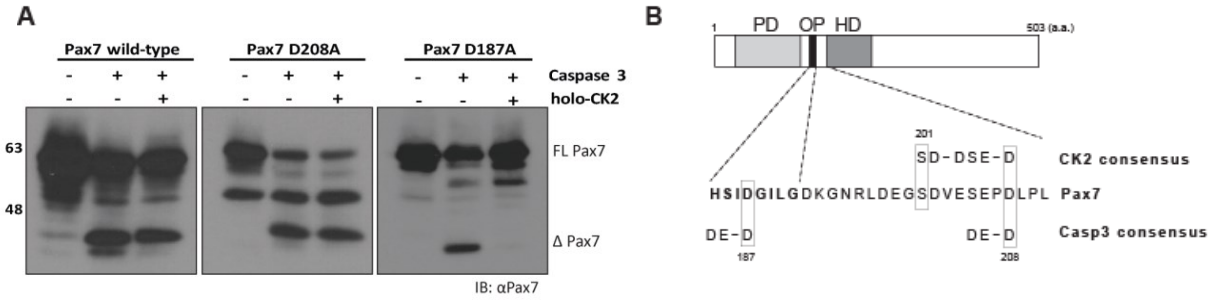

Figure 21 – Casein Kinase 2 (CK2) phosphorylation restricts caspase 3 cleavage of Pax7 protein at D208. (A) Recombinant Pax7 (Pax7 wild-type, Pax7 D208A mutant or D187A mutant) was subjected to an *in vitro* (cold) kinase assay with holo-CK2 (containing both the α and β subunit). Aliquots from each reaction were then subjected to caspase 3 cleavage and to SDS-PAGE and western blot analysis using αPax7. Cleavage of the D187A mutant was impaired by pre-incubation with CK2. (D) Schematic of Pax7 protein indicating the caspase 3 cleavage sites as well as the CK2 phosphorylation site.

CHAPTER 6

6.0 Discussion

6.0: General Discussion

Caspase 3 activation is an essential cue for promoting differentiation of committed progenitor cells (Dick and Megeney, 2013). This study establishes that caspase 3 also acts at a much earlier step in the life cycle of muscle stem cells, by limiting the self-renewal process. Caspase 3 blocks satellite cell self-renewal by cleavage inactivation of Pax7 protein, a mechanism that is counter balanced by CK2 mediated phosphorylation of Pax7. Blockade of caspase activity extends self-renewal in the satellite cell pool, while inhibition of CK2 leads to increased numbers of differentiation committed cells, revealing that satellite cell fate is strongly influenced by competing post-translational modifications of Pax7.

Caspase 3 has been previously reported to inhibit embryonic stem cell (ESC) self-renewal through targeted cleavage of the pluripotency factor Nanog (Fujita et al., 2008). Therefore, it is reasonable to conclude that a similar dichotomous phosphorylation/cleavage modification of Nanog controls ESC self-renewal, with CK2 and caspase 3 acting as the respective competing enzymes. We speculate that the caspase 3/CK2 targeting of self-renewal factors is a broadly conserved phenomenon, affecting cell fate determination across all lineages.

6.1: Regulation of stem cell fate via caspase 3 through targeted cleavage of transcription factors and transcriptional co-regulators.

In organisms with a high turnover of cells, stem cells must be strictly regulated to ensure a balance between the preservation of the stem cell pool and differentiation to replace mature cells lost due to injury, disease or wear. Our data support a novel role for proteases, in regulating the stem cell compartment. In addition to modulating a variety of signaling

pathways, our data illustrate that caspase proteases direct cleavage of a transcription factor, Pax7, which leads to an inhibition of stem cell self-renewal.

Our findings that caspase 3 acts as a mediator of stem cell fate, down-stream of satellite cell/myogenic commitment, extends prior observations that Pax7 is dispensable for satellite cell specification (Oustanina et al., 2004). Following the identification of Pax7 in satellite cells, there has been considerable debate regarding its core function. Contradictory reports on the presence/absence of satellite cells in the Pax7 null mouse have questioned its role in satellite cell specification (Oustanina et al., 2004; Relaix et al., 2006; Seale et al., 2000). However, it is now widely recognized that satellite cells do exist in their niche despite loss of Pax7 expression, where they are gradually lost during the first few weeks of age (Oustanina et al., 2004; Zammit et al., 2006). These observations shifted the focus of Pax7 from one in specification to a self-renewal regulatory factor, associating the loss of satellite cells to an inability to reconstitute the niche following satellite cell activation associated with post-natal growth. Second, conditional knockout studies have claimed loss of Pax7 after a certain age (P20 in the mouse) does not affect viability and that these animals retain effective regeneration capacity (Lepper et al., 2009). Subsequent observations have disproven this claim, indicating loss of Pax7 at any age results in loss of the satellite cell compartment (Gunther et al., 2013; von Maltzahn et al., 2013). These observations are consistent with *in vitro* studies indicating loss of Pax7 results in spontaneous cell differentiation or death (Relaix et al., 2006).

Here we show inhibition of caspase 3, resulting in persistent Pax7 expression does not alter the satellite "stem" cell compartment based on observations of the Myf5-YFP lineage marker (Figure 8), which constitutes about 10% of quiescent satellite cell (Kuang et al., 2007). Maintenance of a Myf5 negative satellite "stem" cell occurs via asymmetric cell

divisions and precludes the decision of a cell to terminally differentiate. The persistence of a long-term repopulating cell, along with committed progenitors, has been documented for other types of adult stem cells and is required for maintenance of genomic integrity in long lived cells (Milyavsky et al., 2010). Although persistence of Pax7 expression is likely required to inhibit differentiation in both cell types, the presence of satellite cells in the Pax7 null mouse indicate additional, yet minor sources for the origin of the stem cell compartment. Whether or not these satellite cells represent a Myf5-YFP+ or Myf5-YFP- population has not been determined. We surmise that, the increased propensity for self-renewal following caspase 3 inhibition (Figure 7) represents a role for Pax7 in the inhibition of differentiation in committed progenitors. The corollary to this argument is that Pax7 promotes a proliferative phase of cell expansion and ensures self-renewal of this population by allowing them to return to a quiescent state, as would occur during regeneration. Exogenous activation of caspase 3 via Pac1 further supports this role, which demonstrates that a loss of Pax7 expression is commensurate with a decrease in satellite cell self-renewal (Figure 9 and 10).

The cohort of endogenous and exogenous cues that determine satellite cell self-renewal or differentiation remain largely undetermined yet our results identify caspase 3 as one endogenous factor that modifies stem cell fate through direct cleavage and removal of Pax7 protein (Figure 11 and 12). Our observations are reminiscent of a recent study in which caspase 3 was found to target the transcription factor Nanog, a known transducer of the pluripotent state and important regulator of ESC self-renewal (Fujita et al., 2008). Here, loss of caspase 3 in ESCs displayed enhanced self-renewal at the expense of differentiation. As both Pax7 and Nanog are known to promote their own transcription (Fujita et al., 2008; Seale et al., 2004), these findings support a mechanism by which stem cells exploit caspases for rapid and specific deactivation of pluripotent factors to disrupt the autoregulatory circuit that

governs self-renewal in these cells. Such an autoregulatory loop may exist in myogenic progenitors, as treatment with the caspase 3 inhibitor z.DEVD.fmk results in a significant increase in Pax7 mRNA expression following 24hrs of differentiation (Larsen, B., unpublished data).

In light of these observations, caspase targeting of transcription factors may represent a general mechanism to control cell fate in a variety of stem and progenitor cells. Intriguing is the site of caspase cleavage in these two, as of yet identified, caspase targets between two functional domains. The question remains as to whether the position of the caspase cleavage site is functionally relevant or a coincidence due to the accessibility of these highly flexible and exposed linkers. Here we identify two caspase 3 cleavage sites at amino acids D187 and D208, both of which reside between the paired domain (N-terminal) and the homeodomain/transactivation domain (C-terminal) of Pax7 (Figure 14). In ESCs, Nanog is cleaved via caspase 3 at amino acid D63 separating the N-terminal/transcriptional interference domain from the homeodomain/ transactivation domain (Fujita et al., 2008). The interaction between Nanog and transcriptional co-activators via its C-terminal domains has been hypothesized to promote expression of self-renewal/pluripotency genes. Alternatively, interactions with transcriptional repressors via its N-terminal domain is thought to suppress lineage-specific differentiation genes (Chang et al., 2009; Pan and Pei, 2003). Although the functional relevance of cleaved Nanog remains to be addressed, an *in vitro* study demonstrated truncated Nanog, missing its N-terminal domain, enhanced its transcriptional activity on the Oct4 promoter (Chang et al., 2009). Future studies will be required to determine if this arrangement of dual transactivators, separated by a caspase 3 cleavage site, may confer the ability of Nanog to regulate genes critical for both pluripotency and differentiation.

The findings presented here establish that the Pax7 fragments produced via caspase 3 cleavage retain no transcriptional activity on the *Myf5* promoter (Figure 16). Based on known functions for Pax7 domains, we predicted the N-terminal fragment containing the Pairedbox domain, would act in a dominant-negative fashion as the Paired domain is thought to constitute the DNA binding domain of Pax7 (Chi and Epstein, 2002). This model would predict that a separated paired domain would interact with DNA independent of its transcriptional activity, competing with wild-type protein for substrate binding, effectively blocking expression of its own transcriptional targets. By contrast, we saw no evidence of this occurring on the *Myf5* promoter when co-expressing wild-type Pax7 and the N-terminal fragment of Pax7. Interestingly, we failed to detect appreciable levels of endogenous cleavage fragments via western blot during myogenic differentiation, suggesting such fragments do not exert dominant-negative effects because they are rapidly degraded. Such a mechanism is consistent with the N-end rule pathway which serves to label proteins for rapid degradation via the proteasome pathway via their N-terminal residue (Piatkov et al., 2012). As such, caspase cleavage may lead to exposure of the appropriate N-terminal residue, targeting the C-terminal fragment for identification and degradation via the N-end rule pathway. Nevertheless, this hypothesis does not account for the N-terminal fragment of Pax7, which may persist in the cell. Indeed, the data presented here are inconclusive with regards to the functional relevance of the N-terminal Pax7 fragment. Further work should be conducted to follow up on this supposition to determine a physiological role, if any, for truncated Pax7. A technical limitation to detecting endogenous N-terminal Pax7 fragment is the lack of commercially available antibodies for Pax7 N-terminal to the D187 cleavage site. Therefore, we suggest the use of over-expression studies to determine the transcriptional

activities of this fragment as well as its DNA and protein binding profile compared to wild-type Pax7.

The necessity for a rapid decrease in Pax7 levels following induction of differentiation suggest that several mechanisms may exist to suppress its expression. At the transcript level, MyoD mediated expression of two miRNAs, miR-1 and miR-206, target Pax7 mRNA resulting in a decrease in gene synthesis (Chen et al., 2010). In proliferating myoblasts these miRNAs are regulated by the epigenetic repressor YY1 (Yin Yang 1), which recruits the Polycomb complex (PCR2) to block transcription (Lu et al., 2012). Interestingly, YY1 has been shown to be cleaved by Caspase 7 in apoptotic conditions in HEK293 cells, an event which is blocked by CK2 phosphorylation of YY1 (Riman et al., 2012). Based on these observations it is a reasonable conjecture that caspase activation may act at an additional level to repress Pax7 translation through cleavage of YY1, resulting in the derepression of miR-1 and miR-206. In contrast with this supposition is the observation that YY1 is required for the p38-mediated recruitment of the PCR2 complex (specifically the enzymatic subunit EZH2) to the Pax7 promoter resulting in repressive epigenetic marks limiting its expression (Palacios et al., 2010). Together, these observations suggests a dynamic role for YY1 in mediating Pax7 expression during myogenesis, either positively via repression of miR-1 and miR-206 in proliferating myoblasts or negatively via repression of Pax7 itself in differentiating myoblasts. Whether or not YY1 is regulated by the caspase/CK2 axis in this context remains to be determined. The indication that truncated YY1 retains some function following caspase cleavage, resulting in removal of the transactivation domain (Krippner-Heidenreich et al., 2005), may explain the divergence in its apparent functions pre- and post-caspase activation.

The findings presented here support a role for caspase 3 in the cleavage inactivation of Pax7 protein during the commitment phase of satellite cells to terminal differentiation. Maintenance of Pax7 expression in a small percent of these cells is necessary for their return to quiescence and self-renewal (Olguin and Olwin, 2004). A significant loss in this population due to deregulated caspase 3 activation (or Pac1 stimulation) would result in a loss of self-renewal, exhaustion of the satellite cell pool and ultimately a defect in skeletal muscle repair. Further *in vivo* examination would be required to confirm a repair defect.

6.2: Casein Kinase 2 (CK2) as a regulator of caspase 3 activity during stem cell differentiation.

Here we demonstrate a CK2-dependent mechanism which regulates caspase 3 activity at the level of post-translational modifications on the target protein. Our *in vitro* analysis revealed CK2 phosphorylates Pax7 at S201 and that phosphorylated Pax7 is resistant to caspase 3 cleavage at site D208 (Figure 20 and 21). This is in line with previous observations demonstrating CK2 phosphorylated proteins are resistant to caspase 3-mediated cleavage (Duncan et al., 2010). Recently, a bioinformatics approach determined CK2 and caspase 3 have similar and often overlapping consensus sequences (Duncan et al., 2011) suggesting they may act in the same regulatory pathway mediating protein stability. This mechanism is critical to control a broad range of cellular functions that have been attributed to caspase 3, including stimulation of apoptosis as well as the induction of cell differentiation. Therefore, caspase activity must be tightly regulated to ensure proper development and avoidance of disease (Lockshin and Zakeri, 2007). For example, loss of caspase inhibition leading to inadvertent caspase activation results in degenerative diseases such as Alzheimer's, while a block in caspase activation or insensitization to caspase

mediated cell death is a hallmark of many cancer cells. Additionally, the advent of caspases in non-death functions further highlights the requirement for a finely regulated mechanism which mediates caspase activity. The targeting of CK2 to caspase substrates, including caspase 3 itself, may be a critical component to ensure appropriate caspase function.

Phosphorylation of protein substrates can mediate susceptibility to caspase 3 directed cleavage by various mechanisms. First, phosphorylation could result in a conformational change of the tertiary structure of the protein which impedes the ability of caspase 3 to access the cleavage site. Moreover, the phosphorylation event could promote binding of a cofactor/binding partner which blocks the cleavage site. Interestingly, the caspase 3 cleavage sites identified in this study reside within (D187) or close to (D208) in the Pax7 octapeptide. The octapeptide is a highly conserved eight amino acid domain located between the paired domain and the homeobox domain of all Pax proteins (with the exception of Pax4 and Pax6) (Chi and Epstein, 2002). Although very little is known about this small domain it is thought to harbour protein binding capabilities (Eberhard et al., 2000). This agrees with the second model presented above by which the phospho-dependent binding of a secondary protein blocks caspase 3 cleavage of Pax7. Although CK2 phosphorylation was sufficient to block cleavage at D208, it is difficult to attribute significance of this phosphorylation event to cleavage of D187. Further studies will be required to attribute physiological relevance to this site.

CK2 is a ubiquitously expressed enzyme, which is constitutively active in many cell types (Turowec et al., 2010). Therefore, the regulation of the CK2 phosphoproteome is likely dependent on the matching dephosphorylation of its targets. What the regulatory phosphatases are, and how they manage the efficacy of CK2 inhibition remains to be clarified.

6.3: A role for CK2 in myogenesis

CK2 is present in proliferating and differentiating myoblasts (Johnson et al., 1996), as well as during satellite cell activation/proliferation (Figure 18). CK2 has been well studied for its role in mediating transcription factor activity including several MRFs (Hunter and Karin, 1992; Johnson et al., 1996). Phosphorylation via CK2 directly enhances Myf5 transcriptional activity (Winter et al., 1997) and Mef2C DNA binding (Molkentin et al., 1996) and over expression of CK2 results in enhanced MyoD and MRF4 transcriptional activity (Johnson et al., 1996). In addition, phosphorylation of Pax3 has been implicated in enhancing its DNA binding and transcriptional activity (Amstutz et al., 2008). The role CK2 plays in regulating the protein stability of these factors has yet to be studied for all but Pax3 (Dietz et al., 2009). Pax3 is phosphorylated at S205 in proliferating myoblasts in a CK2-dependent manner. This phosphorylation is quickly lost upon induction of differentiation (within 15min) and is thought to be related to its subsequent degradation at around 10 hours post-induction (Dietz et al., 2009). Although this study did not discuss the mode of degradation, we predict it may be targeted by caspase 3, similar to what we have shown here for its paralogue Pax7. Consistent with this theory is the presence of two conserved caspase 3 consensus sites near the site of phosphorylation at D206 and D212 (personal observations). The lack of phosphor specific antibodies for Pax7 precluded an assessment of Pax7 phosphorylation *in vivo* and *in situ*. Nevertheless, based on the findings for Pax3 and the enhanced protein stability shown here for CK2-phosphorylated Pax7, we predict the loss of Pax7 protein during differentiation is mediated via a dephosphorylation event at S201 followed by caspase 3 cleavage.

CK2 phsophorylation of Pax proteins may also impact the etiology and biology of skeletal muscle cancer. Importantly, both Pax3 and Pax7 play a role in the tumorigenicity of

a rare childhood muscle cancer termed alveolar rhabdomyosarcoma (ARMS). Transformed cells contain a characteristic t(2;13)(p35;q14) or t(1;13)(p36;q14) chromosomal translocation resulting in the fusion gene Pax3-FOXO1 or Pax7-FOXO1 respectively (Barr, 2001). The resultant protein contains the DNA binding and protein-protein interacting domains of the Pax3/7 protein with its transcriptional coactivator domain being replaced by the partial DNA binding domain and potent transcriptional activation domain of FOXO1. In addition to promoting cell survival and proliferation the fusion protein has greater post-transcriptional stability and persists in myogenic cells even when subjected to differentiation cues (Dietz et al., 2009). In contrast with what was observed for wild-type Pax3, the Pax3-FOXO1 fusion protein failed to lose its phosphorylation at S205 following induction of differentiation. It is not determined whether the persistence of the phosphorylation on S205 on Pax3-FOXO1 is a *result* of the highly proliferative state of the transformed cells or the *cause* of the inability of these cells to terminally differentiate. In support of the latter, our results presented here demonstrate inhibition of CK2 promotes satellite cell differentiation (Figure 19). This suggests a possible mechanism by which the Pax3/7-FOXO1 fusion protein escapes degradation and inhibits differentiation contributing to the tumorigenicity of these cells, in addition to identifying novel targets for the development of therapies for the treatment of ARMS. The question remains as to why there is a difference in phosphorylation patterns between wild-type Pax3/7 and their corresponding fusion proteins. Among possible explanations is the increase in CK2 seen in these tumor cells (Izeradjene et al., 2004) and/or the loss of a putative phosphatase promoting a dephosphorylation event allowing for the predicted caspase 3-mediated degradation.

6.4: Future Directions

One outstanding question, which is critical to any evaluation of caspases in the context of non-death roles, is why doesn't caspase 3 activity self-amplify, as seen in an apoptosis setting? Several theories have been put forth on the matter, including caspases being restricted to a subcellular compartment, as is seen during spermatid differentiation (Kaplan et al., 2010); the regulation of caspase activity directly, through their interactions with inhibitors such as the IAP family of proteins and the role of the XIAP inhibitor ARTS (unpublished results); and finally, presented in detail here, is the role of post-translational modifications on caspase substrates, such as phosphorylation. The role of CK2 is of particular interest as it phosphorylates and regulates cleavage of pro-caspase 3 itself (Turowec et al., 2014) providing a mechanism to limit its own auto-activation. In addition, caspase 9, p53 and Bid have all be shown to be phosphorylated by CK2 (Bian et al., 2013) providing several levels of regulation in the caspase activation pathway. It is likely these pathways of regulation are not mutually exclusive and further investigation into the crosstalk between these pathways in a non-death setting will aid our understanding of how caspases can mediate distinct cell fates.

The distinct and coinciding roles of the effector caspases is also of particular interest based on the known overlap in substrate specificity between caspase 3, 6 and 7. Although caspase 3 is absolutely required for differentiation of certain cell types, as evident by the severe hydro exencephaly seen in the caspase 3 null mouse (Fernando et al., 2005), these mice are developmentally viable. This is believed to be due to the functional overlap between caspase 3 and 7 (and to a lesser extent caspase 6) for a large cohort of substrates, leading to compensation following loss of only one of these caspases. In support of this notion, the caspase 3/7 double knockout mouse is lethal immediately following birth (Lakhani et al.,

2006) and the severity of the caspase $3^{-/-}$ mouse is dependent on the genetic background of the mouse and the levels of endogenous caspase 7 present (Houde et al., 2004). As the effector caspases are very similar in regards to their structure and activation some of the reagents used in this study to inhibit (z.DEVD.fmk) or activate (Pac1) caspase 3 may also affect caspase 7. It will be interesting to examine the role of caspase 7 in the context of cleavage-mediated degradation of Pax7 during satellite cell differentiation and whether or not the cleavage sites are targeted with similar specificity and kinetics as we have presented here for caspase 3.

With specific regard to this project it will be important to follow up on a functional role for the Pax7 cleavage fragments. Previous observations support our findings that dominant-negative Pax7 preferentially affects MyoD (Relaix et al., 2006). Furthermore, Pax7 (specifically the homeodomain) is critical in directing MyoD function, negatively regulating myogenin expression independent of Pax7 transcriptional activity as well as MyoD protein stability (Olguin et al., 2007). Future experiments should focus on the expression of the dominant-negative constructs, their cellular localization and potential binding partners.

As the delicate balance between Pax7 and MyoD protein has been shown to play a critical role in whether or not a satellite cell self-renews or differentiates, it would be interesting to further investigate the mechanism behind how caspases mediate this balance. In this regard, there are two interesting regulatory links which may provide insight. First is the observation that Pax3 promotes the expression of the anti-apoptotic factors BcL-2 and BcL-xL and that Pax3 itself is negatively regulated by MyoD (Hirai et al., 2010). A MyoD mediated down-regulation of Pax3 could provide the derepression of the caspase pathway necessary for the activation of caspase 9/3 and thus degradation of Pax7 protein. Second is the observation that siRNA mediated knock-down of myogenin showed sustained Pax7

protein levels, suggesting myogenin negatively regulates Pax7 protein stability (Olguin et al., 2007). A mechanism for myogenin in regulating caspase 3 activity has yet to be shown, however evidence that myogenin protein itself is unaffected by caspase 3 inhibition (Fernando et al., 2002) suggests it may be upstream of caspases during myogenesis.

6.5: Conclusion

Taken together our results support a model in which CK2 and caspase 3 act in an adversarial relationship, CK2 targeting and inhibiting caspase directed cleavage of Pax7, which acts to maintain satellite cell self-renewal capacity (Figure 22). The removal of Pax7 from the differentiating cell is critical as prolonged and/or over-expression of this transcription factor impairs the proper differentiation of activated myoblasts and thus can negatively affect the efficient repair and regeneration of skeletal muscle (Olguin and Olwin, 2004). Conversely, loss of stem cell self-renewal and the satellite cell pool could negatively affect the long-term health of the muscle resulting in muscle weakening and degeneration over time. This work will greatly contribute to establishing a role for caspase 3 in skeletal muscle development and also to our overall understanding of satellite stem cell regulation.

This study is the first to demonstrate that caspase 3 limits self-renewal of a lineage restricted stem/progenitor cell. We speculate that the caspase 3/CK2 targeting of self-renewal factors is a broadly conserved phenomenon, affecting cell fate determination across all lineages. Based on the evidence collected thus far, from our group and others, it is becoming evident apoptotic proteins have emerged as key regulatory proteins in a wide variety of cellular contexts, independent of inducing cell death (Dick and Megeney, 2013). The results presented in this thesis expand the non-death attributes for caspase proteases, confirming a role for these proteins in the management of stem cell self-renewal.

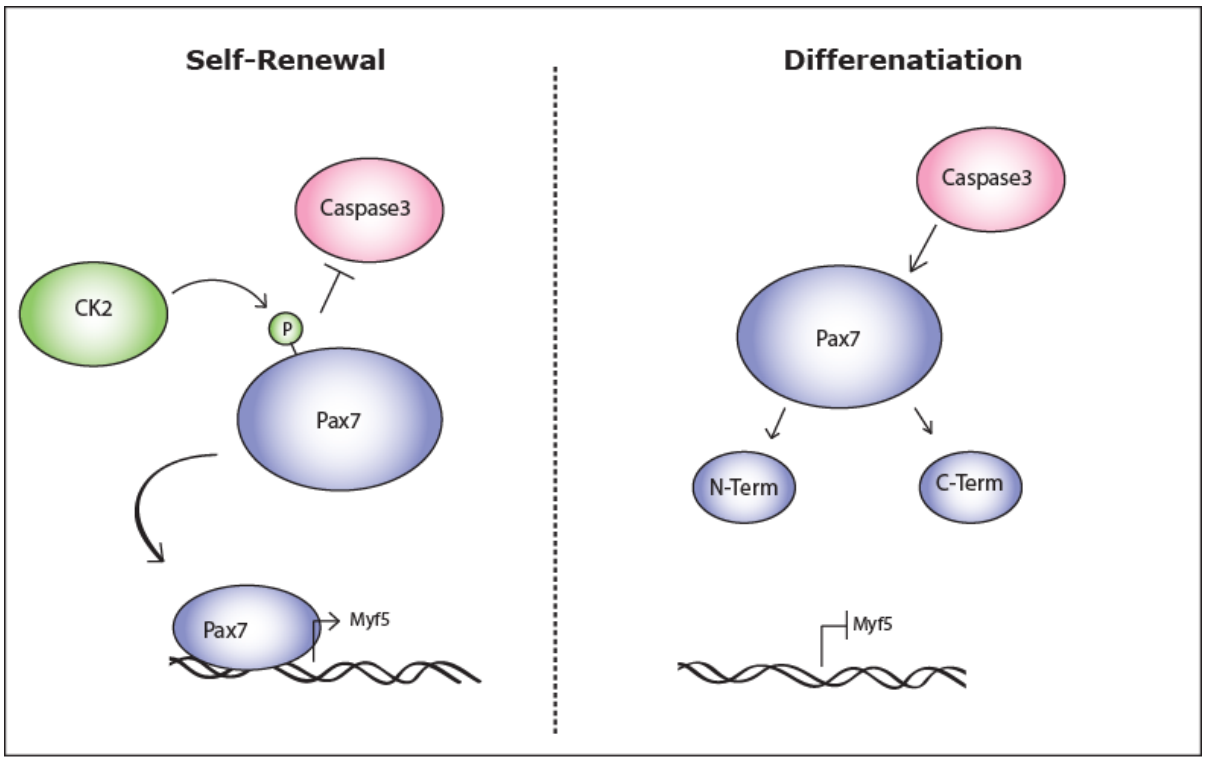

Figure 22 – Working model. During satellite cell self-renewal CK2 phosphorylates Pax7 to protect it from caspase 3 cleavage and maintain protein stability. During myogenic differentiation an unphosphorylated Pax7 protein is susceptible to caspase 3 cleavage resulting in the production of two fragments which hinders the protein inactive.

References

Abdul-Ghani, M., Dufort, D., Stiles, R., De Repentigny, Y., Kothary, R., and Megeney, L.A. (2011). Wnt11 promotes cardiomyocyte development by caspase-mediated suppression of canonical Wnt signals. Mol Cell Biol *31*, 163-178.

Abdul-Ghani, M., and Megeney, L.A. (2008). Rehabilitation of a contract killer: caspase-3 directs stem cell differentiation. Cell stem cell *2*, 515-516.

Aizenman, E., Engelberg-Kulka, H., and Glaser, G. (1996). An Escherichia coli chromosomal addiction module regulated by guanosine [corrected] 3',5'-bispyrophosphate a model for programmed bacterial cell death. Proceedings of the National Academy of Sciences of the United States of America *93*, 6059-6063.

Alfaro, L.A., Dick, S.A., Siegel, A.L., Anonuevo, A.S., McNagny, K.M., Megeney, L.A., Cornelison, D.D., and Rossi, F.M. (2011). CD34 promotes satellite cell motility and entry into proliferation to facilitate efficient skeletal muscle regeneration. Stem cells *29*, 2030-2041.

Amstutz, R., Wachtel, M., Troxler, H., Kleinert, P., Ebauer, M., Haneke, T., Oehler-Janne, C., Fabbro, D., Niggli, F.K., and Schafer, B.W. (2008). Phosphorylation regulates transcriptional activity of PAX3/FKHR and reveals novel therapeutic possibilities. Cancer Res *68*, 3767-3776.

Arama, E., Agapite, J., and Steller, H. (2003). Caspase activity and a specific cytochrome C are required for sperm differentiation in Drosophila. Developmental cell *4*, 687-697.

Asally, M., Kittisopikul, M., Rue, P., Du, Y., Hu, Z., Cagatay, T., Robinson, A.B., Lu, H., Garcia-Ojalvo, J., and Suel, G.M. (2012). Localized cell death focuses mechanical forces during 3D patterning in a biofilm. Proceedings of the National Academy of Sciences of the United States of America *109*, 18891-18896.

Bader, M., Arama, E., and Steller, H. (2010). A novel F-box protein is required for caspase activation during cellular remodeling in Drosophila. Development *137*, 1679-1688.

Bader, M., Benjamin, S., Wapinski, O.L., Smith, D.M., Goldberg, A.L., and Steller, H. (2011). A conserved F box regulatory complex controls proteasome activity in Drosophila. Cell *145*, 371-382.

Bai, L., Smith, D.C., and Wang, S. (2014). Small-molecule SMAC mimetics as new cancer therapeutics. Pharmacology & therapeutics.

Barr, F.G. (2001). Gene fusions involving PAX and FOX family members in alveolar rhabdomyosarcoma. Oncogene *20*, 5736-5746.

Bayles, K.W. (2007). The biological role of death and lysis in biofilm development. Nature Reviews Microbiology *5*, 721-726.

Beauchamp, J.R., Heslop, L., Yu, D.S.W., Tajbakhsh, S., Kelly, R.G., Wernig, A., Buckingham, M., Partridge, T.A., and Zammit, P.S. (2000). Expression of CD34 and Myf5 defines the majority of quiescent adult skeletal muscle satellite cells. Journal of Cell Biology *151*, 1221-1233.

Bentzinger, C.F., Wang, Y.X., and Rudnicki, M.A. (2012). Building muscle: molecular regulation of myogenesis. Cold Spring Harbor perspectives in biology *4*, a008342.

Bentzinger, C.F., Wang, Y.X., von Maltzahn, J., Soleimani, V.D., Yin, H., and Rudnicki, M.A. (2013). Fibronectin regulates Wnt7a signaling and satellite cell expansion. Cell stem cell *12*, 75-87.

Berthelet, J., and Dubrez, L. (2013). Regulation of Apoptosis by Inhibitors of Apoptosis (IAPs). Cells *2*, 163-187.

Beug, S.T., Tang, V.A., LaCasse, E., Cheung, H.H., Beauregard, C.E., Brun, J., Nuyens, J.P., Earl, N., St-Jean, M., Holbrook, J.*, et al.* (2014). Smac mimetics and innate immune stimuli synergize to promote tumor death. Nat Biotechnol *32*, 182-190.

Bian, Y., Ye, M., Wang, C., Cheng, K., Song, C., Dong, M., Pan, Y., Qin, H., and Zou, H. (2013). Global Screen of CK2 Kinase Substrates by an Integrated Phosphoproteomics Workflow. Scientific Reports *3*, 3460.

Boyer, L.A., Lee, T.I., Cole, M.F., Johnstone, S.E., Levine, S.S., Zucker, J.P., Guenther, M.G., Kumar, R.M., Murray, H.L., Jenner, R.G.*, et al.* (2005). Core transcriptional regulatory circuitry in human embryonic stem cells. Cell *122*, 947-956.

Bozhkov, P.V., Smertenko, A.P., and Zhivotovsky, B. (2010). Aspasing out metacaspases and caspases: proteases of many trades. Science signaling *3*, pe48.

Brack, A., Conboy, I.M., Conboy, M.J., Shen, J., and Rando, T.A. (2008). A temporal switch from notch to Wnt signaling in muscle stem cells is necessary for normal adult myogenesis. Cell stem cell *2*, 50-59.

Braun, T., Buschhausen-Denker, G., Bober, E., Tannich, E., and Arnold, H.H. (1989). A novel human muscle factor related to but distinct from MyoD1 induces myogenic conversion in 10T12 fibroblasts. The EMBO journal *8*, 701-709.

Braun, T., Rudnicki, M.A., Arnold, H.H., and Jaenisch, R. (1992). Targeted inactivation of the muscle regulatory gene Myf-5 results in abnormal rib development and perinatal death. Cell *71*, 369-382.

Buckingham, M., Bajard, L., Chang, T., Daubas, P., Hadchouel, J., Meilhac, S., Montarras, D., Rocancourt, D., and Relaix, F. (2003). The formation of skeletal muscle: from somite to limb. J Anat *202*, 59-68.

Burkin, D.J., and Kaufman, S.J. (1999). The alpha7beta1 integrin in muscle development and disease. Cell Tissue Res *296*, 183-190.

Cairns, J. (2006). Cancer nad the immortal strand hypothesis. Genetics *174*, 1069-1072.

Chakkalakal, J.V., Christensen, J., Xiang, W., Tierney, M.T., Boscolo, F.S., Sacco, A., and Brack, A. (2014). Early forming label-retaining muscle stem cells require p27kip1 for maintenance of the primitive state. Development *141*, 1649-1659.

Chang, D.F., Tsai, S.C., Wang, X.C., Xia, P., Senadheera, D., and Lutzko, C. (2009). Molecular characterization of the human NANOG protein. Stem cells *27*, 812-821.

Chargé, S.B., and Rudnicki, M.A. (2004). Cellular and molecular regulation of muscle regeneration. Physiological reviews *84*, 209-238.

Chen, J.F., Tao, Y., Deng, Z., Yan, Z., Xiao, X., and Wang, D.Z. (2010). microRNA-1 and microRNA-206 regulate skeletal muscle satellite cell proliferation and differentiation by repressing Pax7. Journal of Cell Biology *190*, 867-879.

Chen, S., Jin, B., and Li, Y. (2007). TNF-a regulates myogenesis and muscle regeneration by activating p38 MAPK. American journal of physiology Cell physiology *292*, 1660-1671.

Cheng, W., Wang, L., Yang, B., Zhang, R., Yao, C., He, L., Liu, Z., Du, P., Hammache, K., Wen, J.*, et al.* (2014). Self-renewal and Differentiation of Muscle Satellite Cells Are Regulated by the Fas-associated Death Domain. The Journal of biological chemistry *289*, 5040-5050.

Chi, N., and Epstein, J.A. (2002). Getting your Pax straight: pax proteins in development and disease. Trends in Genetics *18*, 41-47.

Choul-Li, S., Leroy, C., Leprivier, G., Laitem, C., Tulasne, D., and Aumercier, M. (2010). Caspase cleavage of Ets-1 p51 generates fragments with transcriptional dominant-negative function. Biochem J *426*, 229-241.

Conradt, B., and Horvitz, H.R. (1998). The C. elegans protein EGL-1 is required for programmed cell death and interacts with the Bcl-2-like protein CED-9. Cell *93*, 519-529.

Cornelison, D.D., Filla, M.S., Stanley, H.M., Rapraeger, A.C., and Olwin, B.B. (2001). Syndecan-3 and syndecan-4 specifically mark skeletal muscle satellite cells and are implicated in satellite cell maintenance and muscle regeneration. Developmental biology *239*, 79-94.

Cossu, G., and Biressi, S. (2005). Satellite cells, myoblasts and other occasional myogenic progenitors: possible origin, phenotypic features and role in muscle regeneration. Semin Cell Dev Biol *16*, 623-631.

D'Amelio, M., Sheng, M., and Cecconi, F. (2012). Caspase-3 in the central nervous system: beyond apoptosis. Trends in neurosciences *35*, 700-709.

Davis, R.L., Weintraub, H., and Lassar, A.B. (1987). Expression of a single transfected cDNA converts fibroblasts to myoblasts. Cell *51*, 987-1000.

de la Vega, L., Hornung, J., Kremmer, E., Milanovic, M., and Schmitz, M.L. (2013). Homeodomain-interacting protein kinase 2-dependent repression of myogenic differentiation is relieved by its caspase-mediated cleavage. Nucleic acids research *41*, 5731-5745.

Dey, B.K., Gagan, J., and Dutta, A. (2011). miR-206 and -486 induce myoblast differentiation by downregulating Pax7. Mol Cell Biol *31*, 203-214.

Dick, S.A., and Megeney, L.A. (2013). Cell death proteins: an evolutionary role in cellular adaptation before the advent of apoptosis. BioEssays : news and reviews in molecular, cellular and developmental biology *35*, 974-983.

Dietz, K.N., Miller, P.J., and Hollenbach, A.D. (2009). Phosphorylation of serine 205 by the protein kinase CK2 persists on Pax3-FOXO1, but not Pax3, throughout early myogenic differentiation. Biochemistry *48*, 11786-11795.

Dietz, K.N., Miller, P.J., Iyengar, A.S., Loupe, J.M., and Hollenbach, A.D. (2011). Identification of serines 201 and 209 as sites of Pax3 phosphorylation and the altered phosphorylation status of Pax3-FOXO1 during early myogenic differentiation. The international journal of biochemistry & cell biology *43*, 936-945.

Duncan, J.S., Turowec, J.P., Duncan, K.E., Vilk, G., Wu, C., Luscher, B., Li, S.S., Gloor, G.B., and Litchfield, D.W. (2011). A peptide-based target screen implicates the protein kinase CK2 in the global regulation of caspase signaling. Science signaling *4*, ra30.

Duncan, J.S., Turowec, J.P., Vilk, G., Li, S.S., Gloor, G.B., and Litchfield, D.W. (2010). Regulation of cell proliferation and survival: convergence of protein kinases and caspases. Biochimica et biophysica acta *1804*, 505-510.

Duszenko, M., Figarella, K., Macleod, E.T., and Welburn, S.C. (2006). Death of a trypanosome: a selfish altruism. Trends in parasitology *22*, 536-542.

Eberhard, D., Jimenez, G., Heavey, B., and Busslinger, M. (2000). Transcriptional repression by pax5 (BSAP) through interaction with corepressors of the Groucho family. The EMBO journal *19*, 2292-2303.

Edison, N., Zuri, D., Maniv, I., Bornstein, B., Lev, T., Gottfried, Y., Kemeny, S., Garcia-Fernandez, M., Kagan, J., and Larisch, S. (2012). The IAP-antagonist ARTS initiates caspase activation upstream of cytochrome C and SMAC/Diablo. Cell death and differentiation *19*, 356-368.

Fabrizio, P., Battistella, L., Vardavas, R., Gattazzo, C., Liou, L.L., Diaspro, A., Dossen, J.W., Gralla, E.B., and Longo, V.D. (2004). Superoxide is a mediator of an altruistic aging program in Saccharomyces cerevisiae. The Journal of cell biology *166*, 1055-1067.

Fabrizio, P., and Longo, V.D. (2008). Chronological aging-induced apoptosis in yeast. Biochimica et biophysica acta *1783*, 1280-1285.

Fernando, P., Brunette, S., and Megeney, L.A. (2005). Neural stem cell differentiation is dependent upon endogenous caspase 3 activity. FASEB *19*, 1671-1673.

Fernando, P., Kelly, J.F., Balazsi, K., Slack, R.S., and Megeney, L.A. (2002). Caspase 3 activity is required for skeletal muscle differentiation. Proceedings of the National Academy of Sciences of the United States of America *99*, 11025-11030.

Florentin, A., and Arama, E. (2012). Caspase levels and execution efficiencies determine the apoptotic potential of the cell. The Journal of cell biology *196*, 513-527.

Frohlich, K.U., and Madeo, F. (2000). Apoptosis in yeast--a monocellular organism exhibits altruistic behaviour. FEBS Letters *473*, 6-9.

Fuchs, Y., and Steller, H. (2011). Programmed cell death in animal development and disease. Cell *147*, 742-758.

Fuentes-Prior, P., and Salvesen, G.S. (2004). The protein structures that shape caspase activity, specificity, activation and inhibition. Biochem J *384*, 201-232.

Fujita, E., Egashira, J., Urase, K., Kuida, K., and Momoi, T. (2001). Caspase-9 processing by caspase-3 via a feedback amplification loop in vivo. Cell death and differentiation *8*, 335-344.

Fujita, J., Crane, A.M., Souza, M.K., Dejosez, M., Kyba, M., Flavell, R.A., Thomson, J.A., and Zwaka, T.P. (2008). Caspase activity mediates the differentiation of embryonic stem cells. Cell stem cell *2*, 595-601.

Galluzzi, L., Kepp, O., Trojel-Hansen, C., and Kroemer, G. (2012). Non-apoptotic functions of apoptosis-regulatory proteins. EMBO reports *13*, 322-330.

Garcia-Fernandez, M., Kissel, H., Brown, S., Gorenc, T., Schile, A.J., Rafii, S., Larisch, S., and Steller, H. (2010). Sept4/ARTS is required for stem cell apoptosis and tumor suppression. Genes & development *24*, 2282-2293.

Gillespie, M.A., Le Grand, F., Scime, A., Kuang, S., Von Maltzahn, J., Seale, V., Cuenda, A., Ranish, J.A., and Rudnicki, M. (2009). p38-γ–dependent gene silencing restricts entry into the myogenic differentiation program. J Cell Biology *187*, 991.

Gomes, D.S., Pereira, M.D., Panek, A.D., Andrade, L.R., and Eleutherio, E.C. (2008). Apoptosis as a mechanism for removal of mutated cells of Saccharomyces cerevisiae: the role of Grx2 under cadmium exposure. Biochimica et biophysica acta *1780*, 160-166.

Gottfried, Y., Rotem, A., Lotan, R., Steller, H., and Larisch, S. (2004). The mitochondrial ARTS protein promotes apoptosis through targeting XIAP. The EMBO journal *23*.

Graves, J.D., Draves, K.E., Gotoh, Y., Krebs, E.G., and Clark, E.A. (2001). Both phosphorylation and caspase-mediated cleavage contribute to regulation of the Ste20-like protein kinase Mst1 during CD95/Fas-induced apoptosis. The Journal of biological chemistry *276*, 14909-14915.

Gunther, S., Kim, J., Kostin, S., Lepper, C., Fan, C.M., and Braun, T. (2013). Myf5-Positive Satellite Cells Contribute to Pax7-Dependent Long-Term Maintenance of Adult Muscle Stem Cells. Cell stem cell.

Hasty, P., Bradley, A., Morris, J.H., Edmondson, D.G., Venuti, J.M., Olson, E.N., and Klein, W.H. (1993). Muscle deficiency and neonatal death in mice with a targeted mutation in the myogenin gene. Nature *364*, 501-506.

Hazan, R., Sat, B., and Engelberg-Kulka, H. (2004). Escherichia coli mazEF-mediated cell death is triggered by various stressful conditions. Journal of bacteriology *186*, 3663-3669.

Hill, S.M., Hao, X., Liu, B., and Nystrom, T. (2014). Life-span extension by a metacaspase in the yeast Saccharomyces cerevisiae. Science *344*, 1389-1392.

Hirai, H., Verma, M., Watanabe, S., Tastad, C., Asakura, Y., and Asakura, A. (2010). MyoD regulates apoptosis of myoblasts through microRNA-mediated down-regulation of Pax3. The Journal of cell biology *191*, 347-365.

Houde, C., Banks, K.G., Coulombe, N., Rasper, D., Grimm, E., Roy, S., Simpson, E.M., and Nicholson, D.W. (2004). Caspase-7 expanded function and intrinsic expression level underlies strain-specific brain phenotype of caspase-3-null mice. The Journal of neuroscience : the official journal of the Society for Neuroscience *24*, 9977-9984.

Hunt, L.C., Upadhyay, A., Jazayeri, J.A., Tudor, E.M., and White, J.D. (2011). Caspase-3, myogenic transcription factors and cell cycle inhibitors are regulated by leukemia inhibitory factor to mediate inhibition of myogenic differentiation. Skeletal muscle *1*, 17.

Hunter, T., and Karin, M. (1992). The regulation of transcription by phosphorylation. Cell *70*, 375-387.

Hutcheson, D.A., Zhao, J., Merrell, A., Haldar, M., and Kardon, G. (2009). Embryonic and fetal limb myogenic cells are derived from developmentally distinct progenitors and have different requirements for beta-catenin. Genes Dev *23*, 997-1013.

Ishizaki, Y., Jacobson, M.D., and Raff, M.C. (1998). A role for caspases in lens fiber differentiation. Journal of Cell Biology *140*, 153-158.

Iyengar, A.S., Loupe, J.M., Miller, P.J., and Hollenbach, A.D. (2012). Identification of CK2 as the kinase that phosphorylates Pax3 at Ser209 in early myogenic differentiation. Biochemical and biophysical research communications *428*, 24-30.

Izeradjene, K., Douglas, L., Delaney, A., and Houghton, J.A. (2004). Influence of casein kinase II in tumor necrosis factor-related apoptosis-inducing ligand-induced apoptosis in human rhabdomyosarcoma cells. Clin Cancer Res *10*, 6650-6660.

Janzen, V., Fleming, H.E., Riedt, T., Karlsson, G., Riese, M.J., Lo Celso, C., Reynolds, G., Milne, C.D., Paige, C.J., Karlsson, S.*, et al.* (2008). Hematopoietic stem cell responsiveness to exogenous signals is limited by caspase-3. Cell stem cell *2*, 584-594.

Johnson, S.E., Wang, X., Hardy, S., Taparowsky, E.J., and Konieczny, S.F. (1996). Casein kinase II increases the transcriptional activities of MRF4 and MyoD independently of their direct phosphorylation. Mol Cell Biol *16*, 1604-1613.

Jones, N.C., Tyner, K.J., Nibarger, L., Stanley, H.M., Cornelison, D.D., Fedorov, Y.V., and Olwin, B.B. (2005). The p38alpha/beta MAPK functions as a molecular switch to activate the quiescent satellite cell. The Journal of cell biology *169*, 105-116.

Kang, J.S., and Krauss, R.S. Muscle stem cells in developmental and regenerative myogenesis. Curr Opin Clin Nutr Metab Care *13*, 243-248.

Kaplan, Y., Gibbs-Bar, L., Kalifa, Y., Feinstein-Rotkopf, Y., and Arama, E. (2010). Gradients of a Ubiquitin E3 Ligase Inhibitor and a Caspase Inhibitor Determine Differentiation or Death in Spermatids. Developmental cell *19*, 160-173.

Kawabe, Y., Wang, Y.X., McKinnell, I.W., Bedford, M.T., and Rudnicki, M.A. (2012). Carm1 regulates Pax7 transcriptional activity through MLL1/2 recruitment during asymmetric satellite stem cell divisions. Cell stem cell *11*, 333-345.

Kissel, H., Georgescu, M.M., Larisch, S., Manova, K., Hunnicutt, G.R., and Steller, H. (2005). The Sept4 septin locus is required for sperm terminal differentiation in mice. Developmental cell *8*, 353-364.

Kobayashi, T., Manno, A., and Kakizuka, A. (2007). Involvement of valosin-containing protein (VCP)/p97 in the formation and clearance of abnormal protein aggregates. Genes to cells : devoted to molecular & cellular mechanisms *12*, 889-901.

Krippner-Heidenreich, A., Walsemann, G., Beyrouthy, M.J., Speckgens, S., Kraft, R., Thole, H., Talanian, R.V., Hurt, M.M., and Luscher, B. (2005). Caspase-dependent regulation and subcellular redistribution of the transcriptional modulator YY1 during apoptosis. Mol Cell Biol *25*, 3704-3714.

Kuang, S., Gillespie, M.A., and Rudnicki, M.A. (2008). Niche regulation of muscle satellite cell self-renewal and differentiation. Cell stem cell *2*, 22-31.

Kuang, S., Kuroda, K., Le Grand, F., and Rudnicki, M.A. (2007). Asymmetric self-renewal and commitment of satellite stem cells in muscle. Cell *129*, 999-1010.

Kuang, S., and Rudnicki, M.A. (2008). The emerging biology of satellite cells and their therapeutic potential. Trends in molecular medicine *14*, 82-91.

Lakhani, S.A., Masud, A., Kuida, K., Porter, G.A., Jr., Booth, C.J., Mehal, W.Z., Inayat, I., and Flavell, R.A. (2006). Caspases 3 and 7: key mediators of mitochondrial events of apoptosis. Science *311*, 847-851.

Lamkanfi, M., Festjens, N., Declercq, W., Vanden Berghe, T., and Vandenabeele, P. (2007). Caspases in cell survival, proliferation and differentiation. Cell death and differentiation *14*, 44-55.

Larisch, S., Yi, Y., Lotan, R., Kerner, H., Eimerl, S., Parks, W.T., Gottfried, Y., Reffey, S.B., de Caesteckert, M.P., Danielpour, D*., et al.* (2000). A novel mitochondrial septin-like protein, ARTS, mediates apoptosis dependent on its P-loop motif. Nature cell biology *2*, 915-921.

Larsen, B.D., Rampalli, S., Burns, L.E., Brunette, S., Dilworth, F.J., and Megeney, L.A. (2010). Caspase 3/caspase-activated DNase promote cell differentiation by inducing DNA strand breaks. Proceedings of the National Academy of Sciences of the United States of America *107*, 4230-4235.

Le Grand, F., Jones, A.E., Seale, V., Scime, A., and Rudnicki, M.A. (2009). Wnt7a activates the planar cell polarity pathway to drive the symmetric expansion of satellite stem cells. Cell stem cell *4*, 535-547.

Lee, R.E., Brunette, S., Puente, L.G., and Megeney, L.A. (2010). Metacaspase Yca1 is required for clearance of insoluble protein aggregates. Proceedings of the National Academy of Sciences of the United States of America *107*, 13348-13353.

Lee, R.E., Puente, L.G., Kaern, M., and Megeney, L.A. (2008). A Non-Death Role of the Yeast Metacaspase: Yca1p Alters Cell Cycle Dynamics. PloS one *3*, 2956.

Lepper, C., Conway, S.J., and Fan, C.M. (2009). Adult satellite cells and embryonic muscle progenitors have distinct genetic requirements. Nature *460*, 627-631.

Lluis, F., Ballestar, E., Suelves, M., Esteller, M., and Munoz-Canoves, P. (2005). E47 phosphorylation by p38 MAPK promotes MyoD/E47 association and muscle-specific gene transcription. The EMBO journal *24*, 974-984.

Lockshin, R.A., and Zakeri, Z. (2007). Cell death in health and disease. Journal of cellular and molecular medicine *11*, 1214-1224.

Lu, L., Zhou, L., Chen, E.Z., Sun, K., Jiang, P., Wang, L., Su, X., Sun, H., and Wang, H. (2012). A Novel YY1-miR-1 regulatory circuit in skeletal myogenesis revealed by genome-wide prediction of YY1-miRNA network. PloS one *7*, e27596.

Madeo, F., Herker, E., Maldener, C., Wissing, S., Lachelt, S., Herlan, M., Fehr, M., Lauber, K., Sigrist, S., Wesselborg, S*., et al.* (2002). A caspase-related protease regulates apoptosis in yeast. Molecular cell *9*, 911-917.

Mahrus, S., Trinidad, J.C., Barkan, D.T., Sali, A., Burlingame, A.L., and Wells, J.A. (2008). Global sequencing of proteolytic cleavage sites in apoptosis by specific labeling of protein N termini. Cell *134*, 866-876.

Mai-Prochnow, A., Webb, J.S., Ferrari, B.C., and Kjelleberg, S. (2006). Ecological advantages of autolysis during the development and dispersal of Pseudoalteromonas tunicata biofilms. Applied and environmental microbiology *72*, 5414-5420.

Mandel-Gutfreund, Y., Kosti, I., and Larisch, S. (2011). ARTS, the unual septin: structural and functional aspects. Biol Chem *392*, 783-790.

Mauro, A. (1961). Satellite cell of skeletal muscle fibers. J Biophys Biochem Cytol *9*, 493-495.

Megeney, L.A., Kablar, B., Garrett, K., Anderson, J.E., and Rudnicki, M.A. (1996). MyoD is required for myogenic stem cell function in adult skeletal muscle. Genes & development *10*, 1173-1183.

Messina, G., and Cossu, G. (2009). The origin of embryonic and fetal myoblasts: a role of Pax3 and Pax7. Genes & development *23*, 902-905.

Milyavsky, M., Gan, O.I., Trottier, M., Komosa, M., Tabach, O., Notta, F., Lechman, E., Hermans, K.G., Eppert, K., Konovalova, Z.*, et al.* (2010). A distinctive DNA damage response in human hematopoietic stem cells reveals an apoptosis-independent role for p53 in self-renewal. Cell stem cell *7*, 186-197.

Miura, M., Chen, X.-D., Allen, M.R., Bi, Y., Gronthos, S., Seo, B.-M., Lakhani, S., Flavell, R.A., Feng, X.-H., Robey, P.G.*, et al.* (2004). A crucial role of caspase-3 in osteogenic differentiation of bone marrow stromal stem cells. Journal of Clinical Investigation *114*, 1704-1713.

Molkentin, J.D., Li, L., and Olson, E.N. (1996). Phosphorylation of the MADS-Box transcription factor MEF2C enhances its DNA binding activity. The Journal of biological chemistry *271*, 17199-17204.

Murray, T.V., McMahon, J.M., Howley, B.A., Stanley, A., Ritter, T., Mohr, A., Zwacka, R., and Fearnhead, H.O. (2008). A non-apoptotic role for caspase-9 in muscle differentiation. Journal of Cell Science *121*, 3786-3793.

Nhan, T.Q., Liles, W.C., and Schwartz, S.M. (2006). Physiological functions of caspases beyond cell death. The American journal of pathology *169*, 729-737.

Ohsawa, S., Hamada, S., Kuida, K., Yoshida, H., Igaki, T., and Miura, M. (2010). Maturation of the olfactory sensory neurons by Apaf-1/caspase-9-mediated caspase activity. Proceedings of the National Academy of Sciences of the United States of America *107*, 13366-13371.

Okasha, S. (2005). Altruism, Group Selection and Correlated Interaction. The British Journal for the Philosophy of Science *56*, 703-725.

Olguin, H.C., and Olwin, B.B. (2004). Pax-7 up-regulation inhibits myogenesis and cell cycle progression in satellite cells: a potential mechanism for self-renewal. Developmental biology *275*, 375-388.

Olguin, H.C., Yang, Z., Tapscott, S.J., and Olwin, B.B. (2007). Reciprocal inhibition between Pax7 and muscle regulatory factors modulates myogenic cell fate determination. The Journal of cell biology *177*, 769-779.

Oustanina, S., Hause, G., and Braun, T. (2004). Pax7 directs postnatal renewal and propagation of myogenic satellite cells but not their specification. The EMBO journal *23*, 3430-3439.

Palacios, D., Mozzetta, C., Consalvi, S., Caretti, G., Saccone, V., Proserpio, V., Marquez, V.E., Valente, S., Mai, A., Forcales, S.V.*, et al.* (2010). TNF/p38alpha/polycomb signaling to Pax7 locus in satellite cells links inflammation to the epigenetic control of muscle regeneration. Cell stem cell *7*, 455-469.

Pan, G.J., and Pei, D.Q. (2003). Identification of two distinct transactivation domains in the pluripotency sustaining factor nanog. Cell Res *13*, 499-502.

Pasut, A., Jones, A.E., and Rudnicki, M. (2013). Isolation and culture of individual myofibers and their satellite cells from adult skeletal muscle. J Vis Exp *73*, e50074.

Pasut, A., Oleynik, P., and Rudnicki, M. (2012). Isolation of muscle stem cells by fluorescence activated cell sorting cytometry. Methods Mol Biol *798*, 53-64.

Piatkov, K.I., Brower, C.S., and Varshavsky, A. (2012). The N-end rule pathway counteracts cell death by destroying proapoptotic protein fragments. Proceedings of the National Academy of Sciences of the United States of America *109*, E1839-1847.

Pinan-Lucarre, B., Gabel, C.V., Reina, C.P., Hulme, S.E., Shevkoplyas, S.S., Slone, R.D., Xue, J., Qiao, Y., Weisberg, S., Roodhouse, K.*, et al.* (2012). The core apoptotic executioner proteins CED-3 and CED-4 promote initiation of neuronal regeneration in Caenorhabditis elegans. PLoS biology *10*, e1001331.

Popgeorgiev, N., Bonneau, B., Ferri, K.F., Prudent, J., Thibaut, J., and Gillet, G. (2011). The apoptotic regulator Nrz controls cytoskeletal dynamics via the regulation of Ca2+ trafficking in the zebrafish blastula. Developmental cell *20*, 663-676.

Putinski, C., Abdul-Ghani, M., Stiles, R., Brunette, S., Dick, S.A., Fernando, P., and Megeney, L.A. (2013). Intrinsic-mediated caspase activation is essential for cardiomyocyte hypertrophy. Proceedings of the National Academy of Sciences of the United States of America *110*, E4079-4087.

Putt, K.S., Chen, G.W., Pearson, J.M., Sandhorst, J.S., Hoagland, M.S., Kwon, J.T., Hwang, S.K., Jin, H., Churchwell, M.I., Cho, M.H.*, et al.* (2006). Small-molecule activation of procaspase-3 to caspase-3 as a personalized anticancer strategy. Nature chemical biology *2*, 543-550.

Relaix, F., Montarras, D., Zaffran, S., Gayraud-Morel, B., Rocancourt, D., Tajbakhsh, S., Mansouri, A., Cumano, A., and Buckingham, M. (2006). Pax3 and Pax7 have distinct and overlapping functions in adult muscle progenitor cells. The Journal of cell biology *172*, 91-102.

Relaix, F., Rocancourt, D., Mansouri, A., and Buckingham, M. (2004). Divergent functions of murine Pax3 and Pax7 in limb muscle development. Genes Dev *18*, 1088-1105.

Ribeil, J.A., Zermati, Y., Vandekerckhove, J., Cathelin, S., Kersual, J., Dussiot, M., Coulon, S., Moura, I.C., Zeuner, A., Kirkegaard-Sorensen, T.*, et al.* (2007). Hsp70 regulates erythropoiesis by preventing caspase-3-mediated cleavage of GATA-1. Nature *445*, 102-105.

Riman, S., Rizkallah, R., Kassardjian, A., Alexander, K.E., Luscher, B., and Hurt, M.M. (2012). Phosphorylation of the transcription factor YY1 by CK2alpha prevents cleavage by caspase 7 during apoptosis. Mol Cell Biol *32*, 797-807.

Rocheteau, P., Gayraud-Morel, B., Siegl-Cachedenier, I., Blasco, M.A., and Tajbakhsh, S. (2012). A subpopulation of adult skeletal muscle stem cells retains all template DNA strands after cell division. Cell *148*, 112-125.

Rudnicki, M., Schnegelsberg, P.N., Stead, R.H., Braun, T., Arnold, H.H., and Jaenisch, R. (1993). MyoD or Myf5 is required for the formation of skeletal muscle. Cell *75*, 1351-1359.

Sabourin, L.A., and Rudnicki, M.A. (2000). The molecular regulation of myogenesis. Clin Genet *57*, 16-25.

Seale, P., Ishibashi, J., Scime, A., and Rudnicki, M. (2004). Pax7 is necessary and sufficient for the myogenic specification of CD45+Sca1+ stem cells from injured muscle. PLoS biology *2*, 0664-0672.

Seale, P., Sabourin, L.A., Girgis-Gabardo, A., Mansouri, A., Gruss, P., and Rudnicki, M. (2000). pax7 is required for the specification of myogenic sat cells. Cell *102*, 777-786.

Segovia, M., Haramaty, L., Berges, J.A., and Falkowski, P.G. (2003). Cell death in the unicellular chlorophyte Dunaliella tertiolecta. A hypothesis on the evolution of apoptosis in higher plants and metazoans. Plant physiology *132*, 99-105.

Shimizu, K., and Sawasaki, T. (2013). Nek5, a novel substrate for caspase-3, promotes skeletal muscle differentiation by up-regulating caspase activity. FEBS Letters *587*, 2219-2225.

Shrestha, A., Puente, L.G., Brunette, S., and Megeney, L.A. (2013). The role of Yca1 in proteostasis. Yca1 regulates the composition of the insoluble proteome. Journal of proteomics *81*, 24-30.

Siegel, A.L., Kuhlmann, P.K., and Cornelison, D.D. (2011). Muscle satellite cell proliferation and association: new insights from myofiber time-lapse imaging. Skeletal muscle *1*, 7.

Simone, C., Forcales, S.V., Hill, D.A., Imbalzano, A.N., Latella, L., and Puri, P.L. (2004). p38 pathway targets SWI-SNF chromatin-remodeling complex to muscle-specific loci. Nature genetics *36*, 738-743.

Soleimani, V.D., Punch, V.G., Kawabe, Y., Jones, A.E., Palidwor, G.A., Porter, C.J., Cross, J.W., Carvajal, J.J., Kockx, C.E., van, I.W.F*., et al.* (2012). Transcriptional dominance of Pax7 in adult myogenesis is due to high-affinity recognition of homeodomain motifs. Developmental cell *22*, 1208-1220.

Sordet, O., Rebe, C., Plenchette, S., Zermati, Y., Hermine, O., Vainchenker, W., Garrido, C., Solary, E., and Dubrez-Daloz, L. (2002). Specific involvement of caspases in the differentiation of monocytes into macrophages. Blood *100*, 4446-4453.

Thornberry, N.A., Rano, T.A., Peterson, E.P., Rasper, D.M., Timkey, T., Garcia-Calvo, M., Houtzager, V.M., Nordstrom, P.A., Roy, S., Vaillancourt, J.P*., et al.* (1997). A combinatorial approach defines specificities of members of the caspase family and granzyme B. Journal of Biological Chemistry *272*, 17907-17911.

Troy, A., Cadwallader, A.B., Fedorov, Y., Tyner, K., Tanaka, K.K., and Olwin, B.B. (2012). Coordination of satellite cell activation and self-renewal by Par-complex-dependent asymmetric activation of p38alpha/beta MAPK. Cell stem cell *11*, 541-553.

Turowec, J.P., Duncan, J.S., French, A.C., Gyenis, L., St. Denis, N.A., Vilk, G., and Litchfield, D.W. (2010). Protein kinase CK2 is a constitutively active enzyme that promotes cell survival-strategies to identify CK2 substrates and manipulate its activity in mammalian cells. Methods of Enzymology *484*.

Turowec, J.P., Zukowski, S.A., Knight, J.D.R., Smalley, D.M., Graves, L.M., Johnson, G.L., Li, S.S.C., Lajoie, G.A., and Litchfield, D.W. (2014). An unbiased proteomic screen reveals caspase

cleavage is positively and negatively regulated by substrate phosphorylation. Molecular and Cellular Proteomics *13*, 1184-1197.

Uren, A.G., O'Rourke, K., Aravind, L., Pisabarro, M.T., Seshagirl, S., Koonin, E.V., and Dixit, V.M. (2000). Identification of paracaspases and metacaspases two ancient families of caspase-like proteins, one of which plays a key role in MALT lymphoma. Molecular cell *6*, 961-967.

Vachova, L., and Palkova, Z. (2005). Physiological regulation of yeast cell death in multicellular colonies is triggered by ammonia. The Journal of cell biology *169*, 711-717.

von Maltzahn, J., Jones, A.E., Parks, R.J., and Rudnicki, M.A. (2013). Pax7 is critical for the normal function of satellite cells in adult skeletal muscle. Proceedings of the National Academy of Sciences of the United States of America *110*, 16474-16479.

Weber, G.F., and Menko, A.S. (2005). The canonical intrinsic mitochondrial death pathway has a non-apoptotic role in signaling lens cell differentiation. The Journal of biological chemistry *280*, 22135-22145.

Wen, Y., Bi, P., Liu, W., Asakura, A., Keller, C., and Kuang, S. (2012). Constitutive Notch activation upregulates Pax7 and promotes the self-renewal of skeletal muscle satellite cells. Mol Cell Biol *32*, 2300-2311.

West, S.A., Griffin, A.S., and Gardner, A. (2007). Social semantics: altruism, cooperation, mutualism, strong reciprocity and group selection. Journal of evolutionary biology *20*, 415-432.

Winter, B., Kautzner, I., Issinger, O.G., and Arnold, H.H. (1997). Two putative protein kinase CK2 phosphorylation sites are important for Myf-5 activity. Biol Chem *378*, 1445-1456.

Yang, Q.H., and Du, C. (2004). Smac/DIABLO selectively reduces the levels of c-IAP1 and c-IAP2 but not that of XIAP and livin in HeLa cells. The Journal of biological chemistry *279*, 16963-16970.

Yuan, J., Shaham, S., Ledoux, S., Ellis, H., and Horvitz, H.R. (1993). The C. elegans cell death gene Ced-3 encodes a protein similar to Mammalian Interleukin-1B-Converting Enzyme. Cell *75*, 641-652.

Zammit, P.S., Golding, J.P., Nagata, Y., Hudon, V., Partridge, T.A., and Beauchamp, J.R. (2004). Muscle satellite cells adopt divergent fates: a mechanism for self-renewal? The Journal of cell biology *166*, 347-357.

Zammit, P.S., Relaix, F., Nagata, Y., Perez-Ruiz, A., Collins, C.A., Partridge, T.A., and Beauchamp, J.R. (2006). Pax7 and myogenic progression in skeletal muscle satellite cells. Journal of Cell Science *119*, 1824-1832.

Zermati, B.Y., Garrido, C., Amsellem, S., Fishelson, S., Bouscary, D., Valensi, F., Varet, B., Solary, E., and Hermine, O. (2001). Caspase activation is required for terminal erythroid differentiation. Journal of Experimental Medicine *193*, 247-254.

Appendix I

Manuscript:

Alfaro LA, Dick SA, Siegel AL, Anonuevo AS, McNagny KM, Megeney LA, Cornelison DD, Rossi FM. (2011) CD34 promotes satellite cell motility and entry into proliferation to facilitate efficient skeletal muscle regeneration. *Stem Cells* **29**(12): 2030-41

STEM CELLS®

TISSUE-SPECIFIC STEM CELLS

CD34 Promotes Satellite Cell Motility and Entry into Proliferation to Facilitate Efficient Skeletal Muscle Regeneration

LESLIE ANN SO ALFARO,[a,b] SARAH A. DICK,[c,d] ASHLEY L. SIEGEL,[e] ADAM S. ANONUEVO,[a] KELLY M. MCNAGNY,[a] LYNN A. MEGENEY,[c,d] D.D.W. CORNELISON,[e] FABIO M.V. ROSSI[a,f]

[a]Biomedical Research Centre, [f]Department of Medical Genetics, and [b]Department of Experimental Medicine Graduate Program, University of British Columbia, Vancouver, British Columbia, Canada; [c]Ottawa Hospital Research Institute, Sprott Centre for Stem Cell Research, Regenerative Medicine Program, Ottawa, Ontario, Canada; [d]Department of Cellular and Molecular Medicine, University of Ottawa, Ottawa, Ontario, Canada; [e]Christopher H. Bond Life Sciences Center, Columbia, Missouri, USA

Key Words. CD34 • Satellite cell activation • Muscle regeneration

ABSTRACT

Expression of the cell surface sialomucin CD34 is common to many adult stem cell types, including muscle satellite cells. However, no clear stem cell or regeneration-related phenotype has ever been reported in mice lacking CD34, and its function on these cells remains poorly understood. Here, we assess the functional role of CD34 on satellite cell-mediated muscle regeneration. We show that *Cd34*$^{-/-}$ mice, which have no obvious developmental phenotype, display a defect in muscle regeneration when challenged with either acute or chronic muscle injury. This regenerative defect is caused by impaired entry into proliferation and delayed myogenic progression. Consistent with the reported antiadhesive function of CD34, knockout satellite cells also show decreased motility along their host myofiber. Altogether, our results identify a role for CD34 in the poorly understood early steps of satellite cell activation and provide the first evidence that beyond being a stem cell marker, CD34 may play an important function in modulating stem cell activity. STEM CELLS *2011;29:2030–2041*

Disclosure of potential conflicts of interest is found at the end of this article.

INTRODUCTION

Skeletal muscle exhibits a remarkable capacity to regenerate and completely restore its mass and function rapidly after injury. Upon muscle damage, muscle stem cells, known as satellite cells, exit a normally quiescent state to self-renew and produce myoblasts, which then commit to terminal differentiation and fuse with each other or to existing myofibers to repair damage [1]. Although composing only a small fraction of the nuclei found in adult muscle, satellite cells are the primary source of new myogenic nuclei that contribute to efficient hypertrophy and regeneration, overall having a tremendous capacity to repair damage [2–7].

During regeneration, satellite cells migrate from a necrotic area toward the periphery as well as in the opposite direction, from the viable area to the site of damage [8, 9]. Recently, Siegel et al. [10] used time-lapse imaging of satellite cells on single fibers to show that satellite cells become extremely motile, crossing the basement membrane to leave their niche as early as 12 hours after culture initiation. Since the initial observation of satellite cell migration [11], there has been a concerted effort to identify factors that regulate this process. While numerous proteins have been proposed to modulate satellite cell migration [12–16], their specific roles have been difficult to define.

In this study, we focus on the sialomucin CD34. Although it is a marker commonly used to identify and purify satellite cells [17–21], its role in skeletal muscle regeneration remains to be explored. A report by Jankowski et al. [22] showed that CD34 could be used to separate defined subpopulations of preplated myogenic progenitors, with CD34^{+} cells having the greatest regenerative capacity. Furthermore, Beauchamp et al. [18] reported a rapid decrease in CD34 mRNA expression in

Author contributions: L.A.S.A.: conception and design, collection and/or assembly of data, data analysis and interpretation, manuscript writing, and final approval of manuscript; S.A.D. and A.L.S.: conception and design, collection and/or assembly of data, data analysis and interpretation and final approval of manuscript; A.S.A.: collection and/or assembly of data and final approval of manuscript; K.M.M.: conception and design, provision of study material, data interpretation, manuscript writing, and final approval of manuscript; L.A.M.: conception and design, data interpretation, and final approval of manuscript; D.D.W.C.: conception and design, collection and/or assembly of data, data analysis and interpretation, manuscript writing, final approval of manuscript, and financial support; F.M.V.R.: conception and design, data interpretation, manuscript writing, final approval of manuscript, and financial support. S.A.D. and A.L.S. contributed equally to this article.

Correspondence: Fabio M.V. Rossi, M.D., Ph.D., Biomedical Research Centre, University of British Columbia, 2222 Health Sciences Mall, Vancouver, British Columbia V6T 1Z3, Canada. Telephone: 604-822-7138; Fax: 604-822-7815; e-mail: fabio@brc.ubc.ca; or D.D. W. Cornelison, Ph.D., Division of Biology, 346 LSC, University of Missouri, 1201 E Rollins Road, Columbia, Missouri 65211, USA. Telephone: 573-882-9690; Fax: 573-884-0802; e-mail: cornelisond@missouri.edu Received July 11, 2011; accepted for publication September 23, 2011; first published online in STEM CELLS *EXPRESS* October 13, 2011. 1066-5099/2011/$30.00/0 doi: 10.1002/stem.759

satellite cells from cultured single fibers early in myogenic progression. Overall, these led us to hypothesize that, as proposed in other cell types [23–28], CD34 could function during activation, initial proliferation, or migration of adult skeletal muscle progenitors.

Here, we describe the regulation of CD34 expression on myogenic cells in vitro and in vivo. Furthermore, we use *Cd34*-deficient (*Cd34*$^{-/-}$) mice to show that CD34 is essential for efficient satellite cell-mediated muscle regeneration in vivo. Our analysis of satellite cells on single fibers and sorted myogenic progenitor cells (MPCs) from *Cd34*$^{-/-}$ animals reveals a role for CD34 in promoting efficient myogenic progression, specifically in satellite cell migration and entry into cell cycle. Together, our results provide novel insights into the significance and function of CD34 in muscle regeneration as well as in the early steps underlying this complex process.

Materials and Methods

Mice

Animals were housed in the animal facility of the Biomedical Research Centre in the University of British Columbia (UBC). Mice were kept under sterile conditions, bred in-house, and handled following guidelines approved by the UBC Animal Care Committee. *Cd34*$^{-/-}$ mice were provided by Dr. Kelly McNagny. *Cd34*$^{-/-}$ mice were crossed onto the green fluorescent protein (GFP)$^{+}$CD45.2 background to obtain CD34$^{-/-}$GFP^{+}CD45.2 mice. LacZ in the Z/AP mice and enhanced GFP expression in the GFP^{+}CD45.2 C56BL/6 mice are both under the control of cytomegalovirus enhancer-chicken β-actin hybrid promoter. These strains were used as wild-type (WT) controls. The Z/AP and GFP^{+}CD45.2 mice were provided by Dr. Corrinne Lobe (MaRS Centre) and Dr. Irving Weissman (Stanford University), respectively. *Mdx* mice contain a point mutation in the dystrophin gene yielding complete absence of the protein. Myf5/LacZ animals express the β-galactosidase gene under the control of the Myf5 promoter. Both strains were provided by Dr. Michael Rudnicki (Ottawa Health Research Institute). Mice genotypes for CD34$^{-/-}$, *mdx*, GFP^{+}, and LacZ^{+} were determined by polymerase chain reaction (PCR), fluorescence microscopy, or β-galactosidase activity using X-gal.

Acute Muscle Damage

To induce acute damage, 10 μL of notexin (NTX; Latoxan# L8104, 10 μg/mL) was injected in the *Tibialis anterior (TA*) muscle. WT and *Cd34*$^{-/-}$ mice were age- (8–9 weeks of age at the time of injection) and sex-matched accordingly. Muscles were harvested at days 5, 7, 10, 14, 21 post-NTX damage, paraffin embedded, and serially sectioned at 5 μm. Slides were H&E stained following standard procedures. Paraffin-embedded tissues were sectioned and stained by Wax-it Histology Services, Inc.

Cross-Sectional Area Measurements

Area measurements were performed using images taken from H&E-stained slides of cross-sectioned muscle. Images were taken with a light microscope (Zeiss Axioplan2 Imaging), and measurements were done on density slices calculated with OpenLab software (version 4.0.4). All measured fibers were verified to ensure that the measurements were done on individual fibers. Regenerating fibers were defined as centrally nucleated fibers (CNFs). Non-regenerating fibers were defined as fibers with peripherally located nuclei.

MPC Preparation, Flow Cytometry Analysis, and Fluorescence-Activated Cell Sorting Isolation

Fluorescence-activated cell sorting (FACS) isolation of myogenic progenitors was performed as previously published [29]. Briefly, primary murine myogenic progenitors were obtained from whole hind limb or *TA* muscles, carefully harvested from adult mice (6–12 weeks of age), and minced into small pieces. Muscles then underwent enzymatic digestion with 0.2% collagenase type II (Roche# C6885) for 30 minutes followed by collagenase D (Roche# 1088882, 1.5 U/mL) and dispase type II (Roche# 295825, 2.4 U/mL) at 37°C for 1 hour. The homogenized muscle samples were then filtered through a 40-μm cell strainer and the cell suspension was stained with antibodies against CD45, CD31, Sca1, and α7 integrin, along with Hoechst and propidium iodide (PI). All cell surface staining was done on ice. Isotype controls were used to determine gating. Antibodies to CD34 were used when needed. Cells were sorted with BD FACSVantageSE (BD FACSDiva version 4.0.1.2 software). Purity checks were done to ensure sorting efficiency and accuracy. Analyses of samples were performed using FlowJo (version 8.7).

Cytospin and LacZ Stain of Sorted MPCs

Following FACS isolation of MPCs, cells were cytospun at 750 rpm for 5 minutes. Samples were then fixed with 2% paraformaldehyde (PFA) and underwent standard staining for LacZ with X-gal and X-gal staining buffer for detection of β-galactosidase activity.

Quantitative Real-Time and Reverse-Transcription PCR (RT-PCR) Primers

Probes for quantitative PCR (qPCR) analysis of CD34 were purchased from Applied Biosystems (Mm00519283_m1*). RT-PCR primers used to distinguish transcripts for full-length CD34 and truncated CD34 isoforms were 5′-AGCACAGAACTTCCCAGCAA-3′ in exons5/6 and 5′-CCTCCACCATTCTCCGTGTA-3′ in exon8.

Transplantation and Engraftment

Freshly sorted MPCs were obtained from Z/AP^{+}, *Cd34*$^{-/-}$ GFP^{+}CD45.2, and GFP^{+}CD45.2 adult mice (8–12 weeks of age). A total of 20,000 GFP^{+} cells from either WT or *Cd34*$^{-/-}$ animals were mixed with 40,000 LacZ^{+} cells in PBS. Mixed cells were then injected into the *TA* muscles of adult WT mice in a 20 μL volume of PBS. Recipient mice were sacrificed 3 weeks post-transplant and perfused with PBS + 10 mM EDTA followed by 4% PFA. Hind limb muscles were harvested and left overnight in 20% sucrose at 4°C. Serial 20-μm sections of optimal cutting temperature TissueTek-embedded muscles were analyzed for engraftment of GFP^{+} and LacZ^{+} cells. A ratio was then obtained by taking the maximum number of GFP^{+} fibers and dividing it by the maximum number of LacZ^{+} fibers on an adjacent section.

5-Bromo-2′-Deoxyuridine (BrdU) Analysis

Following NTX damage, mice were i.p. injected twice daily with 200 μL BrdU (10 mg/mL) for the first 10 days following muscle damage and once daily after day 10. BrdU (0.8 mgl/mL) was also added to the drinking water. All mice were analyzed on the same day to ensure consistency among samples. Individual *TA*s were maintained as separate samples. Muscle tissues were processed as per our normal MPC protocol. Permeabilization and denaturation with 0.1% saponin and DNAse (300 μg/mL) treatment were performed followed by addition of anti-BrdU antibody. All data samples were collected by flow cytometry using a BD FACSLSRII machine (BD FACSDiva version 4.0.1.2 software). Analysis of samples was performed using FlowJo (version 8.7). NTX-damaged *TA*s from mice that did not receive BrdU were used as controls.

Single Fiber Isolations and Confocal Analysis

Single fiber isolations were performed as per standard protocol. Briefly, the *extensor digitorum longus (EDL)* muscle was gently harvested following sacrifice of the mouse. Collagenase I (Worthington# LS004197, 400 U/mL) digestion for approximately 1 hour in 37°C was performed to obtain single fibers. Fibers were then cultured, harvested, and fixed with 4% PFA at specific time points. Immunofluoresecent staining was done using antibodies to Pax7 (Developmental Studies Hybridoma Bank), MyoD (clone C20, Santa Cruz# sc-304), and CD34 (clone RAM34, eBioscience# 13-0341) diluted in 0.3% TritonX. Analysis was done by confocal microscopy (Nikon C1 laser scanning confocal microscope).

Doubling Time

Calculation of doubling time was performed using the algorithm provided by Roth V. in 2006 that is available at http://www.doubling-time.com/compute.php.

Three-Dimensional Video Time-lapse Microscopy

Real-time video imaging and analysis was performed on WT and *Cd34*$^{-/-}$ single fiber cultures as initially described in the study of Siegel et al. [10].

Statistical Analysis

Student's two-tailed *t* test was used on all statistical analyzes performed between groups. Statistical significance was set at $p \leq .05$.

Results

CD34 Is Necessary for Efficient Muscle Regeneration in Adult Mice

Cd34$^{-/-}$ mice show no obvious phenotypes under homeostatic conditions [30, 31]. To assess whether CD34 is required for skeletal muscle regeneration, we tested the response of these mice to acute damage induced by NTX injection [32, 33]. *Tibialis anterior (TA)* muscles from adult WT and *Cd34*$^{-/-}$ mice were harvested at days 0, 5, 10, 14, and 21 postdamage (Fig. 1A-1J). No differences between WT and *Cd34*$^{-/-}$ muscle were noticeable prior to damage (Fig. 1A, 1F). At day 5 postdamage, although the size of the damaged areas in the two groups was comparable, a significant increase in the amount of necrotic myofibers was visible in *Cd34*$^{-/-}$ animals (Fig. 1K). Elevated levels of necrosis can be observed in *Cd34*$^{-/-}$ animals at all postdamage time points analyzed, indicating a consistent difference in regeneration efficiency between WT and *Cd34*$^{-/-}$ animals. Furthermore, the appearance of CNFs, characteristic of regenerating myofibers, was delayed in *Cd34*$^{-/-}$ groups (Fig. 1B vs. 1H) and consistently appeared to be smaller in size (Fig. 1C-1E vs. 1H-1J). Cross-sectional area (CSA) measurements on nondamaged fibers and regenerating CNFs from both WT and *Cd34*$^{-/-}$ animals confirmed that WT CNFs, but not undamaged fibers, are significantly larger than those from *Cd34*$^{-/-}$ animals (Fig. 1L, 1M). This suggests that although *Cd34*$^{-/-}$ animals are capable of initiating repair, their regenerating fibers fail to undergo hypertrophy, a necessary component of muscle regeneration [3, 34].

As the kinetics of satellite cell activation and proliferation may differ between acute and chronic muscle damage, we asked whether the regeneration defect observed in acutely damaged *Cd34*$^{-/-}$ mice is also present during chronic damage, as for example seen in *mdx* mice, the murine model for Duchenne muscular dystrophy. Thus, we subjected *mdx* and *mdx*/*Cd34*$^{-/-}$ animals of different ages to the same histological and morphometric analyses. H&E staining shows histological differences reminiscent of those observed after NTX damage (Fig. 1N-1S). In addition, relative to *mdx* controls, CSA measurements showed a significant decrease in regenerating myofiber sizes of *mdx*/*Cd34*$^{-/-}$ animals at 4 weeks of age, a time when the first wave of myodegeneration takes place, and at 6 months of age. Interestingly, when 18-month old mice were analyzed, no significant differences were observed between the two groups (Fig. 1T). Together, our data from acute and chronic damage models support a key role for CD34 in ensuring efficient muscle repair.

Prospective Isolation of Adult Skeletal MPCs and Characterization of CD34 Expression

FACS can be used to prospectively isolate myogenic progenitors from adult mice [19, 20, 29, 35, 36]. Thus, we used FACS to explore the expression of CD34 on purified myogenic progenitors, isolated as Hoechst^{+}, PI^{-}, CD45^{-}, CD31^{-}, Sca1^{-}, α7 integrin^{+} cells, hereafter referred to as MPCs (Supporting Information Fig. S1A). This population contains all myogenic activity found in adult skeletal muscle [21, 29].

As CD34 expression has been reported on most, but not all, myogenic cells, we assessed the myogenic potential of the CD34^{+} and CD34^{-} MPC fractions. MPCs isolated from Myf5^{LacZ} mice, which express β-galactosidase in satellite cells under the control of the Myf5 promoter [37], showed β-galactosidase activity only in the CD34^{+} fraction (Fig. 2B, 2C). Furthermore, limiting dilution assays showed that the frequency of cells capable of initiating colonies containing multinucleated, myosin heavy chain (MyHC) positive, myotubes is negligible within the CD34^{-} fraction (1 in 31 cells in CD34^{+} fraction vs. 1 in 2,921 cells in CD34^{-} fraction). In summary, our results show that essentially all myogenic activity in sorted MPCs is contained within the CD34^{+} subset.

CD34 expression on myofiber-associated satellite cells is extinguished shortly after the isolated fibers are placed in culture [18]. As the conditions used in these cultures promote satellite cells expansion, likely by mimicking the environment of damaged muscle, we hypothesized that a similar downregulation may be observed following damage in vivo. Indeed, FACS analysis revealed that CD34 is downregulated from the surface of MPCs starting at day 3 postdamage and is essentially absent by day 5. At day 10, a time that follows the cessation of their proliferation [29], MPCs begin to re-express CD34 on their surface and by day 21, CD34 surface expression is fully restored (Fig. 2C). Real-time qPCR (qRT-PCR) analysis of sorted MPCs confirmed the downregulation of total CD34 mRNA soon after damage (Fig. 2D). In contrast, the expression of CD34 on Sca1^{+} α7 integrin^{-} fibro-adipogenic progenitors (FAPs) remains constant throughout the time course (data not shown), despite the fact that FAPs proliferate to the same extent as myogenic cells [29], indicating that CD34 regulation is specific to MPCs.

Additionally, we assessed whether CD34 regulation also occurs at the level of isoform expression. Two different isoforms of CD34 have been described, a full-length (CD34^{FL}) and a truncated version (CD34^{CT}), which lacks most of the cytoplasmic domain [38]. A switch in expression from CD34^{CT} to CD34^{FL} has been reported on cultured satellite cells [18]. Using endpoint RT-PCR, our investigation of CD34 isoform expression in vivo shows that in nondamaged muscle, MPCs exclusively express CD34^{FL}. On satellite cell activation and proliferation (days 1–5 post-NTX damage), both CD34^{FL} and CD34^{CT} are coexpressed. By day 7, when

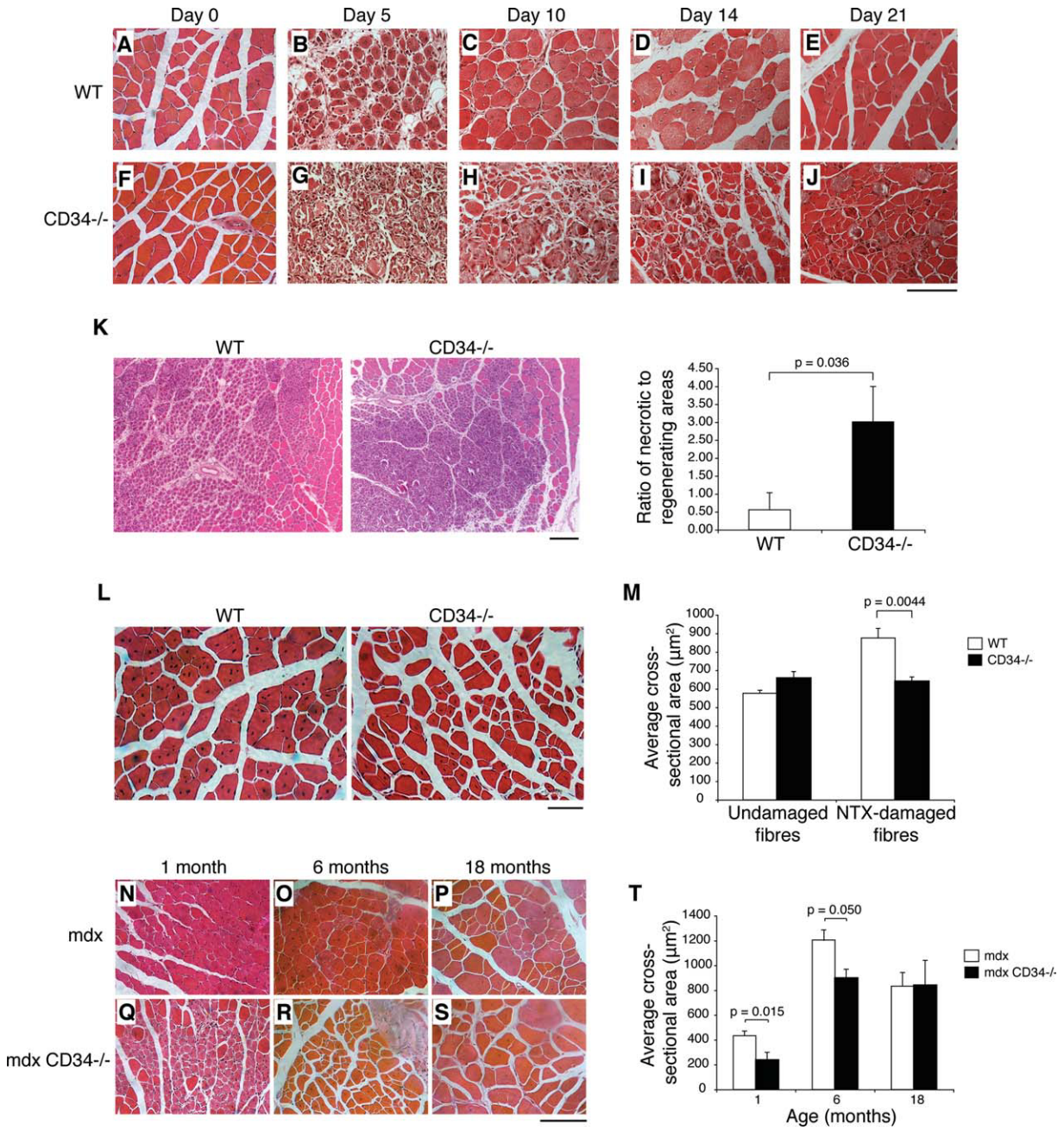

Figure 1. Impaired skeletal muscle regeneration in Cd34$^{-/-}$ mice. (**A–J**): H&E staining of WT and *Cd34*$^{-/-}$ muscles following acute NTX damage. *Tibialis anterior* muscles were analyzed at days 0 (A, F), 5 (B, G), 10 (C, H), 14 (D, I), and 21 (E, J) post-NTX damage (n = 5–6 mice). Scale bar = 100 μm. (**K**): Quantification of necrotic and regenerating areas of damage 5 days after NTX. Error bars represent ± SEM for n = 4–6 mice. Scale bar = 200 μm. (**L**): H&E staining of muscle sections showing centrally nucleated myofibers 21 days after NTX damage. Scale bar = 50 μm. (**M**): Myofiber cross-sectional area (CSA) measurements were performed on undamaged (day 0) and damaged (day 21) myofibers. Error bars represent ± SEM for n = 5–6 animals with >200 fibers per animal. (**N–S**): H&E staining of *mdx* and *mdx*/*Cd34*$^{-/-}$ muscle sections at 1 (N, Q), 6 (O, R), and 18 (P, S) months of age. Scale bar = 100 μm. (**T**): CSA measurements performed on regenerating myofibers of *mdx* and *mdx*/*Cd34*$^{-/-}$ muscles at 1, 6, and 18 months of age. Error bars represent ± SEM for n = 3–5 mice with >200 fibers per animal. Abbreviations: NTX, notexin; WT, wild type.

regeneration is well underway, the CD34^{FL} again becomes the predominant isoform (Fig. 2E). As CD34^{FL} and CD34^{CT} are distinct in their ability to interact with cytoplasmic proteins [39, 40], a change in isoform expression may lead to changes in CD34 localization. However, confocal analysis of CD34 localization on Pax7^{+} satellite cells associated to cultured single fibers from the *EDL* muscle failed to reveal any obvious changes beyond surface down-regulation (Fig. 2F-2Q).

Our analysis confirms that CD34 expression is rapidly downregulated on satellite cells following damage. This tight regulation, together with the observed muscle regeneration defect in *Cd34*$^{-/-}$ mice, provides support to the notion that CD34 plays a fundamental role in the myoregenerative process. As CD34 is no longer expressed in MPCs entering differentiation, such role is likely to be in satellite cell activation, migration, or proliferation.

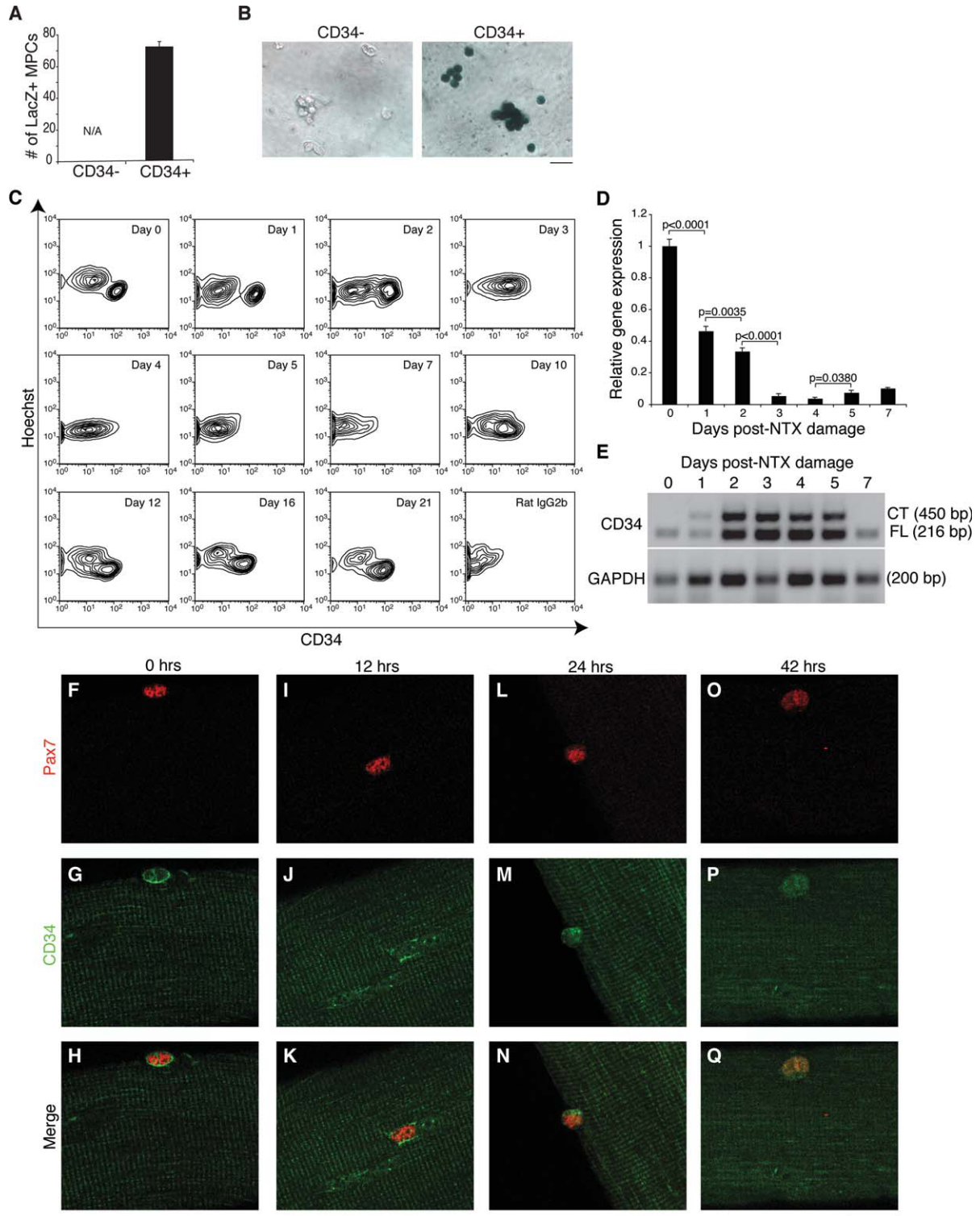

Figure 2. CD34 is expressed on myogenic cells and this expression is dynamically regulated during in vivo and in vitro myogenesis. (**A**): $CD34^-$ and $CD34^+$ fractions were isolated from $Myf5^{LacZ}$ animals and stained for LacZ to assess β-galactosidase activity. Quantification of $LacZ^+$ cells was performed. Error bars represent ± SEM for $n = 3$ mice. (**B**): Representative image of LacZ-stained $CD34^-$ and $CD34^+$ MPCs is shown ($LacZ^+$, blue). Scale bar = 16 μm. (**C**): Representative fluorescence-activated cell sorting plots showing regulated CD34 expression on MPCs following NTX damage ($n = 3$–5 mice per time-point). An isotype antibody control was used to verify specificity. (**D**): qRT-PCR analysis of total CD34 expression in purified MPCs after NTX damage. Error bars represent ± SEM for $n = 3$ independent experiments with 10–20 mice per time point. (**E**): End-point RT-PCR analysis of FL and CT isoform expression from purified MPCs. (**F–Q**): Analysis of CD34 localization (G, J, M, P) in $Pax7^+$ cells (F, I, L, O) on WT fibers at 0, 12, 24, and 42 hours postculture (Pax7, red; CD34, green; Hoechst, blue). Scale bar = 20 μm. Abbreviations: CT, truncated CD34; FL, full-length CD34; GAPDH, glyceraldehyde 3-phosphate dehydrogenase; MPC, myogenic progenitor cell; RT-PCR, reverse-transcriptase polymerase chain reaction.

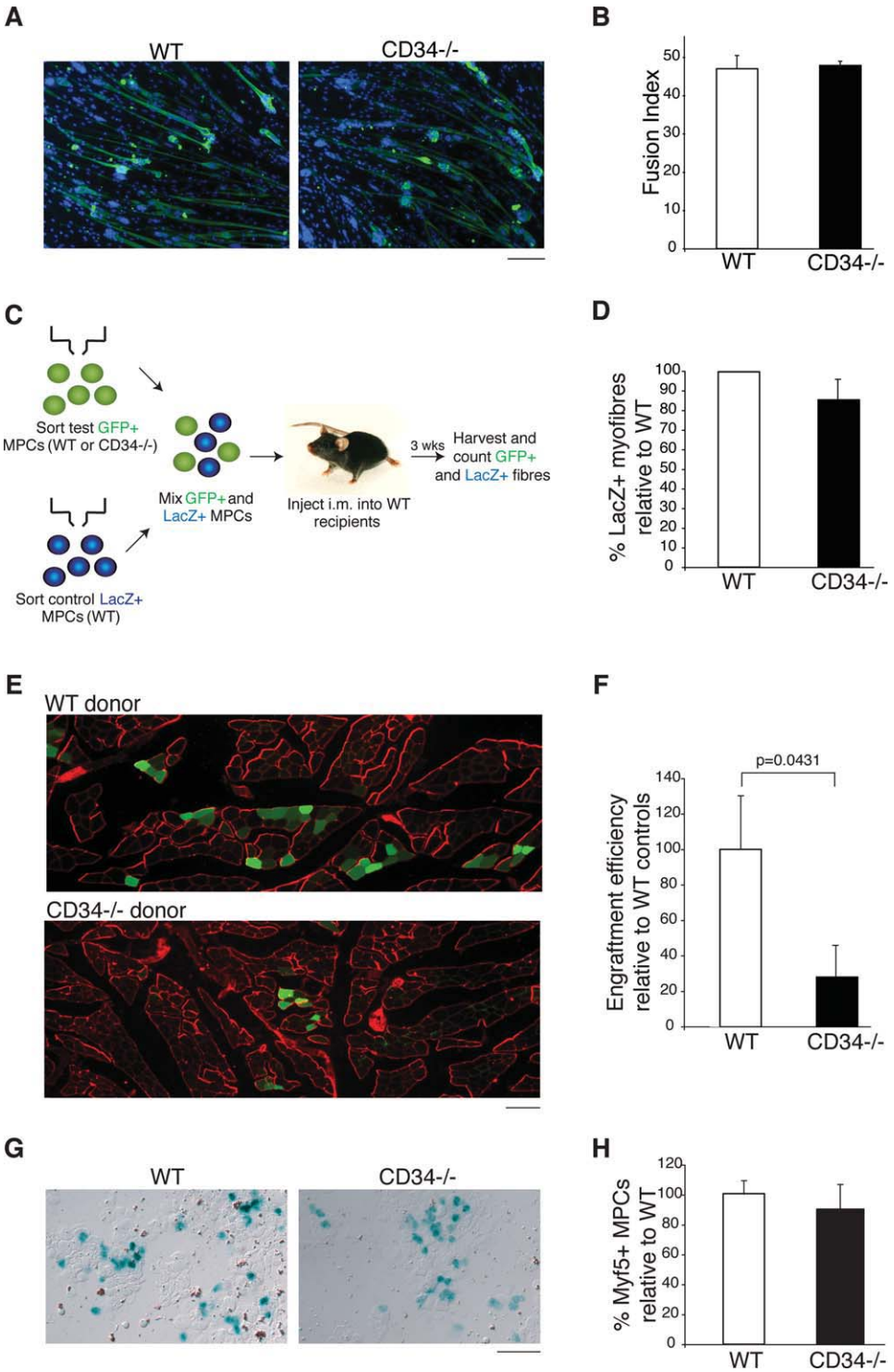

Figure 3. In vitro and in vivo functional assessment of WT and *Cd34*$^{-/-}$ MPCs. (**A**): Representative images showing WT and *Cd34*$^{-/-}$ differentiated MPCs forming multinucleated myotubes (MyHC, green; Hoechst, blue). Scale bar = 65 μm. (**B**): Fusion index (percent of total nuclei found in myotubes) for WT and *Cd34*$^{-/-}$ myotubes. Error bars represent ± SEM for $n = 3$ mice with 15 random fields of view per animal. (**C**): Schematic of the transplant experiment. (**D**): Direct enumeration and comparison of WT LacZ^{+} donor-derived myofibers used as internal standards in transplantation experiments. Bar graphs displaying the relative amount of LacZ^{+} fibers injected with WT/GFP^{+} or *Cd34*$^{-/-}$/GFP^{+} MPCs. Error bars represent ± SEM for $n = 3$ mice. (**E**): Representative image showing engraftment of WT/GFP^{+} and *Cd34*$^{-/-}$/GFP^{+} MPCs 3 weeks following injection into nondamaged WT recipients (GFP, green; Laminin, red). Scale bar = 95 μm. (**F**): Quantification of engraftment. GFP^{+} donor-derived myofibers were counted and normalized to the number of LacZ^{+} donor fibers. Ratios were then normalized to WT controls. Error bars represent ± SEM for $n = 3$–5. (**G**): MPCs from WT and *Cd34*$^{-/-}$ mice on a Myf5^{LacZ} background were sorted, cytospun, and stained for LacZ to assess β-galactosidase activity. Representative images displaying LacZ^{+} cells in both groups are shown. Scale bar = 50 μm. (**H**): Frequency of LacZ^{+} cells in WT and *Cd34*$^{-/-}$ sorted MPCs. Error bars represent ± SEM for $n = 3$ mice. Abbreviations: GFP, green fluorescent protein; MPC, myogenic progenitor cell; WT, wild type.

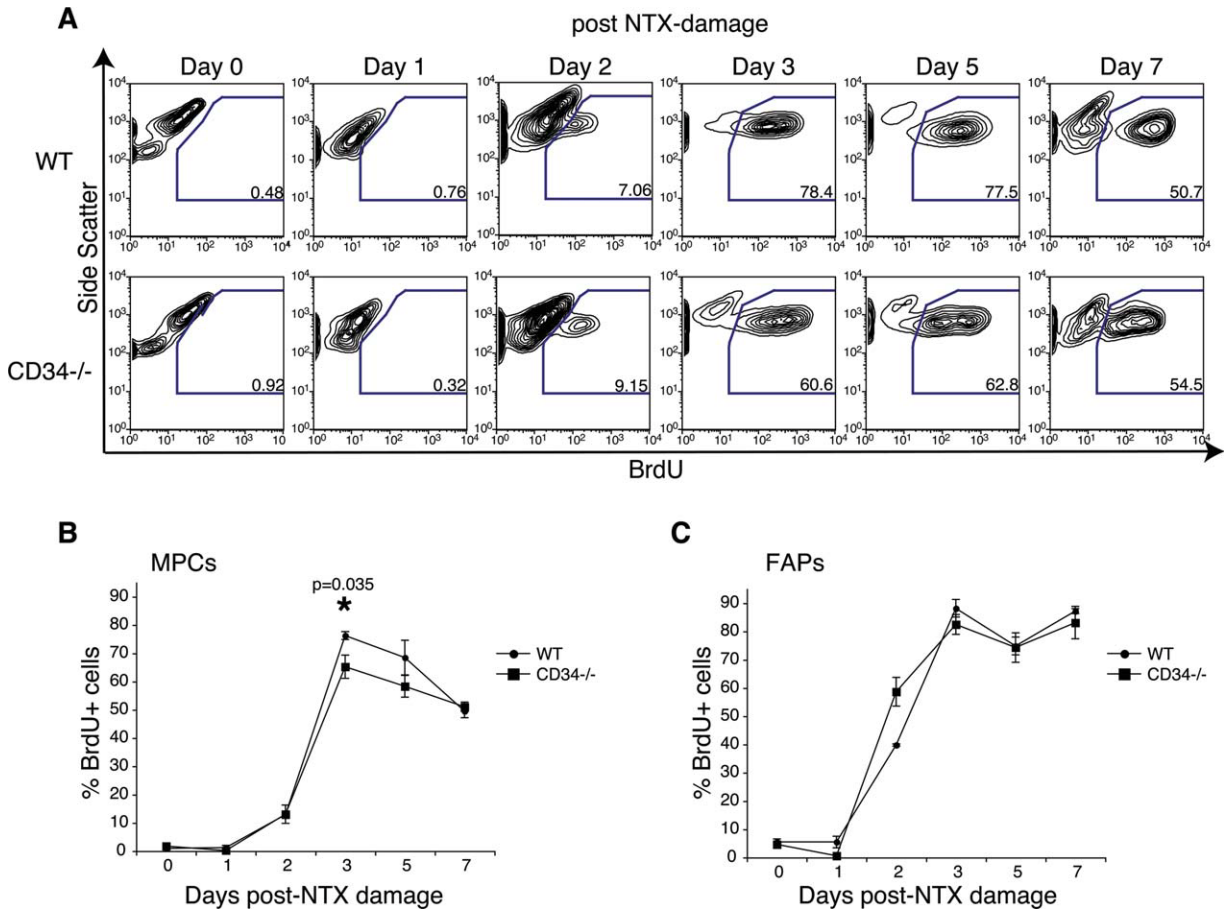

Figure 4. Inefficient in vivo proliferation of myogenic progenitor cells (MPCs) lacking CD34. (**A**): Representative fluorescence-activated cell sorting plots showing detection of a distinct BrdU$^+$ MPC population at 0, 1, 2, 3, 5, and 7 days following NTX damage in WT and *Cd34*$^{-/-}$ animals. (**B**): Graph showing the frequency of BrdU$^+$ WT and *Cd34*$^{-/-}$ MPCs at 0, 1, 2, 3, 5, and 7 days following NTX damage. Error bars represent ± SEM for $n = 3$–5 mice per time point. (**C**): Frequency of BrdU$^+$ WT and *Cd34*$^{-/-}$ FAPs at 0, 1, 2, 3, 5, 7 days post-NTX damage. Error bars represent ± SEM for $n = 3$–5 mice per time point. Abbreviations: BrdU, 5-bromo-2′-deoxyuridine; FAP, fibro-adipogenic progenitor; NTX, notexin; WT, wild type.

Defective Engraftment of Cd34$^{-/-}$ MPCs

Many CD34$^+$ cell types [29, 38, 41, 42] have been proposed to participate in muscle regeneration. To test whether the observed muscle regeneration defect in *Cd34*$^{-/-}$ animals reflects a direct effect of CD34 loss in MPCs, we functionally compared WT and *Cd34*$^{-/-}$ MPCs. We began by testing their ability to differentiate in vitro. Sorted cells were expanded under growth conditions for 5 days and then exposed to differentiation conditions for 5 days. Multinucleated, MyHC$^+$ myotubes were readily observed in both WT and *Cd34*$^{-/-}$ samples (Fig. 3A). Fusion index calculations, a standard measure of differentiation efficiency, confirmed that *Cd34*$^{-/-}$ MPCs differentiate in vitro as efficiently as WT (Fig. 3B). These results are consistent with the observation that CD34 disappears from the cell surface prior to the appearance of mature myofibers, suggesting that it would have little impact on the ability of MPCs to differentiate.

Nevertheless, because in vitro differentiation conditions may not faithfully recapitulate the in vivo environment [43], we further tested the myogenic potential *Cd34*$^{-/-}$ MPCs in vivo using cell transplantation. MPCs were freshly sorted from three groups of mice: (1) Z/AP mice ubiquitously expressing LacZ, (2) WT mice ubiquitously expressing GFP (WT/GFP$^+$), and (3) GFP$^+$ mice lacking CD34 (*Cd34*$^{-/-}$/GFP$^+$). LacZ$^+$ MPCs, initially used as internal standards, were mixed with either WT/GFP$^+$ or *Cd34*$^{-/-}$/GFP$^+$ MPCs prior to transplantation into nondamaged *TA* muscles of WT recipients. Engraftment was assessed 3 weeks later by quantifying donor-derived, GFP$^+$ myofibers (Fig. 3C). Comparable numbers of LacZ$^+$ fibers were observed in all samples (Fig. 3D and Supporting Information Fig. S2A), confirming that no bias was introduced prior to injection. In support of a cell autonomous role of CD34 in MPCs, our results reveal that *Cd34*$^{-/-}$/GFP$^+$ MPCs engraft with significantly decreased efficiency compared to WT/GFP$^+$ MPCs (Fig. 3E, 3F and Supporting Information Fig. S2B).

To exclude a difference in the frequency of myogenic cells contained within WT and *Cd34*$^{-/-}$ MPCs as the cause for our observation, we sorted MPCs from WT and *Cd34*$^{-/-}$ mice carrying a Myf5^{LacZ} transgene. No significant difference in the number of β-galactosidase$^+$ cells, indicative of MPC frequency, was noted between the two groups (Fig. 3G, 3H, and Supporting Information Fig. S2C). Overall, these data demonstrate that CD34 expression on MPCs is required for the efficient generation of myofibers following transplant and suggest that the muscle regeneration defect seen in *Cd34*$^{-/-}$ mice can be attributed to a cell autonomous defect of MPCs.

Loss of CD34 on MPCs Leads to Impaired Proliferation In Vivo Following Acute Damage

Recent publications suggest that a burst of proliferation occurs following transplant of MPCs to recipient muscle [19, 44]. As

WT and *Cd34*$^{-/-}$ MPCs are equally able to generate myotubes in vitro (Fig. 3A, 3B), we hypothesized that inefficient proliferation of *Cd34*$^{-/-}$ MPCs may underlie the phenotype observed in *Cd34*$^{-/-}$ mice. To assess MPC proliferation in vivo, mice were treated with BrdU and injected with NTX. FACS analysis show significantly decreased BrdU incorporation in *Cd34*$^{-/-}$ MPCs 3 days postdamage, when WT MPCs proliferation is maximal (Fig. 4A, 4B). A similar trend of inefficient *Cd34*$^{-/-}$ MPC proliferation is observed at day 5. This proliferation defect is not observed in FAPs, providing further evidence that CD34 plays a selective role in MPC function (Fig. 4C).

The lower frequency of BrdU^{+} MPCs could reflect either a reduction in their proliferative response or the selective loss of *Cd34*$^{-/-}$ cells. To distinguish between these possibilities, we used terminal deoxynucleotidyl transferase dUTP nick end labeling staining of WT and *Cd34*$^{-/-}$ muscle sections to detect apoptotic cells 3 days postdamage. We observed little to no apoptosis in either groups (data not shown), indicating that the decreased amount of *Cd34*$^{-/-}$ MPCs is not due to increased apoptosis. Thus, our results suggest that CD34 is required for the efficient expansion of MPCs after muscle injury in vivo.

CD34 Is Necessary for the Efficient Entry of Satellite Cells into Proliferation

One potential explanation for the observed reduction in proliferating MPCs could be delayed satellite cell entry into proliferation. To test this hypothesis, we cultured fibers from adult *EDL* muscles of WT and *Cd34*$^{-/-}$ animals. No difference in numbers of Pax7^{+} satellite cells was apparent immediately after fiber isolation (Fig. 5A), indicating that CD34 is dispensable for the maintenance of satellite cell numbers during homeostasis.

We then examined the progression of satellite cells through the myogenic program by assessing Pax7 and MyoD expression. Pax7 is highly expressed in quiescent satellite cells; but, on entry into cycle, these cells initiate expression of MyoD and eventually downregulate Pax7 as they commit to differentiation [45, 46]. Thus, two myogenic progenitor populations can then be identified: activated satellite cells (Pax7^{+} MyoD^{+}) and differentiation-committed myoblasts (Pax7^{-} MyoD^{+}) (Fig. 5B). Analyses of these populations over time in WT and *Cd34*$^{-/-}$ single fiber cultures revealed no significant difference in the frequency of Pax7^{+} cells that activate MyoD expression. However, analysis of the differentiation-committed myoblast population shows that while these cells become evident in WT samples, they are absent in *Cd34*$^{-/-}$ fibers after 48 hours of culture. At the 72-hour time point, although differentiation-committed myoblasts are now readily detectable on *Cd34*$^{-/-}$ fibers, their frequency remains significantly lower than on WT fibers (Fig. 5C). Thus, the lack of CD34 on satellite cells results in a significant delay in their progression along the myogenic program.

We next examined whether their proliferation is also similarly delayed. On WT fibers, an increase in the total number of myogenic cells, defined as cells expressing Pax7 and/or MyoD, is clearly observed at 48 hours following culture initiation. In contrast, no such increase is detected on *Cd34*$^{-/-}$ fibers until 72 hours following culture. At this point, WT fibers harbor significantly more myogenic cells than *Cd34*$^{-/-}$ fibers (Fig. 5D). Because these differences were not present initially, they reveal a striking reduction in the ability of *Cd34*$^{-/-}$ satellite cells to expand. *Cd34*$^{-/-}$ myogenic progenitors do proliferate, as can be seen by their sharp increase between 48 and 72 hours in culture. However, this proliferation is delayed when compared to WT fibers, whose associated myogenic progenitor numbers begin to increase between 24 and 48 hours in culture (Fig. 5D). In addition, the in vitro doubling time of *Cd34*$^{-/-}$ myogenic progenitors was considerably longer than that of WT cells (45.31 hours vs. 30.81 hours, respectively), providing further evidence that the lack of CD34 on myogenic progenitors indeed results in reduced proliferation.

To further confirm these results, we performed time-lapse imaging of cultured single fibers [10], which allows us to directly monitor satellite cell divisions. We observed fewer divisions on *Cd34*$^{-/-}$ fibers between 24 and 48 hours of culture compared to WT controls (Fig. 5E), reflecting a smaller percentage of *Cd34*$^{-/-}$ cells entering the cell cycle (44.2% vs. 20.6%). Furthermore, the first division of *Cd34*$^{-/-}$ satellite cells was significantly delayed (Fig. 5F). Altogether, these data argue that CD34 is essential for satellite cells to efficiently enter their first cell cycle. Subsequently, the lack of CD34 results in reduced expansion of myogenic cells as well as delayed progression through the myogenic program.

CD34 Is Essential for Efficient Satellite Cell Motility

CD34 has been proposed to promote the efficient migration of hematopoetic cells through its antiadhesive functions [23, 39, 40]. Since Siegel et al. [10] have established that satellite cells undergo extensive movement and migratory behavior during culture, we evaluated the motility of *Cd34*$^{-/-}$ satellite cells on their native substrate, the myofiber.

Live imaging of WT and *Cd34*$^{-/-}$ single fibers was initiated 24 hours after isolation and continued for an additional 24 hours [10]. During this period, both WT and *Cd34*$^{-/-}$ cells were found to be actively motile, but WT cells exhibited substantially more movement than *Cd34*$^{-/-}$ cells (Supporting Information videos S1, S2). Direct tracking of individual satellite cells over time revealed a dramatic reduction in average speed and overall distance traveled by *Cd34*$^{-/-}$ cells in comparison to WT controls (Fig. 6A-6C). Evaluation of the instantaneous velocities show that WT cells move faster throughout this period, suggesting that the decreased motility of *Cd34*$^{-/-}$ cells is not due to a delay in initiating movement but rather to a defect in migration (Fig. 6D). Overall, these data support a key role for CD34 in promoting efficient satellite cell movement.

One of the earliest motility-associated phenomena that take place during satellite cell activation is their exit from the niche. To test whether this process is also delayed in *Cd34*$^{-/-}$ animals, the position of individual Pax7^{+} satellite cells on cultured fibers relative to the laminin^{+} basement membrane was assessed by confocal microscopy. We observed no difference in the proportion of WT and *Cd34*$^{-/-}$ cells located above or below the basement membrane, indicating that the inefficient motility of *Cd34*$^{-/-}$ satellite cells does not affect their ability to exit from the niche (Supporting Information Fig. S3A).

Discussion

CD34 is a well-known surface marker used to isolate various progenitor cells, yet is also notorious for leaving researchers questioning its exact functional role. Previous reports speculated that CD34 may function as a homing receptor, a blocker of differentiation, a proadhesive receptor, or, conversely, an antiadhesion molecule [40]. Efforts to directly reveal a function for CD34 have been hampered by the fact that CD34 is one member of a functionally redundant family of three

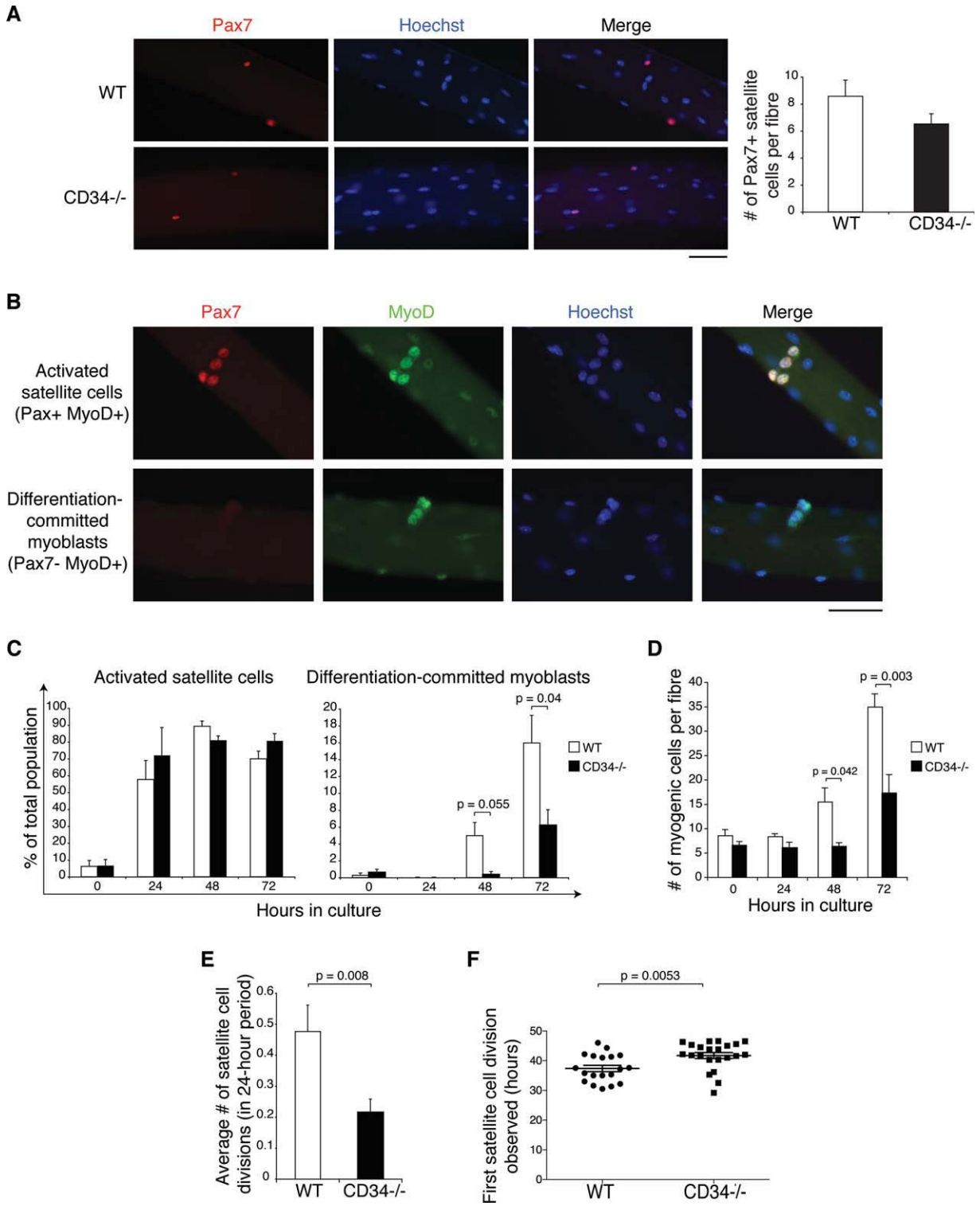

Figure 5. Defective activation of *Cd34*$^{-/-}$ satellite cells. (**A**): Immunofluorescent detection and enumeration of satellite cells on WT and *Cd34*$^{-/-}$ single fibers (Pax7, red; Hoechst, blue). Scale bar = 50 μm. Error bars represent ± SD for n = 5–7 animals. (**B**): Combined Pax7 and MyoD staining on single fibers identify two subpopulations of myogenic progenitors: Pax7^{+} MyoD^{+} as activated satellite cells and Pax7^{-} MyoD^{+} as differentiation-committed myoblasts (Pax7, red; MyoD, green; Hoechst, blue). Scale bar = 50 μm. (**C**): Quantification of activated satellite cells and differentiation committed myoblasts on WT and *Cd34*$^{-/-}$ cultured fibers. Error bars represent ± SD for n = 3–7 animals per time point. (**D**): Total myogenic cells counted per fiber. Error bars represent ± SEM for n = 3–7 animals per time point. (**E**): Number of satellite cell divisions detected using time-lapse microscopy between 24 and 48 hours after fiber culture initiation. Error bars represent ± SEM for n = 42–107 satellite cells. (**F**): Timing of first division of individual satellite cell. Line represents the mean values ± SEM for n = 19–22 satellite cells in 5–7 mice. Abbreviation: WT, wild type.

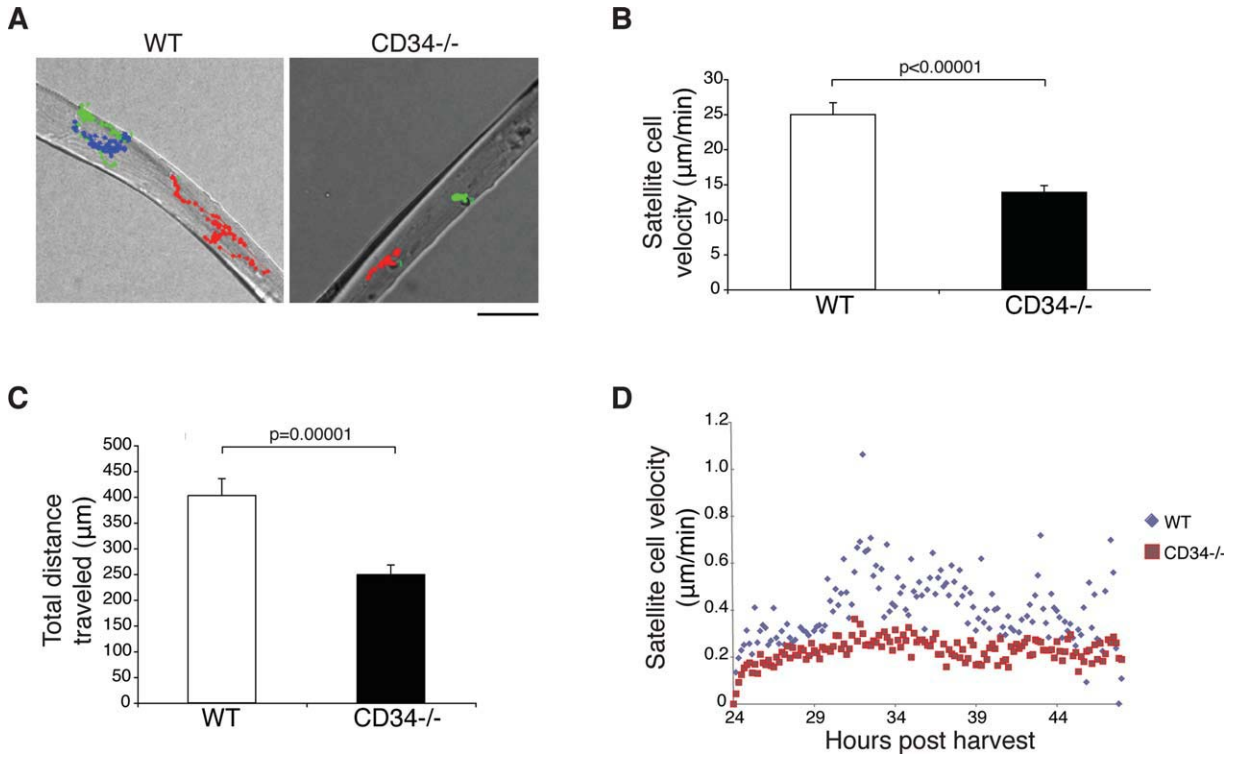

Figure 6. CD34 is necessary for efficient satellite cell motility. (**A**): Representative images of WT and *Cd34*$^{-/-}$ satellite cell tracking on single fibers based on time-lapse microscopy imaging. Each color represents a different cell tracked. Scale bar = 50 μm. (**B**): WT and *Cd34*$^{-/-}$ satellite cell velocities as determined using time-lapse microscopy. Error bars represent ± SEM for n = 42–107 satellite cells. (**C**): Total distances traveled for WT and *Cd34*$^{-/-}$ satellite cell were determined. Error bars represent ± SEM for n = 42–107 satellite cells. (**D**): Measurement of frame-by-frame instantaneous velocities for WT and *Cd34*$^{-/-}$ cells. Abbreviation: WT, wild type.

sialomucins (CD34, podocalyxin, and endoglycan) with an overlapping tissue distribution [40, 47, 48]. This may, in part, explain why *Cd34*$^{-/-}$ mice show no obvious defects in tissues where its homologues are expressed. Recent studies, however, showed that phenotypes in these mice can be revealed when a specific system is challenged, thus leading to more precise hypotheses of CD34's function [23, 49–51].

In this study, we evaluated muscle regeneration in adult *Cd34*$^{-/-}$ animals and observed a clear impairment in both acute and chronic damage models. Notably, in the chronic damage model, this defect was no longer apparent in aged, 18-month-old animals. However, as impaired regeneration in *mdx* mice has been attributed to satellite cell exhaustion [52, 53], the defects in satellite cell function caused by the lack of CD34 could be masked in aged animals.

A detailed analysis of CD34 expression on normal MPCs at steady state and during regeneration following acute damage showed that, consistent with previous results in vitro, CD34 expression is regulated during in vivo regeneration and is downregulated prior to differentiation. However, on analysis of CD34 isoform expression, we find our results from sorted MPCs in apparent contradiction with those published using individual satellite cells from single fibers [18], despite our use of the same primers on multiple experiments. One possible explanation for this discrepancy could be that some of the cells assayed in the study of Beauchamp et al. may have been FAPs, which can contaminate fiber preparations [54]. Nevertheless, in support for our hypothesis that CD34's role is likely in the early stages of myogenesis, our results show that it is during the stages prior to differentiation, when CD34 is regulated, that defects are observed in *Cd34*$^{-/-}$ myogenic cells. The defective engraftment of *Cd34*$^{-/-}$ MPCs in WT recipients conclusively supports the notion that CD34 plays a cell autonomous role in MPCs.

More specifically, our data demonstrates that CD34 is required for MPCs and satellite cells to proceed through the early stages of myogenic progression, defined here as the period spanning from the onset of damage to the first satellite cell division. Three main events take place during this time. (1) Satellite cells exit the niche by crossing the basement membrane. Presumably, this requires the cells to be motile; however, no defect in this first step was observed in *Cd34*$^{-/-}$ fiber cultures, suggesting the effect of CD34 on motility is not generalized. (2) Satellite cells move rapidly at relatively large distances. In vitro, this movement takes place on the outside surface of the basement membrane ensheathing the myofibers, which likely represents the interstitial space in regenerating tissue in vivo. (3) Myogenic cells begin to proliferate. We have found that these latter two processes, movement and proliferation, are clearly defective in *Cd34*$^{-/-}$ myogenic progenitors.

The relationship between satellite cell movement and proliferation remains debatable. Some published work suggests that movement follows division [35], while our data demonstrates that satellite cells can become motile before dividing (Supporting Information videos S1, S2). However, it has been shown that proliferation can proceed despite blocked movement [10]. Evidence that both proliferation and motility are affected in *Cd34*$^{-/-}$ mice suggests that a functional link between the two may exist. But, it is also possible that CD34 plays independent roles in each of these processes. Interestingly, links between CD34 and both proliferation and motility have been independently established in other systems. *Cd34*$^{-/-}$ mast cells and eosinophils display defective inflammatory migration, an effect that has been ascribed to the loss

of CD34 antiadhesive properties [23, 39]. In support of a role for CD34 in facilitating the entry of quiescent cells into proliferation, Trempus et al. [28] reported that *Cd34*$^{-/-}$ animals failed to develop papillomas upon 7,12-dimethyl-benz[a]anthracene/phorbol ester 12-O-tetradecanoylphorbol-13 acetate induction, a phenomenon attributed to inefficient hair follicle stem cell activation. Finally, studies comparing CD34^{+} and CD34^{-} hematopoietic stem cell subsets show a higher percentage of proliferating cells in the CD34^{+} population [27] providing a link between CD34 and proliferation. Our data lend further support to this concept as we find a clear role for CD34 in mediating activation, proliferation, and motility of myogenic cells.

Although the reported antiadhesive properties of CD34 are likely to be at the basis for its function in promoting cell motility, the molecular link between this molecule and proliferation is still unresolved. Interestingly, another sialomucin, CD164, has been described to regulate myoblast motility and fusion through modulation of satellite cell responses to the chemokine stromal cell–derived factor 1 (SDF-1) [55]. Moreover, it has been shown that CD34^{+} myogenic cells express higher levels of the SDF-1 receptor, C-X-C chemokine receptor 4 (CXCR4), compared to the CD34^{-} population [56], suggesting a role for CD34 in CXCR4 signaling. However, we failed to detect any change in the ability of *Cd34*$^{-/-}$ cells to migrate in response to SDF-1 (data not shown), suggesting that CD34 acts through other mechanisms, the elucidation of which requires further investigation.

Conclusion

In summary, we have shown that CD34 is necessary for efficient muscle regeneration in response to both acute and chronic damage. The downregulation of both mRNA and surface protein levels of CD34 expression on myogenic precursors shortly following damage in combination with the defective engraftment of *Cd34*$^{-/-}$ MPCs indicates that CD34 plays a cell autonomous role on myogenic progenitors during the early phase of adult myogenesis. Our data demonstrating impaired motility and delayed entry into proliferation of *Cd34*$^{-/-}$ satellite cells further support this notion. Overall, we show that CD34 is not just a useful marker of MPCs, but it is required for efficient myogenic progression.

Acknowledgments

We thank L. Yi, J. Duenas, J. Kang, S. Boumahdi, A. Johnson, J. Wong, the BRC animal facility and BRC Core Staff for their expert technical assistance; Dr. B. Ajami, Dr. G. Alfaro, B. Paylor, and Dr. M. Long for help in editing the manuscript. This research was supported by grants from CIHR (MOP-82864) to F.M.V.R; D.D.W.C is supported by the National Institute of Health (NIH, 1R21AR056814-01); and K.M.M. is supported by CIHR (MOP-84545) and is a Michael Smith Foundation for Health Research Senior Scholar. L.A.S.A was supported by fellowships from the Natural Sciences and Engineering Research Council of Canada (NSERC, PGSD2-362406-2008) and the Michael Smith Foundation for Health Research (MSFHR, ST-JGS-062(06-1)BM).

Disclosure of Potential Conflicts of Interest

The authors indicate no potential conflicts of interest.

References

1 Hawke TJ, Garry DJ. Myogenic satellite cells: Physiology to molecular biology. J Appl Physiol 2001;91:534–551.
2 Moss FP, Leblond CP. Satellite cells as the source of nuclei in muscles of growing rats. Anat Rec 1971;170:421–435.
3 Snow MH. Satellite cell response in rat soleus muscle undergoing hypertrophy due to surgical ablation of synergists. Anat Rec 1990;227:437–446.
4 Schultz E. Satellite cell proliferative compartments in growing skeletal muscles. Dev Biol 1996;175:84–94.
5 Mauro A. Satellite cell of skeletal muscle fibers. J Biophys Biochem Cytol 1961;9:493–495.
6 Collins CA, Olsen I, Zammit PS et al. Stem cell function, self-renewal, and behavioral heterogeneity of cells from the adult muscle satellite cell niche. Cell 2005;122:289–301.
7 Snow MH. An autoradiographic study of satellite cell differentiation into regenerating myotubes following transplantation of muscles in young rats. Cell Tissue Res 1978;186:535–540.
8 Schultz E, Jaryszak DL, Valliere CR. Response of satellite cells to focal skeletal muscle injury. Muscle Nerve 1985;8:217–222.
9 Phillips GD, Hoffman JR, Knighton DR. Migration of myogenic cells in the rat extensor digitorum longus muscle studied with a split autograft model. Cell Tissue Res 1990;262:81–88.
10 Siegel AL, Atchison K, Fisher KE et al. 3D timelapse analysis of muscle satellite cell motility. Stem Cells 2009;27:2527–2538.
11 Bischoff R. Chemotaxis of skeletal muscle satellite cells. Dev Dyn 1997;208:505–515.
12 Germani A, Di Carlo A, Mangoni A et al. Vascular endothelial growth factor modulates skeletal myoblast function. Am J Pathol 2003;163:1417–1428.
13 Griffin CA, Apponi LH, Long KK et al. Chemokine expression and control of muscle cell migration during myogenesis. J Cell Sci 2010;123:3052–3060.
14 Griffin CA, Kafadar KA, Pavlath GK. MOR23 promotes muscle regeneration and regulates cell adhesion and migration. Dev Cell 2009;17:649–661.
15 Horsley V, Jansen KM, Mills ST et al. IL-4 acts as a myoblast recruitment factor during mammalian muscle growth. Cell 2003;113:483–494.
16 Salerno MS, Dyer K, Bracegirdle J et al. Akirin1 (Mighty), a novel promyogenic factor regulates muscle regeneration and cell chemotaxis. Exp Cell Res 2009;315:2012–2021.
17 Conboy MJ, Cerletti M, Wagers AJ et al. Immuno-analysis and FACS sorting of adult muscle fiber-associated stem/precursor cells. Methods Mol Biol 2010;621:165–173.
18 Beauchamp JR, Heslop L, Yu DS et al. Expression of CD34 and Myf5 defines the majority of quiescent adult skeletal muscle satellite cells. J Cell Biol 2000;151:1221–1234.
19 Sacco A, Doyonnas R, Kraft P et al. Self-renewal and expansion of single transplanted muscle stem cells. Nature 2008;456:502–506.
20 Montarras D, Morgan J, Collins C et al. Direct isolation of satellite cells for skeletal muscle regeneration. Science 2005;309:2064–2067.
21 Sherwood RI, Christensen JL, Conboy IM et al. Isolation of adult mouse myogenic progenitors: Functional heterogeneity of cells within and engrafting skeletal muscle. Cell 2004;119:543–554.
22 Jankowski RJ, Deasy BM, Cao B et al. The role of CD34 expression and cellular fusion in the regeneration capacity of myogenic progenitor cells. J Cell Sci 2002;115:4361–4374.
23 Blanchet MR, Maltby S, Haddon DJ et al. CD34 facilitates the development of allergic asthma. Blood 2007;110:2005–2012.
24 Blanchet MR, McNagny KM. Stem cells, inflammation and allergy. Allergy Asthma Clin Immunol 2009;5:13.
25 Nielsen JS, McNagny KM. CD34 is a key regulator of hematopoietic stem cell trafficking to bone marrow and mast cell progenitor trafficking in the periphery. Microcirculation 2009;16:487–496.
26 Sato T, Laver JH, Ogawa M. Reversible expression of CD34 by murine hematopoietic stem cells. Blood 1999;94:2548–2554.
27 Shman TV, Savitski VP, Fedasenka UU et al. Apoptosis and proliferation differences between CD34^{+} and CD34^{-} leukemic subpopulations in childhood acute leukemia. Hematology 2007;12:403–407.

28 Trempus CS, Morris RJ, Ehinger M et al. CD34 expression by hair follicle stem cells is required for skin tumor development in mice. Cancer Res 2007;67:4173–4181.
29 Joe AW, Yi L, Natarajan A et al. Muscle injury activates resident fibro/adipogenic progenitors that facilitate myogenesis. Nat Cell Biol 2010;12:153–163.
30 Cheng J, Baumhueter S, Cacalano G et al. Hematopoietic defects in mice lacking the sialomucin CD34. Blood 1996;87:479–490.
31 Suzuki A, Andrew DP, Gonzalo JA et al. CD34-deficient mice have reduced eosinophil accumulation after allergen exposure and show a novel crossreactive 90-kD protein. Blood 1996;87:3550–3562.
32 Harris JB. Myotoxic phospholipases A2 and the regeneration of skeletal muscles. Toxicon 2003;42:933–945.
33 Harris JB, Vater R, Wilson M et al. Muscle fibre breakdown in venom-induced muscle degeneration. J Anat 2003;202:363–372.
34 Adams GR. Satellite cell proliferation and skeletal muscle hypertrophy. Appl Physiol Nutr Metab 2006;31:782–790.
35 Kuang S, Kuroda K, Le Grand F et al. Asymmetric self-renewal and commitment of satellite stem cells in muscle. Cell 2007;129: 999–1010.
36 Mitchell KJ, Pannerec A, Cadot B et al. Identification and characterization of a non-satellite cell muscle resident progenitor during postnatal development. Nat Cell Biol 2010;12:257–266.
37 Tajbakhsh S, Bober E, Babinet C et al. Gene targeting the myf-5 locus with nlacZ reveals expression of this myogenic factor in mature skeletal muscle fibres as well as early embryonic muscle. Dev Dyn 1996;206:291–300.
38 Krause DS, Ito T, Fackler MJ et al. Characterization of murine CD34, a marker for hematopoietic progenitor and stem cells. Blood 1994;84: 691–701.
39 Drew E, Merzaban JS, Seo W et al. CD34 and CD43 inhibit mast cell adhesion and are required for optimal mast cell reconstitution. Immunity 2005;22:43–57.
40 Nielsen JS, McNagny KM. Novel functions of the CD34 family. J Cell Sci 2008;121:3683–3692.
41 Baumhueter S, Dybdal N, Kyle C et al. Global vascular expression of murine CD34, a sialomucin-like endothelial ligand for L-selectin. Blood 1994;84:2554–2565.
42 Drew E, Merkens H, Chelliah S et al. CD34 is a specific marker of mature murine mast cells. Exp Hematol 2002;30:1211–1218.
43 Cornelison DD. Context matters: In vivo and in vitro influences on muscle satellite cell activity. J Cell Biochem 2008;105:663–669.
44 Xu X, Yang Z, Liu Q et al. In vivo fluorescence imaging of muscle cell regeneration by transplanted EGFP-labeled myoblasts. Mol Ther 2010;18:835–842.
45 Cornelison DD, Wold BJ. Single-cell analysis of regulatory gene expression in quiescent and activated mouse skeletal muscle satellite cells. Dev Biol 1997;191:270–283.
46 Zammit PS, Relaix F, Nagata Y et al. Pax7 and myogenic progression in skeletal muscle satellite cells. J Cell Sci 2006;119:1824–1832.
47 Doyonnas R, Kershaw DB, Duhme C et al. Anuria, omphalocele, and perinatal lethality in mice lacking the CD34-related protein podocalyxin. J Exp Med 2001;194:13–27.
48 Sassetti C, Van Zante A, Rosen SD. Identification of endoglycan, a member of the CD34/podocalyxin family of sialomucins. J Biol Chem 2000;275:9001–9010.
49 Maltby S, Wohlfarth C, Gold M et al. CD34 is required for infiltration of eosinophils into the colon and pathology associated with DSS-induced ulcerative colitis. Am J Pathol 2010;177:1244–1254.
50 Blanchet MR, Gold M, Maltby S et al. Loss of CD34 leads to exacerbated autoimmune arthritis through increased vascular permeability. J Immunol 2010;184:1292–1299.
51 Strilic B, Kucera T, Eglinger J et al. The molecular basis of vascular lumen formation in the developing mouse aorta. Dev Cell 2009;17: 505–515.
52 Luz MA, Marques MJ, Santo Neto H. Impaired regeneration of dystrophin-deficient muscle fibers is caused by exhaustion of myogenic cells. Braz J Med Biol Res 2002;35:691–695.
53 Sacco A, Mourkioti F, Tran R et al. Short telomeres and stem cell exhaustion model Duchenne muscular dystrophy in mdx/mTR mice. Cell 2010;143:1059–1071.
54 Starkey JD, Yamamoto M, Yamamoto S et al. Skeletal muscle satellite cells are committed to myogenesis and do not spontaneously adopt nonmyogenic fates. J Histochem Cytochem 2011;59:33–46.
55 Bae GU, Gaio U, Yang YJ et al. Regulation of myoblast motility and fusion by the CXCR4-associated sialomucin, CD164. J Biol Chem 2008;283:8301–8309.
56 Ieronimakis N, Balasundaram G, Rainey S et al. Absence of CD34 on murine skeletal muscle satellite cells marks a reversible state of activation during acute injury. PLoS ONE 2010;5:e10920.

See www.StemCells.com for supporting information available online.

Appendix II

Manuscript:

Dick and Megeney (2013) Cell death proteins: An evolutionary role in cellular adaptation before the advent of apoptosis. *BioEssays* **35**(11):974-83

Cell death proteins: An evolutionary role in cellular adaptation before the advent of apoptosis

Sarah A. Dick[1)2)] *and Lynn A. Megeney*[1)2)*]

Programmed cell death (PCD) or apoptosis is a broadly conserved phenomenon in metazoans, whereby activation of canonical signal pathways induces an ordered dismantling and death of a cell. Paradoxically, the constituent proteins and pathways of PCD (most notably the metacaspase/caspase protease mediated signal pathways) have been demonstrated to retain non-death functions across all phyla including yeast, nematodes, drosophila and mammals. The ancient conservation of both death and non-death functions of PCD proteins raises an interesting evolutionary conundrum: was the primordial intent of these factors to induce cell death or to regulate other cellular adaptations? Here, we propose the hypothesis that apoptotic behaviour of PCD proteins evolved or were co-opted from core non-death functions.

Keywords:
apoptosis; caspase; differentiation; metacaspase; multicellularity; non-death

DOI 10.1002/bies.201300052

[1)] Sprott Center for Stem Cell Research, Regenerative Medicine Program, Ottawa Hospital Research Institute, Ottawa, ON, Canada
[2)] Department of Cellular and Molecular Medicine, University of Ottawa, Ottawa, ON, Canada

***Corresponding author:**
Lynn A. Megeney
E-mail: lmegeney@ohri.ca

Abbreviations:
PCD, programmed cell death; **PS,** phosphatidylserine.

Introduction: The evolutionary paradox of programmed cell death in unicellular life forms

We would like to emphasize that while many forms of programmed cell death (PCD) have been characterized, the following discussion will focus on caspase-mediated pathways as the proxy to address a general evolutionary origin and intent of cell death proteins.

PCD is a biochemical process in which a single cell actively commits to death through an ordered deconstruction and dismantling of organelles. A key feature that distinguishes PCD from other forms of cell demise is the high level of regulation, initiated or inhibited by a variety of environmental and intracellular controls [1]. The most common form of PCD is apoptosis, a well-defined cellular signaling cascade that culminates in the activation of caspase proteases, enzymes that once activated dismantle the proteome within the cell [2].

From the vantage point of a complex organism, apoptosis is an essential feature that coordinates normal body patterning during embryonic development and tissue homeostasis in the adult, facilitating the removal of damaged or supernumery cells [3]. The discovery of caspase homologs in single-celled species, termed metacaspases [4], has provided support for the basic contention that PCD evolved from an ancient function in early eukaryotic organisms. Indeed, forced expression and activation of these caspase homologs has been shown to yield a PCD like phenotype in various model systems such as *Saccharomyces cerevisiae* [5], suggesting that PCD is an ancient and conserved cell fate. Several prokaryotes, including various bacterial species, have now been shown to exhibit PCD in response to environmental stresses [6, 7] and during biofilm development [8, 9]. Numerous hypotheses have been posited to rationalize PCD in single-celled organisms, prominent among which is altruistic sacrifice of the individual cell for colony benefit [10–13]: a reasonable notion given the clonal nature of such cellular communities. Within this context, two arguments are commonly put forth to support the evolution of PCD in a single-celled organism. For example, PCD represents an efficient mechanism to remove otherwise

damaged or aged cells from the population [14–16]. In turn, self-sacrifice via PCD would act to provide nutrient supply for neighboring cells, maximizing population dynamism [17–19].

Despite the obvious theoretical appeal of an entrenched biochemical pathway devoted to inducing PCD, the utility of such a process in single-celled organisms is not without controversy. Foremost in the argument against an exclusive evolved PCD pathway is the simple observation that there is no evolutionary advantage for PCD in a single-celled entity. Cell death defies the basic precept of maintaining and replicating life; therefore the retention of an exclusive PCD pathway would be subject to strong negative selection pressures over the evolutionary timescale that would be required to entrench this cell fate. To rationalize this contradiction, we propose the hypothesis that apoptotic or death-centric proteins evolved from a primordial non-death role in the cell. The corollary to this premise is that PCD is a process that evolved via co-option or co-evolution from a cohort of essential proteins with canonical functions unrelated to cell death.

A non-death origin for apoptotic proteins and pathways is not a conventional perspective in the field. Indeed, while reviews over the preceding decade have highlighted the broad role of these biochemical cascades including non-death outcomes, the general consensus remains that any physiologic function is ancillary to the core death role (as reviewed in [20–22]). Here, we will present the argument for a non-death origin of this cellular machinery.

The conservation of programmed cell death pathways in complex eukaryotes

Across the broad phyla of multicellular organisms apoptosis is a highly conserved phenomenon characterized by ordered phenotypic events [23]. The penultimate step in apoptosis is often considered to be the activation of caspases, aspartic acid-directed, cysteine proteases. The caspase-mediated cleavage of cellular proteins results in reorganization of the cytoskeleton, nuclear condensation and DNA fragmentation. This promotes membrane blebbing and compaction of the cellular content in membrane bound vesicles known as apoptotic bodies. Late stage apoptosis involves flipping the membrane bound protein phosphatidylserine (PS) from its typical intercellular location to protrude outside the cell. This signals macrophages to engulf these apoptotic bodies without eliciting a traditional immune response [23]. Not surprisingly, the caspases involved in mediating these phenotypic events, and the proteins that regulate caspase activity are highly conserved.

Here we suggest that these pathways co-evolved from a single-celled ancestor common to all multicellular eukaryotes. Indication of a conserved pathway for cell death was first gleaned from studies in the simple nematode *Caenorhabditis elegans*. Genetic and biochemical evidence established a linear pathway of apoptotic induction in which there is only one caspase, CED-3 [24]. In response to a death signal, EGL-1 is actively transcribed and acts as an antagonist against the anti-apoptotic protein CED-9. Under homeostatic conditions, CED-9 is bound to the adaptor protein CED-4. Once CED-4 is released from CED-9, CED-4 oligomerizes and activates CED-3, which carries out the proteolysis typical of PCD [25](Fig. 1).

In more complex organisms the apoptotic program evolved additional modes of regulation, whereby multiple caspase enzymes interact in a coordinated signal pathway, comprising initiator caspases and effector caspases. This basic signal relationship emerged from the study of two key model systems, the fruit fly (*Drosophila melanogaster*) and the common mouse (*Mus musculus*). These dissimilar species share a remarkable number of functional orthologs with *C. elegans*, as well as with each other, indicating that these protein interactions evolved early as a requisite for normal development. The initiator and effector caspase enzymes exist within two well-defined PCD pathways, commonly referred to as the extrinsic and intrinsic pathway [26]. The extrinsic pathway is engaged by extracellular signals that bind receptors on the cell membrane, promoting oligomerization of a death inducing signaling complex (DISC). This complex is responsible for the activation of an initiator caspase, caspase-8/10, which subsequently targets an effector caspase (caspase-3, 6, and 7), in addition to other pro-apoptotic proteins. The intrinsic pathway originates within the cell in response to cellular stresses such as DNA damage, promoting the depolarization of the outer mitochondrial membrane, leading to an efflux of vital mitochondrial proteins such as cytochrome *c*, which prompts the formation of a tripartite protein complex (via binding to the adaptor protein Apaf-1 and the initiator caspase, caspase-9). The resulting complex, termed the apoptosome, promotes self-activation of caspase-9, acting as a scaffold to recruit and cleave caspase-3. Recent proteomic studies have identified close to 300 protein targets of caspase-3 within a single cell type [27], confirming the centrality of this enzyme for the proteome-wide alterations that occur during PCD.

Orthologs of Apaf-1 are found in both *C. elegans* (CED-4) and *Drosophila* (Dapaf-1 aka Dark) and are indispensable for the activation of the caspase cascade. In addition, the nematode anti-apoptotic protein CED-9, and pro-apoptotic protein EGL-1 (functional homologs to the mammalian BCL-2 and BID/BIM proteins, respectively) form the mitochondrial pore complex that acts as the conduit for cytochrome *c* release (see [2] for complete review). Interestingly, genetic analysis has identified Drp-1, a protein that promotes mitochondrial fission in *Drosophila*, and appears to induce PCD independent of cytochrome *c* release [28], suggesting a divergent origin for mitochondrial control of PCD in invertebrate animals. Nevertheless, mitochondrial membrane polarization and cytochrome *c* release during apoptosis in the metazoan, planarian *Platyhelminthes* (flat worm) [29] suggests that a mitochondrion-derived PCD signal was an early adaptation in the evolution of a common ancestor to extant multicellular organisms.

Cell death/apoptosis in single-celled life forms

As noted, PCD as a defined molecular program was initially characterized in vertebrate and invertebrate animals, yet a robust scepticism remained as to whether this cell fate/program evolved from or was present within single-celled organisms. In

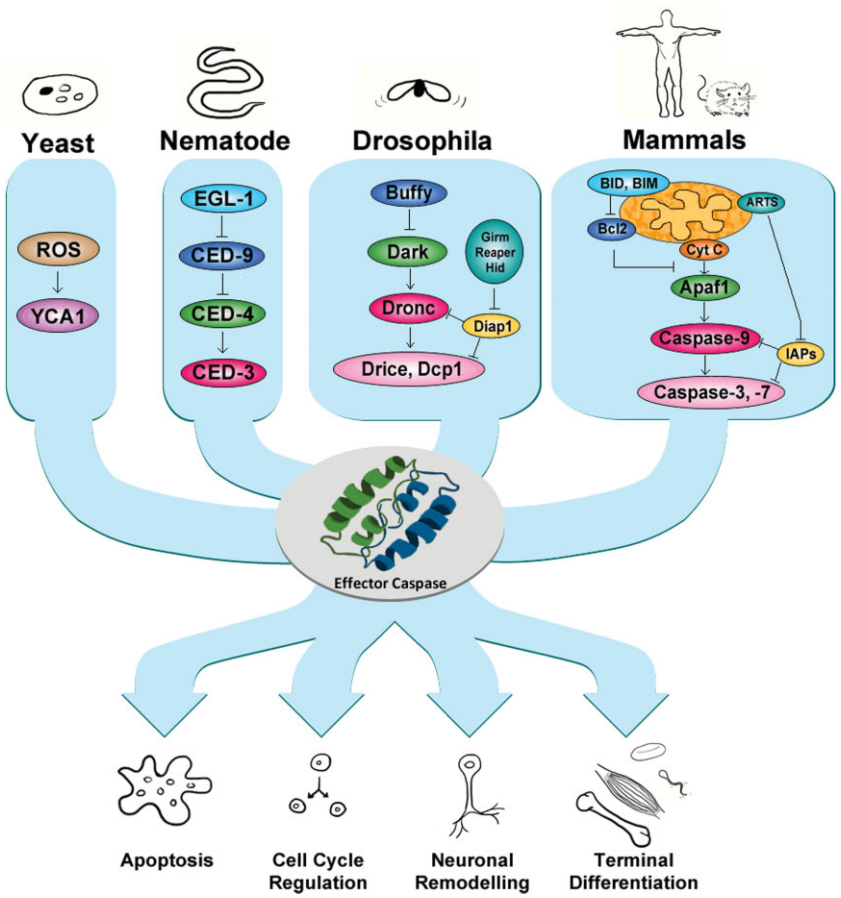

Figure 1. Conservation of the molecular pathway of caspase activation across the major species studied and its divergent physiological roles. Caspase 3 and caspase 7 in mammals, and Drice and Dcp1 in *Drosophila*, are classified as effector caspases. CED-3 in the nematode *C. elegans* functions as both the initiator and effector caspase. Effector caspases dictate diverse cell fates including apoptosis, cell cycle regulation, neuronal remodelling and terminal differentiation of a number of different cell types. The sole metacaspase in the yeast, *S. cerevisiae*, Yca1, functions similarly to an effector protease, and has been implicated in yeast apoptosis, cell cycle regulation and proteostasis. Functional homologs found within each species are indicated by the same colour.

this category, phenotypic characterization of PCD began with investigations using the budding yeast model, *S. cerevisiae* [30]. An apoptosis-like mechanism had been observed in unicellular life forms comprising the ordered dismantling of the cell, nuclear fragmentation, PS exposure [31] and compartmentalization of its nutrients and organelles into autophagic bodies [32]. High levels of reactive oxygen species (ROS) were also reported to initiate this apoptosis-like process [33]. The existence of PCD in the yeast model was strengthened with the publication of two insightful studies. First, Uren et al. [4] described a family of caspase-like proteins, termed metacaspases, present in plants, protists, and fungi. Similar to caspases, metacaspases contain a histidine/cysteine dyad in the active site and require proteolytic cleavage for activation [5, 34]. Subsequently, Madeo et al. [5] identified the sole metacaspase present in yeast, termed Yca1, demonstrating that Yca1 mediated the PCD associated with both oxidative stress and chronological aging. Overexpression of Yca1 induced PCD as defined by ordered proteolysis and membrane blebbing, while deletion of Yca1 protected the cell from PCD agonists.

Following these paradigm-setting studies, a wealth of data has established metacaspases as a probable evolutionary origin for caspase like enzymes [35]. In addition to ROS signaling, Yca1-mediated PCD is also linked to alterations in mitochondrial function [36]. For example, the mitochondrial permeability transition pore complex is required for Yca1-mediated apoptosis [31]. In addition, YCA1 is also implicated in virus-induced cell death [37] and metabolic and DNA replication defect-associated cell death [38], suggesting that metacaspases act as global conveyors of cell death akin to their respective caspase counterparts.

Metacaspases have also been identified for their role in PCD in additional fungal species as well as the kinetoplastid parasites, *Trypanosoma* [39], and *Leishmania* [40, 41]. In the fission yeast, *S. pombe*, the metacaspase Pca1 has been implicated in PCD associated with nutrient starvation [42]. In the fungi species *Aspergillus fumigatus* and *A. nidulans*, there are two metacaspases, which act antagonistically, both promoting (CasA) and protecting against (CasB) ER stress-associated cell death [43, 44].

Given the conservation of PCD in the eukaryotic phyla, a reasonable hypothesis would suggest that core PCD protein constituents evolved from a similar cohort of proteins in prokaryotic organisms. A PCD-like cell fate has been described in prokaryotes and shares many morphologic similarities with the classical apoptosis phenotypes [45–47], yet the molecular mechanisms that govern PCD in these phyla are poorly understood, and remain controversial. One protein cascade that is considered to induce PCD is the *Escherichia coli* toxin-antitoxin (TA) module, a major regulatory nodule that ensures quality control of gene expression during stress conditions [48]. Despite inducing a form of PCD, this signal conduit does not have a molecular equivalent in eukaryotes.

Nonetheless, a recent bioinformatic analysis has revealed metacaspase- and paracaspase-like enzymes across a spectrum of bacterial species [49]. Having identified a cast of probable executioner proteins, the challenge will be to substantiate the physiologic role of these factors. Assuming that metacaspase function in single-celled eukaryotes is informative, then one may predict that the prokaryotic counterpart will regulate both vital and death-centric functions.

The perceived benefits of programmed cell death in single-celled life forms

The hypothesized origin of PCD in single-celled life forms is conventionally explained as an act of altruism, a sacrifice of the individual cell for the benefit of a population at large. This is a reasonable context to assume when considering single-celled organisms that have the potential to interact as a colony, such as budding yeast [14]. Here, the cells within the larger structure are propagated by a single founder, such that all cells contain the same genetic material. Given the genetic relatedness of such a population, the benefit of selective removal of individual cells via PCD mitigates the pressure to select against this biochemical pathway over an evolutionary timeframe. Agonists that propagate PCD in yeast colonies include various forms of environmental stress, as well as nutrient starvation [14]. Indeed, studies of yeast have shown that single cells will commit to PCD if such an outcome would benefit the colony as a whole [10, 17]. Retention of a PCD pathway would also arise if there was a strong selective advantage or survival benefit of interacting as a colony versus individual cells [14]. Interestingly, in yeast colonies, cells display PCD, compartmentalizing their amino acids and nutrients for release into the extracellular space, 'feeding' the other cells in times of low nutritional stress [50]. PCD in this setting has been suggested to be an adaptive mechanism to control cell number (as in multicellular organisms) in response to nutrient constraints, while maximizing long-term population survival.

The altruistic hypothesis for the origin of PCD is a reasonable conjecture when considering examples of single-celled organisms that also have a colony-based life stage. In the parasites, *Trypanosoma* and *Leishmania*, PCD is hypothesized to be essential in maintaining the host-parasite equilibrium by controlling cell numbers during infection [51]. The apoptosis-like death of incompetent cells ensures that the current host will avoid a premature lethal infection event, which increases the probability of parasite transmission to the next host. These observations suggest that PCD may have originated from a direct competition between individual cells, which belies a less co-operative origin for PCD. For example, in the quest for genetic survival or supremacy, individual cells may engage a form of 'warfare', where paracrine signals are used to activate a PCD-like pathway in the nearest neighbor. This hypothesis does not depend on the evolution of an altruistic PCD program, which has a noted disadvantage in terms of selection pressure. Rather, one may envision that such PCD pathways have other vital roles within the cell, yet these fixed pathways can be co-opted to engage cell death by sustained activation of an otherwise non-lethal function.

The alternative hypothesis: Apoptotic/PCD proteins evolved as by-products of adaptation or co-option

Despite the perceived benefits for PCD in complex organisms, proteins solely devoted to this cell fate would be subject to enormous evolutionary constraints and selection pressures in single-celled organisms. The cell would require extensive and costly adaptations to ensure that a death centric protein could be restrained and then activated only when a series of coordinated alterations in the internal and external milieu had taken place. A more reasonable hypothesis is that primordial cells did not evolve apoptotic/PCD proteins per se, but rather that cell death evolved from the adaptation or co-option of existing proteins that performed physiologic roles within the cell.

To support the premise that the constituent proteins of PCD evolved from a non-death role in single-celled organisms, it is essential to identify a corresponding physiologic activity (if any) for these proteins. A series of observations in the yeast model *S. cerevisiae*, provided the first robust evidence that apoptotic/PCD proteins in single-celled life forms retain core non-death functions. Here, Lee et al. [52] demonstrated that yeast strains with a genetic deletion of the single metacaspase Yca1, or expressing a catalytically inactive mutant strain of Yca1 (where the catalytic cysteine residue was mutated to an alanine) displayed significant reduction in cell growth/cell fitness. Both Yca1 mutant strains were characterized by a slower G1/S transition, and a failure to respond to reagents that induce G2/M checkpoint [52]. In a subsequent study, Lee et al. characterized the precise molecular role for Yca1. Using a series of complimentary proteomic screens, these investigators noted that 1. Yca1 formed robust physical interactions with proteins that control basic proteostasis functions, including protein folding and aggregate control, and 2. that loss of Yca1 led to accumulation of vaculor structures and protein aggregates during cell cycle progression and heat stress [53]. These results confirm that the core molecular function of Yca1 is to limit protein aggregation within the cell, rather than to promote cell death per se. These observations do not exclude a role for Yca1 in PCD, and suggest that such a role may have been derived from the general aggregate targeting capacity of the protease. Indeed, one may envision conditions in the cell whereby unrestrained activation of Yca1 would lead to widespread protein aggregate disassembly, active inhibition of protein aggregate formation or limitation of the formation of vital multi-protein structures–all changes that are not conducive to basic cell survival/function [54]. The inescapable conclusion is that the PCD capacity of Yca1 may simply be the result of re-purposing a protein, rather than de novo evolution of a death specific factor. Indeed, the very concept that Yca1 manages physiologic cell death is weakened by the observation that apoptosis in multicellular yeast structures occurs independent of Yca1 activity [14].

The validity of a non-death origin for PCD protein function has been reinforced with similar observations across multiple species. In the simple unicellular eukaryote, *Trypanosoma cruzi*, the two prominent metacaspase enzymes impact a range of biological processes [39]. Metacaspase-3 and metacaspase-5 are both found overexpressed during apoptosis in these cells during cellular stress, yet overexpression of

metacaspase-3 resulted in a decreased growth rate due to a stall in the G1/S transition [55]. This metacaspase activity in trypanosomes was reminiscent of the capacity of Yca1 to control cell cycle progression in *S. cerevisieae* [52]. Furthermore, metacaspase-3 activity promoted the transition from the proliferative epimastigote stage to the infective G0-arrested metacyclic trypomastigote [55], indicating an important role for this protein in regulating the balance between life-cycle stages. Similar to Yca1, the type 1 metacaspase from the free living protozoan *Acanthamoeba castellani* has been shown to impact cell growth and also stabilize contractile vacuole formation through multiple protein-protein interactions [56]. Finally, it is germane to note the recent discovery of metacaspase like enzymes in bacteria and phytoplankton [57]. A careful molecular dissection of these enzymes may shed more light on the origin of PCD proteins and whether this cell fate emerged as a result of co-option or as a fully independent cell behavior.

In addition to metacaspases, other well-described PCD proteins have been reported to manifest non-death activities in single-celled eukaryotes. The yeast homolog of endonuclease G, Nuc1, is notable in this regard. Early studies of Nuc1 indicated a defined role in yeast PCD, yet the loss of Nuc1 also resulted in diminished cell growth capacity [31]. In addition, Nuc1 activity has been linked to the focal destruction of nuclei during yeast sporulation, a process that occurs without engaging a complete PCD response in the larger cell mass [58]. Meiotic sporulation is an alternative to asexual reproduction in yeast and occurs during times of nutrient stress. The result is the production of two surviving haploid cells while the additional nuclei are degraded through a phagocytosis-dependent process. This active nuclear destruction was shown to be dependent on Nuc1 and combined apoptotic-like genome fragmentation, while conserving the adjacent haploid structures [58]. Although not investigated in this study, the concurrent vacuolar-mediated autophagy of cell components during sporulation is consistent with the known aggregate remodeling activity of Yca1 [53], a distinctly non-apoptotic function of this protease.

Conductors of the orchestra: Apoptotic proteins as determinants of multiple cell fates

The cogent interpretation of the metacaspase and Nuc1 studies suggest that PCD evolved from or co-evolved with another cellular adaptation that utilized a similar cohort of proteins. A probable cell fate that may share this common ancestry with PCD is the process of cell differentiation. In general terms, differentiation is a final disposition where the cell ceases to divide and adopts a specialized function. This cell specialization is a critical adaptation, allowing multicellular organisms to thrive and exploit their ambient environment. Both PCD and cell differentiation involve similar morphologic and biochemical alterations that appear to be conserved across the multicellular metazoan phyla. Therefore, a co-evolution of these critical cell fates and their respective regulatory proteins is a reasonable proposition. The relevant question is whether experimental evidence can be found to support this hypothesis, or whether we are limited to reconstructing a first approximation based on observed activities of proteins in current extant organisms.

The seminal study by Ratcliff et al. [59] provides compelling evidence that PCD and differentiation may well have a common root. Here, the investigators utilized a model where they established the development of multicellularity in yeast over the course of a single experiment. Using gravity to select for multicellular clusters in the yeast, they noted that the yeast colonies arranged themselves in a snow-flake formation and employed a reproductive mechanism whereby multicellular 'propagules' or the arms of the cluster were sequentially released from the parent structure via apoptotic cell death of the centric (oldest) cells [59]. The evolution of a centric cell that would sacrifice its own direct reproduction in favor of the colony as a whole represents a division of labor, or differentiation event that is synonymous with a somatic cell and germ cell lineage. Indeed, prior to death, the centric cells displayed a basic morphology that was distinct from the cells in the "arms", suggesting that a differentiation program had been instituted.

A similar phenomenon is present in yeast grown on solid nutrient agar [50]. The yeast cells coalesce to form complex three-dimensional bodies that are composed of two distinct cell types, with different metabolic activities and distinct gene expression profiles. The lower cells (L cells), which sit directly on the medium have high metabolic activities, slow growth rates, with a definitive size in total cell number. Upper cells (U cells) are more proliferative and are more stress-resistant [50]. In this system the U cells utilize nutrients expressed by the L cells and the L cells repress growth to the benefit of the U cells. Consistent with their location in a hypoxic environment, L cells produce high levels of ROS, and are more susceptible to cell death, hence providing an additional source of nutrients to the U cells [50]. As in the study of Ratcliff et al., these observations indicate a clear division of labor or differentiation of cell types concurrent to the emergence of PCD. Moreover, ROS a well-defined apoptogen, appears to influence this division of labor between U and L cells [50], signifying a common biochemical root between PCD and differentiation. Of paramount importance will be defining the molecular basis of these induced multicellular models and the role (if any) of PCD proteins (metacaspases, etc.) in establishing these basic morphologies.

Apoptotic proteins in eukaryotes are general cell fate determinants

These elegant multicellularity studies in yeast have provided support for the hypothesis that PCD and cell differentiation may derive from a common source and utilize the same biochemical controls. However, the primary support for this supposition has been gleaned from studies involving complex cell types of vertebrate and invertebrate animals. Early studies using lens fiber epithelial cells [60] and erythrocytes [61] demonstrated that caspase 3 is essential for the differentiation of these cell types. The role of caspase 3 in these cell lineages was interpreted to be merely an attenuated form of apoptosis, as the differentiation program in each of these cell lineages is

characterized by nuclei removal and dissolution, akin to PCD. However, this death-centric view of caspase function was challenged with the publication of three landmark papers. First, Fernando et al. reported that caspase 3 activation was essential for the differentiation and formation of murine skeletal muscle [62]. Loss of caspase 3 activity through peptide inhibition, or via the generation of caspase 3 null mice, led to a drastic reduction in the endogenous differentiation capacity of skeletal muscle progenitor cells. While skeletal muscle differentiation shares phenotypic characteristics of apoptosis, myofibers are long-lived cell types that retain their nuclei in a functional syncytium. Next, Sordet et al. [63] demonstrated that the differentiation of monocytes into macrophages was dependent on the activity of a number of caspase proteases, again macrophages being cell types that retain their nuclei and defy simple characterization as an attenuated apoptotic cell. Finally, a study examining *Drosophila* spermatid maturation, provided compelling evidence for a conserved non-death role of the intrinsic cell death pathway [64]. Spermatid individualization, the final step in sperm development, is characterized by chromatin condensation along with bulk removal of the majority of cytoplasm and alterations in cytoarchitecture. Closer examination of this process revealed that Apaf-1 and cytochrome *c*, as well as the effector caspase Drice, were active during spermatid differentiation [64]. Drice activity is initially restricted to the cytoplasmic bulge, known as the individualization complex, then travels along the length of the elongated spermatid removing the bulk of the cytoplasm – a spatial and temporal regulation of caspase activity that is essential for maturation of the developing sperm.

Building on these initial observations, a plethora of studies has confirmed the requirement of PCD proteins for cell differentiation in general. To date, transient activation of caspase-mediated signaling has been found to be indispensable for the differentiation of the various haematopoietic cell lineages [65], epithelial derivatives [66], skeletal muscle [62, 67, 68], neural progenitors [69], cardiac myocytes [70], osteogenic derivatives [71], embryonic stem cells [72], etc. This caspase-dependent control of cell differentiation is also broadly conserved, having been demonstrated in vertebrate (zebrafish [73], murine, and human) and invertebrate (*Drosophila*) cells. This degree of conservation may also extend to the penultimate enzymatic step associated with PCD, caspase directed genome wide DNA damage. The differentiation of skeletal muscle myoblasts is characterized by genome wide DNA strand breaks [67], a phenomenon that is essential for the differentiation program, and has been demonstrated to be mediated by caspase 3 activation of caspase activated DNase (CAD). Most interesting is the degree to which the intrinsic PCD pathway is conserved in its entirety for the induction of these various differentiation programs. As noted above, this complete pathway conservation was initially demonstrated in *Drosophila* spermatid maturation [64], then corroborated in the study of differentiation of lens fiber epithelial cells [66], skeletal muscle myoblasts [68], and neural progenitor cells [74]. In an ironic twist, the intrinsic PCD pathway has also been implicated in the promotion of cell differentiation in *C. elegans* [75]: *C. elegans* was the pivotal model used to discover and construct the biochemical relationships that constitute caspase mediated PCD. CED-3, along with the cognate activator CED-4, acts in a calcium dependent manner to promote efficient regeneration initiation in part via the kinase DLK-1 and dependent on CED-3 protease activity [75]. Both the rate and extent of new outgrowth were dramatically reduced in CED-3 null nematodes, indicating defects in early filopodia extension. This phenotype was also observed in CED-4 null as well as the CED-3/CED-4 double mutants [75], again highlighting the conservation of the intrinsic PCD pathway in a non-death cell fate.

In addition to cell death and differentiation, caspase proteases have also emerged as critical regulatory factors in neuronal adaptation. At the cellular level, the proteolytic activity of caspase 3 has been found to be indispensable for synaptic plasticity by regulating the formation and retraction of axonal projections and dendrites (reviewed in D'Amelio et al. [76]). At the organ level, caspase 3 activity has been shown to be vital for memory, learning, and consolidation, remarkable tasks for a protein that is often considered to be the primary mediator of PCD.

Accepting the alternative hypothesis: A deeper understanding of death-centric proteins in development

There is a predilection for regarding the non-death related function of caspases and PCD pathways as ancillary or recent adaptations of a core death activity [3]. The wealth of data obtained from single-celled and multicellular organisms refute this core argument and suggest that PCD proteins evolved as general determinants of cell adaptation and cell fate (Fig. 1). The new interpretation of PCD protein biology raises a number of critical questions. First, what are the constraints and factors that direct these proteins to engage death versus non-death outcomes? Second, is elevated PCD protein activity a primary contributor to disease pathology, or do these proteins serve a physiologic role? i.e. do these proteins have a role in limiting disease pathology?

The available evidence suggests that altering the timing, duration or intensity of flux through PCD signaling pathways and proteins is a definitive step in directing divergent cell fates. The differentiation of lens fiber epithelial cells has provided an excellent model in this regard; demonstrating that cell differentiation was associated with intrinsic PCD pathway activation, accompanied by elevated expression of caspase inhibitory proteins [from the inhibitors of apoptosis (IAP) family] [66]. In contrast, cells displayed excessive levels of caspase activation during apoptosis, a level that was sufficient to overcome the threshold provided by the IAP content. PCD pathway selection of cell fate may also depend on reinforcing feedback loops between caspase proteases. Caspase 3 has been shown to cleavage-activate caspase 9, thus propagating the signal, during apoptosis [77]. Furthermore, cleavage of the caspase 7 ortholog in *Drosophila*, Dcp1, activates the caspase 3 ortholog, Drice, but not vice versa [78]. Despite having overlapping target sequences Drice and Dcp1 have very different affinities for the same death-associated targets, and Dcp1 is very inefficient at inducing cell death [78]. Post-translation modification of caspase enzymes may also

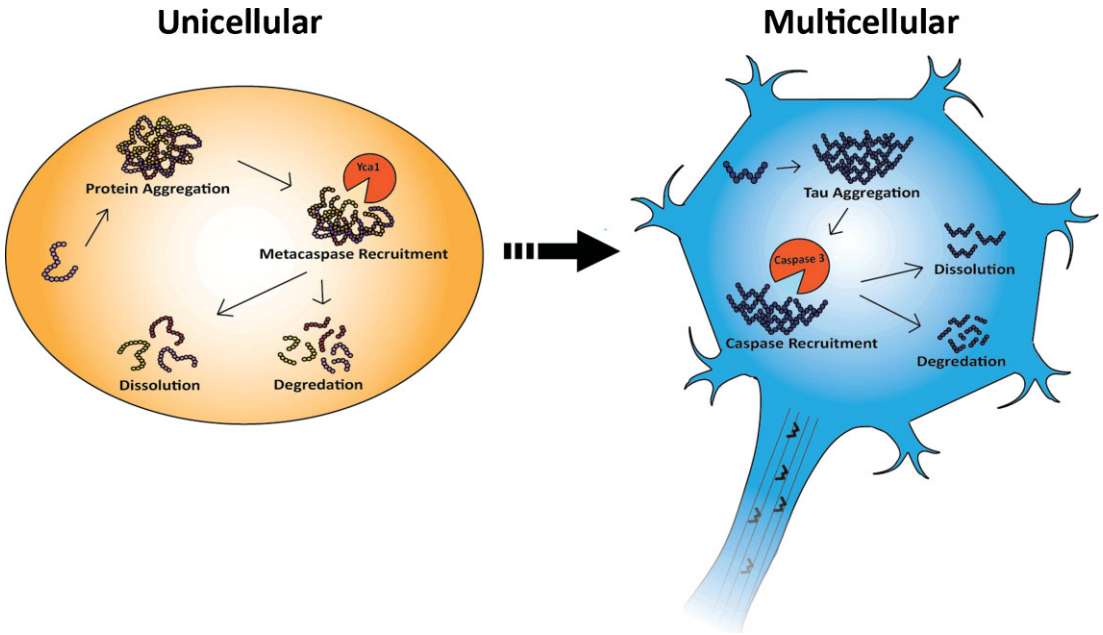

Figure 2. A model for metacaspase/caspase-mediated dissolution of protein aggregates. The yeast metacaspase Yca1 is recruited to protein aggregates during stress and participates in their dissolution. In human neurons afflicted with neurodegenerative disease, deposition of protein aggregates (represented here by Tau protein deposits as observed in Alzheimer's disease) is concurrent to caspase 3 activation. We predict that the concurrent activation of caspase in protein aggregation disease is an evolved compensatory response, engaged to rid the cell of toxic aggregate accumulation. This caspase-directed clearance of protein aggregates may be applicable to the broader class of degenerative disease that is characterized by proteostasis disruption, including ALS, Huntingtin's disease and inclusion body myopathies.

provide a rapid and convenient mechanism for a cell to guide PCD pathways to divergent outcomes. Fbox proteins that mediate degradation of caspase inhibitory proteins and stimulate proteasome activation have been demonstrated to modify the Drice/casapse 3 activity during *Drosophila* spermatid differentiation [79, 80]. Most interestingly, caspase 3, and the CK2 kinase have been shown to share an overlapping recognition motif in targeted substrates [81]. CK2 phosphorylation of a wide range of proteins prevents cleavage by caspase 3, a biochemical event that extends even to pro-caspase 3 itself [82]. Although this reciprocal relationship was only examined in conditions of apoptosis, one may envision this rheostat mechanism being directed to control caspase activity and drive non-death outcomes.

Revisiting the function of death-centric proteins in disease progression

The original discovery and characterization of PCD pathways implied that inappropriate activity of the constituent proteins may form the basis of human disease conditions, where excessive cell death is the defining characteristic. PCD has been theorized to contribute to the evolving pathology of ischemic disease, pathogen-initiated organ damage and a broad range of degenerative conditions [3, 83]. Many investigators have noted a strong association between elevated caspase activity and the cell death that characterizes neurodegenerative disorders [84]. However, caspase inhibition in many of these models does not limit the progress of disease: large numbers of neurons continue to die via caspase-independent mechanisms [85, 86]. We do not rule out the potential for these cells to engage additional cell death pathways, but propose an alternative point of view. If, as these studies suggest, caspase activation is not a core contributor to the degenerative process, then perhaps the elevated protease activity reflects a beneficial adaptive response. For example, elevated caspase 3 is known to promote synaptic plasticity and neuronal adaptation [76]. Therefore, engagement of this protease may simply reflect a compensatory mechanism to restore neuron function during neurodegeneration. The global increase in caspase activation is also consistent with the differentiation of neural progenitors, cells that may be recruited in response to damage/tissue loss (recall that neural differentiation is dependent on the intrinsic PCD pathway).

Tauopathies and proteinopathies present a most fascinating case study to re-examine caspase function in disease progression. Tauopathy and proteinopathy represent a class of neurodegenerative disease where depositions of insoluble protein aggregates represent the primary cause or contributing pathology [87]. Tauopathy is associated with detrimental amyloid protein fibril deposition (Alzheimer's being the prototypical condition), whereas proteinopathy is a more generalized disease phenotype with damaging protein inclusions and insoluble protein aggregates (ALS features prominently in this category). Both disease categories are characterized by a significant elevation in effector caspase activity and premature death of affected neurons [88]. Based on the traditional model, caspase activation is viewed as a secondary stress response, which is detrimental to the survival of the affected neuron. However, when we view these human pathologies through the prism of evolution, our knowledge of

metacaspase biology instructs that caspase activation may be engaged for the clearance of protein aggregates, a function that would maintain cell viability (Fig. 2). This supposition has not been exhaustively tested, yet supportive evidence is beginning to accrue. A significant portion of ALS patients present with protein inclusions/aggregates that contain TDP-43 protein (TAR DNA binding protein-43), and elevated expression of TDP-43 in cell and animal models replicates the essential features of ALS pathology [89]. Suzuki et al. [89] have demonstrated that TDP-43 aggregate deposition leads to the activation of caspase 3 and targeted cleavage of TDP-43. Expression of caspase cleavage-resistant forms of TDP-43 produced a dramatic increase in cell death, while expression of the cleavage fragments per se resulted in a resistance to cell death. Lastly, a recent study in yeast supports the contention that the metacaspase/caspase targeting of insoluble aggregates may have a relevant bearing on a human disease [54]. Here, Yca1 was observed to form a strong physical association with Cdc48, a protein that modifies protein aggregation. Loss of Yca1 led to a dramatic reduction in the recruitment of Cdc48 to the insoluble protein fraction, concurrent with increased aggregate formation [54]. Cdc48 is the homolog of the human AAA^{+} ATPase VCP, and substitution mutations in VCP have been shown to give rise to a progressive form of damaging protein aggregation (inclusion body myopathy with pagets disease of the bone and frontotemporal dementia) [90]. How mutations in VCP give rise to progressive aggregate formation remains unknown; nonetheless, impaired recruitment of a caspase/disaggregase would be consistent with this disease etiology.

Conclusion

In this essay we have argued that PCD proteins likely arose originally as components of the cellular adaptation machinery rather than the cell death apparatus. The prominence of PCD protein involvement in basic cell function from unicellular to multicellular organisms argues against the simple interpretation that activation of these proteins is a harbinger of cell death and hence human disease. The field must support an approach where we categorize PCD protein function in an unbiased setting and attribute outcomes or disease relevance based on clear cause and effect experiments rather than guilt by association. To further substantiate the model that caspases exert positive aggregate dissolution activity (Figure 2), priority should be given to examining whether these proteases interact (genetically or physically? or both?) with a broad range of inclusion-susceptible proteins. The potential roles of such interactions in the progression of the respective disease need to be investigated. If caspase proteases (and other PCD signaling components) evolved (in part) as a reactive mechanism to mitigate the effects of harmful protein inclusions, then implementing strategies to block caspase function during neurodegeneration might have the unintended consequence of accelerating the disease.

Acknowledgments

The authors thank members of the Megeney Laboratory for insightful discussion and comment. Due to space constraints we were not able to present all of the relevant publications in the field, we apologize to those whose work is not represented. Sarah A. Dick is supported by QEII-GSST and Lynn A. Megeney held the Mach Gaennslen Chair in Cardiac Research. Work in the laboratory of Lynn A. Megeney was supported by grants from the Canadian Institute of Health Research, The Muscular Dystrophy Association USA, and the Ontario Research Fund.

The authors have declared no conflict of interest.

References

1. **Kerr JFR, Wyllie AH, Currie AR**. 1972. Apoptosis: a basic biological phenomenon with wide-ranging implications in tissue kinetics. *Br J Cancer* **26**: 239–57.
2. **Riedl SJ, Shi Y**. 2004. Molecular mechanisms of caspase regulation during apoptosis. *Nat Rev Mol Cell Biol* **5**: 897–07.
3. **Fuchs Y, Steller H**. 2011. Programmed cell death in animal development and disease. *Cell* **147**: 742–58.
4. **Uren AG, O'Rourke K, Aravind L, Pisabarro MT**, et al. 2000. Identification of paracaspases and metacaspases two ancient families of caspase-like proteins, one of which plays a key role in MALT lymphoma. *Mol Cell* **6**: 961–7.
5. **Madeo F, Herker E, Maldener C, Wissing S**, et al. 2002. A caspase-related protease regulates apoptosis in yeast. *Mol Cell* **9**: 911–7.
6. **Aizenman E, Engelberg-Kulka H, Glaser G**. 1996. An *Escherichia coli* chromosomal addiction module regulated by guanosine [corrected] 3',5'-bispyrophosphate a model for programmed bacterial cell death. *Proc Natl Acad Sci USA* **93**: 6059–63.
7. **Hazan R, Sat B, Engelberg-Kulka H**. 2004. *Escherichia coli* mazEF-mediated cell death is triggered by various stressful conditions. *J Bacteriol* **186**: 3663–9.
8. **Bayles KW**. 2007. The biological role of death and lysis in biofilm development. *Nat Rev Microbiol* **5**: 721–6.
9. **Asally M, Kittisopikul M, Rue P, Du Y**, et al. 2012. Localized cell death focuses mechanical forces during 3D patterning in a biofilm. *Proc Natl Acad Sci USA* **109**: 18891–6.
10. **Frohlich KU, Madeo F**. 2000. Apoptosis in yeast – a monocellular organism exhibits altruistic behaviour. *FEBS Lett* **473**: 6–9.
11. **Okasha S**. 2005. Altruism, group selection and correlated interaction. *Br J Philos Sci* **56**: 703–25.
12. **West SA, Griffin AS, Gardner A**. 2007. Social semantics: altruism, cooperation, mutualism, strong reciprocity and group selection. *J Evol Biol* **20**: 415–32.
13. **Duszenko M, Figarella K, Macleod ET, Welburn SC**. 2006. Death of a trypanosome: a selfish altruism. *Trends Parasitol* **22**: 536–42.
14. **Vachova L, Palkova Z**. 2005. Physiological regulation of yeast cell death in multicellular colonies is triggered by ammonia. *J Cell Biol* **169**: 711–7.
15. **Fabrizio P, Longo VD**. 2008. Chronological aging-induced apoptosis in yeast. *Biochim Biophys Acta* **1783**: 1280–5.
16. **Gomes DS, Pereira MD, Panek AD, Andrade LR**, et al. 2008. Apoptosis as a mechanism for removal of mutated cells of *Saccharomyces cerevisiae*: the role of Grx2 under cadmium exposure. *Biochim Biophys Acta* **1780**: 160–6.
17. **Fabrizio P, Battistella L, Vardavas R, Gattazzo C**, et al. 2004. Superoxide is a mediator of an altruistic aging program in *Saccharomyces cerevisiae*. *J Cell Biol* **166**: 1055–67.
18. **Segovia M, Haramaty L, Berges JA, Falkowski PG**. 2003. Cell death in the unicellular chlorophyte *Dunaliella tertiolecta*. A hypothesis on the evolution of apoptosis in higher plants and metazoans. *Plant Physiol* **132**: 99–105.
19. **Mai-Prochnow A, Webb JS, Ferrari BC, Kjelleberg S**. 2006. Ecological advantages of autolysis during the development and dispersal of *Pseudoalteromonas tunicata* biofilms. *Appl Environ Microbiol* **72**: 5414–20.
20. **Galluzzi L, Kepp O, Trojel-Hansen C, Kroemer G**. 2012. Non-apoptotic functions of apoptosis-regulatory proteins. *EMBO Rep* **13**: 322–30.
21. **Lamkanfi M, Festjens N, Declercq W, Vanden Berghe T**, et al. 2007. Caspases in cell survival, proliferation and differentiation. *Cell Death Differ* **14**: 44–55.
22. **Bozhkov PV, Smertenko AP, Zhivotovsky B**. 2010. Aspasing out metacaspases and caspases: proteases of many trades. *Sci Signal* **3**: pe48.

23. **Elmore S**. 2007. Apoptosis: a review of programmed cell death. *Toxicol Pathol* **35**: 495–516.
24. **Yuan J, Shaham S, Ledoux S, Ellis H**, et al. 1993. The *C. elegans* cell death gene Ced-3 encodes a protein similar to Mammalian Interleukin-1B-Converting Enzyme. *Cell* **75**: 641–52.
25. **Conradt B, Horvitz HR**. 1998. The *C. elegans* protein EGL-1 is required for programmed cell death and interacts with the Bcl-2-like protein CED-9. *Cell* **93**: 519–29.
26. **Taylor RC, Cullen SP, Martin SJ**. 2008. Apoptosis: controlled demolition at the cellular level. *Nat Rev Mol Cell Biol* **9**: 231–41.
27. **Mahrus S, Trinidad JC, Barkan DT, Sali A**, et al. 2008. Global sequencing of proteolytic cleavage sites in apoptosis by specific labeling of protein N termini. *Cell* **134**: 866–76.
28. **Goyal G, Fell B, Sarin A, Youle RJ**, et al. 2007. Role of mitochondrial remodeling in programmed cell death in *Drosophila melanogaster*. *Dev Cell* **12**: 807–16.
29. **Bender CE, Fitzgerald P, Tait SWG, Llambi F**, et al. 2012. Mitochondrial pathway of apoptosis is ancestral in metazoans. *Proc Natl Acad Sci USA* **109**: 4904–9.
30. **Madeo F, Frohlich E, Frohlich KU**. 1997. A yeast mutant showing diagnostic markers of early and late apoptosis. *J Cell Biol* **139**: 729–34.
31. **Buttner S, Eisenberg T, Carmona-Gutierrez D, Ruli D**, et al. 2007. Endonuclease G regulates budding yeast life and death. *Mol Cell* **25**: 233–46.
32. **Vardi A, Eisenstadt D, Murik O, Berman-Frank I**, et al. 2007. Synchronization of cell death in a dinoflagellate population is mediated by an excreted thiol protease. *Environ Microbiol* **9**: 360–9.
33. **Madeo F, Frohlich E, Ligr M, Grey M**, et al. 1999. Oxygen stress a regulator of apoptosis in yeast. *J Cell Biol* **145**: 757–67.
34. **Gonzalez IJ, Desponds C, Schaff C, Mottram JC**, et al. 2007. *Leishmania* major metacaspase can replace yeast metacaspase in programmed cell death and has arginine-specific cysteine peptidase activity. *Int J Parasitol* **37**: 161–72.
35. **Tsiatsiani L, Van Breusegem F, Gallois P, Zavialov A**, et al. 2011. Metacaspases. *Cell Death Differ* **18**: 1279–88.
36. **Mazzoni C, Herker E, Palermo V, Jungwirth H**, et al. 2005. Yeast caspase 1 links messenger RNA stability to apoptosis in yeast. *EMBO Rep* **6**: 1076–81.
37. **Reiter J, Herker E, Madeo F, Schmitt MJ**. 2005. Viral killer toxins induce caspase-mediated apoptosis in yeast. *J Cell Biol* **168**: 353–8.
38. **Weinberger M, Ramachandran L, Feng L, Sharma K**, et al. 2005. Apoptosis in budding yeast caused by defects in initiation of DNA replication. *J Cell Sci* **118**: 3543–53.
39. **Kosec G, Alvarez VE, Aguero F, Sanchez D**, et al. 2006. Metacaspases of *Trypanosoma cruzi*: possible candidates for programmed cell death mediators. *Mol Biochem Parasitol* **145**: 18–28.
40. **Zalila H, Gonzalez IJ, El-Fadili AK, Delgado MB**, et al. 2011. Processing of metacaspase into a cytoplasmic catalytic domain mediating cell death in *Leishmania major*. *Mol Microbiol* **79**: 222–39.
41. **Lee N, Gannavaram S, Selvapandiyan A, Debrabant A**. 2007. Characterization of metacaspases with trypsin-like activity and their putative role in programmed cell death in the protozoan parasite *Leishmania*. *Eukaryot Cell* **6**: 1745–57.
42. **Guerin R, Beauregard PB, Leroux A, Rokeach LA**. 2009. Calnexin regulates apoptosis induced by inositol starvation in fission yeast. *PLoS ONE* **4**: e6244.
43. **Richie DL, Miley MD, Bhabhra R, Robson GD**, et al. 2007. The *Aspergillus fumigatus* metacaspases CasA and CasB facilitate growth under conditions of endoplasmic reticulum stress. *Mol Microbiol* **63**: 591–604.
44. **Colabardini AC, De Castro PA, De Gouvea PF, Savoldi M**, et al. 2010. Involvement of the *Aspergillus nidulans* protein kinase C with farnesol tolerance is related to the unfolded protein response. *Mol Microbiol* **78**: 1259–79.
45. **Dwyer DJ, Camacho DM, Kohanski MA, Callura JM**, et al. 2012. Antibiotic-induced bacterial cell death exhibits physiological and biochemical hallmarks of apoptosis. *Mol Cell* **46**: 561–72.
46. **Pang X, Moussa SH, Targy NM, Bose JL**, et al. 2011. Active Bax and Bak are functional holins. *Genes Dev* **25**: 2278–90.
47. **Amitai S, Kolodkin-Gal I, Hananya-Meltabashi M, Sacher A**, et al. 2009. *Escherichia coli* MazF leads to the simultaneous selective synthesis of both "death proteins" and "survival proteins". *PLoS Genet* **5**: e1000390.
48. **Pandey DP, Gerdes K**. 2005. Toxin-antitoxin loci are highly abundant in free-living but lost from host-associated prokaryotes. *Nucleic Acids Res* **33**: 966–76.
49. **Asplund-Samuelsson J, Bergman B, Larsson J**. 2012. Prokaryotic caspase homologs: phylogenetic patterns and functional characteristics reveal considerable diversity. *PLoS ONE* **7**: e49888.
50. **Cap M, Stepanek L, Harant K, Vachova L**, et al. 2012. Cell differentiation within a yeast colony: metabolic and regulatory parallels with a tumor-affected organism. *Mol Cell* **46**: 436–8.
51. **Debrabant A, Nakhasi H**. 2003. Programmed cell death in trypanosomatids is it an altruistic mechanism for survival of the fittest. *Kinetoplastid Biol Dis* **2**: 7–8.
52. **Lee RE, Puente LG, Kaern M, Megeney LA**. 2008. A non-death role of the yeast metacaspase: Yca1p alters cell cycle dynamics. *PLoS ONE* **3**: 2956.
53. **Lee RE, Brunette S, Puente LG, Megeney LA**. 2010. Metacaspase Yca1 is required for clearance of insoluble protein aggregates. *Proc Natl Acad Sci USA* **107**: 13348–1353.
54. **Shrestha A, Puente LG, Brunette S, Megeney LA**. 2013. The role of Yca1 in proteostasis. Yca1 regulates the composition of the insoluble proteome. *J Proteomics* **81**: 24–30.
55. **Laverriere M, Cazzulo JJ, Alvarez VE**. 2012. Antagonic activities of *Trypanosoma cruzi* metacaspases affect the balance between cell proliferation, death and differentiation. *Cell Death Differ* **19**: 1358–69.
56. **Saheb E, Trzyna W, Bush J**. 2013. An *Acanthamoeba castellanii* metacaspase associates with the contractile vacuole and functions in osmoregulation. *Exp Parasitol* **133**: 314–26.
57. **Choi CJ, Berges JA**. 2013. New types of metacaspases in phytoplankton reveal diverse origins of cell death proteases. *Cell Death Dis* **4**: e490.
58. **Eastwood MD, Cheung SW, Lee KY, Moffat J**, et al. 2012. Developmentally programmed nuclear destruction during yeast gametogenesis. *Dev Cell* **23**: 35–44.
59. **Ratcliff WC, Denison RF, Borrello M, Travisano M**. 2012. Experimental evolution of multicellularity. *Proc Natl Acad Sci USA* **109**: 1595–600.
60. **Ishizaki Y, Jacobson MD, Raff MC**. 1998. A role for caspases in lens fiber differentiation. *J Cell Biol* **140**: 153–8.
61. **Zermati BY, Garrido C, Amsellem S, Fishelson S**, et al. 2001. Caspase activation is required for terminal erythroid differentiation. *J Exp Med* **193**: 247–54.
62. **Fernando P, Kelly JF, Balazsi K, Slack RS**, et al. 2002. Caspase 3 activity is required for skeletal muscle differentiation. *Proc Natl Acad Sci USA* **99**: 11025–30.
63. **Sordet O, Rebe C, Plenchette S, Zermati Y**, et al. 2002. Specific involvement of caspases in the differentiation of monocytes into macrophages. *Blood* **100**: 4446–53.
64. **Arama E, Agapite J, Steller H**. 2003. Caspase activity and a specific cytochrome *c* are required for sperm differentiation in *Drosophila*. *Dev Cell* **4**: 687–97.
65. **Janzen V, Fleming HE, Riedt T, Karlsson G**, et al. 2008. Hematopoietic stem cell responsiveness to exogenous signals is limited by caspase-3. *Cell Stem Cell* **2**: 584–94.
66. **Weber GF, Menko AS**. 2005. The canonical intrinsic mitochondrial death pathway has a non-apoptotic role in signaling lens cell differentiation. *J Biol Chem* **280**: 22135–45.
67. **Larsen BD, Rampalli S, Burns LE, Brunette S**, et al. 2010. Caspase 3/caspase-activated DNase promote cell differentiation by inducing DNA strand breaks. *Proc Natl Acad Sci USA* **107**: 4230–5.
68. **Murray TV, McMahon JM, Howley BA, Stanley A**, et al. 2008. A non-apoptotic role for caspase-9 in muscle differentiation. *J Cell Sci* **121**: 3786–93.
69. **Fernando P, Brunette S, Megeney LA**. 2005. Neural stem cell differentiation is dependent upon endogenous caspase 3 activity. *FASEB J* **19**: 1671–3.
70. **Abdul-Ghani M, Dufort D, Stiles R, De Repentigny Y**, et al. 2011. Wnt11 promotes cardiomyocyte development by caspase-mediated suppression of canonical Wnt signals. *Mol Cell Biol* **31**: 163–78.
71. **Miura M, Chen X-D, Allen MR, Bi Y**, et al. 2004. A crucial role of caspase-3 in osteogenic differentiation of bone marrow stromal stem cells. *J Clin Invest* **114**: 1704–13.
72. **Fujita J, Crane AM, Souza MK, Dejosez M**, et al. 2008. Caspase activity mediates the differentiation of embryonic stem cells. *Cell Stem Cell* **2**: 595–601.
73. **Popgeorgiev N, Bonneau B, Ferri KF, Prudent J**, et al. 2011. The apoptotic regulator Nrz controls cytoskeletal dynamics via the regulation of Ca2+ trafficking in the zebrafish blastula. *Dev Cell* **20**: 663–76.
74. **Ohsawa S, Hamada S, Kuida K, Yoshida H**, et al. 2010. Maturation of the olfactory sensory neurons by Apaf-1/caspase-9-mediated caspase activity. *Proc Natl Acad Sci USA* **107**: 13366–71.
75. **Pinan-Lucarre B, Gabel CV, Reina CP, Hulme SE**, et al. 2012. The core apoptotic executioner proteins CED-3 and CED-4 promote initiation of

neuronal regeneration in *Caenorhabditis elegans*. *PLoS Biol* **10**: e1001331.
76. **D'Amelio M, Sheng M, Cecconi F**. 2012. Caspase-3 in the central nervous system: beyond apoptosis. *Trends Neurosci* **35**: 700–9.
77. **Fujita E, Egashira J, Urase K, Kuida K**, et al. 2001. Caspase-9 processing by caspase-3 via a feedback amplification loop in vivo. *Cell Death Differ* **8**: 335–44.
78. **Florentin A, Arama E**. 2012. Caspase levels and execution efficiencies determine the apoptotic potential of the cell. *J Cell Biol* **196**: 513–27.
79. **Bader M, Benjamin S, Wapinski OL, Smith DM**, et al. 2011. A conserved F box regulatory complex controls proteasome activity in *Drosophila*. *Cell* **145**: 371–82.
80. **Bader M, Arama E, Steller H**. 2010. A novel F-box protein is required for caspase activation during cellular remodeling in *Drosophila*. *Development* **137**: 1679–88.
81. **Duncan JS, Turowec JP, Duncan KE, Vilk G**, et al. 2011. A peptide-based target screen implicates the protein kinase CK2 in the global regulation of caspase signaling. *Sci Signal* **4**: ra30.
82. **Duncan JS, Turowec JP, Vilk G. Li SS**, et al. 2010. Regulation of cell proliferation and survival: convergence of protein kinases and caspases. *Biochim Biophys Acta* **1804**: 505–10.
83. **Lockshin RA, Zakeri Z**. 2007. Cell death in health and disease. *J Cell Mol Med* **11**: 1214–24.
84. **Friedlander RM**. 2003. Apoptosis and caspases in neurodegenerative diseases. *N Engl J Med* **348**: 1365–75.
85. **Lee S, Shea TB**. 2012. Caspase-mediated truncation of tau potentiates aggregation. *Int J Alzheimers Dis* **2012**: 731063.
86. **Zhang Q, Zhang X, Chen J, Miao Y**, et al. 2009. Role of caspase-3 in tau truncation at D421 is restricted in transgenic mouse models for tauopathies. *J Neurochem* **109**: 476–84.
87. **Lee SJ, Lim HS, Masliah E, Lee HJ**. 2011. Protein aggregate spreading in neurodegenerative diseases: problems and perspectives. *Neurosci Res* **70**: 339–48.
88. **Rohn TT**. 2010. The role of caspases in Alzheimer's disease; potential novel therapeutic opportunities. *Apoptosis* **15**: 1403–9.
89. **Suzuki H, Lee K, Matsuoka M**. 2011. TDP-43-induced death is associated with altered regulation of BIM and Bcl-xL and attenuated by caspase-mediated TDP-43 cleavage. *J Biol Chem* **286**: 13171–83.
90. **Kobayashi T, Manno A, Kakizuka A**. 2007. Involvement of valosin-containing protein (VCP)/p97 in the formation and clearance of abnormal protein aggregates. *Genes Cells* **12**: 889–901.

Appendix III

Manuscript:

Putinski C, Abdul-Ghani M, Stiles R, Brunette S, Dick SA, Fernando P, Megeney LA. (2013) Intrinsic-mediated caspase activation is essential for cardiomyocyte hypertrophy. *Proc Natl Acad Sci USA* **110**(43):E4079-87

Intrinsic-mediated caspase activation is essential for cardiomyocyte hypertrophy

Charis Putinski[a,b], Mohammad Abdul-Ghani[a,b], Rebecca Stiles[a,b], Steve Brunette[a], Sarah A. Dick[a,b], Pasan Fernando[b,c,d], and Lynn A. Megeney[a,b,e,1]

[a]Ottawa Hospital Research Institute, Sprott Centre for Stem Cell Research, Regenerative Medicine Program, Ottawa Hospital, Ottawa, ON, Canada K1H 8L6; [b]Department of Cellular and Molecular Medicine, Faculty of Medicine, and [e]Department of Medicine, University of Ottawa, Ottawa, ON, Canada K1H 8M5; [c]Division of Cardiology, Canadian Molecular Imaging Centre of Excellence, University of Ottawa Heart Institute, Ottawa, ON, Canada K1Y 4W7; and [d]Nordion, Ottawa, ON, Canada K2K 1X8

Edited* by Eric N. Olson, University of Texas Southwestern Medical Center, Dallas, TX, and approved September 4, 2013 (received for review August 17, 2013)

Cardiomyocyte hypertrophy is the cellular response that mediates pathologic enlargement of the heart. This maladaptation is also characterized by cell behaviors that are typically associated with apoptosis, including cytoskeletal reorganization and disassembly, altered nuclear morphology, and enhanced protein synthesis/translation. Here, we investigated the requirement of apoptotic caspase pathways in mediating cardiomyocyte hypertrophy. Cardiomyocytes treated with hypertrophy agonists displayed rapid and transient activation of the intrinsic-mediated cell death pathway, characterized by elevated levels of caspase 9, followed by caspase 3 protease activity. Disruption of the intrinsic cell death pathway at multiple junctures led to a significant inhibition of cardiomyocyte hypertrophy during agonist stimulation, with a corresponding reduction in the expression of known hypertrophic markers (atrial natriuretic peptide) and transcription factor activity [myocyte enhancer factor-2, nuclear factor kappa B (NF-κB)]. Similarly, in vivo attenuation of caspase activity via adenoviral expression of the biologic effector caspase inhibitor p35 blunted cardiomyocyte hypertrophy in response to agonist stimulation. Treatment of cardiomyocytes with procaspase 3 activating compound 1, a small-molecule activator of caspase 3, resulted in a robust induction of the hypertrophy response in the absence of any agonist stimulation. These results suggest that caspase-dependent signaling is necessary and sufficient to promote cardiomyocyte hypertrophy. These results also confirm that cell death signal pathways behave as active remodeling agents in cardiomyocytes, independent of inducing an apoptosis response.

The vertebrate heart is structurally complex, yet this organ retains a remarkable ability to adjust intrinsic cell properties to alterations in the exterior milieu. A most critical aspect of this phenomenon is hypertrophic growth of individual cardiomyocytes. This form of cell adaptation is a vital feature that matches physiologic enlargement of the heart to the growth of the organism, yet compensatory hypertrophy is also a prominent feature of cardiac disease. Consequently, disease hypertrophy has been intensely studied, resulting in the identification of a consistent cellular pathology. In general, the pathologic condition derives from an agonist or trigger that stimulates key intracellular signaling pathways, which converge on transcription factors to reengage the fetal gene expression program in cardiomyocytes. Prominent examples of this molecular circuit are agonist-induced mitogen-activated protein kinase (MAPK)/CAMK (Ca^{2+}/calmodulin-dependent kinase) activation of myocyte enhancer factor-2 (MEF2) transcription and calcineurin activation of nuclear factor of activated T cells (NFAT) transcription (1–3).

Despite the success in identifying the key transcription control events during cardiomyocyte hypertrophy, the pathways or proteins that couple the fetal gene expression program with the structural reorganization of the cell remain largely unknown. One notable facet of hypertrophy is the degree to which this cell morphology shares overlapping features of programmed cell death or apoptosis. For example, hypertrophy is characterized by standard hallmarks of programmed cell death, including cytoskeletal reorganization and disassembly, altered nuclear morphology, and enhanced protein synthesis/translation (4, 5). Moreover, although cardiomyocyte hypertrophy is initially adaptive, hypertrophy often transits to a myopathic response that results in dilation, a latter event that is concurrent with an increased incidence of caspase-mediated cell death (6, 7). Therefore, a reasonable supposition is that activation of canonical cell death pathways may contribute to the initiation and/or progression of hypertrophy.

In addition to these general features, a number of proapoptotic agonists have been directly implicated in the development of cardiac hypertrophy, including tumor necrosis factor alpha (TNF-α) and the cognate FAS receptor. Antibody blockade of TNF-α leads to diminished overload-induced hypertrophy (8), and mice with genetic deletion of TNF-α display similar attenuation of an overload-induced hypertrophy response (9). Similarly, Fas ligand activation of the Fas receptor has been noted to prompt the induction of cardiomyocyte hypertrophy, and loss of the Fas receptor in vivo was reported to result in a dramatic reduction in compensatory hypertrophy through an as yet undefined signal (10). Interestingly, the apoptotic endonuclease EndoG has recently been shown to play a critical nonapoptotic role in maintaining mitochondrial bioenergetics, and defects in EndoG have directly been linked to the subsequent development of maladaptive hypertrophy (11).

These phenotypic and biochemical intersections raise the provocative hypothesis that a caspase signaling mechanism may propagate or direct the hypertrophy response in cardiomyocytes. This is not an unreasonable premise, as a growing body of literature has demonstrated that caspase-dependent apoptosis pathways act as essential drivers of cell differentiation, including the differentiation of cardiac progenitor cells (12, 13). Canonical cell

Significance

Cardiac hypertrophy is a pathologic enlargement of the heart, an alteration that leads to contractile dysfunction and eventual organ failure. The hypertrophy phenotype originates from concentric growth of heart muscle cells and shares many biochemical features with programmed cell death, implying a common molecular origin. Here, we show cell-autonomous activation of a mitochondrial cell death pathway during initial stages of muscle cell hypertrophy, a signal that is essential and sufficient to promote hypertrophy. Targeting individual cell death proteins may offer an effective means to limit the initial stage of cardiac disease, and forgo the transition to heart failure.

Author contributions: C.P., M.A.-G., R.S., S.B., P.F., and L.A.M. designed research; C.P., M.A.-G., R.S., S.B., S.A.D., and P.F. performed research; C.P., M.A.-G., R.S., and L.A.M. analyzed data; and C.P., M.A.-G., and L.A.M. wrote the paper.

The authors declare no conflict of interest.

*This Direct Submission article had a prearranged editor.

[1]To whom correspondence should be addressed. E-mail: lmegeney@ohri.ca.

This article contains supporting information online at www.pnas.org/lookup/suppl/doi:10.1073/pnas.1315587110/-/DCSupplemental.

death pathways derive from an intrinsic source originating from the mitochondria, or an extrinsic source as mediated by prodeath ligand/receptor interactions. Once engaged, these pathways ultimately converge, activating caspase proteases (such as caspase 3), which cleave vital protein substrates that usher in the cell death response. Here, we demonstrate that agonist-induced cardiomyocyte hypertrophy is associated with and critically dependent on the transient activation of the mitochondrial/intrinsic cell death pathway. Inhibition of the intrinsic pathway (at multiple levels) led to a dramatic attenuation of hypertrophy, whereas small-molecule induction of caspase activation alone was sufficient to recapitulate the phenotypic and biochemical characteristics of cell hypertrophy.

Results and Discussion

Activation of the Intrinsic Cell Death Pathway During Agonist-Induced Cardiomyocyte Hypertrophy. To begin to address the role of caspase-mediated signaling in cardiomyocyte adaptation, we used immunofluorescence microscopy to detect caspase activity during agonist-induced hypertrophy (Fig. 1 and Figs. S1–S3). Given the prominent role of caspase 3 as a mediator of cell fate determination, we initially examined the activity kinetics for this effector protease. Treatment of primary cardiomyocytes with the hypertrophy agonist phenylephrine (PE) resulted in rapid formation of active caspase 3 foci in the cytoplasm and within a nuclear/perinuclear compartment (Fig. 1*A*, *c* and *d*). Similar to PE, isoproterenol (ISO) treatment also resulted in nuclear localized active caspase 3 foci (Fig. 1 *A*, *e* and *f*). Caspase 3 activation and localization was also analyzed for additional hypertrophic agonists, including angiotensin II (AngII) and endothelin 1 (ET1), which displayed a similar caspase 3 activation pattern (Fig. S1 *A*, *c* and *d* and *e* and *f*, respectively). Within only 30 min of PE treatment, the number of cardiomyocytes expressing active caspase 3 increased compared with cells not treated with PE (Fig. S2, green, *e* and *f* vs. *g* and *h*; white arrows indicate nuclear and perinuclear localization patterns). Similar caspase 3 activation and localization was observed at 1 h (Fig. 1 *A*, *a* and *b* vs. *c* and *d*) and 3 h (Fig. S2, *i* and *j* vs. *k* and *l*) of PE exposure. Following 24 h of PE treatment, the caspase 3 activation pattern was detectable yet diminished, with limited cytoplasmic and perinuclear/nuclear activity (Fig. S2, green, *m* and *n* vs. *o* and *p*). Caspase 3 localization was quantified based on the number of cardiomyocytes expressing nuclear activated caspase 3 and the number of active caspase 3 foci per nuclei (Fig. 1*A*). A significant increase in the number of nuclei with active caspase 3 as well as total foci number was observed during agonist-induced hypertrophy (Fig. 1*A* and Fig. S1*A*). Furthermore, caspase 3 nuclear specificity was demonstrated by *z*-stack confocal imaging (Fig. S4). The focal activity pattern for caspase 3 suggested that the cardiomyocyte may restrict the protease activity to discrete compartments to engage nonapoptotic cellular functions. Indeed, otherwise lethal caspase activity can be refocused and restrained to effect targeting of particular cellular structures during remodeling and differentiation (14–16). Preliminary experiments indicate that caspase 3 activity in the total soluble protein fraction/lysate does not change during PE-induced hypertrophy (Fig. S5), suggesting that the active protease may be directed to a unique insoluble compartment within the cell.

α-Adrenergic stimulation via PE exposure has been reported to alter mitochondrial calcium leak and membrane potential (17, 18). As such, we reasoned that the source of caspase 3 activation during hypertrophy stimulation may originate from transient activation of the intrinsic/mitochondrial cell death pathway rather than the ligand-associated extrinsic-mediated cell death pathway. Caspase 9 activity represents an immediate downstream proxy for mitochondrial-derived signals whereby, in response to an apoptogen, the mitochondria releases cytochrome *c* (cyt *c*), promoting activation of procaspase 9 within the multiprotein apoptosome complex. Immunofluorescence analysis revealed a caspase 9 activation pattern as early as 15 min post hypertrophic induction (Fig. S3 *A*, *a* and *b* vs. *c* and *d*), with a peak of activation at 1 to 3 h after PE exposure in healthy, intact cardiomyocytes (Fig. 1 *B*, *a* and *b* vs. *c* and *d*; and Fig. S3 *A*, *m* and *n* vs. *o* and *p*). Additional hypertrophic agonists ISO (Fig. 1 *B*, *a* and *b* vs. *e* and *f*; and Fig. S3*A*), AngII (Fig. S1 *B*, *a* and *b* vs. *c* and *d*; and Fig. S3*B*), and ET1 (Fig S1 *B*, *a* and *b* vs. *e* and *f*; and Fig. S3*B*) showed similar caspase 9 activation patterns. With all hypertrophic agonists, caspase 9 activity was dispersed throughout the cell, reminiscent of a typical mitochondrial distribution pattern. Activation of the intrinsic (caspase 9-mediated) pathway was further confirmed by measuring the drop in mitochondrial membrane potential, which is an early essential step in this pathway. PE and ISO treatments led to a similar induction of the intrinsic pathway as early as 5 min after hypertrophic induction (see number symbols in Fig. 1 *C*, *Left* and *Right*, respectively). Together, these data demonstrate that agonist-induced hypertrophy leads to activation of the intrinsic cell death signal pathway in a temporally restricted manner.

It is important to note that this initiation signal (caspase 9 and caspase 3 activation) is not followed by induction of apoptosis per se. Extensive analysis of cardiomyocyte viability during agonist-induced hypertrophy was conducted by annexin V/propidium iodide (PI) labeling, TUNEL labeling of apoptosis-induced DNA damage, and analysis of nuclear integrity via DAPI staining (Fig. 1*D*). These efforts indicate that there is no significant increase in apoptotic cell death during hypertrophic agonist stimulation.

Activation of the Intrinsic Cell Death Pathway Is Required for Cardiomyocyte Hypertrophy. Next, we investigated the requirement of the intrinsic mediated cell death pathway for mediating the hypertrophy response. Presumably, if the agonist-induced hypertrophy response required sequential activation of the intrinsic pathway, inhibition of this signal should reduce or block hypertrophy. Primary cardiomyocytes were treated with PE in the presence or absence of the caspase 9 peptide inhibitor *N*-benzyloxycarbonyl-Leu-Glu-His-Asp-fluoromethylketone (z-LEHD-fmk). A significant attenuation of cardiomyocyte cell size (~39%) was noted after caspase 9 inhibition (Fig. 2 *A*, *b* vs. *c*). In addition to cell size, a significant reduction in the expression of the prohypertrophic marker atrial natriuretic peptide (ANP; ~62%) (19) was also observed following caspase 9 inhibition (Fig. 2 *A*, *e* vs. *f*). Although caspase 9 represents an accurate proxy for intrinsic pathway activation, we sought to confirm the mitochondria as the de facto initiation signal. Here, the intrinsic pathway was inhibited during agonist stimulation by infection with an adenovirus (AdV) expressing the myeloid cell leukemia 1 (Mcl-1) protein. Mcl-1 binds to various proapoptotic Bcl-2 homology 3 (BH3)-only proteins such as Bid and Bim and multiple BH domain proteins Bax and Bak, inhibiting BH3 pore formation in the mitochondrial membrane, squelching cyt *c* release, and effectively blocking activation of the intrinsic apoptotic pathway (20, 21). A significant decrease in cell size (~33%) and ANP levels (~61%) was noted in Mcl-1-AdV–infected cardiomyocytes compared with PE treatment alone (Fig. 2 *B*, *b* and *h* vs. *c* and *i*). ISO treatment (Fig. 2 *C*, *b* and *h* vs. *c* and *i*) and additional hypertrophic agonists, AngII and ET1, yielded similar reductions in cell size and ANP levels (Fig. S6). The decrease in cell size and ANP levels resulting from Mcl-1-AdV infection mirrors the observations with caspase 9 peptide inhibition, suggesting an essential role for the intrinsic cell death pathway in promoting hypertrophic induction.

Effector Caspase/Caspase 3 Activation Is Essential for Cardiomyocyte Hypertrophy in Vitro and in Vivo. We next examined the requirement of caspase 3 activity in the development of the hypertrophy response. Primary cardiomyocytes were treated with the caspase 3-specific peptide inhibitor N-benzyloxycarbonyl-Asp-Glu-Val-Asp-fluoromethylketone (z-DEVD-fmk), followed by cell size and ANP quantifications. The PE-induced hypertrophic pheno-

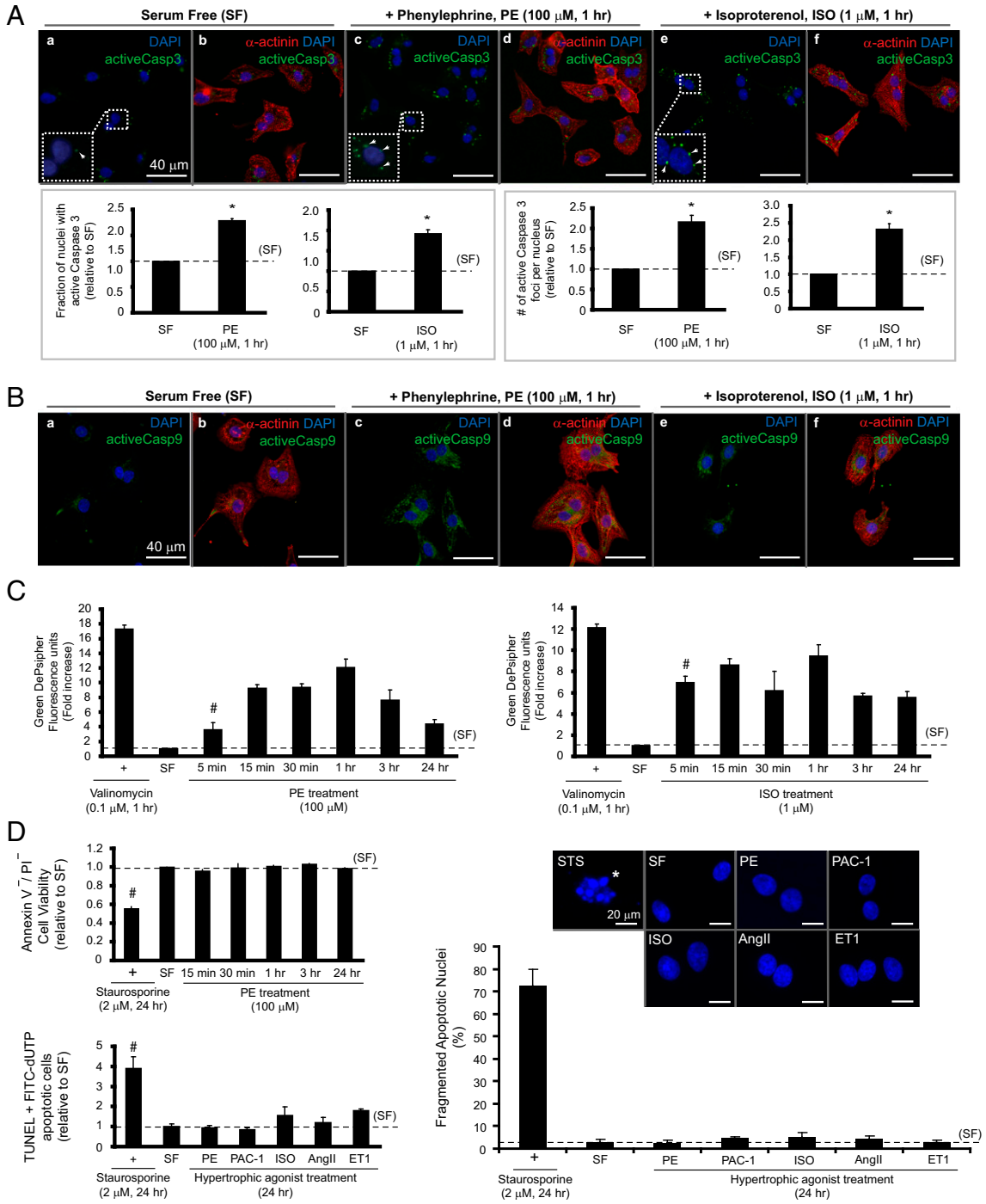

Fig. 1. Increased caspase 3 and 9 activation during early stages of PE- and ISO-induced cardiomyocyte hypertrophy. (*A*) Cardiomyocytes were treated with hypertrophic agonists PE (100 μM; *c* and *d*) or ISO (1 μM; *e* and *f*) to induce hypertrophy for 1 h. Immunofluorescence was used to detect activated caspase 3 (green), α-actinin (red), and DAPI (blue). Exposure to PE or ISO for only 1 h resulted in a significant increase in the number of cardiomyocytes expressing activated caspase 3 (green; PE, *c* and *d*; ISO, *e* and *f*) compared with SF media-treated cells (*a* and *b*). Activated caspase 3 displayed localization to the perinuclear and nuclear regions during hypertrophic induction (compare *c* and *d* and *e* and *f* vs. *a* and *b*). Magnified views are shown in boxed regions (white arrows; *a* and *c* vs *a* and *e*). The fraction of nuclei with active caspase 3 and the fraction of active caspase 3 foci per nucleus during PE and ISO treatment significantly increased after 1 h compared with SF controls ($n = 3$; $^{*}P < 0.05$; Figs. S1*A* and S2). (*B*) Cardiomyocytes were treated as in *A* and stained for activated caspase 9 (green). Caspase 9 activation was readily detected during PE and ISO treatment (green; *c* and *d* and *e* and *f*) compared with SF media-treated control cells (*a* and *b*; Figs. S1*B* and S3). (Scale bars: 40 μm.) (*C*) Activation of the intrinsic (caspase 9-mediated) pathway was also evaluated by use of the DePsipher kit. Green DePsipher fluorescence was quantified during PE- and ISO-induced hypertrophy from 5 min to 24 h. A significant increase in green fluorescence was observed after only 5 min of hypertrophic induction, suggesting early intrinsic pathway activation ($n = 3$; $^{\#}P < 0.05$). (*D*) Caspase activation during agonist-induced hypertrophy occurs in viable cardiomyocytes. Cardiomyocyte viability was evaluated by analysis of annexin V/PI double-negative cell population, fragmented apoptotic nuclei quantifications (asterisk), and TUNEL assay. Staurosporine treatment led to a significant reduction in cardiomyocyte viability ($n = 3$; $^{\#}P < 0.05$). Cardiomyocyte viability remained intact after 24 h hypertrophic induction with PE (100 μM), PAC-1 (25 μM), ISO (1 μM), AngII (100 nM), and ET1 (20 nM). (Scale bars: 20 μm.)

type was abrogated by caspase 3 inhibition, as demonstrated by reduced cell size (~36%) and ANP levels (~42%; Fig. 3 *A*, *b* and *e* vs. *c* and *f*). Caspase 3 inhibition was also accomplished by infection of primary cardiomyocytes with an AdV expressing the baculoviral protein p35 (22). p35 acts to competitively inhibit effector caspases by an irreversible chemical process. The caspase recognition sequence of p35 is targeted by the effector caspase (3, 6, 7), forming a thioester bond between the active cysteine and the P_1 residue, resulting in a completely disabled enzyme (23). p35 is the most potent inhibitor of caspases identified to date, providing an irreversible inhibition of all caspase enzymes except caspase 9 (23, 24). Importantly, the infection of cardiomyocytes with p35-AdV led to a similar reduction in the hypertrophic response following exposure to PE and ISO (decreased ANP levels in Fig. 3*B*), as well AngII and ET1 (decreased ANP and cell size in Fig. S7 *A–C*). Finally, we demonstrate that, within the same cardiomyocyte culture, cells that are infected with caspase signaling inhibitors (p35-AdV) do not respond to hypertrophy agonists, whereas the uninfected cardiomyocytes in the same culture undergo hypertrophy (Fig. S8). Taken together, these data confirm that secondary paracrine effects of caspase activity in adjacent apoptotic cells do not significantly impact the hypertrophy response.

To further confirm the caspase 3-induced hypertrophy response, we measured the transcriptional response of known prohypertrophic markers [MEF2, NF-κB, ANP, (B-type natriuretic peptide (BNP)]. Primary cardiomyocytes were transfected with MEF2, NF-κB, ANP, or BNP plasmids (with a *Renilla* luciferase internal control plasmid) and monitored for the response to agonist and caspase activation (SF plus DMSO, PE plus DMSO, PE plus z-DEVD-fmk or z-LEHD-fmk). PE treatment resulted in a significant increase in all hypertrophic markers compared with cardiomyocytes treated with SF plus DMSO media (Fig. 3*C*), whereas PE treatment followed by caspase 3 or caspase 9 inhibition led to a dramatic reduction in reporter activation compared with PE plus DMSO treatment (Fig. 3*C*).

We next sought to identify a molecular cascade whereby caspase 3 activity engages the hypertrophy response. In this regard, the MEF2 pathway was of considerable interest. The MEF2 family functions as a point of convergence for a variety of hypertrophic signals, including the fetal gene program (3, 25). MEF2 transcriptional activity is suppressed by the binding of histone deacetylases (HDACs), and relief of this repression has been well documented as a key step in the hypertrophic response (3). Of interest, caspase 3 has been shown to cleave HDAC3 and HDAC4, resulting in their cytoplasmic relocalization during apoptotic signaling (26–28). Moreover, cardiac-specific deletion of HDAC3 is synonymous with a pronounced cardiac hypertrophy phenotype (29). To address our supposition that caspase 3 activity is restrained in insoluble foci, we first examined levels of activated caspase 3 in the soluble and insoluble fractions. We observed a significant increase in the level of active caspase 3 within the insoluble fraction of PE-treated cardiomyocytes as early as 30 min, followed by a transient decrease and then a latter-stage increase in activity (Fig. S7*D*). We observed a specific and temporal decline in levels of full-length HDAC3 at early time points following PE-induced hypertrophy in the soluble fraction, whereas HDAC4 protein levels remained unchanged (Fig. S7*D*). Furthermore, infection of cardiomyocytes with p35-AdV blocked the temporal decline in HDAC3 protein levels, suggesting that the HDAC3 decrease was caspase 3-dependent (Fig. S7*D*). Finally, we noted a large concentration of full-length HDAC3 (~48 kDa) within the insoluble protein fraction, which was associated with a cleavage event that was attenuated with p35-AdV (Fig. S7*D*, asterisk). The size of the putative fragment (~44 kDa) corresponds to the predicted size of the caspase 3-mediated large C-terminal cleavage fragment of HDAC3 observed by others (26). Interestingly, a classic caspase 3 cleavage site is present at Asp-391 of the C terminus of HDAC3 that would produce this putative large HDAC3 fragment. Prior observations in the literature also suggest that HDAC proteins do segregate and associate with an insoluble fraction (30, 31). Liu et al. noted that Hos2 (yeast HDAC) and Yca1 (yeast metacaspase) were contained within insoluble stress granules (30). Our group has previously demonstrated that the core molecular function of Yca1 is to limit protein aggregate formation in response to stress (16). As such, a reasonable conjecture is that the colocalization of caspase 3 and HDAC3 (and the caspase-mediated processing of HDAC3) may represent an adaptive stress response in cardiomyocytes, a response that has been conserved from single-celled eukaryotes. This is a topic of considerable interest and will require additional experimental validation to confirm this hypothesis.

Consistent with a model of caspase-mediated derepression of MEF2, we also observed that MEF2 transcriptional activity (via an MEF2-dependent reporter assay) was dramatically attenuated (~80%) in cardiomyocytes with impaired caspase activation via p35-AdV during PE stimulation (Fig. 3*D*). An additional hypertrophic transcription signal that may respond to and translate caspase activity is the NF-κB pathway. NF-κB is a transcription factor that responds to stress signaling to promote or enhance cell survival, yet this factor is also a prominent feature in pathological cardiac hypertrophy (32). Interestingly, caspase proteases have been shown to activate NF-κB signaling in a variety of noncardiac settings, steps that involve cleavage-activation of the inhibitor of kappa B kinase (IKK) kinases, as well as targeted cleavage and removal of the inhibitor of kappa B alpha (IκBα), the NF-κB inhibitor protein (33–35). PE-treated cardiomyocytes displayed a significant increase in NF-κB reporter activity, yet caspase inhibition via p35-AdV infection resulted in complete blockade of the NF-κB–induced response (~84%; Fig. 3*D*). These results suggest that the hypertrophy-associated engagement of NF-κB activity is caspase 3-responsive, yet we have been unable to identify the precise caspase 3 substrate that is targeted in this pathway.

Caspase 3-mediated induction of cardiomyocyte hypertrophy was also examined in the intact myocardium. PE control and experimental groups were subject to ultrasound-guided microinjection of the left ventricle wall with control GFP-AdV or p35-AdV expressing AdVs. After 3 d, osmotic minipumps were implanted in rats containing saline solution (control) or PE (PE control and experimental groups) to induce pathologic hypertrophy. Subsequently, hearts were retrieved at 3 wk after treatment, to coincide with the early stages of adaptive hypertrophy. Hearts treated with PE and infected with p35-AdV displayed a significant reduction in heart weight to body weight (HW/BW) ratio (~12%) and cardiomyocyte cell size (~37%) compared with the PE-treated GFP-AdV–infected group (Fig. 4*A*). Similarly, ISO-induced hypertrophy in vivo (2 wk) was significantly blunted in the presence of p35-AdV, with a decreased HW/BW ratio (~12%) and cardiomyocyte cell size (~42%) compared with the ISO-treated GFP-AdV–infected group (Fig. 4*B*). Therefore, similar to the in vitro experimental observations, inhibition of effector caspase activity (caspase 3) attenuates cardiomyocyte hypertrophy in the intact heart.

Caspase 3 Activation Is Sufficient to Induce Cardiomyocyte Hypertrophy. The combination of peptide and biologic inhibitor experiments demonstrate that intrinsic-mediated cell death signaling is required for the development of cardiomyocyte hypertrophy. As such, we next examined whether caspase activation was sufficient to engage hypertrophy, independent of any agonist stimulation. To test this premise, we used a small molecule that specifically stimulates caspase 3 activation, termed procaspase 3 activating compound 1 (PAC-1). PAC-1 is a potent and specific activator of procaspase 3 that acts via sequestration of the inhibitory zinc ions at the catalytic site on the pro form of caspase 3 (36, 37). As unrestricted caspase 3 activation leads to induction of apoptosis, we conducted a dose range experiment to establish

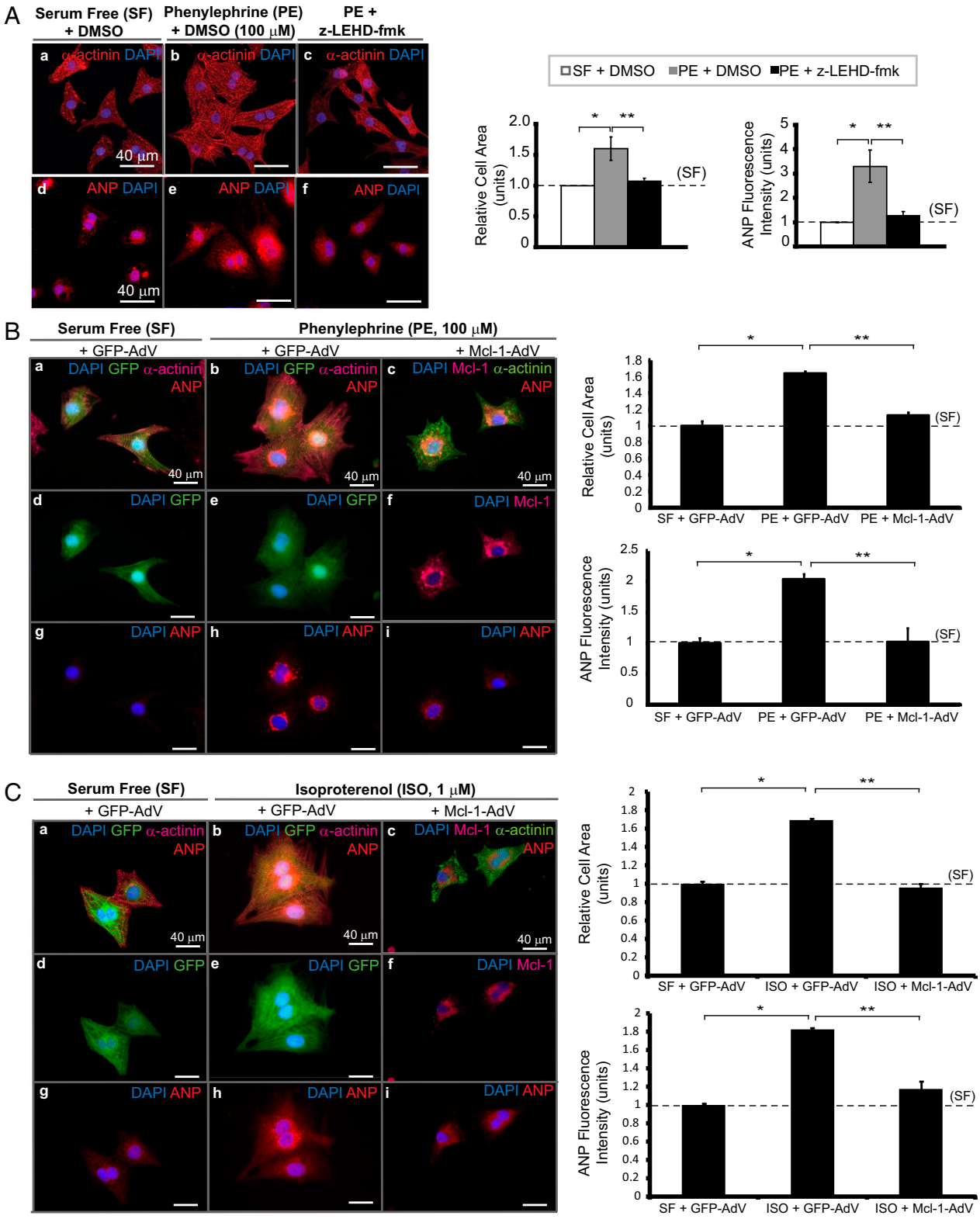

Fig. 2. The intrinsic mitochondrial/caspase 9 cell death pathway is required for PE- and ISO-induced cardiomyocyte hypertrophy. (*A*) Cardiomyocytes were treated for 24 h with SF medium (*a* and *d*), 100 μM PE (*b* and *e*), and PE plus 20 μM caspase 9 inhibitor z-LEHD-fmk (*c* and *f*). PE treatment increased cell size, which was significantly attenuated in the presence of z-LEHD-fmk (*Left*; $n = 3$, $^{**}P < 0.05$). ANP levels were significantly reduced in the presence of z-LEHD-fmk compared with PE-treated cells (*Right*; $n = 3$, $^{**}P < 0.05$). (*B*) Mcl-1-AdV inhibition of the intrinsic caspase 9 pathway, with GFP-AdV used as a control. Infection with Mcl-1-AdV significantly decreased cell size and ANP levels compared with PE plus GFP-AdV–treated cardiomyocytes ($n = 3$; $^{**}P < 0.05$). (*C*) Cardiomyocytes were treated as in *B* except ISO was the hypertrophic agonist (1 μM). Similarly, intrinsic pathway inhibition by Mcl-1-AdV infection led to significantly reduced cell size and ANP levels ($n = 3$; $^{**}P < 0.05$). For *B* and *C*, Mcl-1 expression was detected with anti-myc antibody and an Alexa 647 (pink)-conjugated secondary antibody (Fig. S6). Cell sizes analyzed by using ImageJ software. (Scale bars: 40 μM.)

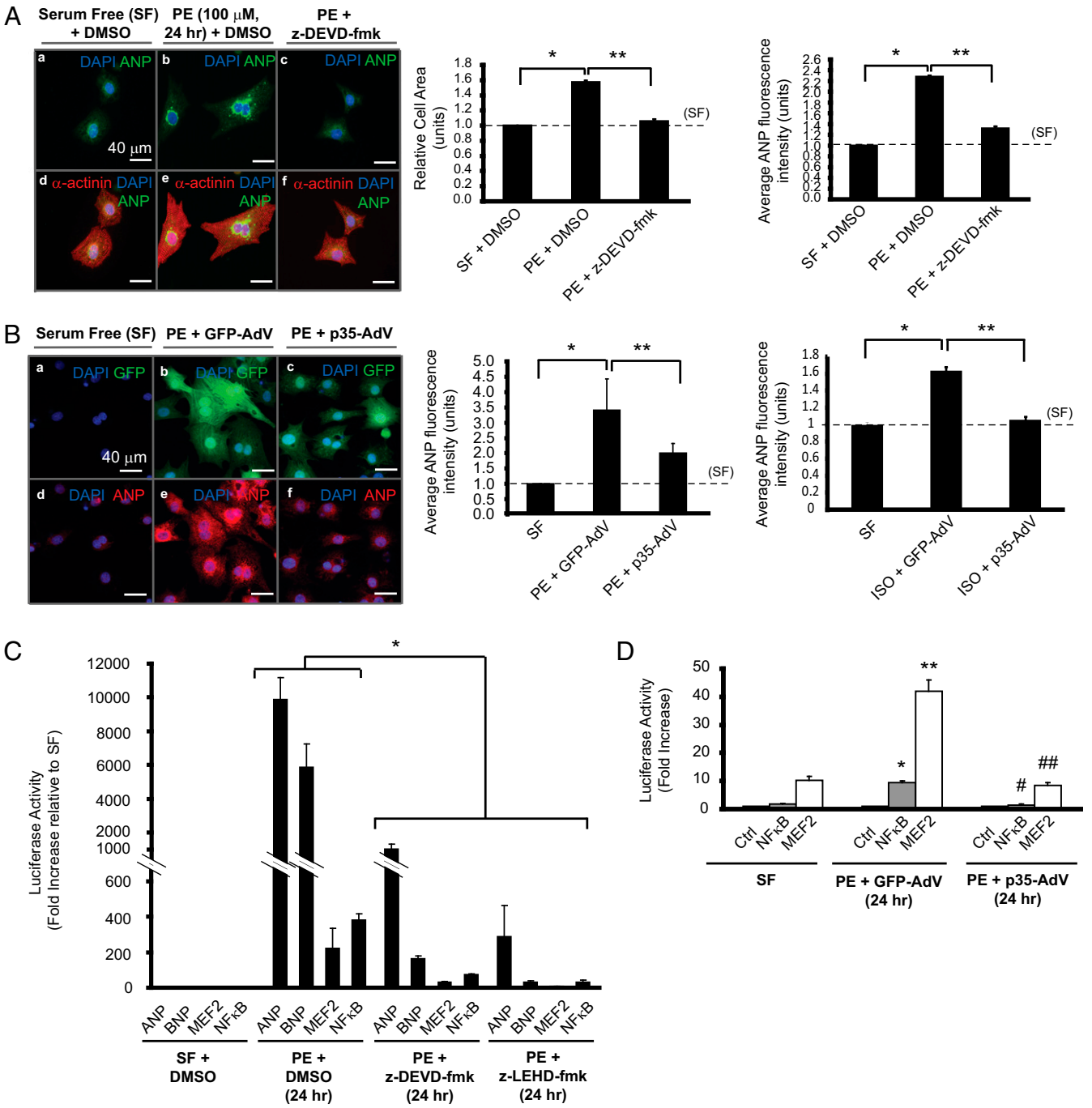

Fig. 3. Caspase 3 activation is required for PE- and ISO-induced cardiomyocyte hypertrophy. (*A*) Cardiomyocytes were treated for 24 h with SF medium (*a* and *d*), 100 μM PE (*b* and *e*), and PE plus 20 μM caspase 3 inhibitor z-DEVD-fmk (*c* and *f*). PE induced a significant increase in cell size, which was inhibited by z-DEVD-fmk (*Left*; $n = 3$; $^{**}P < 0.05$). PE also increased the levels of ANP, whereas the presence of z-DEVD-fmk reduced ANP expression (*Right*; $n = 3$; $^{**}P < 0.05$). (*B*) Cardiomyocytes were treated with SF medium (*a* and *d*), 100 μM PE plus GFP-AdV (*b* and *e*), and PE plus p35-AdV (*c* and *f*). During PE treatment, a significant increase in ANP was detected, whereas p35-AdV decreased ANP levels (*Left*; $n = 3$; $^{**}P < 0.05$). p35-AdV infection also led to significantly reduced ANP levels during ISO-induced hypertrophy (*Right*; $n = 3$, $^{**}P < 0.05$; Fig. S7). (*C*) Cardiomyocytes were transfected with luciferase reporter plasmids for prohypertrophic markers (ANP, BNP, MEF2, and NF-κB), and reporter activity was measured after treatments with SF plus DMSO, PE plus DMSO, and PE plus z-DEVD-fmk or z-LEHD-fmk inhibitors for 24 h. PE plus z-DEVD-fmk or z-LEHD-fmk inhibition led to a significant reduction in PE-induced reporter activation ($n = 3$; $^{*}P < 0.05$). (*D*) Cardiomyocytes were transfected with NF-κB, MEF2, or control luciferase hypertrophic reporter plasmids followed by infection with GFP-AdV or p35-AdV. PE-induced hypertrophy resulted in a significant increase in NF-κB ($n = 3$, $^{*}P < 0.05$) and MEF2 ($n = 3$, $^{**}P < 0.05$) activation compared with SF control. Caspase inhibition with p35-AdV infection suppressed NF-κB ($n = 3$, $\#P < 0.05$) and MEF2 ($n = 3$, $\#\#P < 0.05$) activation. (Scale bars: 40 μm.)

a concentration of PAC-1 that was compatible with maintaining cell viability. Primary cardiomyocytes treated with high doses of PAC-1 (100 μM) displayed decreased viability (i.e., increased cell death) relative to control cells, an outcome that was comparable to a standard apoptotic treatment with staurosporine (Fig. S9). However, low-dose PAC-1 administration (12.5–25 μM) maintained cell viability (i.e., no significant decrease in cell viability) while inducing cardiomyocyte hypertrophy, a response that was

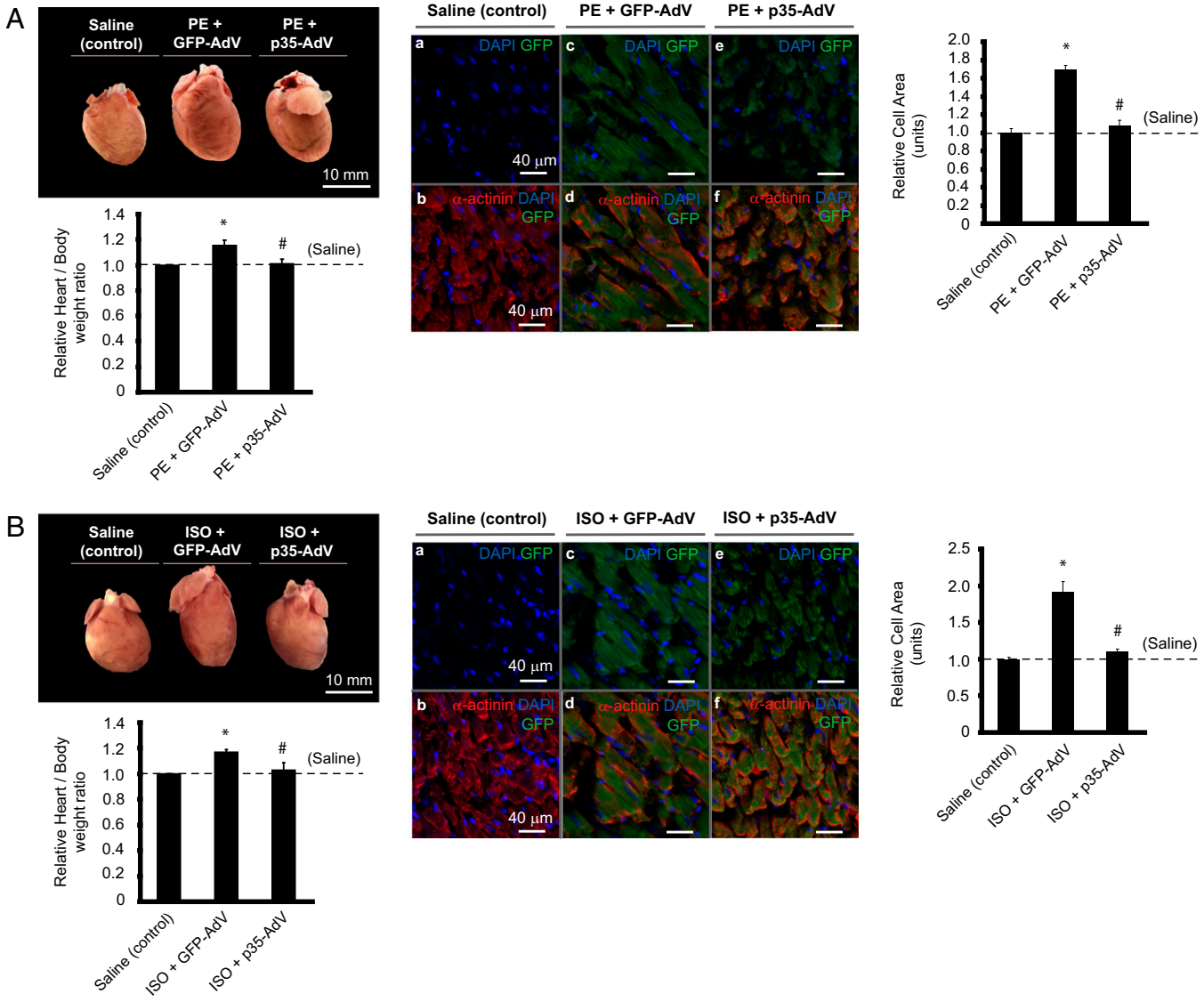

Fig. 4. Inhibition of caspase 3 activity attenuates cardiomyocyte hypertrophy in the intact myocardium. (*A*) Osmotic minipumps were implanted in rats containing saline solution (control) or PE (PE control and experimental) to induce hypertrophy over 3 wk at 10 mg/kg/d. PE control and experimental groups were subjected to GFP-AdV or a GFP tagged p35 expressing AdV (p35-AdV) infection via echo-directed microinjections into the ventricle wall. After 3 wk, whole hearts were isolated, cryosectioned, and stained for α-actinin (red) and DAPI (blue). PE induced an increase in HW/BW ratio of 15% and an increase in cardiomyocyte cell area of 69% compared with control ($n = 3$; $^{*}P < 0.05$) whereas p35-AdV significantly reduced these effects ($n = 3$; $^{\#}P < 0.05$). (*B*) Hypertrophy was induced (as described earlier) using ISO at 1 mg/kg/d for 2 wk. HW/BW ratio and cell size were increased (17% and 90%, respectively) compared with control ($n = 3$; $^{*}P < 0.05$), and p35-AdV treatment led to a significant reduction in these hypertrophic effects ($n = 3$; $^{\#}P < 0.05$). Cell area of GFP (green)-positive cardiomyocytes was evaluated by using ImageJ software. (Scale bars: 40 μm.)

comparable with the hypertrophic agonist PE (Fig. S9 and Fig. 5*A*). Specifically, cardiomyocytes treated with low PAC-1 concentrations (25 μM, 24 h) displayed a significant increase in cell size (~65%) and ANP expression (approximately threefold; Fig. 5 *A*, *a* and *f* vs. *c* and *h*). To further validate the PAC-1/caspase 3-induced hypertrophy response, we measured the transcriptional response of known prohypertrophic markers (MEF2, NF-κB, ANP, BNP) after 1 h, 3 h, and 24 h of PAC-1 (25 μM) treatment. Similar to PE treatment, PAC-1 administration resulted in a significant increase in all hypertrophic markers compared with cardiomyocytes treated with SF plus DMSO media as early as 1 h after exposure to PAC-1 (Fig. 5*B*, *Left*). After 3 h of PAC-1 treatment, significant elevations in reporter activity were observed which were comparable to those following PE exposure (Fig. 5*B*, *Center*). Significant reporter activity after 24 h of PAC-1 treatment was also observed (Fig. 5*B*, *Right*). The differences in the fold activation noted at the 24-h time point in PE treated vs. PAC-1–treated cardiomyocytes may derive from the probability that PE engages additional signaling events, signals that extend beyond the intrinsic cell death pathway and that converge to amplify the hypertrophic gene expression program.

Finally, to confirm specificity of action for PAC-1, we conducted two additional experiments. Assuming PAC-1 stimulates cardiomyocyte hypertrophy through a strict activation of caspase 3, then (*i*) use of an irreversible inhibitor of caspase 3 activity should block the ability of PAC-1 to induce hypertrophy, and (*ii*) limiting activation of the intrinsic pathway should not impact the ability of PAC-1 to promote hypertrophy. Importantly, a significant reduction in cell size (~39%) and ANP expression (~56%) was observed in cardiomyocytes treated with the caspase 3 inhibitor during PAC-1 administration (Fig. 5 *A*, *c* and *h* vs. *d* and *i*). Conversely, caspase 9 inhibition was not able to significantly

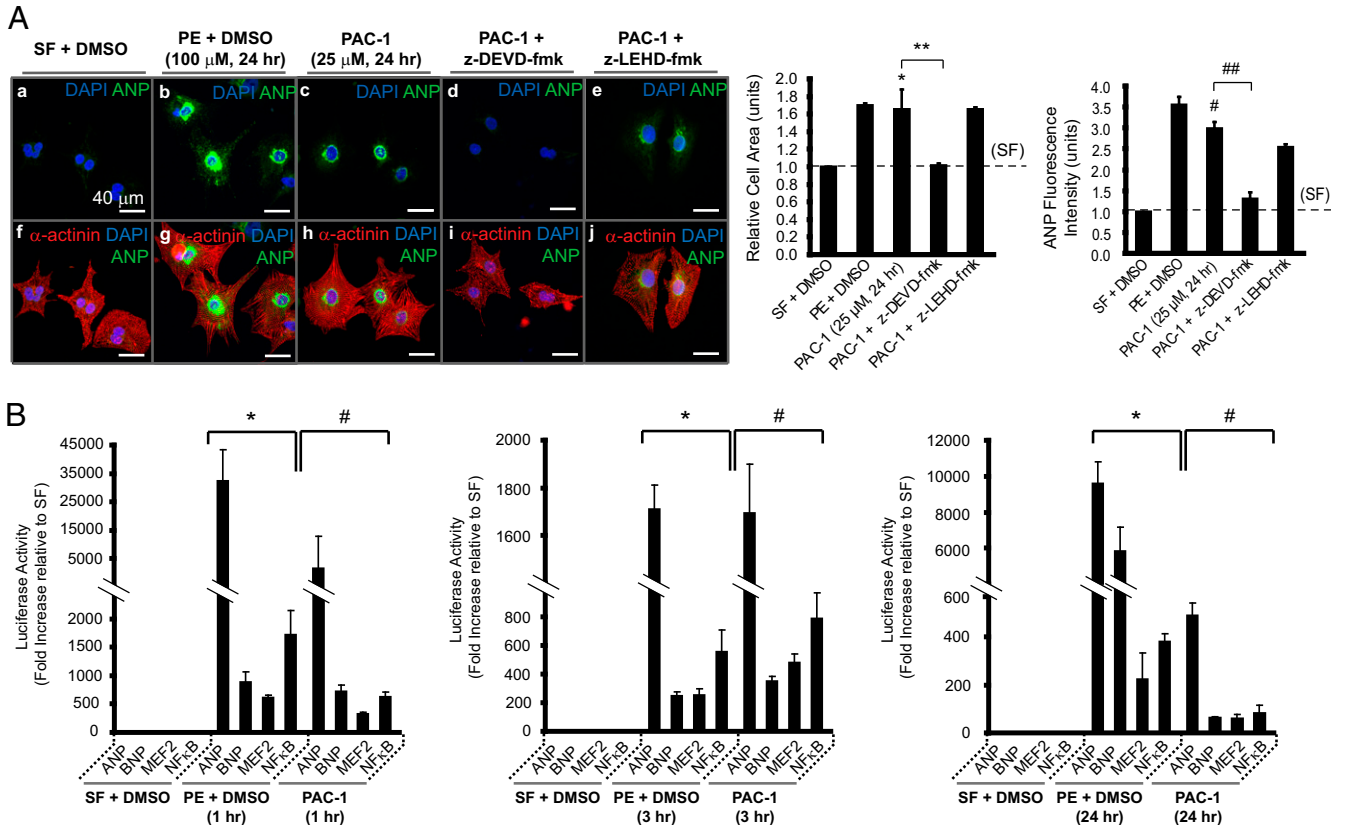

Fig. 5. Caspase 3 activation is sufficient to induce cardiomyocyte hypertrophy. (*A*) Cardiomyocytes were treated with SF media (*a* and *f*), PE (100 μM; 24 h; *b* and *g*), PAC-1 (25 μM; 24 h; *c* and *h*), PAC-1 and caspase 3 inhibitor z-DEVD-fmk (*d* and *i*), or PAC-1 and caspase 9 inhibitor z-LEHD-fmk (*e* and *j*). Cells were stained for α-actinin (red), ANP (green), and DAPI (blue). PAC-1 treatment resulted in a significant increase in cell area and ANP levels, whereas inhibition with z-DEVD-fmk resulted in a significant reduction in cell size ($n = 3$, $^{**}P < 0.05$) and ANP levels ($n = 3$, $^{\#\#}P < 0.05$). Conversely, caspase 9 inhibition was not able to significantly reduce the hypertrophic phenotype induced by PAC-1 treatment (compare *c* and *h* vs. *e* and *j*). (Scale bars: 40 μm.) (*B*) The transcriptional response of known prohypertrophic markers was evaluated following 1, 3, and 24 h of PAC-1 treatment. Cardiomyocytes were transfected with luciferase reporter plasmids for prohypertrophic markers (MEF2, NF-κB, ANP, and BNP), and reporter activity was measured after treatments with SF, PE, and PAC-1. PAC-1 treatment resulted in a significant increase ($n = 3$; $^{\#}P < 0.05$) in all hypertrophic markers compared with SF media during early (1–3 h) and late (24 h) time points.

reduce the hypertrophic phenotype induced by PAC-1 treatment, demonstrating that PAC-1 activates caspase 3 downstream of caspase 9 (Fig. 5 *A*, *c* and *h* vs. *e* and *j*). These results establish that small molecule induction of caspase 3 activation is sufficient to recapitulate the phenotypic and biochemical characteristics of cardiomyocyte hypertrophy, independent of any agonist costimulation. To address the involvement of nonspecific protease activity or other calcium activated proteases as probable contributors to caspase induction of hypertrophy, we analyzed calpain activity during PE- and PAC-1–induced hypertrophy in the presence of caspase and calpain inhibitors (p35-AdV and calpastatin, respectively; Fig. S7*E*). Neither PE stimulation nor PAC-1 treatment of primary cardiomyocytes leads to any appreciable increase in calpain activity at later time points in the hypertrophy cycle (Fig. S7*E*). Although our observations do not preclude a role for calpains in the hypertrophic remodeling process, the data and reagents used in this study demonstrate a caspase specific role that cannot be attributed directly to calpain activity.

The present study establishes the intrinsic/mitochondrial cell death pathway as a central conduit for adrenergic-induced cardiomyocyte hypertrophy. To date, cell death signal pathways have been associated with the transition to end-stage heart failure. For example, long-term caspase inhibition has been reported to reduce cardiomyocyte apoptosis, attenuate cardiac remodeling, while preserving myocardial function in models of cardiomyopathy and pressure overload (6, 38–40). Here, our observations indicate that elevated caspase 3 activity is an early and essential step in the promotion of cardiomyocyte hypertrophy, a cellular response that is not associated with the apoptosis program per se. The ability of caspase signaling to induce hypertrophy or apoptosis may appear to be an incompatible feature for a single pathway, yet may simply reflect alterations in signal intensity or duration. In such a model, transient and low-level activation of intrinsic signaling would be predicted to promote the hypertrophic adaptation, whereas sustained and high level activation would result in apoptosis. Indeed, a similar dichotomy has been reported for many neurohormonal agonists that trigger adrenergic receptor signaling events in the myocardium (e.g., PE, norepinephrine, AngII, and ET1). AdV expression of WT Gαq has been reported to induce compensatory/adaptive hypertrophic growth in cultured cardiomyocytes at 24 h; however, expression of a constitutively active Gαq mutant produced hypertrophy, which rapidly progressed to apoptotic cell death (41). These observations were supported by in vivo studies where transgenic mice overexpressing WT Gαq developed compensatory hypertrophy that rapidly transitioned to progressive heart failure (41, 42). Although these studies did not investigate the requirement for caspase activity, adrenergic stimulation of intrinsic cell death signaling may explain the accelerated progression from hypertrophy to failure.

We favor the hypothesis that caspase 3 cleavage inactivation of MEF2 and NF-κB inhibitory proteins releases the respective transcription factors to induce the cardiomyocyte hypertrophy program. Nevertheless, it is reasonable to conclude that other caspase-related signaling events augment the hypertrophy tran-

sition. Caspase activity can be localized to promote dismantling of specific subcellular structures during cellular differentiation and remodeling (13, 14). In the context of prohypertrophic remodeling, localized/restricted caspase activity may trigger the dynamic reorganization of cytoskeletal and contractile protein components, thus allowing for the subsequent addition to and growth of sarcomeres (43). Communal et al. (43) have reported that β-adrenergic stimulation via norepinephrine exposure in adult rat ventricular cardiomyocytes triggered a caspase 3 targeting of α-actin, α-actinin, and cardiac troponin T before the onset of apoptosis. More recently, other sarcomeric proteins have been shown to be direct caspase targets in apoptotic models including, myosin heavy chain and ventricular myosin light chain (44–46). The ability of caspase 3 to directly modify cellular structure while altering the activity of key gene expression programs implies that this protease (and the intrinsic pathway) may serve as a fulcrum for agonist-induced hypertrophy in general.

In summary, we have provided clear evidence that the mitochondrial/intrinsic caspase-mediated pathway is essential for cardiomyocyte hypertrophy. Currently, antagonists of the upstream adrenergic receptors (e.g., β-blockers) are one of several mainstay treatments of heart failure (47). Based on our results, targeting downstream components of the intrinsic pathway, specifically caspase 3 or 9 protease function, may allow for therapeutic intervention in patients at the earlier compensatory stage of the disease process, limiting cardiomyocyte cell size and forgoing the maladaptive transition to heart failure.

Materials and Methods

Primary neonatal rat cardiomyocytes were isolated from hearts of 2-d-old Sprague–Dawley rats, and ventricles were digested with collagenase II. Subsequently, cardiomyocytes were resuspended in DMEM. Cells were allowed to recover in DMEM culture media for 24 h, followed by a change to serum-free (SF) media for another 24 h before cardiomyocyte treatments with hypertrophic agonists: PE (100 μM), ISO (1 μM), AngII (100 nM), or ET1 (20 nM). Caspase 3 and 9 signaling was inhibited by using 20 μM of a chemical peptide inhibitor (z-DEVD-fmk and z-LEHD-fmk, respectively). Inhibition of the intrinsic and effector caspase pathways was accomplished by infecting primary cardiomyocytes with AdVs expressing the biological caspase inhibitors (Mcl-1-AdV and p35-AdV, respectively).

Additional details regarding materials and methods are provided in *SI Materials and Methods*.

ACKNOWLEDGMENTS. The authors thank Drs. Duncan Stewart, Michael Rudnicki, and Peter Liu for helpful discussions; Rick Seymour and Ali Ahmadi for performing ultrasound-guided intracardiac injections (University of Ottawa Heart Institute); Paul Oleynik for assistance with flow cytometry analyses (StemCore); and Dr. Ruth Slack for providing the Mcl-1–expressing adenovirus. This work was supported by grants (to L.A.M.) from the Ontario Research Fund, The Heart and Stroke Foundation of Canada, and the Canadian Institutes of Health Research. L.A.M. held the Mach Gaensslen Chair in Cardiac Research.

1. Kolodziejczyk SM, et al. (1999) MEF2 is upregulated during cardiac hypertrophy and is required for normal post-natal growth of the myocardium. *Curr Biol* 9(20):1203–1206.
2. Liu Q, Chen Y, Auger-Messier M, Molkentin JD (2012) Interaction between NFκB and NFAT coordinates cardiac hypertrophy and pathological remodeling. *Circ Res* 110(8):1077–1086.
3. Olson EN, Backs J, McKinsey TA (2006) Control of cardiac hypertrophy and heart failure by histone acetylation/deacetylation. *Novartis Found Symp* 274:3–12.
4. Nicol RL, Frey N, Olson EN (2000) From the sarcomere to the nucleus: role of genetics and signaling in structural heart disease. *Annu Rev Genomics Hum Genet* 1:179–223.
5. Oka T, Komuro I (2008) Molecular mechanisms underlying the transition of cardiac hypertrophy to heart failure. *Circ J* 72(Suppl A):A13–A16.
6. Dorn GW, 2nd (2009) Having a change of heart: reversing the suicidal proclivities of cardiac myocytes. *Trans Am Clin Climatol Assoc* 120:189–198.
7. van Berlo JH, Maillet M, Molkentin JD (2013) Signaling effectors underlying pathologic growth and remodeling of the heart. *J Clin Invest* 123(1):37–45.
8. Jobe LJ, et al. (2009) TNF-alpha inhibition attenuates adverse myocardial remodeling in a rat model of volume overload. *Am J Physiol Heart Circ Physiol* 297(4): H1462–H1468.
9. Sun M, et al. (2007) Tumor necrosis factor-alpha mediates cardiac remodeling and ventricular dysfunction after pressure overload state. *Circulation* 115(11):1398–1407.
10. Badorff C, et al. (2002) Fas receptor signaling inhibits glycogen synthase kinase 3 beta and induces cardiac hypertrophy following pressure overload. *J Clin Invest* 109(3): 373–381.
11. McDermott-Roe C, et al. (2011) Endonuclease G is a novel determinant of cardiac hypertrophy and mitochondrial function. *Nature* 478(7367):114–118.
12. Abdul-Ghani M, et al. (2011) Wnt11 promotes cardiomyocyte development by caspase-mediated suppression of canonical Wnt signals. *Mol Cell Biol* 31(1):163–178.
13. Abdul-Ghani M, Megeney LA (2008) Rehabilitation of a contract killer: caSpase-3 directs stem cell differentiation. *Cell Stem Cell* 2(6):515–516.
14. Fuchs Y, Steller H (2011) Programmed cell death in animal development and disease. *Cell* 147(4):742–758.
15. Larsen BD, et al. (2010) Caspase 3/caspase-activated DNase promote cell differentiation by inducing DNA strand breaks. *Proc Natl Acad Sci USA* 107(9):4230–4235.
16. Lee RE, Brunette S, Puente LG, Megeney LA (2010) Metacaspase Yca1 is required for clearance of insoluble protein aggregates. *Proc Natl Acad Sci USA* 107(30): 13348–13353.
17. Coll KE, Joseph SK, Corkey BE, Williamson JR (1982) Determination of the matrix free Ca2+ concentration and kinetics of Ca2+ efflux in liver and heart mitochondria. *J Biol Chem* 257(15):8696–8704.
18. Nagendran J, et al. (2008) A dynamic and chamber-specific mitochondrial remodeling in right ventricular hypertrophy can be therapeutically targeted. *J Thorac Cardiovasc Surg* 136(1):168–178.e3.
19. Garcia R, Thibault G, Cantin M (1987) Correlation between cardiac hypertrophy and plasma levels of atrial natriuretic factor in non-spontaneous models of hypertension in the rat. *Biochem Biophys Res Commun* 145(1):532–541.
20. Ploner C, Kofler R, Villunger A (2008) Noxa: At the tip of the balance between life and death. *Oncogene* 27(Suppl 1):S84–S92.
21. Zhuang J, Brady HJ (2006) Emerging role of Mcl-1 in actively counteracting BH3-only proteins in apoptosis. *Cell Death Differ* 13(8):1263–1267.
22. Ryan CA, et al. (2002) Inhibitor specificity of recombinant and endogenous caspase-9. *Biochem J* 366(pt 2):595–601.
23. Fuentes-Prior P, Salvesen GS (2004) The protein structures that shape caspase activity, specificity, activation and inhibition. *Biochem J* 384(pt 2):201–232.
24. Clem RJ (2001) Baculoviruses and apoptosis: The good, the bad, and the ugly. *Cell Death Differ* 8(2):137–143.
25. Zhang CL, et al. (2002) Class II histone deacetylases act as signal-responsive repressors of cardiac hypertrophy. *Cell* 110(4):479–488.
26. Escaffit F, et al. (2007) Cleavage and cytoplasmic relocalization of histone deacetylase 3 are important for apoptosis progression. *Mol Cell Biol* 27(2):554–567.
27. Liu F, Dowling M, Yang XJ, Kao GD (2004) Caspase-mediated specific cleavage of human histone deacetylase 4. *J Biol Chem* 279(33):34537–34546.
28. Paroni G, et al. (2004) Caspase-dependent regulation of histone deacetylase 4 nuclear-cytoplasmic shuttling promotes apoptosis. *Mol Biol Cell* 15(6):2804–2818.
29. Montgomery RL, et al. (2008) Maintenance of cardiac energy metabolism by histone deacetylase 3 in mice. *J Clin Invest* 118(11):3588–3597.
30. Liu IC, Chiu SW, Lee HY, Leu JY (2012) The histone deacetylase Hos2 forms an Hsp42-dependent cytoplasmic granule in quiescent yeast cells. *Mol Biol Cell* 23(7):1231–1242.
31. Waltregny D, et al. (2005) Histone deacetylase HDAC8 associates with smooth muscle alpha-actin and is essential for smooth muscle cell contractility. *FASEB J* 19(8):966–968.
32. Gordon JW, Shaw JA, Kirshenbaum LA (2011) Multiple facets of NF-κB in the heart: To be or not to NF-κB. *Circ Res* 108(9):1122–1132.
33. Lamkanfi M, Declercq W, Vanden Berghe T, Vandenabeele P (2006) Caspases leave the beaten track: caspase-mediated activation of NF-kappaB. *J Cell Biol* 173(2): 165–171.
34. Rathore N, Matta H, Chaudhary PM (2004) An evolutionary conserved pathway of nuclear factor-kappaB activation involving caspase-mediated cleavage and N-end rule pathway-mediated degradation of IkappaBalpha. *J Biol Chem* 279(38):39358–39365.
35. Su H, et al. (2005) Requirement for caspase-8 in NF-kappaB activation by antigen receptor. *Science* 307(5714):1465–1468.
36. Peterson QP, et al. (2009) PAC-1 activates procaspase-3 in vitro through relief of zinc-mediated inhibition. *J Mol Biol* 388(1):144–158.
37. Putt KS, et al. (2006) Small-molecule activation of procaspase-3 to caspase-3 as a personalized anticancer strategy. *Nat Chem Biol* 2(10):543–550.
38. Adams JW, et al. (2000) Cardiomyocyte apoptosis induced by Galphaq signaling is mediated by permeability transition pore formation and activation of the mitochondrial death pathway. *Circ Res* 87(12):1180–1187.
39. Balakumar P, Singh M (2006) The possible role of caspase-3 in pathological and physiological cardiac hypertrophy in rats. *Basic Clin Pharmacol Toxicol* 99(6):418–424.
40. Balsam LB, Kofidis T, Robbins RC (2005) Caspase-3 inhibition preserves myocardial geometry and long-term function after infarction. *J Surg Res* 124(2):194–200.
41. Adams JW, et al. (1998) Enhanced Galphaq signaling: A common pathway mediates cardiac hypertrophy and apoptotic heart failure. *Proc Natl Acad Sci USA* 95(17): 10140–10145.
42. D'Angelo DD, et al. (1997) Transgenic Galphaq overexpression induces cardiac contractile failure in mice. *Proc Natl Acad Sci USA* 94(15):8121–8126.
43. Communal C, et al. (2002) Functional consequences of caspase activation in cardiac myocytes. *Proc Natl Acad Sci USA* 99(9):6252–6256.
44. Fischer U, Jänicke RU, Schulze-Osthoff K (2003) Many cuts to ruin: A comprehensive update of caspase substrates. *Cell Death Differ* 10(1):76–100.
45. Moretti A, et al. (2002) Essential myosin light chain as a target for caspase-3 in failing myocardium. *Proc Natl Acad Sci USA* 99(18):11860–11865.
46. Solinet S, Vitale ML (2008) Isoform B of myosin II heavy chain mediates actomyosin contractility during TNFalpha-induced apoptosis. *J Cell Sci* 121(pt 10):1681–1692.
47. Deedwania PC, Carbajal E (2012) Evidence-based therapy for heart failure. *Med Clin North Am* 96(5):915–931.